Effects of antimalarial treatments and febrile temperatures on *Plasmodium falciparum* cytoadherence

Thesis submitted in accordance with the requirements of the University of Liverpool for the degree of Doctor in Philosophy

by

Katie Ruth Hughes

December 2008

TABLE OF CONTENTS

LIST OF FIGURES

LIST OF ABBREVIATIONS

ACT	artemisinin based combination therapies
art	artesunate
BBB	Blood brain barrier
CIDR	Cysteine Rich Interdomain Region
CSA	Chondroitin Sulfate A
D1	Domain 1 (of ICAM-1)
DBL	Duffy Binding Like
dPBS	Dulbecco's PBS
FACS	Fluorescence activated cell sorter
f-actin	Filamentous actin
Fur	Furosemide
HBEC	Human Brain Endothelial Cells
hct	Haematocrit
HDMEC	Human Dermal Microvascular Endothelial Cells
HLEC	Human Pulmonary Vein (lung) Endothelial Cells
HNE	4-hydroxynonenal
Hpi	Hours Post Invasion
HRP	Horseradish Peroxidase
HSF-1	Heat Shock (transcription) Factor 1
HSP	Heat Shock Protein
HUVEC	Human Umbilical Vein Endothelial cells
ICAM-1	Intercellular Cell Adhesion Molecule 1
Ig	Immunoglobulin
KAHRP	knob associated histidine rich protein
LFA-1	Lymphocyte function associated antigen 1
LORCA /Lorca	laser assisted optical rotational cell analyser (analysis)
Lum	Lumefantrine
mAb	Monoclonal Antibody
NCAM	Neural cell adhesion molecule
PBS	Phosphate buffered saline
PECAM-1	Platelet/endothelial cell adhesion molecule-1
Pexel	Plasmodium pentamaric export element
PfEMP-1	*Plasmodium falciparum* erythrocyte membrane protein 1
Pip	Piperaquine
PRBC	Parasitised Red Blood Cell(s)
PV	Parasitophorous Vacuole
PVM	Parasitophorous Vacuole Membrane
Qn	Quinine
RBC	Red Blood Cell (s)
SD	Standard Deviation
SP	sulfadoxine-pyrimethamine
TBS	Tris-buffered saline
TBST	Tris-buffered saline with 0.1% Tween 20
TNF	Tumour necrosis factor
VCAM-1	Vascular cell adhesion moleclue-1
WHO	World Health Organisation

ABSTRACT

The *Plasmodium falciparum* parasite is thought to be responsible for more than a million deaths every year from severe malaria. Although malaria is a treatable disease, many of the mortalities occur in the first 24 – 48 hours after hospital admission, despite administration of antimalarial drugs. An important contributory factor to severe disease is the ability of the parasite, during the intraerythrocytic development phase, to cause infected red blood cells to sequester in host microvasculature. These sequestered parasitized red blood cells (PRBC) contribute to severe disease by impeding microcirculatory flow and possibly contributing to damage to the host endothelium. Sequestration is a result of the cytoadherence interaction between parasite proteins on the surface of the PRBC, and host endothelial adhesion molecules. Whilst many adhesion receptors have been identified, adhesion to ICAM-1 has been, in some cases, potentially linked with one of the most severe forms of malaria, cerebral malaria.

We have investigated what might happen in terms of cytoadherence during the first 24 hours after administration of antimalarials. We find that despite loss of viability, parasites are still able to cytoadhere at significant levels for many hours after administration of antimalarials. These results indicate that changes made by the parasite to a PRBC are stable even after parasite death, and any pathophysiological effects resulting from the ability of the PRBC to sequester in microvasculature may be continuing for long after parasite death. We also investigate the increased rigidity of PRBC, and find that this feature is also maintained long after administration of antimalarials.

These results highlight a potential need for adjunct therapy that could be administered along with antimalarial treatment which may reverse sequestration of PRBC. Whilst many studies have investigated the inhibition of adhesion, few have looked at the potential to reverse sequestered populations. We show for the first time that the strong adhesion of PRBC to ICAM-1 can be not only inhibited, but also reversed by both a monoclonal antibody and a recombinant protein. This suggests that the reversal of cytoadherence and removal of sequestered populations may be feasible.

Finally, we have investigated a natural host response to infection, fever, which is an almost ubiquitous symptom of *P. falciparum* infection as a result of parasite stimulation of inflammatory responses. We find that the levels of cytoadherence are reduced following exposure of host endothelial cells to febrile temperatures. This illustrates the potentially protective nature of host responses to infection.

CHAPTER 1 - INTRODUCTION

Plasmodium falciparum is the intracellular protozoan parasite that is responsible for over a million deaths from severe malaria every year. During one stage of its complex life cycle, the intraerythrocytic asexual development stage, the parasite can cause the potentially fatal symptoms of severe malaria. This thesis focuses on the interactions that occur during this life cycle stage between the parasite and the human host. An important aspect of *P. falciparum* malaria is the intimate cytoadherence process that leads to the sequestration of *P. falciparum* infected red blood cells (PRBC) in microvasculature. We investigate how natural host responses (fever) and artificial interventions (antimalarial treatments) may affect this cytoadherence interaction and look at the potential for adjunct therapies to prevent or reverse this potentially pathophysiological interaction.

1-1 Malaria Parasites – *Plasmodium* Species

The most severe form of malaria is caused by *Plasmodium falciparum* parasites. Recent work suggests that over 2 billion people live in areas at risk of *P. falciparum* transmission (Guerra *et al.*, 2008), with parasite distribution encompassing much of Africa, South-east Asia, and South and Central America. There are five species of *Plasmodium* that can cause human malaria, however, malaria caused by *P. falciparum* is thought to account for around 50% of infections and 95% of global malaria mortalities. There are still up to 2 million deaths a year attributed to *P. falciparum* malaria, with many of these deaths occurring in young children in sub-Saharan Africa. The four other *Plasmodium* species that infect humans and cause disease are: *Plasmodium vivax, Plasmodium ovale, Plasmodium malariae* and recently recognised as causing human disease is *Plasmodium knowlesi.*

Symptoms of *P. vivax* infection are generally less severe than *P. falciparum*, but it is thought that as much of the world's population is at risk of *P. vivax* infection as is at risk of *P. falciparum* infection. Up to 50% of malaria cases in South and Southeast Asia are attributed to *P. vivax*, and this figure is up to 70% for South and Central America (Price *et al.*, 2007). The parasite is largely absent from Western Africa, probably due to a common blood type mutation which renders the parasite unable to invade host red blood cells.

The impact of *P. ovale* and *P. malariae* is less than that of *P. falciparum* or *P. vivax*, however still could be important. *P. malariae* has been detected in most malaria endemic countries, including those in Asia, the Middle East, S. and Central America, although it is most common in sub-Saharan Africa and SW Pacific. *P. ovale* infections are less common, both in distribution and frequency. While both infections result in mild symptoms there is the possibility for chronic infections, and recurrence of infection decades after original exposure (Mueller *et al.*, 2007). Recently identified as being an important human pathogen in its own right is *P. knowlesi,* which had previously been described as a primate species (Singh *et al.*, 2004, Cox-Singh *et al.*, 2008). Using PCR genotyping techniques increasing numbers of cases are now being attributed to *P. knowlesi* rather than the morphologically indistinguishable *P. malariae* (Ng *et al.*, 2008, Luchavez *et al.*, 2008), although questions still remain as to whether the parasite is transmitted between humans.

One interesting difference between the parasite species is that only the most virulent of the established human malaria parasites, *P. falciparum*, has been shown to sequester

in microvasculature. Cytoadherence of *P. falciparum* PRBC is thought to be an important determinant in the severity of disease and is the focus of this thesis.

1-2 *Plasmodium falciparum* life cycle

The vector for *P. falciparum* transmission is the female anopheline mosquito, which passes on around 15 – 150 sporozoites from her salivary gland whilst taking a blood meal. On biting a mammalian host the mosquito injects from her salivary gland factors to help facilitate her ingestion of the blood meal, including vasodilators and anti-coagulants. If the mosquito is infected, sporozoites are injected into the host skin from where they travel rapidly via the bloodstream to the liver. Interaction between a sporozoite and liver cells seems to be mediated by the parasite circumsporozoite protein (CSP) interacting with Heparan Sulphate proteoglycans (HSPGs) on liver cells.

Within the liver the sporozoite passes through several cells before coming to rest in a hepatocyte in which it forms a parasitophorous vacuole. Within this the parasite develops into thousands of merozoites. These are released into the blood stream following the budding off of a merozoite-filled vesicle which is probably then proteolytically degraded in the blood stream to release the merozoites (Prudencio *et al.*, 2006). The liver stage is largely asymptomatic and for *P. falciparum* lasts around 5½ days. The resulting merozoites then are able to initiate rounds of asexual multiplication inside red blood cells.

A merozoite, although small at 1.5 µm by 1 µm (Baum *et al.*, 2005), the size of most bacteria, is a highly specialised polar cell. The pear-shaped merozoite attaches to the surface of an RBC then must then orient itself so that the apical end of the cell is attached to the RBC surface. After reorientation a tight junction is formed which moves around the cell to engulf the parasite in its parasitophorous vacuole (Gaur *et al.*, 2004). Key to these processes are the specialised microneme and rhoptry structures underneath the apical surface membrane of the merozoite.

In the host RBC the parasite develops within the parasitophorous vacuole (PV). Young parasites are termed "rings" due to their characteristic ring-shaped appearance. Over the next 48 hours of development in the RBC the parasite makes many changes to the cell which will be described in more detail later. For the first 18 hours of development *P. falciparum* PRBC are freely circulating in the bloodstream, however the mature trophozoite stages from around 18 hours post invasion (hpi) disappear from peripheral circulation and become sequestered in microvasculature (Fig 1.2). This sequestration is a result of the cytoadherence interaction between parasite protein, (mainly PfEMP-1) on the surface of a PRBC, and host endothelial cell adhesion receptors. From around 34 – 48 hours the parasite is undergoing schizogony, nuclear division. By 48 hours

following initial merozoite invasion the PRBC is packed with up to 32 daughter merozoites ready for release to begin a new invasion cycle.

Release of merozoites from a PRBC is a disruptive process destroying the cell; the resulting loss of RBC may contribute to the anaemia often seen in severe malaria. Merozoites have to escape from two membranes, the PV membrane and the RBC plasma membrane. Although several models for the release of PRBC have previously been proposed (Rayner, 2006), recently, careful microscopy has suggested that an explosive release of merozoites is preceded by some swelling of the schizont before almost simultaneous rupture of the PVM and RBC PM (Glushakova *et al.*, 2005).

Once the *P. falciparum* asexual infection is established, parasites adapted for mosquito transmission, the gametocytes, start to emerge. The commitment to form gametocytes occurs during schizont development, such that all merozoites from a committed schizont once reinvaded will not only all develop into gametocytes, but will all become the same sex. The precise triggering factor for gametogenesis is unknown, but stressful conditions encountered at high parasite densities are known to be involved. Gametogenesis takes around 10 days for *P. falciparum* and during most of this time, as seen with mature trophozoites, the cells are absent from peripheral circulation. Unlike mature trophozoites which sequester in a variety of tissues, gametocytes can be found specifically in bone marrow. Whereas it is well established that the protein responsible for adhesion of asexual stages is PfEMP-1 (see later), it is less clear what is mediating the cytoadherence and sequestration of developing gametocytes in the bone marrow. The developing gametocytes have been shown to have low levels of *var* transcripts and PfEMP-1, and do not express the knob structures that are necessary for correct display of PfEMP-1 and efficient cytoadherence. The mature gametocytes (known as stage V) which have a characteristic crescent shaped appearance and show no cytoadherence phenotype are found in peripheral circulation. It is these cells that, after being taken into a mosquito in her blood meal, are capable of developing and further transmission (Alano, 2007).

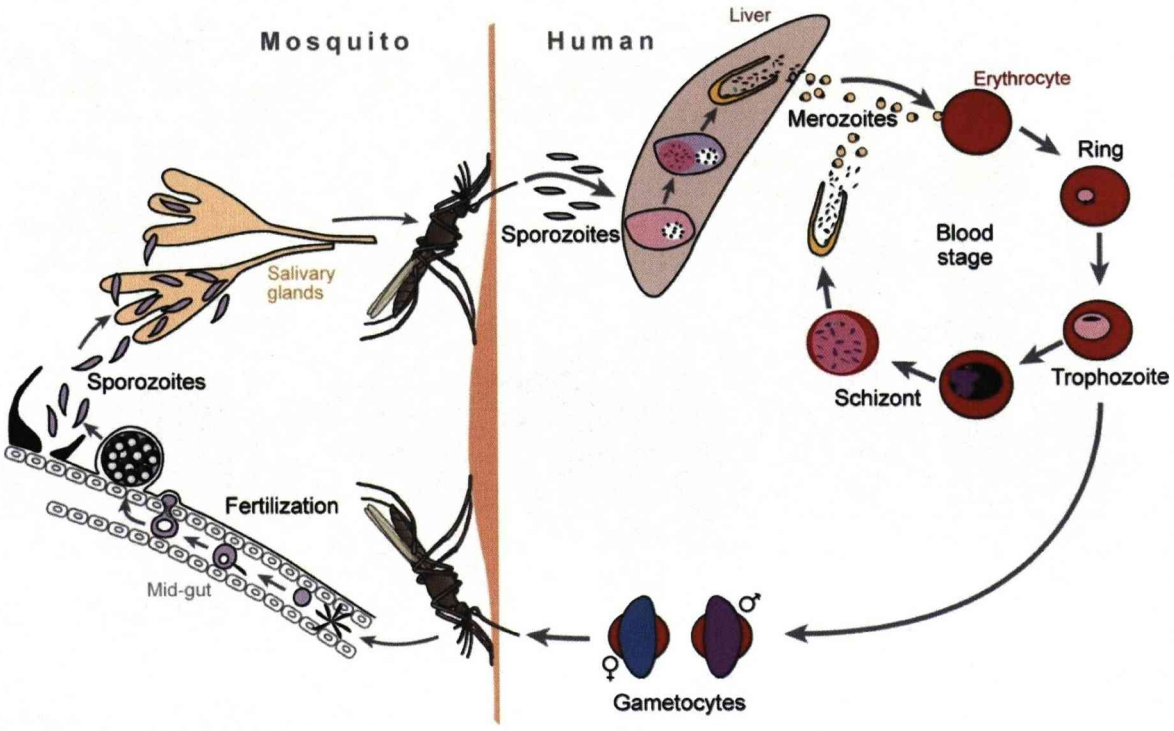

Figure 1.1. Life cycle of *Plasmodium falciparum* (Figure taken from Scherf 2008 (Scherf *et al.*, 2008)). See text for life cycle description.

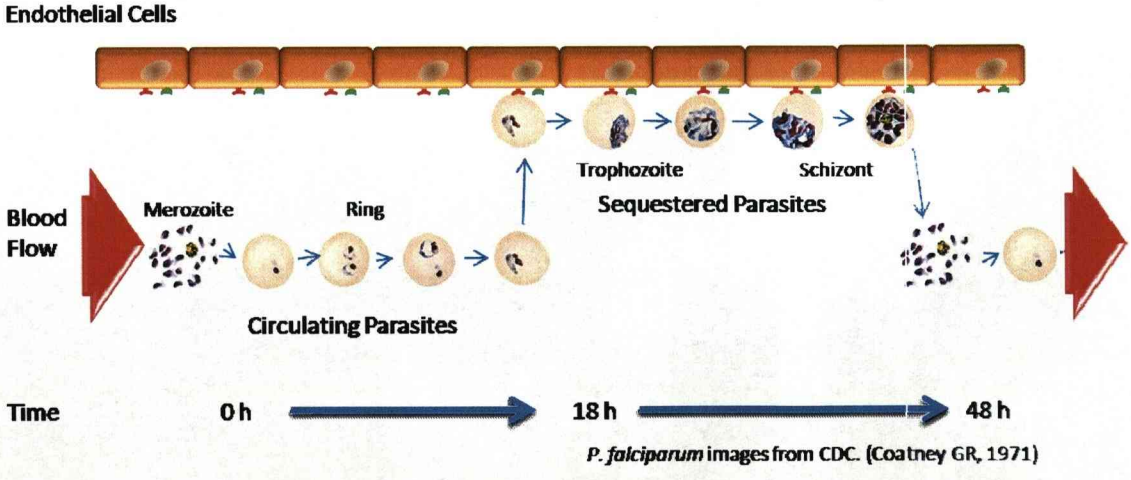

Figure 1.2. Development and cytoadherence of intraerythrocytic stages of *P. falciparum*. Illustrating the morphology of the developing parasite from Ring stage (0h – 14h). Ring-trophozoite transition stage (14-18h). Young trophozoite (18-24h). Mid-trophozoite (24-28h). Mature trophozoite (28-32h). Developing Schizont (32-42h). And Schizont (42-48h). Cytoadherence to endothelial cells and sequestration in microvasculature occurring from around 18 h onwards.

1-3 The Infected Red Blood Cell

As a parasite matures inside a host red blood cell, the cell becomes capable of cytoadherence, adhesion to the endothelial cells that line blood vessel walls. Infected red blood cells are also significantly more rigid than the highly deformable red blood cell (Cranston *et al.*, 1984). It is widely thought that it is the increased rigidity of *P. falciparum* PRBC is responsible for the ability of the spleen to recognise and clear PRBC, either through destruction of the PRBC, or through removal of the parasite by the mechanical process of pitting (Engwerda *et al.*, 2005, Chotivanich *et al.*, 2002, Angus *et al.*, 1997, Safeukui *et al.*, 2008). Sequestration in the microvasculature is a mechanism by which the rigid PRBC can escape from circulation and avoid passage through, and destruction by, the spleen. *P. vivax* PRBC are not known to cytoadhere, so remain in peripheral circulation during intraerythrocytic development. However, *P. vivax* infection does not lead to increased rigidity of the PRBC. It has been suggested that the *P. vivax* PRBC are more deformable than uninfected RBC (Suwanarusk *et al.*, 2004). An alternative mechanism for avoidance of splenic clearance of *P. vivax* PRBC has been proposed based on adhesion of *P. vivax* PRBC to barrier cells in the spleen preventing entry into the spleen and subsequent clearance (del Portillo *et al.*, 2004), but there is little evidence to support this.

The many modifications that a parasite makes to the host red blood cell might contribute to the decreased deformability of the PRBC (Cooke *et al.*, 2001). Changes made by the parasite to the RBC include: i) Expression of parasite proteins on the cytoplasmic face of the RBC membrane; ii) Expression of parasite proteins on the surface of the PRBC and insertion of novel, or modification of existing channels in the RBC membrane to form the new permeation pathways (NPP); iii) The modification of RBC membrane cytoskeletal components. These structural changes made by the parasite occur alongside the increasing physical size of the parasite within the RBC, and the increase in components of the RBC cytoplasm such as solutes being taken up into the cell by the parasite (Kirk, 2001). The resulting increased rigidity may be a factor in impairing microcirculatory blood flow (Dondorp *et al.*, 2008), and determination of disease severity (Dondorp *et al.*, 2000).

RBC Membrane Cytoskeleton

A red blood cell needs to be highly deformable to allow passage through small blood vessels throughout its 120 day lifespan. This deformability is a result of a highly specialised membrane cytoskeleton structure with elastic properties. Spectrin is the main component of the cytoskeleton, and is composed of an α and a β chain that form

antiparallel heterodimers which then associate to form tetramers. Junctional complexes connecting spectrin tetramers comprise mainly of protein 4.1, and actin. These are connected to the membrane through interactions between protein 4.1 and ankyrin to the integral membrane proteins band 3 and glycophorin C. In PRBC this membrane cytoskeleton is altered by parasite proteins that interact with the host membrane or cytoskeleton, as well as parasite induced modifications to endogenous host proteins (Cooke et al., 2001). Some of these changes may contribute to the increased rigidity of PRBC compared to uninfected RBC (Cranston et al., 1984).

Protein 4.1

Protein 4.1 appears to be essential for the proper development of *P. falciparum*. It has been shown that protein 4.1 is phosphorylated to a greater extent in PRBC than in uninfected RBC, and the parasite protein, mature parasite-infected erythrocyte surface antigen, (MESA) is known to interact with protein 4.1 (Bennett *et al.*, 1997). Failure to interact with protein 4.1 leads to accumulation of MESA in the RBC cytoplasm and reduced parasite viability. However, the precise role of MESA is unknown and MESA is not thought to be important for the formation of knobs or cytoadherence (Lustigman *et al.*, 1990, Magowan *et al.*, 1995).

Knobs

A major change to the PRBC is the formation of knobs which anchor the variant protein PfEMP-1 on the surface of the PRBC; knobs have been shown to be essential for the ability of PRBC to cytoadhere under flow conditions (Crabb *et al.*, 1997). Knobs are formed from the interaction with parasite proteins PfEMP3 and knob associated histidine rich protein (KAHRP) with host spectrin, actin and ankyrin. PfEMP-1 protein is anchored to knobs through association between the PfEMP-1 cytoplasmic C-terminal domain acidic terminal segment (ATS) and KAHRP (Rug *et al.*, 2006, Pei *et al.*, 2005, Oh *et al.*, 2000).

KAHRP

KAHRP has binding sites for Spectrin, Ankyrin and PfEMP-1. The presence of KAHRP is essential for formation of knobs on the surface of PRBC, and also for the display of PfEMP-1, and proper cytoadherence. In the absence of KAHRP, whether through chromosomal deletion or targeted genetic deletion, the level of PfEMP-1 on the surface is reduced, the distribution of the protein is altered, and cytoadherence under flow is not possible (Horrocks *et al.*, 2005, Crabb et al., 1997). The formation of knobs has been shown to be a major determinant in the reduced rigidity of PRBC (Paulitschke &

Nash, 1993), and KAHRP specifically has been shown to have an important role in this reduced rigidity (Glenister *et al.*, 2002).

PfEMP-3

PfEMP-3 has been shown to interact with spectrin and actin (Waller *et al.*, 2007), destabilising the RBC membrane cytoskeleton (Pei *et al.*, 2007) and playing a role in the reduced deformability of PRBC (Glenister et al., 2002). PfEMP-3 is located in the PRBC membrane cytoskeleton and can be found in knobs (as well as distributed throughout the cytoskeleton) but is not essential for their formation. A truncated mutant of PfEMP-3 fails to reach the surface and also disrupts proper PfEMP-1 trafficking (Waterkeyn *et al.*, 2000).

Band 3 and Glycophorin

Parasites also induce changes to erythrocyte proteins. Components of the red blood cells cytoskeleton Band 3 and Glycophorin show restricted mobility within the membrane as compared with uninfected erythrocytes. This could to be due to the effect of parasite proteins or due to oxidative stress induced by the parasite (Parker *et al.*, 2004). Modified band 3, (previously known as Pfalhesin) may have a role in cytoadherence to CD36 (Crandall *et al.*, 1994).

NPP

Proteins inserted into the erythrocyte membrane form, or partly make up, components of the new permeation pathways (NPP). These pathways induced by the parasite enable it to take up the nutrients needed for rapid growth and differentiation. The NPP increases flux of many solutes, including amino acids, sugars, nucleosides, vitamins and other inorganic and organic anions and cations. (Kirk, 2001). Although precise components of the NPP are unknown, and they may consist of modified host pathways (Kirk *et al.*, 1994), the involvement of parasite proteins in these pathways has been shown (Baumeister *et al.*, 2006).

Surface Exposed Proteins

Parasite proteins including the protein responsible for cytoadherence, PfEMP-1 (see below), are known to be exposed on the surface of a PRBC (Fig. 1.3) (Craig & Scherf, 2001). Other major proteins exposed on the surface of the PRBC are another family of variant proteins, RIFINs, as well as the modified host Band 3.

PfEMP-1

PfEMP-1 is the major exposed parasite protein, it is the protein responsible for cytoadherence, and, encoded for by the family of *var* genes is the major antigenically variant protein. One of around 60 *var* genes is expressed at a time, each encoding a PfEMP-1 variant with unique antigenic and cytoadherent properties. The structure of PfEMP-1 and its role in antigenic variation and cytoadherence is discussed in more detail later. PfEMP-1 has a large extracellular portion comprising several DBL domains, and a small intracellular domain which interacts with KAHRP to localise PfEMP-1 to knobs.

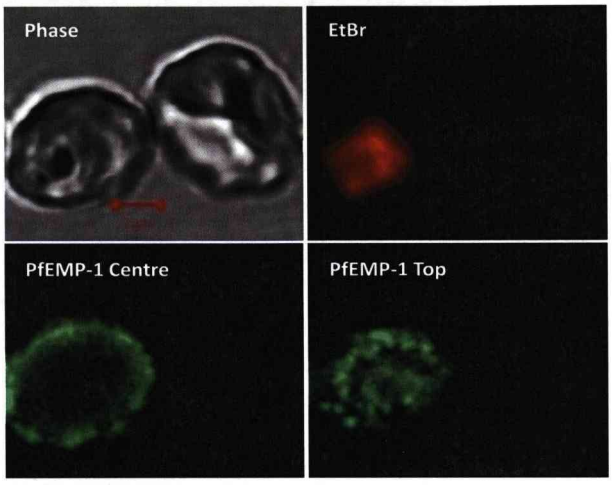

Figure 1.3. Parasite protein on the surface of a PRBC (See chapter 3). Example of parasite protein PfEMP-1 expressed on the surface of an infected red blood cell. Confocal immunofluorescence microscopy image of (unfixed) infected (left) and uninfected (right) RBC. Showing phase contrast image (Phase), ethidium bromide staining for parasite (EtBr) and top plane and centre plane of PfEMP-1 on the PRBC surface.

RIFINs

RIFINs are encoded by the clonally variant *rif* family of genes. There are an estimated 200 copies of *rif* per haploid genome and the genes are located subtelomerically, close to *var* genes. mRNA encoding rifins is detectable in trophozoite-stage parasites from around 18–23 hours post-invasion, i.e. slightly later than seen for *var* genes. RIFINs are 27–34 kDa proteins and are detectable in the RBC cytoplasm as well as associated with the mature PRBC membrane (Kyes *et al.*, 1999). RIFINs were originally identified as being involved in rosetting (Helmby *et al.*, 1993), a virulence associated phenotype involving the adhesion of a PRBC with one or more uninfected RBC through the complement receptor CR1 (Cockburn *et al.*, 2004). However, it is now thought that PfEMP-1 is the major ligand mediating rosetting (Rowe *et al.*, 1997).

STEVOR is a third large family of clonally variant proteins which although expressed in many life cycle stages is now not thought to be exposed on the surface of asexual stage PRBC (Blythe *et al.*, 2004).

Protein trafficking in the PRBC

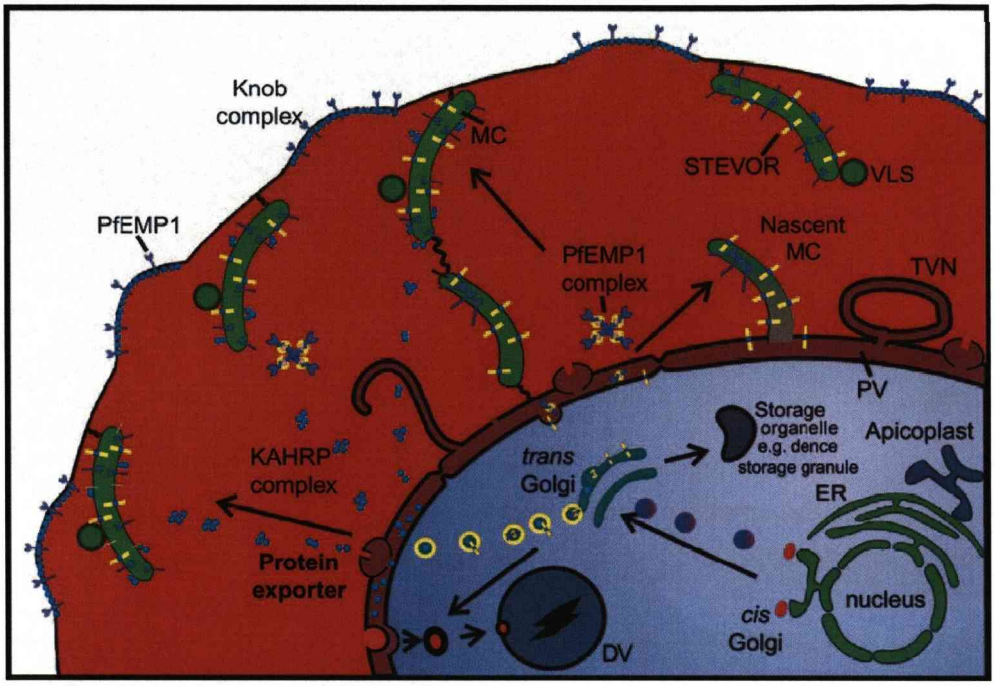

Figure 1.4. Trafficking pathways in trophozoite stage PRBC. (Figure taken from Tilley 2008 (Tilley *et al.*, 2008)) Soluble proteins destined for export are directed into the ER and pass through cis-Golgi and trans Golgi compartments en route to the parasitophorous vacuole (PV). Some proteins are retrieved from the plasma membrane or diverted from the ER or Golgi to intracellular organelles, such as the digestive vacuole (DV) and the apicoplast or (in the schizont stage) to regulated secretory compartments, such as the dense granules, rhoptries and micronemes. Following transport across the PV membrane, soluble proteins (such as KAHRP) may form complexes as they diffuse across the RBC cytoplasm and interact with the cytoplasmic surface of the MC before redistribution to the RBC membrane skeleton. *Plasmodium falciparum* erythrocyte membrane protein-1 may also be trafficked in protein complexes and may become membrane-embedded by inserting into MC from the RBC cytoplasm. Integral membrane proteins destined for the MC (such as STEVOR) may be transferred to the PV membrane and then accumulate in nascent MC. Vesicle-like structures are observed in the infected RBC cytoplasm; however, their role in protein trafficking is unclear. TVN, tubulovesicular network.

As illustrated in figure 1.4, trafficking of *Plasmodium* proteins destined for outside of the parasitophorous vacuole (PV) is a complicated process. Proteins targeted to the outside of the PV, (i.e. KAHRP and PfEMP-1) are first targeted to the PV by a hydrophobic signal sequence (Wickham *et al.*, 2001). A further signal sequence then targets them for export to the RBC cytoplasm, or membrane. This signal sequence has been identified as the Pentameric *Plasmodium* EXport ELement (Pexel) motif which appears to be able to direct the transport of exported proteins to outside of the PV

(Marti *et al.*, 2004). It is predicted that up to 8% of the *Plasmodium* genome (~400 proteins) contain this sequence and are targeted for export, although this number includes multigene families such as *var* (encoding PfEMP-1), *rif* and *stevor* (families containing ~60, ~200 and ~25 paralogues respectively). The study also noted however, that some known exported proteins did not contain a recognisable pexel motif (Marti et al., 2004).

Trafficking of proteins through the RBC cytoplasm to the RBC membrane is thought to be through Maurer's clefts structures (Wickham et al., 2001). These membranous vesicular networks have recently been visualised by electron tomography imaging to be flattened disc-like structures that are tethered to the RBC membrane (Hanssen *et al.*, 2008, Tilley et al., 2008).

The functions of some of the identified exported proteins are known. The surface proteins, PfEMP-1, and the knob associated proteins are thought to have roles in antigenic variation and virulence through cytoadherence phenotypes. Some of the identified exported proteins are known to be located in Maurer's clefts and may play a role in protein trafficking. However, the function of many of the exported proteins, and their role in parasite virulence is unknown. In order to determine the essentiality and role of some of this large number of predicted exported *P. falciparum* proteins, a large project to knock out all of the exported proteins was undertaken (Maier *et al.*, 2008). This work by Maier et. al resulted in successful genetic disruption of 53 genes. The inability to create knock out clones of 30 genes hints that they may be essential for the parasite even under the in-vitro conditions of these experiments.

Potential functions for the 53 knock out proteins were assessed by looking at virulence-related phenotypes of cytoadherence and rigidity in the knock out parasite lines. Analysis of the mutants revealed six clones with very low or reduced level of PfEMP-1 on the surface. These clones also showed no or very low cytoadherence in flow adhesion assays. The identified proteins were shown to act on different stages of the trafficking pathway, with roles apparently specific for the trafficking of PfEMP-1. Three identified proteins acted on early stages of trafficking, as the mutant parasites showed low levels of PfEMP-1 in the RBC. Three other mutants showed PfEMP-1 localised in the Maurer's clefts indicating they had a role in the trafficking of PfEMP-1 from Maurer's clefts to the PRBC surface. Two proteins were identified which disrupted formation of knobs, and as expected these mutants also showed reduced cytoadherence phenotypes. Along with this, several other mutants appeared to show some reduction in the level cytoadherence, although PfEMP-1 was apparently present

on the surface of the PRBC hinting at more subtle roles in PRBC remodelling (Maier et al., 2008). This study makes important contributions into both elucidating the detail of the complex PfEMP-1 trafficking mechanism, and identification of other potential parasite virulence factors.

1-4 PfEMP-1: Cytoadherence and Antigenic Variation

PfEMP-1 is the large variant protein that is implicated in cytoadherence to many host endothelial cell adhesion receptors. The protein is encoded for by *var* genes (Su *et al.*, 1995, Baruch *et al.*, 1995), with one of 60 *var* genes expressed at a time. Different PfEMP-1 proteins have different phenotypes in terms of both antigenicity and adhesion phenotype and are clonally expressed (Smith *et al.*, 1995). As described below there is a large range of endothelial cell adhesion receptors to which PfEMP-1 proteins can adhere. Different PfEMP-1 variants can bind to different receptors potentially mediating sequestration in different tissues (Montgomery *et al.*, 2007). High levels of recombination between *var* genes result in a huge repertoire of unique PfEMP-1 proteins within parasite populations leading to a wide range of antigenic and phenotypic diversity (Kraemer et al., 2007).

PfEMP-1 proteins comprise a domain structure consisting mainly of several Duffy-binding like (DBL) domains and cysteine-rich interdomain (CIDR) regions (Fig. 1.5). The gene structure for PfEMP-1 comprises two exons, with exon two encoding a small conserved C-terminal domain, known as the acidic terminal segment (ATS). This intracellular domain is involved in interaction with KAHRP on the cytoplasmic face of the RBC plasma membrane, resulting in the anchoring of PfEMP-1 in PRBC surface knobs. Exon 1 encodes the extracellular portion of the protein and the huge variability in PfEMP-1 proteins arises from proteins with different combinations of DBL domains, and their high sequence variability of the DBL domains.

At the N terminal end of PfEMP-1 is a semi-conserved head structure consisting of a cysteine-rich interdomain region (CIDR) domain coupled to a DBL-α domain. DBL-α domains have been shown to be able to mediate rosetting, the adhesion of a PRBC to uninfected RBCs, through the complement receptor 1 (CR1) (Rowe et al., 1997). The CIDR region is implicated in the adhesion to CD36 (Smith *et al.*, 1998, Baruch *et al.*, 1997). A portion of the DBL-α domain is often used as a sequence tag to distinguish between and identify different (*var* genes) PfEMP-1 proteins (Kraemer *et al.*, 2003, Bull *et al.*, 2005).

DBL-β type domains are known to bind to Intercellular adhesion molecule 1 (ICAM-1) (Springer *et al.*, 2004, Smith *et al.*, 2000), more detail of ICAM-1 and this adhesion is discussed below. The domain architecture of a commonly used ICAM-1 binding clone, A4, which contains an ICAM-1 binding DBL-β domain is illustrated (Fig. 1.5). DBL-β

sequences are always found in tandem with a C2 domain and are usually referred to together as DBL-β.

Adhesion to chondroitin sulphate A (CSA) as implicated in placental malaria, is mediated through DBL-γ or DBL-3x domains. One *var* gene, *var2csa* implicated in adhesion to CSA (Viebig *et al.*, 2007), is unusually conserved across diverse parasite populations (Fried *et al.*, 1998, Fried & Duffy, 2002, Kraemer *et al.*, 2007). The mechanism for the selection for this PfEMP-1 variant is as yet unknown (Nunes & Scherf, 2007). This adhesion of VAR2CSA to CSA is through a DBL-3X domain (Gamain *et al.*, 2005), the structure of which has recently been solved both alone (Higgins, 2008b) and in co-crystal with CSA (Singh *et al.*, 2008).

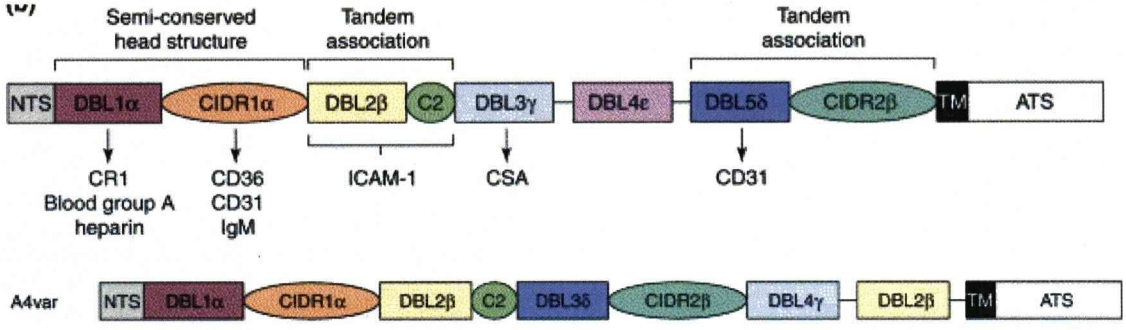

Figure 1.5. *Plasmodium falciparum* erythrocyte membrane protein 1 (PfEMP-1); protein architecture and binding domains. (Figure adapted from Smith 2001 (Smith *et al.*, 2001))

Top illustrates a schematic of possible DBL and CIDR domains that may be found in a PfEMP-1 protein. Below is illustrated the specific architecture for a known PfEMP-1 protein A4var41, from the well characterised ICAM-1 binding A4 clone. The intracellular domain ATS is highly conserved and anchors PfEMP-1 to parasite-induced knobs that facilitate infected erythrocyte sequestration. The extracellular domain is highly variable but is predominantly assembled from four building blocks: NTS, DBL, CIDR and C2 domains. Based on sequence similarity, DBL domains group as five types (α– ε) and CIDR domains as three types (α–γ) The prototypical PfEMP-1 extracellular region (a) consists of an NTS and DBL1α–CIDR1 'semiconserved head structure' followed by a DBL2δ–CIDR2 tandem. Larger PfEMP-1 proteins also include the DBLβ, γ and εtypes arrayed differently. CD36 is considered to be the major endothelial sequestration receptor; other receptors are recognized less frequently but might have important roles in disease. Abbreviation: CR1, complement receptor 1. Abbreviations: ATS, acidic terminal segment; CIDR, cysteine-rich interdomain region; DBL, Duffy-binding-like domain; ICAM-1, intracellular adhesion molecule-1; NTS, N-terminal segment; TM, transmembrane domain.

1-5 Molecular basis of Antigenic Variation

The strategy of antigenic variation is used by many pathogens as a method for evading host antibody-mediated immune defences (Lopez-Rubio *et al.*, 2007b); and parallels are often drawn between antigenic variation in African trypanosomes (*T. brucei*) and *P. falciparum* (Lopez-Rubio et al., 2007b, Borst *et al.*, 1995). As described earlier, a *P. falciparum* genome contains around 60 *var* genes. It is known that host immune responses can result in the production of antibodies targeted to PfEMP-1. Repeated exposure to *P. falciparum* infection is thought to lead to the development of partial immunity through the production of anti PfEMP-1 antibodies (Bull *et al.*, 1998). Switching of expressed PfEMP-1 to an antigenically distinct PfEMP-1 could protect the parasite from destruction and allows for propagation of infection within a host. An important aspect of antigenic variation is the regulation of the expression of *var* genes, and crucially the silencing of the non-expressed, or silent *var* genes.

Expression of *var* genes has been shown to be regulated at the level of transcription initiation (Kyes *et al.*, 2007a, Schieck *et al.*, 2007, Scherf *et al.*, 1998). Switching between expressed *var* genes occurs at this level by the turning on or off of *var* promoters. Switching rates have been estimated at up to roughly 2% per generation (Roberts *et al.*, 1992) but are thought to vary between different *var* genes, with different promoters having different "off" rates (Horrocks *et al.*, 2004). For example, centrally located *var* genes appear to have slower switching rates than telomeric *var* genes (Dzikowski *et al.*, 2007). In *T. brucei* the antigenic surface molecule is the variant surface glycoprotein (VSG), encoded for by a *vsg* gene which is located in a polycistronic, telomeric vsg expression site. Switching of *vsg* expression in *T. brucei* is complicated by the additional possibility of recombination mediated switching. As well as the possibility of switching which *vsg* expression site promoter is active, *T. brucei* often exchange *vsg* within an active expression site by recombination, or, since all *vsg* expression sites are telomerically located, telomere exchange (Aitcheson *et al.*, 2005). In contrast, switching *var* though recombination mechanisms is not thought to occur in *P. falciparum,* although high rates of recombination between *var* genes are responsible for the high sequence diversity observed between parasite populations (Kraemer et al., 2007).

There is evidence that the transcriptional silencing of inactive *var* genes is controlled by epigenetic mechanisms. Most *var* genes have 5' upstream promoter regions of one of three types, upsA, upsB and upsC which appear to be important in the control of the transcriptional silencing (Voss *et al.*, 2006). Epigenetic marks in these regions, i.e.

histone modifications are important in maintaining the transcriptional state of these promoters (Lopez-Rubio *et al.*, 2007a), although the histone marks identified may reflect a general genome wide histone modification pattern (Comeaux & Duraisingh, 2007).

Chromatin at activated *var* loci is remodelled from a transcriptionally inactive heterochromatin structure, maintenance of which requires (in some cases) the PfSir2 protein (Freitas-Junior *et al.*, 2005), to a transcriptionally competent euchromatin. Further to this chromatin remodelling requirement, the transcription of *var* loci appears to be restricted to a specific location on the nuclear periphery (Duraisingh *et al.*, 2005, Ralph *et al.*, 2005). Broad similarities can be seen with control of *vsg* expression site silencing in *T. brucei*. The involvement of chromatin remodelling factor in silencing suggests that chromatin structure may play a role in *vsg* expression site regulation (Hughes *et al.*, 2007). Similarly, restriction of transcription to a unique expression location, in *T. brucei* known as the expression site body (ESB) has been shown (Navarro & Gull, 2001).

The interesting complication of antigenic variation in *Plasmodium falciparum* is the role of the antigenic protein PfEMP-1 as the major cytoadherence ligand, whereas in *T. brucei* no other function for the major antigenically variant protein, VSG, has been established. The requirement for variation as the antigenically variant protein may complement the role for PfEMP-1 as the cytoadherence ligand. Variation of the proteins is a requirement for antigenic variation, and may result in phenotypic variation i.e. the ability to adhere to different host receptors. This is apparent in disease situation where *P. falciparum* populations expressing different variant PfEMP-1 proteins can be found sequestered in different tissues, probably through adhesion to different host receptors (Montgomery et al., 2007).

1-6 Host Adhesion Receptors

Endothelial cells can express many different adhesion molecules on the cell surface, many of which are highly glycosylated proteins which have roles in immune response, often acting as receptors for other immune cells. The expression of many receptors is increased in response to immune stimuli, including Tumor necrosis factor (TNF) which is known to be upregulated in malaria. PRBC have been shown to be able to bind to many of these receptors, and in some cases there is a link with disease phenotype, notably a link between adhesion to ICAM-1 and cerebral malaria, and CSA and placental malaria. In most cases the adhesion has been shown to be mediated by the parasite protein PfEMP-1. The variant properties of PfEMP-1 enable different variant PfEMP-1 proteins to be able to have different cytoadherent properties, resulting in a large range of adhesion receptors to which PRBC expressing different PfEMP-1 proteins can bind. Here we briefly describe some of the endothelial cell receptors involved in cytoadherence. Since most of the work presented in this thesis looks at adhesion to the receptor ICAM-1, this is discussed in detail in a separate section.

Thrombospondin (TSP)

Thrombospondin (TSP) is a large adhesive glycoprotein that is associated with endothelial cell surfaces and has binding sites for a wide range of ligands, from calcium up to glycolipids (Lawler & Hynes, 1986). TSP has been implicated in binding under both static (Roberts *et al.*, 1985) and flow conditions (Rock *et al.*, 1988). However, binding to TSP alone is not thought to be sufficient to mediate cytoadherence (Ho & White, 1999, Cooke *et al.*, 1994). The modified band three protein has been implicated in adhesion to TSP as opposed to the major adhesion ligand PfEMP-1 which is thought to be responsible for adhesion to most other identified receptors (Eda *et al.*, 1999, Lucas & Sherman, 1998).

CD36

CD36 is an important adhesion receptor that was another of the first PRBC receptors to be identified, and it has since been revealed that most *P. falciparum* isolates tested have some ability to adhere to CD36. It was initially identified since adhesion to cells could be inhibited using an antibody to an 88 kDa glycoprotein, subsequently identified as CD36 (Barnwell *et al.*, 1985, Barnwell *et al.*, 1989, Ockenhouse *et al.*, 1989). CD36 is a cell surface class B scavenger receptor with a large highly glycosylated extracellular domain, which can be found on different cell types, including microvascular endothelial cells, and platelets. The endogenous function for CD36 is as a receptor for fatty acids, TSP and collagen, and it is a phagocytic receptor for

apoptotic cells. PRBC were shown to require knobs for adhesion to CD36, and it has been shown that only more mature stages were able to adhere (Ockenhouse et al., 1989). Phosphorylation of the CD36 ectodomain is thought to be important in regulating substrate specificity. Alternative phosphorylation at this site may also play a role in regulating PRBC adhesion, with dephosphorylation of this residue required for optimal adhesion (Ho *et al.*, 2005). Furthermore, an inhibitor of this dephosphorylation reaction (Levamisole) seemed to reduce sequestration *in vivo* (Dondorp *et al.*, 2007). PRBC have also been shown to be able to bind to platelets in both static and flow conditions through binding to platelet-expressed CD36 (Cooke & Nash, 1995). This provides a mechanism for CD36 mediated binding of PRBC to endothelium devoid of CD36 using the platelets as a bridging interaction (Wassmer *et al.*, 2004).

Vascular Cell Adhesion Molecule-1 (VCAM-1)

VCAM-1 is a member of the immunoglobulin (Ig) superfamily of adhesion receptors, along with ICAM-1 and PECAM-1, and is upregulated on endothelium in response to inflammatory mediators. VCAM consists of 6 Ig domains and is predicted to form a bent rod structure protruding out from the endothelial cell surface, similar to ICAM-1. PRBC have been shown to bind to VCAM-1 although VCAM-1 binding under flow conditions may be less important than adhesion to ICAM-1 or CD36 (Ockenhouse *et al.*, 1992b, Yipp *et al.*, 2007).

Platelet/endothelial cell adhesion molecule-1 (PECAM-1/CD31)

PECAM-1/CD31 is another glycosylated member of the Ig superfamily. The protein is 130 kDa consisting of 6 extracellular Ig domains with 9 N-linked glycosylation sites. PECAM is expressed on endothelial cells and intravascular cells i.e. granulocytes, monocytes and platelets and is thought to act as a homing receptor for leukocytes to pass through junctions of endothelial cells (Newman *et al.*, 1990). The protein is normally localized to cell junctions but on stimulation with Interferon-gamma (IFN-γ) can be relocalised to all over the cell surface, increasing binding. Binding of PRBC to CD36 negative but PECAM-1 positive endothelial cells has been shown, as has adhesion to immobilized soluble PECAM-1 (Treutiger *et al.*, 1997).

Neural cell adhesion molecule (NCAM)

Recently the identification of an adhesion receptor on chicken brain tissue, suggested to be NCAM, (another member of the Ig superfamily) illustrates the increasing number of endothelial adhesion molecules known to be important for cytoadherence (Pouvelle *et al.*, 2007). Due to the nature of the PfEMP-1 variation it is possible that variants exist that can adhere to most existing endothelial cell adhesion receptors. NCAM is known

to be expressed on endothelium in two sites where sequestration is commonly observed in severe disease, skin and brain, tempting speculation that it may be an important receptor in severe disease (Pouvelle et al., 2007).

gC1qR/HABP1

Another recently identified receptor for PRBC adhesion is gC1qR/HABP1. This is a 32 kDa membrane protein that is expressed on resting endothelial cells and resting platelets, as well as other cell types. Three out of 8 field isolates tested, and two out of three lab isolates showed ability to bind to this receptor, independent of ability to bind to ICAM-1 or CD36. This receptor was also able to mediate platelet clumping (as can CD36) so may prove to be an important receptor for different types of pathogenesis (Biswas *et al.*, 2007). The existence of gC1qR/HABP1 on resting endothelium may indicate a role in adhesion early on in infection before the cytokine stimulated upregulation of other widely used receptors such as ICAM-1.

P-Selectin

Selectins are characterised by an N-terminal domain of 117 – 120 amino acids that is homologous to Ca^{2+} dependent animal lectins, and P-Selectin has been shown to be involved in PRBC cytoadherence (Udomsangpetch *et al.*, 1997). The binding site for PRBC on P-selectin is thought to be on the lectin domain but distinct from that of a natural ligand PSGL-1 (Ho *et al.*, 1998). A significant point about P-selectin is the distance from the endothelial cell surface that the molecule protrudes, this enables it to be potentially above the glycocalyx, an important consideration in leukocyte recruitment (Patel *et al.*, 1995) which may well also be relevant for PRBC adhesion. E-selectin is another member of the selectin family that has been suggested to be able to be involved in adhesion (Ockenhouse et al., 1992b).

CSA

Adhesion of PRBC to Chondroitin Sulfate A (CSA) is uniquely linked with placental adhesion in malaria in pregnancy (Scherf *et al.*, 2001). Malaria in pregnancy is associated with an increased risk of maternal anaemia, and a low birth weight. Adhesion to CSA has been shown to be a firm adhesion with little rolling interaction, and is able to withstand high shear stress levels (Rogerson *et al.*, 1995, Cooke *et al.*, 1996). Adhesion to CSA has been shown to be mediated by PfEMP-1 (Reeder *et al.*, 1999), and interestingly the PfEMP-1 variant known to be able to adhere to CSA is unusually conserved between different parasite isolates (Fried et al., 1998, Fried & Duffy, 2002, Kraemer et al., 2007).

Cytoadherence to multiple receptors

Cytoadherence under flow conditions is thought to involve multiple adhesion receptors acting cooperatively, shown with CD36, ICAM-1 and P-Selectin (McCormick *et al.*, 1997, Gray *et al.*, 2003, Yipp et al., 2007). A model has been widely proposed where PRBC are captured from flow by one receptor, roll along endothelial cells before firm adhesion, possibly being mediated by a different receptor. This may separate out roles for difference receptor families, where a selectin (i.e. P-selectin) or Ig superfamily receptor (i.e. ICAM-1) may be required to capture PRBC from flow followed by firm adhesion to a different class of receptor i.e. CD36. Firm adhesion may also require or be enhanced by interactions with more than one receptor concurrently (i.e. ICAM-1 and CD36).

1-7 ICAM-1

Adhesion to ICAM-1 has been suggested to be linked with cerebral malaria as post mortem studies showing increased parasite sequestration in the brain of patients diagnosed with severe malaria also showed increased ICAM-1 expression (Turner *et al.*, 1994, Newbold *et al.*, 1997),. Isolates from patients have also shown the ability to adhere *in vitro* to ICAM-1. Most of the work presented in this thesis looks at aspects of cytoadherence to ICAM-1. This is due to interest in this interaction because of the link with cerebral malaria (Chakravorty & Craig, 2005), but also due to the availability of well characterised parasite isolates with known adhesive properties to ICAM-1, and endothelial cells that are known to express ICAM-1.

ICAM-1 is an endothelial cell adhesion receptor that is involved in leukocyte recruitment through the Lymphocyte function-associated antigen-1 (LFA-1). The receptor also has a binding site for rhinovirus (Staunton *et al.*, 1990). ICAM-1 protein expression on many types of endothelium can be stimulated by cytokines including TNF and IL-1; and PRBC have been shown to increase ICAM-1 levels through *Plasmodium* glycosylphosphatidylinositol anchor (GPI) (Schofield *et al.*, 1996) – or directly through adhesion (Tripathi *et al.*, 2006). ICAM-1 consists of 5 Ig domains and is predicted to have a "bent rod" structure (Staunton et al., 1990). Homodimers are formed on the surface of cells with interactions of the transmembrane domain and Ig domain 4 (towards the C terminal, membrane end of the molecule), as well as a weaker interface between domains 1. It is possible that the interactions between transmembrane domains, and the domain 4 interactions allow for dimerisation, and domain 1 interactions allow for multimerisation on the surface (Fig. 1.6) (Yang *et al.*, 2004).

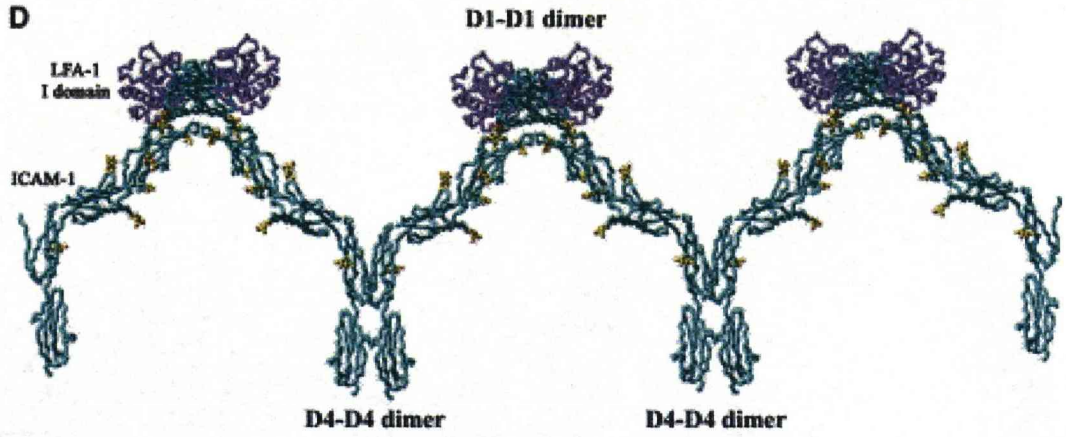

Figure 1.6. ICAM-1 mutimerisation and dimerisation. Figure taken from Yang 2004 (Yang et al., 2004) Illustration of dimerisation of ICAM-1 through D4 and potential multimerisation through D1, the LFA-binding domain.

The binding site for Lymphocyte function-associated antigen-1 (LFA-1, also known as CD11a/CD18, or αLβ2), rhinovirus and *P. falciparum* are on the most N terminal of 5 the Ig domains in ICAM-1 (D1), with the binding site for *P. falciparum* probably distinct but overlapping that of LFA-1 or rhinovirus (Berendt *et al.*, 1992). LFA-1 is an abundant and widely expressed beta2-integrin and is required for many cellular adhesive interactions during the immune response including the adhesion of leukocytes to endothelial cells prior to transmigration through endothelial layers following interaction with ICAM-1. The integrin Mac-1 (also known as αMβ2 or CD11b/CD18) is associated with monocyte adhesion to endothelium and is known to bind to ICAM-1 on domain 3 (Diamond *et al.*, 1991).

Extensive mutagenesis studies have mapped the *P. falciparum* binding site to a region comprising three beta sheet strands known as the BED region of D1 (Tse *et al.*, 2004). Figure 1.7a illustrates the location of residues which when mutated lead to a significant reduction in the adhesion of ItG PRBC to ICAM-1, under both static and flow conditions, as determined by Tse et al (Tse et al., 2004). This work also showed that different PRBC isolates had slightly different binding sites. As illustrated in figure 1.7b, two mutations are used to characterise between the adhesion of two parasite isolates, A4 and ItG. A mutation of K29, as found in the ICAM-1 variant ICAM-1 Kilifi (red residue in figure 1.7b) results in reduced adhesion of A4 PRBC, whereas no effect on ItG PRBC adhesion is seen. Mutation of S22 (purple residue in figure 1.7b) results in loss of ItG PRBC adhesion but does not affect A4 binding. However, the monoclonal antibody mAb 15.2 is known to block adhesion of all tested PRBC isolates, the epitope of mAb 15.2 adhesion involves L42 (blue residue in fig 1.7b).

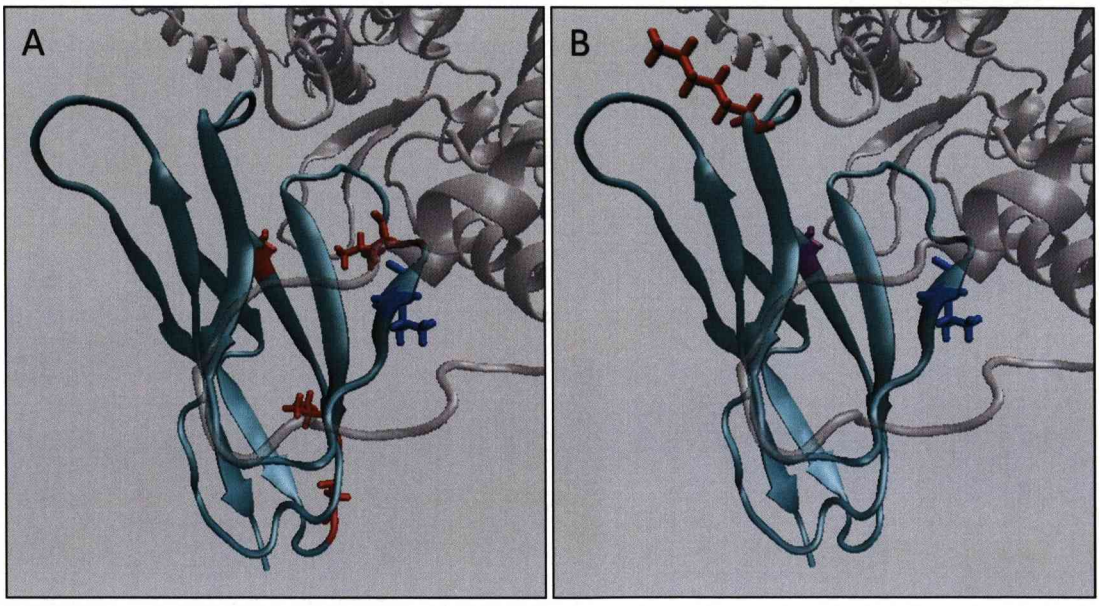

Figure 1.7. Domain 1 of ICAM-1. Domain 1 of ICAM-1 (light blue) shown with part of modelled PfEMP-1 (translucent grey), Model PM0074932 (Bertonati 2007) (Bertonati & Tramontano, 2007) see below. Annotated using VMD. Highlighted residues in A are residues implicated in adhesion of ItG PRBC to ICAM-1 in both static and flow conditions as determined by mutagenesis in (Tse et al., 2004). Highlighted resides in B are: Red - K29 implicated in adhesion of A4 PRBC to ICAM-1; Purple – S22 implicated in adhesion of ItG PRBC to ICAM-1 and Blue L42 implicated in adhesion of general blocking antibody mAb 15.2 to ICAM-1. Orientation of ICAM-1 D1 is shown as in (Tse et al., 2004).

ICAM-1 is known to form homodimers, mainly due to contacts between domain 4 of the protein, but also some interactions at domain 3, and possibly the transmembrane domain. The BED region of D1 is also thought to be involved in dimerisation contacts through weaker polar interactions of side chains. This may be involved in the multimerisation seen on ICAM-1 clustering during activation (Fig. 1.6). If there is a protein-protein interaction interface using this BED region of D1 this puts the binding site for PfEMP-1 in a groove formed between two D1 domains. Figure 1.8 illustrates the residues shown to be involved in a) PfEMP-1 adhesion, and b) dimerisation interface (Casasnovas *et al.*, 1998, Jun *et al.*, 2001a, Jun *et al.*, 2001b), mapped onto a second possibility for PfEMP-1 adhesion as predicted by computation modelling. This recent *in silico* molecular modelling of the interaction suggests that *P. falciparum* could bind slightly further toward the end rather than in the groove of D1 (Fig. 1.8) (Bertonati & Tramontano, 2007).

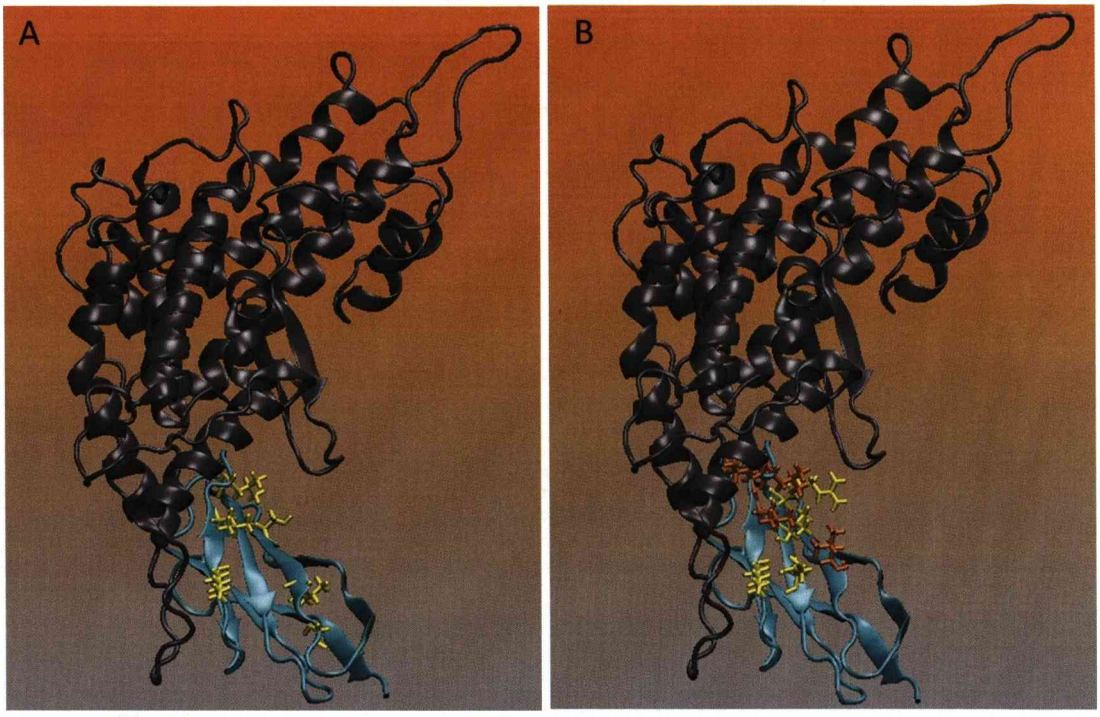

Figure 1.8. Modelled PfEMP-1 bound to ICAM-1. "PfEMP-1" (Grey) bound to ICAM-1 domain 1 (Blue) indicating residues involved in A) cytoadherence and B) D1 dimerisation. Model PM0074932 (Bertonati 2007 (Bertonati & Tramontano, 2007)) annotated using VMD. A) Resides implicated in cytoadherence as in Tse 2003 marked in yellow. B) Resides involved in D1 dimerisation interface in yellow (Casasnovas 1998) and Orange (Jun 2001). ICAM-1 orientation showing BED β sheets facing upwards.

Mutagenesis studies (Tse et al., 2004) showed that different ICAM-1 binding variants appeared to have different binding sites but the modelled interaction was made using a consensus of known binding sequences. Inaccuracies in this model may also occur as the PfEMP-1 DBL-β domain is a modelled structure on a non-PfEMP-1 DBL domain (EBA 175), furthermore modelling of protein-protein interactions is not accurate. Attempts to create a crystal structure of an ICAM-1 binding PfEMP-1 DBL domain are currently in progress (Higgins MK); and the structure of a CSA binding PfEMP-1 DBL domain (DBL-3X) has recently been solved both alone (Higgins, 2008b) and in complex with CSA (Singh et al., 2008). This structure suggests the involvement of conformation changes to the DBL domain on binding such that a hinge region may fold over to create the binding contacts. A co-crystal structure of the DBL-β domain from PfEMP-1 bound to ICAM-1 is essential to resolve the exact DBL-β:ICAM-1 binding mechanism. However, there will still be the limitation that different DBL-β domains may bind differently, and there may be differences in adhesion mechanisms under static and flow conditions. Further knowledge of the detail of the interaction between PfEMP-1 DBL-β domains and ICAM-1 may enable development of targeted anti-adhesion adjunct therapies, as discussed in chapter 6.

1-8 Cytoadherence – Post Adhesion events

PRBC adhesion to endothelial cells may result in damage to the endothelial layer, potentially contributing to pathogenesis. An important consequence of adhesion to host endothelium is the induction of signalling events within endothelial cells (Chakravorty *et al.*, 2008). Signalling pathways in mammalian cells are complex, with many interacting pathways present. In brief, signalling pathways in cells are commonly activated by ligation of adhesion receptors on the cell surface. Adhesion of ligand to the extracellular domains of a receptor can lead to intracellular events, often initiated by phosphorylation events on, or by a cytoplasmic tail of the receptor. Signalling through ICAM-1 results from adhesion of ligands to the extracellular domains of ICAM-1, mainly using binding sites on domain 1. This results in clustering and multimerisation of ICAM-1 on the cell surface (Yang et al., 2004), and signalling requiring the small C terminal cytoplasmic domain (Greenwood *et al.*, 2003). A series of intracellular phosphorylation events, often through MAP kinase signalling cascades can result in nuclear translocation of transcription factors, and activation of transcription of target genes.

It has been shown that MAP kinase signalling pathways, including ERK, JNK and P38 pathways are activated on adhesion of PRBC to ICAM-1 (Jenkins *et al.*, 2007a). Activation of such pathways may result in translocation of transcription factors, i.e. NF-kB to the nucleus (Tripathi et al., 2006) and activation of transcription of many targets. These targets may include adhesion molecules such as ICAM-1. In this way adhesion of PRBC may itself induce increased ICAM-1 expression, leading to greater adhesion. This ability of PRBC to induce ICAM-1 levels has been shown on human brain endothelial cells (HBEC) and also on human umbilical vein endothelial cells (HUVEC) where there was a requirement for very low levels of TNF (Tripathi et al., 2006, Chakravorty *et al.*, 2007).

Another widely discussed consequence of adhesion to endothelial cells is the induction of apoptosis in the endothelial cells. There are three ways in which endothelial cell apoptosis may be stimulated in malaria. It has been shown that soluble parasite derived factors can induce apoptosis in endothelial cells (Wilson *et al.*, 2008). Host derived inflammatory factors present in malaria may influence apoptosis (Combes *et al.*, 2006, Wassmer *et al.*, 2006a, Wassmer *et al.*, 2006b, Hemmer *et al.*, 2005), and there is also evidence suggesting that cytoadherence of PRBC can directly induce apoptosis. All published data showing *in vitro* evidence for cytoadherence-induced apoptosis is based on assays using human lung endothelial cells (Toure *et al.*, 2008,

Pino *et al.*, 2003, Siau *et al.*, 2007). However, it has been suggested that there is upregulation of pathways protective against apoptosis following cytoadherence in some endothelial cell types, i.e. HUVEC (Chakravorty et al., 2007). These differences may reflect differences between endothelial cell types, or illustrate that endothelial cell responses may include activation of a range of signalling pathways, the balance of which may result in either apoptosis, or cellular protection.

1-9 Studying Cytoadherence

Assay Types

Adhesion to endothelial receptors has been assayed *in vitro* in various ways. To assay binding under static conditions protein can be immobilised on a plastic Petri dish, or endothelial cells grown on cover slips. Assays are also carried out under flow conditions, to either immobilised protein or to endothelial cell lines. Flow assays can be carried out using microslides or parallel plate chambers, and are set up to enable a defined physiologically relevant wall shear stress to be created (Cooke et al., 1994). Although animal models of malaria cannot be used for adhesion studies a skin-graft technique has been used where human skin tissue has been grafted onto mice to allow an interesting way to assess cytoadherence *in vivo* (Yipp *et al.*, 2003b). Microfluidics systems have recently been developed that mimic adhesion under both physiologically relevant shear stress and the diameter constriction of narrow vessels (Antia *et al.*, 2007).

Adhesion of PRBC under flow conditions is a more complicated process than static adhesion. Binding mimics that of leukocyte recruitment in that PRBC first have to be captured from flow, often seen as a rolling interaction that occurs along endothelial cells before firm adhesion results. The microfluidics system showed that the rolling interaction was abolished while PRBC traversed a narrow constriction, however, quickly restarted when the channel opened out again. This could be due to the increased shear stress in these constrictions, or physical constraints reducing the interaction between receptor and ligand (Antia et al., 2007).

In this thesis we investigate cytoadherence using static and flow adhesion assays to both endothelial cells and protein.

Parasite Isolates

As described earlier, different PRBC isolates have different cytoadherent characteristics, and by the process of antigenic variation an isolate can change cytoadherent phenotypes by switching of expressed PfEMP-1. In order for comparable results between experiments, PRBC isolates expressing known PfEMP-1 proteins are often used in the study of cytoadherence, and these are regularly maintained by selection for the expected PfEMP-1 expression. For the study of ICAM-1 cytoadherence parasite isolates of the IT lineage are often used. A series of three isogenic isolates with different ICAM-1 avidity are available, ItG (Ockenhouse *et al.*, 1992a) A4 and C24 (Roberts et al., 1992). Of the three, ItG shows the highest levels of

adhesion to ICAM-1, A4 shows moderate levels of adhesion, and C24 shows little or no adhesion to ICAM-1. However, all three bind to CD36. These three were derived by cloning and selection procedures from a single original isolate (Roberts et al., 1992). A fourth isolate often used for ICAM-1 cytoadherence studies is JDP8 (Chattopadhyay *et al.*, 2004), which is known to have a very high ICAM-1 adhesion phenotype but unusually low adhesion to CD36. These isolates are all able to bind to ICAM-1 under both static and flow conditions (Tse et al., 2004, Gray et al., 2003).

Most of the work presented in this thesis uses the parasite isolates ItG and A4, although JDP8, C24 and a recent patient isolate (unpublished) are also used in some experiments.

Endothelial Cells

Primary human endothelial cells can be grown *in vitro* and are often used as models for PRBC adhesion. Primary cells from various sources have been used in the study of PRBC cytoadherence, including human umbilical vein endothelial cells (HUVEC), human dermal microvascular endothelial cells (HDMEC), human pulmonary vein (Lung) endothelial cells (HLEC). All of these cells can be purchased from a commercial supplier (such as Promocell) as pooled batches, and all are routinely assessed by the manufacturers for expression of endothelial cell markers, such as presence of Von Willebrand factor (VWF) (Promocell).

All types of cell mentioned have very low basal expression levels of many endothelial cell receptors in culture conditions, as expected from resting endothelial cells. However, as with the *in vivo* situation, adhesion receptors such as ICAM-1 can be stimulated by the addition of inflammatory cytokines, such as TNF. HUVEC do not express the common receptor CD36, a similar characteristic to brain endothelial cells, and these are often used as a model for ICAM-1 mediated adhesion, without the complication of additional CD36 adhesion. HDMEC and HLEC express CD36 as well as ICAM-1 (after TNF stimulation) making them a useful model for analysis of more complex adhesion phenotypes. Other endothelial cell lines are available, including transformed brain endothelial cells, HBEC (Tripathi et al., 2006, Tripathi *et al.*, 2007) . Similarly to HUVEC, these do not express CD36, and ICAM-1 expression can be stimulated by addition of TNF. While a useful model for cerebral malaria, these cells are transformed therefore one step further away from a physiologically relevant model.

Most of the work presented in this thesis uses HUVEC and HDMEC, although HLEC and HBEC are also used in some experiments.

1-10 Malaria – Severe Disease

Malaria is a complicated disease with possible symptoms that range from asymptomatic parasitaemia, through mild febrile illness to severe disease that may result in death. Clinical symptoms of severe disease include severe malarial anaemia (SMA), respiratory complications (including pulmonary oedema), multi-organ failure, and the coma of cerebral malaria. Many of the disease symptoms may result from general host inflammatory responses to the parasite. As an inflammatory disease malaria results in increased levels of many host cytokines, including TNF, IL-1, IL-6, and TGF-β. Increased levels of host pyrogens, such as TNF, are thought to be responsible for induction of fever in patients, an almost universal symptom of malaria that is discussed in more detail below.

Other factors that contribute to severe disease are related to the parasite induced changes to the red blood cell. Resulting increased rigidity of RBC may be linked to disease severity (Dondorp *et al.*, 1997), as could the ability of PRBC to adhere to uninfected RBC, rosetting (Rowe *et al.*, 1995). Both phenotypes may contribute to microcirculatory dysfunction resulting in complications due to hypoxia. Cytoadherence to endothelium, and post-adhesive changes to endothelium are thought to be a major contributor to the pathophysiology of disease. We will specifically discuss the example of cerebral malaria which has been suggested to result from adhesion of PRBC to cerebral microvasculature (Turner *et al.*, 1994, Newbold *et al.*, 1997), and is responsible for significant numbers of deaths particularly of children in Africa.

A link between sequestration in the brain and cerebral malaria has been shown; examination of post mortem sections of the brain has revealed significant PRBC sequestration in cerebral vasculature of patients dying from cerebral malaria compared with other types of malaria. Furthermore, this has been linked specifically with ICAM-1 upregulation and the ability of PRBC isolates to adhere to ICAM-1 (Turner et al., 1994, Newbold et al., 1997). Although there is no evidence for widespread endothelial damage even in cerebral malaria, there are often observed small ring haemorrhages indicative of some damage resulting in leakage of blood through the endothelial layer. The endothelial layer in the brain is a unique layer with tight junctions between endothelial cells.

Disruption of the blood brain barrier (BBB) is hypothesised to be responsible for many of the symptoms of cerebral malaria, including coma. As illustrated in figure 1.9 (Medana & Turner, 2006), possible damage to the blood brain barrier could have

several causes. Some of these are not directly related to cytoadherence, for example the release of cytokines by leukocytes stimulated by release of malaria toxins on RBC rupture. However, this could be more significant where a large mass of PRBC are present in a small area due to sequestration, concentrating the malaria toxins locally. Altered blood flow resulting in hypoxia could be contributed to by the increased rigidity of PRBC, and PRBC rosetting and clumping. Again, microvascular obstruction due to cytoadherence is likely to play an important role. There are also likely to be direct effects of cytoadherence playing a role in potential damage to BBB. As discussed earlier, cytoadherence has been shown to directly lead to signalling events within endothelial cells. The consequences of these signalling events could lead to increased junctional permeability (Fig. 1.9 (Medana & Turner, 2006, Tripathi et al., 2007)).

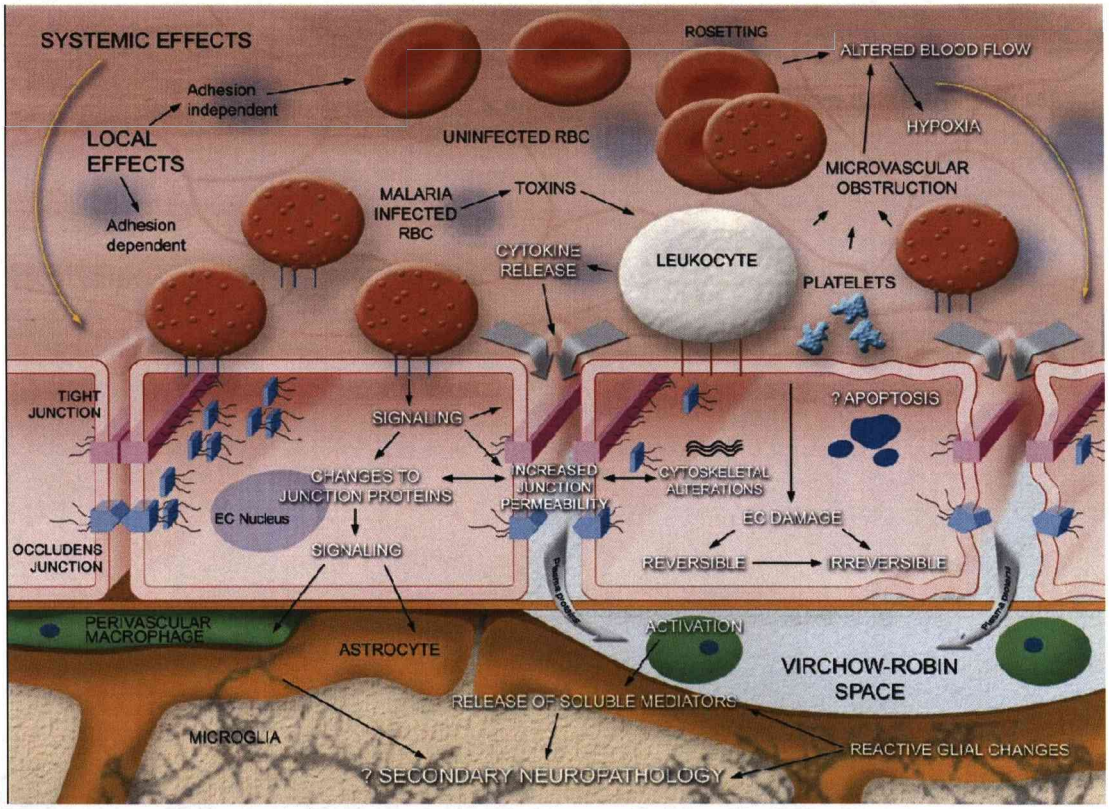

Figure 1.9. The blood–brain barrier (BBB) in malaria. (Figure taken from Medana 2006 (Medana & Turner, 2006)). The diagram shows a schematic representation of the structures forming the BBB, the events occurring during malaria and some of the possible mechanisms that may influence function of the BBB during cerebral malaria (CM). The key structural elements of the BBB include cerebral endothelial cells (EC), with specialised tight junctional complexes regulating the permeability of the paracellular space. Pathological changes to BBB structure, and therefore function, may be broadly divided into 'distant' effects of severe disease, such as acidosis or hypoxia due to anaemia, and local factors acting in the brain. Both may involve cell adhesion-dependent and non-adhesion-dependent pathways. Adhesion to the EC by parasitised red blood cells (PRBC), host leukocytes or platelet-fibrin thrombi, the influence of cytokines or parasite toxins such as pigment may also cause direct cellular damage. These events may initiate signalling within EC that could influence junctional protein expression, and also directly activate perivascular and parenchymal effector cells.

1-11 Antimalarial Treatment

Malaria is a treatable disease, and many anti-malarial drugs are available that kill parasites. However, an emerging problem is that of parasite resistance to many currently used antimalarials. This is particularly a problem with resistance to chloroquine and sulfadoxine-pyrimethamine (SP) mainly seen in SE Asia, however also increasingly a problem throughout Africa (WHO). Resistance to chloroquine and SP has prompted a move to alternative new treatments, particularly artemisinin based combination therapies (ACT). ACTs combine an artemisinin derivative with a partner drug. Here, we briefly introduce artemisinin, along with two of the partner drugs, lumefantrine and piperaquine. Lumefantrine is used in conjunction with the artemisinin derivative artemether, a formulation marketed as "Coartem". Piperaquine is marketed in formulation with dihydroartemisinin as "Artekin". These are compared with traditional quinine, which is used as a first line therapy for severe malaria in many areas.

It is known that all of these treatments are effective on parasites, killing them rapidly, although as described there are different stage-specificities of each treatment, as well as differences in pharmacodynamic properties. However, little is known about the effect of these treatments specifically on cytoadherence. It has been suggested that after treatment with antimalarials PRBC can still cytoadhere to endothelium, however this has not been shown directly. This question will be addressed in this thesis where, in chapter 3, we investigate cytoadherence of PRBC after treatment with these selected antimalarials.

Quinine

Like many antimalarial drugs, including commonly used chloroquine, quinine works by inhibiting haem metabolism by the parasite. The build up of toxic waste products as a result of haemoglobin breakdown is lethal for the parasite. A consequence of this mechanism of action is that the drug is only effective against later stages of parasites, when haem build up reaches toxic levels.

Artemisinins

Artemisinin is derived from the Chinese wormwood plant (*Artemisia annua*) and has been known about as a cure for fever for centuries. Semi-synthetic derivatives of this; artesunate, artemether and dihydroartemisinin are all rapidly acting and effective antimalarials; however, the drugs have a short half life. This short half life increases potential for recrudescence and increases risk of emergence of resistance so

artemisinins are used in combination with a longer lasting partner drug, i.e. piperaquine or lumefantrine.

Antimalarial activity of artemisinins is dependent on an endoperoxide bridge structure and is thought to require the addition of iron or haem. Artemisinin acts rapidly on parasites. After a short time lag of 1 – 4 hours the effect on parasite metabolism is rapid. A similar delay is seen with other drugs i.e. quinine, however killing activity is then slower (ter Kuile *et al.*, 1993). Artemisinins are known to act on young ring stage parasites whereas other treatments, quinine particularly, only acts on mature trophozoites (Skinner *et al.*, 1996). Artesunate (art) and artemether are both hydrolysed *in vivo* to dihydroartemisinin, which is an effective treatment in its own right. The activity of these three different artemisinin derivatives has been shown to be similar (Price *et al.*, 1998).

It has been hypothesised that an advantage of artemisinin based treatments may be the prevention of development of ring stage PRBC to cytoadherent trophozoite stages (Checkley & Whitty, 2007). This was suggested to potentially play a role in the slight advantage of artesunate over quinine that was observed in some groups in a large study, the South East Asian quinine artesunate malaria trial (SEAQUAMAT) (Dondorp *et al.*, 2005). This is discussed in more detail in chapter 3.

Piperaquine

Piperaquine is a 4-aminoquinoline, like chloroquine. However piperaquine is a bisquinoline with two rings, this larger structure is possibly important in reducing resistance to piperaquine. One of the proposed resistance mechanisms to chloroquine involves a transporter, *Plasmodium falciparum* chloroquine resistance transporter (PfCRT) located in the parasite food vacuole (Bray *et al.*, 2005). The transporter may be inhibited by the larger size of the piperaquine molecule. Hence there is limited evidence of cross resistance with chloroquine despite the shared mechanism of action. A by-product of haemoglobin metabolism by the parasite is the toxic molecule haem, which must be rendered harmless by the parasite by conversion to haemozoin crystals (malaria pigment). 4-aminoquinoline drugs work by interfering with this haem metabolism (Davis *et al.*, 2005).

Lumefantrine

Lumefantrine (previously known as Benflumetol) is in the amino alcohol group of antimalarials which includes quinine, mefloquine, and halofantrine. In vitro sensitivity assays suggest no cross-resistance with chloroquine however cross resistance is

possible with mefloquine and halofantrine due to the predicted similar mechanism of action. This is based on a shared hydroxyl group near the ring structure which has been predicted to be crucial for their antimalarial activity (Basco *et al.*, 1998). The antimalarial property is probably a result of interference with haem metabolism. The oral availability of both piperaquine and lumefantrine is increased by addition of fat (Winstanley & Ward, 2006).

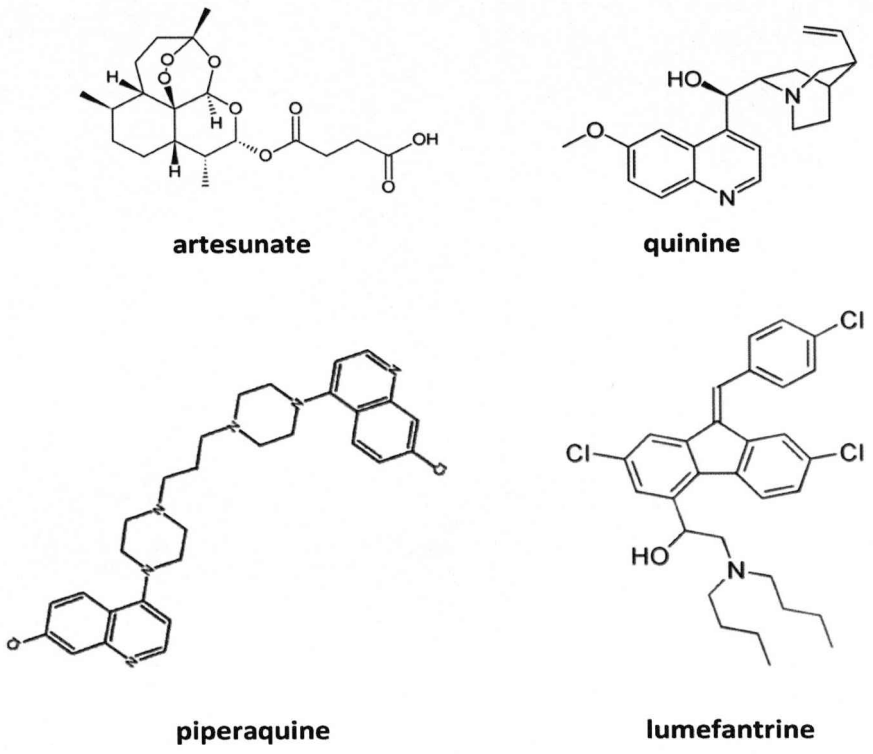

Figure 1.10. Structures of selected antimalarials

1-12 Fever

Fever is induced in *P. falciparum* malaria by factors released on schizont rupture. In a synchronous population of parasites schizont rupture will occur simultaneously giving rise to the classically expected peaks of fever every 48 hours. Fever is thought to be caused by the host pyrogen TNF (Kwiatkowski *et al.*, 1997), production of which is induced by the malarial GPI molecule that is released on schizont rupture (Schofield & Hackett, 1993).

The classic expected pattern for fever in malaria is peaks of fever induced on schizont rupture every 48 hours (WHO). However, in acute infections more commonly observed is a more irregular generally raised temperature (Fig. 1.11) (Peters, 1995).

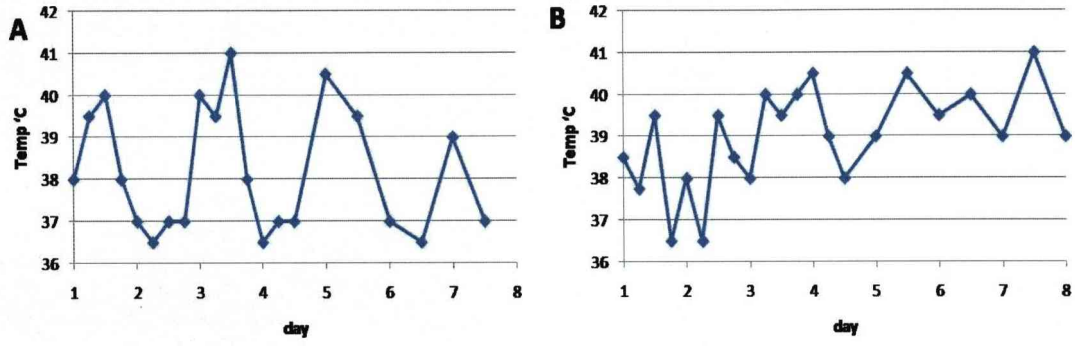

Figure 1.11. Schematic of possible expected patterns of fever in malaria. A) classic expected pattern of fever peaks every 48 hours each lasting around 12 hours (WHO) and B) more commonly observed in acute infections a general irregular raised temperature (Peters, 1995).

Antipyretic (fever-reducing) treatment is standard adjunct therapy for malaria (Winstanley & Ward, 2006), however, studies assessing the effects of antipyretic treatment on disease have not shown evidence for an advantage of giving antipyretic treatment in terms of parasite clearance time or disease outcome (Meremikwu *et al.*, 2000). In one study paracetamol led to a significantly increased time to parasite clearance when compared to mechanical antipyresis alone. (Brandts *et al.*, 1997). Similar results were seen with other antipyretics metamizol and naproxen, where a slight difference in parasite clearance time was observed but this could not be linked to any significant difference in fever reduction compared to controls (Lell *et al.*, 2001). Furthermore, although anti-TNF therapy has been shown to have a significant effect on decreasing fever in cerebral malaria no beneficial effect on disease could be detected (Kwiatkowski *et al.*, 1993).

Some studies have looked at the effect of fever on parasite growth, however almost all cytoadherence studies are carried out at 37°C. One published study assessed the effect of incubation of PRBC at febrile temperatures on subsequent cytoadherence (Udomsangpetch *et al.*, 2002), but no studies report the effect of endothelial cell exposure to febrile temperatures on cytoadherence. There are some studies showing effects of febrile temperatures on endothelial cell characteristics that may be relevant to cytoadherence. However, it is clear that endothelial cell responses may vary depending on cell type and exact conditions used, and it is unclear what the resulting effect on cytoadherence may be. In chapter 5 we specifically address the question of how endothelial cells may respond to febrile temperatures in terms of the ability of PRBC to adhere.

Effect of fever on Parasites

Febrile temperatures have been shown to affect the intra-erythrocytic growth of *P. falciparum* parasites; growth of parasites is generally reduced on exposure to febrile temperatures (~40°C) (Oakley *et al.*, 2007, Kwiatkowski, 1989). Mature parasites (trophozoites in the second half of the 48 hour maturation cycle) appear to be sensitive to increased temperature and may be killed by heat exposure. However, the viability of young ring stage parasites is not reduced by increased temperature, and the growth and development of this stage may even be more rapid at fever range temperatures (Long *et al.*, 2001, Kwiatkowski, 1989, Pavithra *et al.*, 2004). This difference in sensitivity to febrile temperatures of different stages may play a role in increasing the synchronicity of cultures. Febrile episodes in malaria are classically linked with schizont rupture at the end of the 48 hour cycle. The increased resistance of young ring-stage parasites, or even enhanced growth of this stage could increase survival of young ring stage parasites while reducing viability of remaining mature parasites which could result in synchronisation of cultures (Kwiatkowski, 1989, Gravenor & Kwiatkowski, 1998).

A large microarray study has assessed the effects of febrile temperature on expression of parasite genes. Oakley *et.* al. (Oakley et al., 2007) showed up-regulation of a wide array of transcripts after exposure to febrile temperatures (41°C), including families involved in protein stability, i.e. heat shock proteins and other chaperones. Ubiquitination of proteins was reduced, correlating with the reduced expression levels of ubiquitinating enzymes. The up-regulation of several exported parasite proteins potentially involved in parasite sequestration, including *var* and *rif* genes was observed. This might be due to the fact that preferential increased expression of subtelomeric genes was observed – possibly reflecting increased sensitivity of chromatin structure at

chromosome ends to the higher temperatures. Several genes involved in chromatin structure were upregulated, including Pf*Sir2*.

Effect of Fever on Cytoadherence

Exposure of parasites to fever range temperatures has been reported to increase cytoadherence (Udomsangpetch et al., 2002). Binding normally occurs at mature trophozoite-stage, however, exposure to higher temperatures enabled binding slightly (around 2 h) earlier than parasites maintained at 37°C. Some increase in binding of mature trophozoite stage parasites to receptors at higher temperatures was also seen which appeared to correlate with an increased expression of PfEMP-1 on the surface of parasites. However, this up-regulation of PfEMP-1 was not seen in a separate study (Oakley et al., 2007), where an up-regulation of other *var* gene transcripts was reported and hypothesised to increase chances of parasite sequestration.

Effect of fever and heat shock on endothelial cells

Different subsets of endothelial cells vary in many ways, including in their adhesion receptor expression profile. It is also possible that they differ in their response to febrile temperature. While there is a clear effect of febrile temperatures on High Endothelial Venule cells, (HEV), the effect on other endothelial cell lines is less apparent. HEV are reported to be stimulated by febrile temperatures to increase ICAM-1 expression through IL-1. This leads to increased binding and migration of leukocytes (Chen *et al.*, 2006).

It is possible that cells respond differently to heat shock temperature (>~42°C for short periods) as opposed to febrile range temperatures (~38°C – ~41°C), or "mild heat stress". The responses to different conditions have been described as "distinct but partially overlapping processes" (Hasday & Singh, 2000). While the upregulation of heat shock proteins through HSF-1 activation (see below) occurs in both cases, there are differences. Many of the responses to heat shock, or "severe heat stress" result in cell morbidity, whereas responses to "mild heat stress" lead to adaptation of growth conditions to enhance survival (table 1) (Park *et al.*, 2005).

	Mild heat stress	Severe heat stress
Denaturation of		
nascent polypeptides	+	+
pre-existing proteins	–	+
HSF1 activation	+ (Rac1 dependent)	++ (Rac1 independent)
HSP synthesis	+ (Rac1 dependent)	++ (Rac1 independent)
Cell cycle arrest		
p21	–	G1/S and G2/M arrest
Cell proliferation	+/– (depending on cell types)	–
cyclin D1	+	↓
cyclin A	+	–
Differentiation	+/– (depending on cell types)	–
Apoptosis	–	+
Acquisition of thermotolerance	+	+
Signaling pathways		
Ras/Rac 1	+	–
PI3K-AKT	+	–
ERK1/2	+	+
SAPK/JNK	+	+
p38MAPK	+	+
Biological relevance	adaptation of growth conditions	cell death or cell morbidity

Table 1. Comparison of cellular responses to mild and severe heat stress, (Taken from Park 2001)

Heat shock temperatures (> 42°C) for short periods of time have been suggested to increase ICAM-1 levels in the macrovascular endothelial cell line HUVEC (Lefor *et al.*, 1994). However, a recent study using Human Aortic endothelial cells showed reduced stimulation of adhesion molecule expression (E-Selectin and VCAM-1) after TNF stimulation following heat shock (42°C for 1 hour). This was shown to be due to reduced NF-κB signalling pathway response in cells exposed to the heat shock (Nakabe *et al.*, 2007). A separate study (Kohn *et al.*, 2002) also sees reduced ICAM-1 stimulation in response to TNF after heat shock treatment.

Exposure of endothelial cells to lower, fever-range temperatures (39°C – 41°C as opposed to heat shock temperatures of > 42°C) has been reported to show more subtle effects. Expression of various adhesion receptors (including ICAM-1) in HUVEC was not increased after 40°C incubation for 12 hours, and cytokine expression was not affected (Shah *et al.*, 2002). A slightly altered response to TNF was seen in pulmonary artery endothelial cells. A small reduction in adhesion of neutrophils was suggested after incubation at 39.5°C compared to 37°C after TNF stimulation, along with a slight reduction in barrier function (Hasday *et al.*, 2001). Although no effect on the levels of cell surface ICAM-1 has been shown in HUVEC, exposure to febrile temperatures has been shown to slightly increase levels of soluble adhesion receptors. The levels of soluble ICAM-1, PECAM-1 and E-Selectin were slightly increased after TNF stimulation after fever (Gnant *et al.*, 2000).

Heat Shock Response Pathway

The heat shock response pathway is a stress response activated in mammalian cells in response to environmental stresses – including heat shock (temperature of >42°C) (Morimoto, 1998). Environmental stresses result in the activation of production of a number of heat shock proteins (HSPs) including HSP70. These HSPs are well conserved across species and many family members function as chaperones involved in protein folding (Lindquist & Craig, 1988, Hartl, 1996). The transcription factor Heat Shock Transcription Factor 1 (HSF-1) is responsible for the increased transcription of these HSPs. HSF-1 is thought to be maintained in an inactive state through interactions with HSP90. On exposure to heat shock, HSP90 dissociates from HSF-1 allowing HSF-1 to trimerise and autophosphorylate into an active DNA-binding form which can bind to heat shock elements (HSE) upstream of target genes (i.e. *HSP*s) (Morimoto, 1998) (Fig. 1.12 (Powers & Workman, 2007)). Although it was thought that inactive HSF-1 was mainly cytoplasmic, it has now been shown that in many mammalian cells HSF-1 appears to be predominantly localised to the nucleus even in the absence of stress (Mercier *et al.*, 1999). However, on activation HSF-1 appears to redistribute from a general nuclear localisation to localise to nuclear stress granules (Jolly *et al.*, 1999, Nonaka *et al.*, 2003). Similarly, in our HUVEC endothelial cells HSF-1 appears predominantly nuclear localised, with a granular distribution becoming apparent on exposure to heat shock.

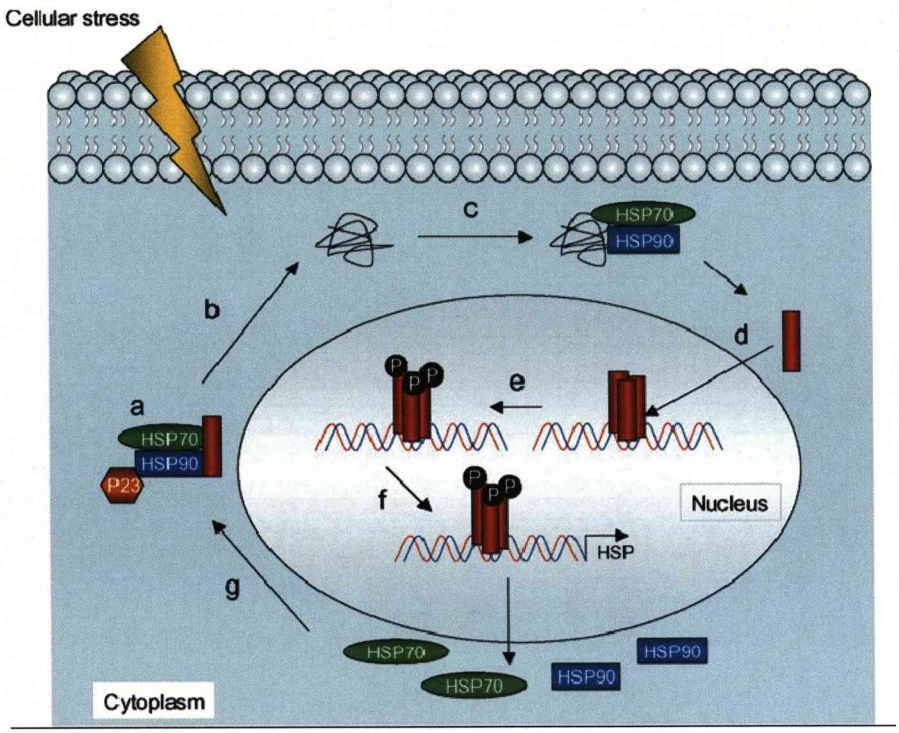

Figure 1.12. Activation and modulation of HSF-1 (Figure taken from Powers 2007 (Powers & Workman, 2007)) transcriptional activity (a) Under normal conditions HSF-1 exists as a monomer held in a repressed state by an interaction with HSP90 and HSP70. (b) Cellular stress causes an increase in denatured proteins (c) which leads to the dissociation of HSP90 and HSP70 from HSF-1. (d) Monomeric HSF-1 is then free to trimerize, translocate to the nucleus and (e) undergo a series of post-translational phosphorylation events. (f) HSF-1 activates the transcription of a number of HSP genes, including HSP90 and HSP70. (g) The increased cellular concentration of these chaperones can then inactivate HSF-1 by binding to monomeric or trimeric forms of the transcription factor.

THESIS AIMS

In the introduction we have discussed how some of the changes that the *P. falciparum* parasite makes to the PRBC may result in the cytoadherence of the PRBC to endothelium. This is an interaction that is thought to contribute to many of the symptoms of severe malaria. We have identified some aspects of the cytoadherence interaction where there are gaps in current knowledge, and address the following questions:

1) What is the potential for non-viable, antimalarial treated PRBC to retain the ability to cytoadhere?
2) How is the rigidity of PRBC affected by antimalarial treatment?
3) What effect does exposure of endothelial cells to fever have on cytoadherence?
4) What is the potential to not only inhibit but to reverse the cytoadherence interaction between PRBC and endothelial cells?

The first question we address is what may happen, in terms of ability to cytoadhere, after parasites have been killed by antimalarial treatment. It is known that many of the deaths from severe malaria occur within the first 24 hours after hospital admission and administration of antimalarials (Marsh *et al.*, 1995). While it has been hypothesised that these drug-treated PRBC may still be able to sequester and contribute to disease this has not previously been shown in controlled *in vitro* experiments. In chapter 3 we show the ability of PRBC to cytoadhere for many hours following loss of viability after antimalarial treatment. This result highlights a potential need for an adjunct therapy to reverse the cytoadherence interaction, which we address in chapter 6.

Directly related to that question is the effect of the antimalarial treatment on another major consequence of *P. falciparum* infection of RBCs, the increased rigidity of the PRBC. In chapter 4 we ask the question of how the rigidity of PRBC is affected by antimalarial treatments. In answering this question we also look into some of the factors affecting the increased PRBC rigidity.

After studying cytoadherence interactions at 37°C we consider how fever, a common consequence of malaria, may affect cytoadherence. While some studies have looked at the effect of fever on parasites there are fewer studies looking at how endothelial cells may respond to fever, and how this may affect cytoadherence. Our striking result that we present in chapter 5 is that natural host responses may be protective against cytoadherence.

A question following on from results presented in chapter 3 is what is the potential to reverse cytoadherence interactions? While many studies have presented work inhibiting, or blocking cytoadherence there are few results showing reversal or desequestration of already adhered PRBC. We address this question in chapter 6 where we show the potential for a monoclonal antibody and a recombinant protein to reverse cytoadherence.

CHAPTER 2 - MATERIALS AND METHODS

2-1 *PLASMODIUM FALCIPARUM* METHODS

Parasite Strains

Parasite lines used were ItG (Ockenhouse et al., 1992a), A4 (Roberts et al., 1992), C24 (Roberts et al., 1992) and JDP8 (Chattopadhyay et al., 2004). All have been previously characterized for their adhesion phenotypes to ICAM-1 and CD36 (Gray et al., 2003). All parasite lines are subject to antigenic switching and so were used for only up to 3 weeks post-selection to minimise the effect of mixed populations. ItG was selected on ICAM-1 protein and expression of the expected *var* gene confirmed by cloning and sequencing a DBLα tag from cDNA (see below). A4 was selected for binding to the monoclonal antibody BC6 (Horrocks *et al.*, 2002, Smith et al., 1995) followed by immunofluorescence analysis of expressed PfEMP-1 and sequencing of the expressed *var* tag. Populations used were ~80% homogeneous for the expected *var* tag.

Parasite Culture

Blood-stage parasites were cultured under standard conditions (Trager & Jensen, 1976). Parasites were maintained in complete parasite medium which consists of HEPES buffered RPMI-1640 medium (Sigma), with the addition of 0.2% Glucose, 2 mM Glutamine and gentamycin along with 10% human serum. Serum was obtained from the Haematology department of the Royal Liverpool University hospital and batches pooled from 10 individuals. Cultures were maintained at 2 – 10% parasitaemia by dilution on trophozoite days in washed red blood cells along with replacement of media. Red blood cells were obtained from the British transfusion service by centrifugation of whole type O + blood through Histopaque (Sigma) to remove plasma and lymphocytes. Washed red blood cells (WRBC) were resuspended to 50% haematocrit (hct) in incomplete parasite medium (as complete medium described above with the exception of serum) and stored at 4°C for up to 10 days. Cultures were maintained at 1% hct and in a gas mixture of 3% CO_2, 1% O_2 maintained by gassing of flasks each time they were opened.

Blood smears for determination of parasitaemia

Parasitaemia and growth stage of parasite culture was determined by daily blood smears. 300 µl of culture was pelleted by centrifugation in an Eppendorf centrifuge for 30 seconds and resuspended in around 50 µl final volume. This was placed on a

microscope slide and a thin smear made using a second slide. The blood smear was dried and fixed by 5 sec incubation in 100% methanol, rinsed and air dried then stained by incubation for 20 min with 5% Giemsa stain (in Giemsa buffer). The slide was rinsed in water and dried before microscopic examination using a 100 X oil immersion objective. At least 400 RBC were counted and the number and stage of infected cells calculated as a percentage of the total RBC counted.

Cryopreservation of Parasites

Parasites were frozen by resuspending a pellet of washed parasite culture at 3 – 5% parasitaemia at ring stage in glycerolyte freezing medium in a ratio of 5 vol freezing medium to 3 vol cell pellet. One volume of freezing medium was added and cells allowed to stand for 5 min before slow addition of the remaining 4 volumes. The solution was gently mixed and transferred to cryovials (0.5 ml per vial) before wrapping in tissue and polystyrene containers to allow slow freezing at -80°C overnight before transfer to liquid nitrogen for long term storage.

Reconstitution of frozen Parasites

After careful removal of stabilate from liquid nitrogen the solution was allowed to thaw rapidly at 37°C. As soon as the stabilate was thawed the 0.5 ml contents were transferred to a 15 ml Falcon conical tube and 100 µl 12% NaCl was added. After 5 min standing at room temperature 2.5 ml 1.8% NaCl was added over 10 min, followed by 2.5 ml 0.9% NaCl containing 0.2% glucose. After 10 min standing the mix was centrifuged at 1600 rpm in bench top centrifuge for 4 min then washed in incomplete parasite medium. The cell pellet was resuspended in 8 ml complete medium, transferred to small culture flask and gassed for 30 seconds before transfer to 37°C incubator. The following day parasitaemia was assessed and washed red blood cells added as appropriate.

Synchronisation of parasites – Sorbitol Lysis

Parasites were synchronised at ring stage using sorbitol lysis. This method works on the basis that sorbitol is taken up through the NPP of mature PRBC causing lysis of the cell, however is excluded from and therefore does not affect uninfected RBC or ring stage parasites. Parasites were resuspended in sterile 5% sorbitol solution for 15 min at 37°C before washing twice in incomplete medium and returned to culture in appropriate volume of complete medium. For increased synchronicity this process was repeated at a 4 – 6 hour interval. For some experiments two parasite cultures were maintained to be at the same stage on alternate days so the sorbitol synchronisation process was carried out at the same time on alternate days to the relevant culture. For

some experiments (notably Lorca) the sorbitol treatment appeared to affect the results on subsequent days so synchronisation was not carried out within 3 days prior to performing experiments.

Trophozoite Enrichment – Plasmagel Flotation

One method used to enrich for trophozoite stage parasite was Plasmagel flotation which is based on the ability of knob positive PRBC to float on 3% gelatin solution (Jensen, 1978). We used Plasmion; a physiological saline solution containing 3% gelatin. The parasite pellet was resuspend in a ratio of 2 vol pellet to 3 vol incomplete medium and 5 vol Plasmagel, and this mixture transferred to suitable tube (15 ml Falcon conical tube for sterile applications or 5 ml FACS tube for non-sterile procedures) and allowed to settle for 30 - 45 min. Trophozoite stage PRBC in the top layer were carefully transferred to a clean tube then washed three times in incomplete medium and parasitaemia assessed by Giemsa stained smear. For most experiments the effect of Plasmagel on the RBC was controlled for by exposing uninfected RBC to Plasmagel in a similar way, however, the cells were retrieved from the bottom Plasmagel layer as no uninfected cells remain in the upper phase.

Trophozoite Enrichment – Magnetic Enrichment

Since the above method of enrichment is dependent on the presence of knobs on the parasites, in some cases a magnetic method was used to enrich for the mature stages (Staalsoe *et al.*, 1999). This method is based on the paramagnetic property of mature parasites due to the stacking of the iron content of the haemozoin product of haemoglobin breakdown (Paul *et al.*, 1981). Parasite culture was resuspended in 15 ml of binding solution, (2% BSA 0.2% glucose in PBS) and applied to a CS column against a VarioMACS magnet (Miltenyi Biotec) (Miltenyi *et al.*, 1990). The column had been pre-washed in the binding solution and was not allowed to dry out at any point during the procedure. The column, against the magnet, was then washed with binding solution to wash off any unbound cells until the flow through was clear. The column was then removed from the magnet and parasites eluted by washing with 15 ml of binding solution (away from the magnet). Parasites were washed in incomplete medium and the parasitaemia was checked as above. After use the columns were washed three times in each of: binding solution; 1% Tween20; distilled water; and finally 100% Ethanol. After drying under vacuum the columns were stored for re-use.

Selection on ICAM-1

To increase the homogeneity of the ItG parasite population which expresses a PfEMP-1 protein with a high affinity for ICAM-1, the population was subject to selection on

ICAM-1 protein. ICAM-1 protein (Craig *et al.*, 1997) (prepared by Tadge Szestak) was diluted to 20 µg/ml in sterile dPBS. 1.5 ml was used to coat a sterile 60 mm diameter bacteriological petri dish (Falcon #351007) at 37°C in a humid chamber for 2 hours. The dish was blocked overnight at 4°C in sterile PBSBSA (dPBS containing 1% BSA). ItG Parasites at mid-trophozoite stage were enriched by Plasmagel separation to 60% parasitaemia then washed 3 x 10 ml warm incomplete medium, 1 x 10 ml binding buffer (RPMI1640 with 5 mM glucose at pH 7.2) then resuspended at 1% haematocrit in binding buffer. The blocked ICAM-1 coated dish was warmed to 37°C and block solution removed. 1.25 ml parasite mix was added to the dish and incubated at 37°C for 30 min with gentle mixing every 10 min. Unbound parasites were removed by pipetting and washing with approx 5 x 2 ml of binding buffer (37°C) until few loose cells were visible. Bound red blood cells were removed by scraping with a sterile cell scraper and returned to culture in fresh warm medium (25 ml) with fresh washed red blood cells (200 µl pellet). This was repeated on the same dish 3 times until all parasite culture had been used and all bound parasites pooled. After expansion for one week under normal culture conditions RNA was isolated from ring stage parasites, expressed *var* tag was checked by cloning from cDNA and sequencing and a large batch of stabilates frozen. These were then used for a maximum of three weeks. (Alternatively, a method using selection on magnetic beads was used. This was as described below for selection on BC6, except that beads were coated with 2.5 µg ICAM-1 protein per 50 µl of protein A Dynabeads).

Selection on BC6

BC6 antibody (Horrocks et al., 2002, Smith et al., 1995) (B Pinches, Oxford) was used to coat Protein A Dynabeads (Invitrogen #100.01D). 50 µl of Magnetic beads were washed twice in 1 ml of Dulbecco's PBS (Sigma #D8537) with 1% Bovine serum albumin (BSA) (PBSBSA) (Filter sterilised) in a 1.5 ml sterile Eppendorf. Beads were resuspended by gentle pipetting in PBSBSA then the Eppendorf placed next to the magnet for 10 seconds before careful removal of wash solution. Beads were gently resuspended in 380 µl of PBSBSA and 20 µl of BC6 monoclonal antibody was added and incubated for 1 hour at room temperature with gentle rotation. Unbound antibody was removed by 1 x wash with 1 ml PBSBSA and beads resuspended in 200 µl of PBSBSA. A4 parasite culture (50 ml at 10% mid-trophozoite parasitaemia) was enriched for trophozoites using Plasmagel flotation to achieve 50% parasitized RBC. 50 µl pellet was washed 2 x 5 ml of yellow medium, 1 x 5 ml PBSBSA and resuspended by adding 150 µl of PBSBSA. Resuspended parasites (200 µl) were added to 200 µl of prepared beads and allowed to bind at room temperature for 40 minutes with gentle rotation. Unbound parasites were removed by placing the

Eppendorf tube next to the magnet for 10 seconds and careful aspiration of supernatant. Beads were gently resuspended in 1 ml of PBSBSA and wash solution removed as above. Beads were resuspended in 1 ml of culture medium and transferred to culture in 25 ml of medium with addition of 200 µl of washed red blood cells (50%). Parasitaemia was checked and adjusted to <2% for normal culture. After 1 week of culture, selection was repeated and immunofluorescence analysis used to confirm the homogeneity of the resulting culture. Stabilates were made after 1 week expansion and used for no more than three weeks of further culture.

2-2 EXPRESSED *VAR* TAG ANALYSIS

RNA Isolation and cDNA Preparation

RNA was isolated from approx 10 ml culture at around 5% parasitaemia synchronised ring stage parasites (approx 12 – 18 hours post-invasion) using Trizol (Kyes *et al.*, 2000). RNA was resuspended in 40 µl diethylpyrocarbonate (DEPC) treated water. Half of the RNA prep was treated using DNAse I (Ambion) as instructions and cDNA synthesised using Bioline reverse transcription kit. Random hexamers were used as primers and synthesis was at 45°C for 1 hour after a 3 minute 96°C denaturation of the RNA. As a control a reaction was set up in parallel that did not include the reverse transcriptase enzyme.

Var tag PCR

cDNA was used as a template for PCR using primers 2002αAF and alphaBR (Bull et al., 2005). PCR amplification was using Qiagen Taq polymerase $MgCl_2$ concentration of 1.5 mM, and primers at 4 µM and dNTPs at 0.2 µm (each). A reaction size of 50 µl was used for cloning. The PCR was an initial 95°C melt for 2 min followed by 30 cycles of 30 sec 95°C melt then annealing step at 45°C for 30 seconds and elongation at 72°C for 30 seconds. A 10 min final elongation was included. The negative control of RNA treated with no reverse transcriptase was also used as a control template. 5 µl of each reaction was checked on a 2% agarose gel to ensure no product was seen in the no-RT reactions. The remaining 45 µl of the reaction was then run and the ~400 bp PCR product was excised from a 1% agarose gel (in Tris-Acetic acid EDTA buffer (TAE) Sambrook *et al.*) and purified using an Amicon column.

Cloning into TOPO

4.5 µl of purified PCR product was added to 0.5 µl of TOPO TA vector (Invitrogen) and 1 µl salt solution (1.2 M NaCl and 0.06 M $MgCl_2$) (as manufacturer's recommendations) and ligation at room temperature for 5 min. Chemically competent Top10 *Escherichia coli* cells were prepared as Sambrook et. al and aliquots stored at -80°C with the addition of 10% glycerol. One 100 µl aliquot of cells was thawed rapidly then placed on ice and ½ the ligation reaction added. Cells were left on ice for 20 min with occasional gentle mixing by tapping. Heat shock was at 42°C for 1 min 15 seconds, then cells were placed on ice for 2 minutes before addition of 400 µl LB (Luria-Bertani broth (Miller) Sigma #L3152). After 45 min at 37°C with shaking the cells were plated onto LB agar plates containing ampicillin (50 µg/ml) and X-gal (40 µg/ml) coating to facilitate blue-white selection. The following day white colonies were picked into 1 ml LB plus

ampicillin (50 µg/ml) for 4-6 hours then grown overnight in 5 ml LB plus ampicillin (50 µg/ml).

Mini Preps

DNA was prepped from 5 ml overnight cultures using Qiagen mini prep kit as the standard manufacturer's protocol, final resuspension of DNA was in 40 µl of distilled water. Alternatively an alkaline lysis method based on Sambrook et. al was used. DNA concentration and quality were checked by spectrometry and running a sample on an agarose gel.

Restriction Digest Mapping

*Eco*RI digestion was used to confirm the presence of an insert, then restriction mapping of the fragment was carried out by digesting 2 µg of DNA (~5 µl from mini prep as above) with *Eco*RI in double digests with *Ssp*I, *Dra*I and *Rsa*I. Double digests were performed using 0.25 µl EcoRI and 0.5 µl of the second enzyme in appropriate buffer for 2 – 4 h at 37°C. The enzymes were chosen based on a high frequency of cutting in *P. falciparum* genome but few sites in the TOPO vector (table 2.1)

Enzyme	Buffer	Sequence	Pf. Freq	TOPOpCR2.1	Fragment Size
*Ssp*I	EcoR1	AATATT	304	None	3900*
*Dra*I	4	TTTAAA	394	3	19; 692; 3189
*Rsa*I	1	GTAC	206	3	684; 1511; 1705

Table 2.1 Restriction Digests for analysis of expressed var tag. Pf. Freq is the frequency of sites (if they were evenly distributed) in bp. Cuts in the TOPOpCR2.1 vector and fragment sizes are based on the vector backbone.

Patterns were analysed by running digests on a 2% agarose gel. The expected pattern of the vector backbone served as a control for complete digestion. Analysis of published *var* tag sequences from A4 and 3D7 strains available in the EBI database using NEB digest tool suggest that the enzymes used should not result in identical restriction patterns for any different *var* gene tags so far published (although clearly this method would not detect point mutations or smaller changes within *var* tags unless occurring in an enzyme site). Also given the variation in *var* tags it is probable that similar restriction patterns could emerge from unrelated *var* tags from different isolates. Selected clones were sent for sequencing by the LSTM sequencing service in forward and reverse directions using M13 forward and reverse primers. Freely available

software Chromas lite and packages from EBI (www.ebi.ac.uk) were used to analyse sequences.

BC6 Immunofluorescence for microscopy

Trophozoite stage A4 parasites (approx 5 µl pellet) were washed once with 5 ml serum-free culture medium, followed by washing with 1 ml Dulbecco's PBS with 1% BSA (PBSBSA) and resuspended in 50 µl of BC6 antibody diluted 1:25 in PBSBSA. These were incubated at room temperature for 1 hour, then washed 2 x 0.5 ml PBSBSA. The pellet was resuspended in 50 µl of rabbit anti-mouse antibody (Abcam) diluted 1:50 in PBSBSA. After 40 min incubation at RT cells washed 2 x 0.5 ml in PBSBSA and resuspended in 50 µl of Alexa 488 goat anti-rabbit antibody (Invitrogen) diluted 1:1000. This was incubated at room temperature for 40 minutes then washed 1 x 0.5 ml PBSBSA. For IFA parasites were stained with 10 µg/ml Ethidium Bromide (EtBr) for 5 min at RT before washing. Parasites were wet mounted on a slide under a cover-slip, sealed with nail varnish and visualised immediately using Confocal microscopy.

BC6 Immunofluorescence for Flow Cytometry Analysis

A 10 µl pellet of trophozoite stage parasites at 3-10% parasitaemia was washed in serum-free culture medium and resuspended in 100 µl of BC6 antibody diluted 1:50 in PBSBSA. This was incubated at 37°C for 30 min, washed 3 x 1 ml in PBSBSA and resuspended in 100 µl secondary rabbit anti-mouse antibody diluted 1:100 in PBSBSA. After 30 minutes at 37°C the cells were washed as above then resuspended in 100 µl goat anti-mouse alexa 488 conjugated antibody at 1:2500 dilution in PBSBSA containing 1 µg/ml ethidium bromide. The cell pellet was washed 3 x 1 ml PBS after 30 minutes incubation at 37°C and resuspended in 100 µl PBS. 25 µl was diluted into 1 ml PBS for FACS analysis (Williams & Newbold, 2003) using Beckman Coulter XL flow cytometer.

2-3 ENDOTHELIAL CELL METHODS

Endothelial Cell Culture

HUVEC and HDMEC were obtained from Promocell and cultured as per manufacturer's instructions. Cells between passage 3 and 6 were used for experiments. Before assays cells were generally stimulated by the addition of 1 ng/ml TNF for 18-20 hours. This was shown by immunofluorescence and FACS using anti ICAM-1 monoclonal antibody 15.2 (Serotec), to induce the surface expression of ICAM-1.

Endothelial Cell Immunofluorescence staining for ICAM-1 expression analysis by FACS

One confluent well of a 6 well plate was washed 2 x Dulbecco's PBS and trypsinised by addition of 0.5 ml trypsin/EDTA solution (Promocell). After cells were observed to have rounded up and detached trypsinisation was stopped by addition of 0.5 ml trypsin neutralisation solution (TNS) (Promocell). After careful mixing the cells were split to two Eppendorfs and pelleted by centrifugation at 3500 rpm in an Eppendorf centrifuge for 5 min. Cells were washed 2 x in Dulbecco's PBS with 1% BSA (PBSBSA) then resuspended in 50 µl PBSBSA with primary ICAM-1 monoclonal Ab 15.2 (Serotec) 1:50 dilution, or negative control with no primary antibody. Cells were incubated at 37°C for 45 min then washed 3 x in PBSBSA and incubated for 45 min at 37°C with secondary antibody FITC conjugated goat anti-mouse (Sigma) 1:100 dilution in PBSBSA. Alternatively a FITC-conjugated version of the same anti-human ICAM-1 monoclonal antibody 15.2 (Sigma) was used at 1:50 dilution along with the FITC-conjugated matched isotype control (Sigma). (No difference was seen between the two labelling techniques). After staining cells were washed 3 x in PBSBSA and resuspended in 250 µl 4% paraformaldehyde in PBS pH 7.2. Fixed cells were stored at 4°C and washed 3 x in PBS by centrifuging at 5000 rpm 5 min and resuspension in 500 µl PBS for FACS analysis. An example of ICAM-1 expression in shown in figure 2.1.

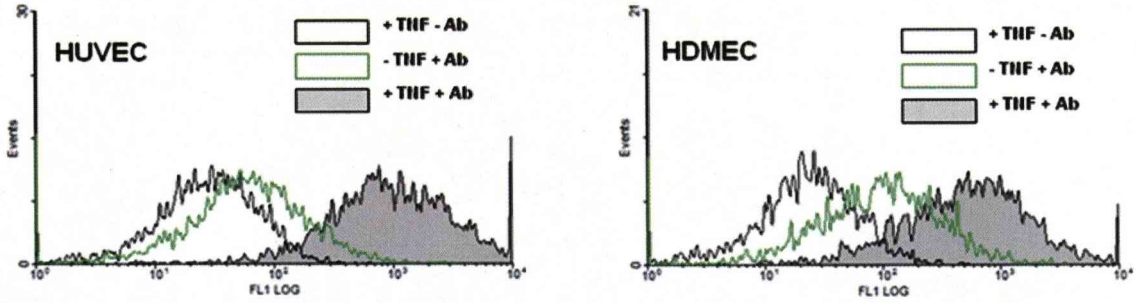

Figure 2.1. ICAM-1 expression on endothelial cells. Characterisation of ICAM-1 expression after 16 h stimulation with 1 ng/ml TNF. Staining as described above on HUVEC (left) and HDMEC (right). Negative controls shown (black open line) are with TNF stimulation and secondary antibody but no primary antibody (+TNF –Ab). Other negative controls (no primary antibody and no TNF) gave the same result as + TNF - Ab. ICAM-1 levels shown without TNF stimulation (open green line) and with TNF stimulation (grey solid)

2-4 ADHESION ASSAYS

Static Protein Assay

Static protein binding assays were carried out as previously described. ICAM-1-Fc (Craig et al., 1997) (Prepared by Tadge Szestak, LSTM) was diluted to 50 µg/ml and 25 µg/ml in PBS and 2 µl spots were placed around a defined diameter of a sterile 60 mm diameter bacteriological Petri dish (Falcon 351007). CD36 protein (R&D) was spotted at 25 µg/ml, and a negative control PBS spot included. Triplicate spots per dish were prepared, and usually two or three dishes prepared per parasite line/experimental condition. Dishes were incubated in a humidified chamber for 2 h at 37°C. Protein spots were aspirated off and dishes blocked overnight at 4°C in 1% BSA in PBS. After overnight incubation blocking solution was removed and the dish washed in warm binding buffer (37°C). Parasites were prepared after appropriate treatment and washed 1 x 5 ml in binding buffer then resuspended in warm binding buffer to 1% Hct and 3% parasitaemia. 1.25 ml of parasite suspension was added to each dish. Dishes were incubated at 37°C for 1h, with re-suspension by gentle rotation for approx 30 seconds every 10 min. Unbound RBC were removed by approx 10 x 2 ml washes with binding buffer and bound cells fixed with 1% glutaraldehyde for at least 1h. Dishes were stained with 5% Giemsa stain for 20 min, washed 2 x 4 ml in water and levels of adhesion were quantitated microscopically. Six independent fields per spot were counted at 200 x magnification, and calculated to the mean binding per mm^2. The mean of the three spots per dish for each protein was calculated.

Flow Protein Assays

Microslides were pre-prepared by coating with amino-propyl-tri-ethoxy-silane (APES) following nitric acid treatment to allow for protein/cell adherence, then autoclaved. Before the experiment a small piece (1.5 cm) of thin wall rubber tubing was attached to one end of the microslide, marked to indicate orientation of the coated surface, and slides were autoclaved. Slides were then coated with ICAM-1 at 50 µg/ml or 25 µg/ml by drawing up 65 µl of solution using a pipette tip connected to the tubing. Protein was allowed to adhere to the microslide by incubation in a humid 37°C chamber for 2 hours then washed by drawing through 4 x 65 µl of PBS with 1% BSA (PBSBSA). Slides were blocked in PBSBSA overnight at 4°C. Parasites were prepared as for static protein assay and everything warmed to 37°C before use. The microslide was connected to flow apparatus and binding buffer (37°C) flowed through for at least 2 min before the experiment started. Prepared parasites were flowed through at pump speed of 0.186 ml/min to give an appropriate shear stress of 0.05 pascal Pa (Cooke *et al.*, 2002). To

ensure comparable experiments timings were strictly adhered to. Parasites were flowed through for 2 min then image capture was started. 80 images at 1 sec intervals were obtained at 10 x magnification over 6 areas of slide. Immediately following this 80 images were obtained in the same way at 20 x magnification. Parasite flow was swapped to binding buffer flow to wash for 2 minutes before counting bound parasites over 6 areas of slide. When rolling images were not captured parasite flow culture was initiated using a syringe, then flow at the correct rate was timed for 5 min. The slide was washed for 2 min with binding buffer to clear the lines and slide of unbound RBC before counting stationary adhered parasites. To enable re-use of the slide parasites were removed by washing the slide through 2 x 2 ml with water then 2 x 2 ml binding buffer. To ensure this had no effect on binding, a positive control was carried out as the last run on a slide in each experiment. Slides were not re-used more than 6 times.

Static Cell Assays

Endothelial cells cultured as above were seeded onto 13 mm coverslips coated in 1% gelatin in 24 well plates. One confluent T25 flask was trypsinised and used to coat 12 – 24 coverslips. After leaving overnight for cells to adhere the medium was changed and cells cultured until confluent (2 – 5 days). Cells were induced with 1 ng/ml TNF for 20 hours and washed 1 x in culture medium before an assay. Parasites were prepared as above to 1% hct and 3% parasitaemia in binding buffer. 0.5 ml of parasite mix was applied to each well and incubated at 37°C for 1 hour with gentle resuspension by rotating every 10 min. Unbound cells were removed by washing by 2 x 2 sec dips in binding buffer followed by 2 x 30 min gravity washes in binding buffer. Bound cells were then fixed by incubation in 1% glutaraldehyde in PBS for at least 1 hour. After staining with Giemsa for 30 min coverslips were washed in water, air dried and mounted using DPX hard set mounting medium. 6 – 10 areas of each slide were counted under 200 X magnification for the number of bound parasites.

Flow Cell Assays – Using Microslides

Microslides were prepared as for protein assays then coated with collagen/1% gelatin for 45 minutes at 37°C. One confluent T25 flask of endothelial cells was trypsinised and was sufficient for 6 microslides. Slides were washed extensively after collagen/gelatin coating by aspirating through PBS, and left to dry. Trypsinised cells were resuspended in 400 µl of culture medium with the addition of 25 µg/ml gentamicin, and approx 65 µl sucked into each microslide ensuring no air bubbles. Cells were allowed to settle for 2 hours at 37°C then slides connected to a flow system to allow media exchange every hour. After overnight growth, TNF (1 ng/ml) was added to confluent cells for 20 hours before the assay. Assay conditions were as for the protein flow assay except that slides

were not re-used, and extra care was taken to ensure no entry of air bubbles into the system. See figure 2.3 for schematic of growth and assay conditions.

Flow Cell Assays - Using Chamber Slides

Chamber slides (Permanox Lab-teK chamber slides Nunc #177410) were coated with gelatin for 30 min at 37°C. One confluent T25 flask of endothelial cells was trypsinised and used to seed 3 (for next day assay) or 6 (For 2-4 days growth before assay) chamber flasks. 2.5 ml trypsinised cells were added per flask. After settling overnight the medium was changed and cells cultured until confluent. Cells were generally stimulated using 1 ng/ml TNF overnight before assays. For assays the medium was aspirated off and the chamber removed from the chamber slide flask using the special tool. The slide was immediately placed cell side down on the gasket of an immunogenetics flow chamber. Vacuum was applied to the chamber to seal the slide then flow connected. Buffer was flowed through at a rate of 0.24 ml/min to give a shear stress of 0.05 Pa. See figure 2.4 for schematic, and table 2.2 and figure 2.5 for comparison of flow assays using microslides or chamber slides.

Growth and adhesion assay under flow conditions using microslides

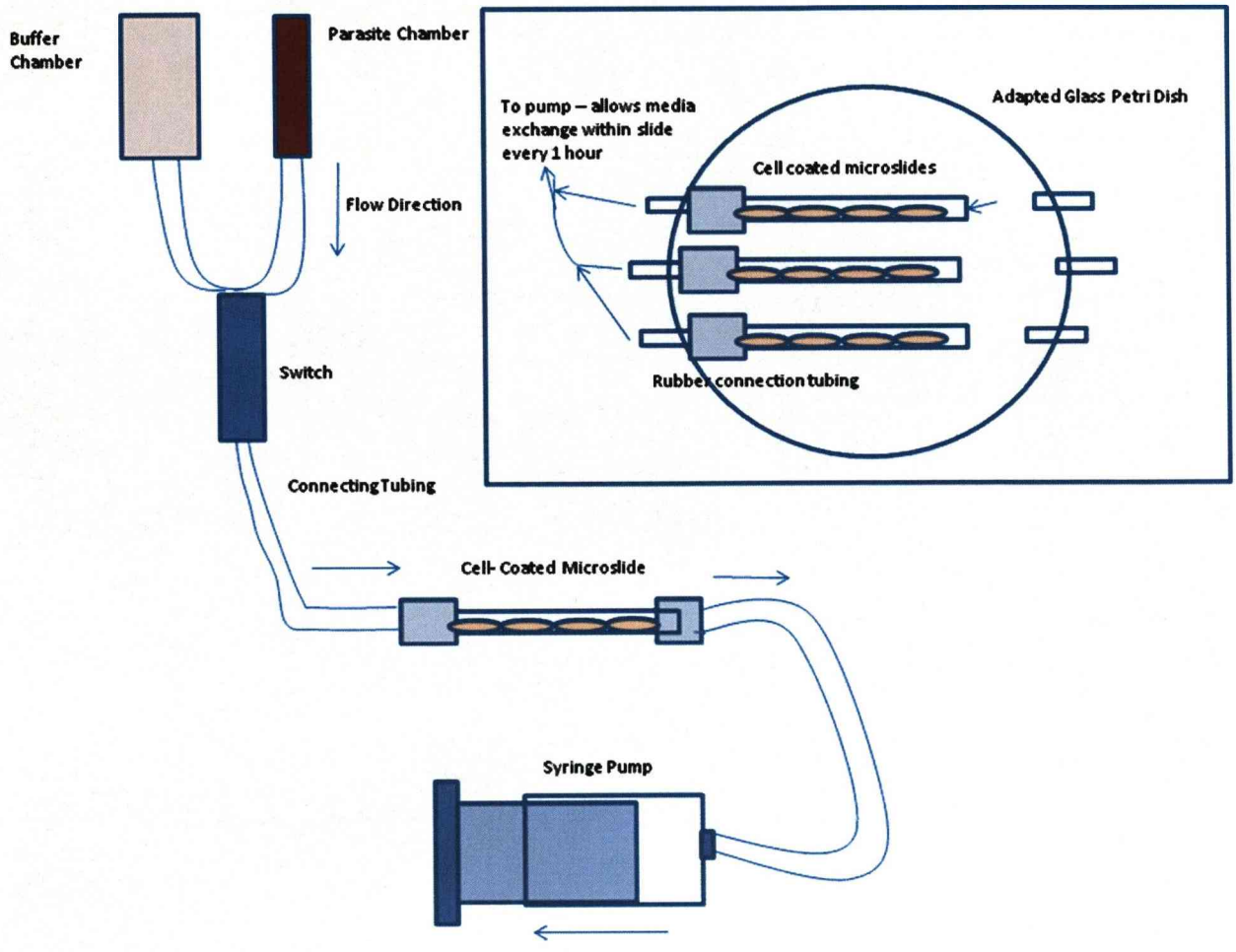

Figure 2.3. Schematic of growth and adhesion under flow conditions using microslides. Cells are seeded onto microslides and allowed to adhere for 2 h before connection to the media exchange system. Slides are placed in 50 ml medium in an adapted glass petri dish (inset picture), each slide is attached using rubber tubing to an outlet connected via tubing to a pump. The pump is on a timer which is active every hour to remove enough medium to exchange medium within each microslide. After overnight growth TNF can be added as required to the dish. The microslide is placed under a microscope to allow for visualisation, imaging and counting of assays. The syringe pump can be set to suitable speed to allow flow at appropriate shear stress levels. During the assay the flow can be switched from the parasite or the medium reservoirs.

Growth and assay under flow conditions using chamber slides

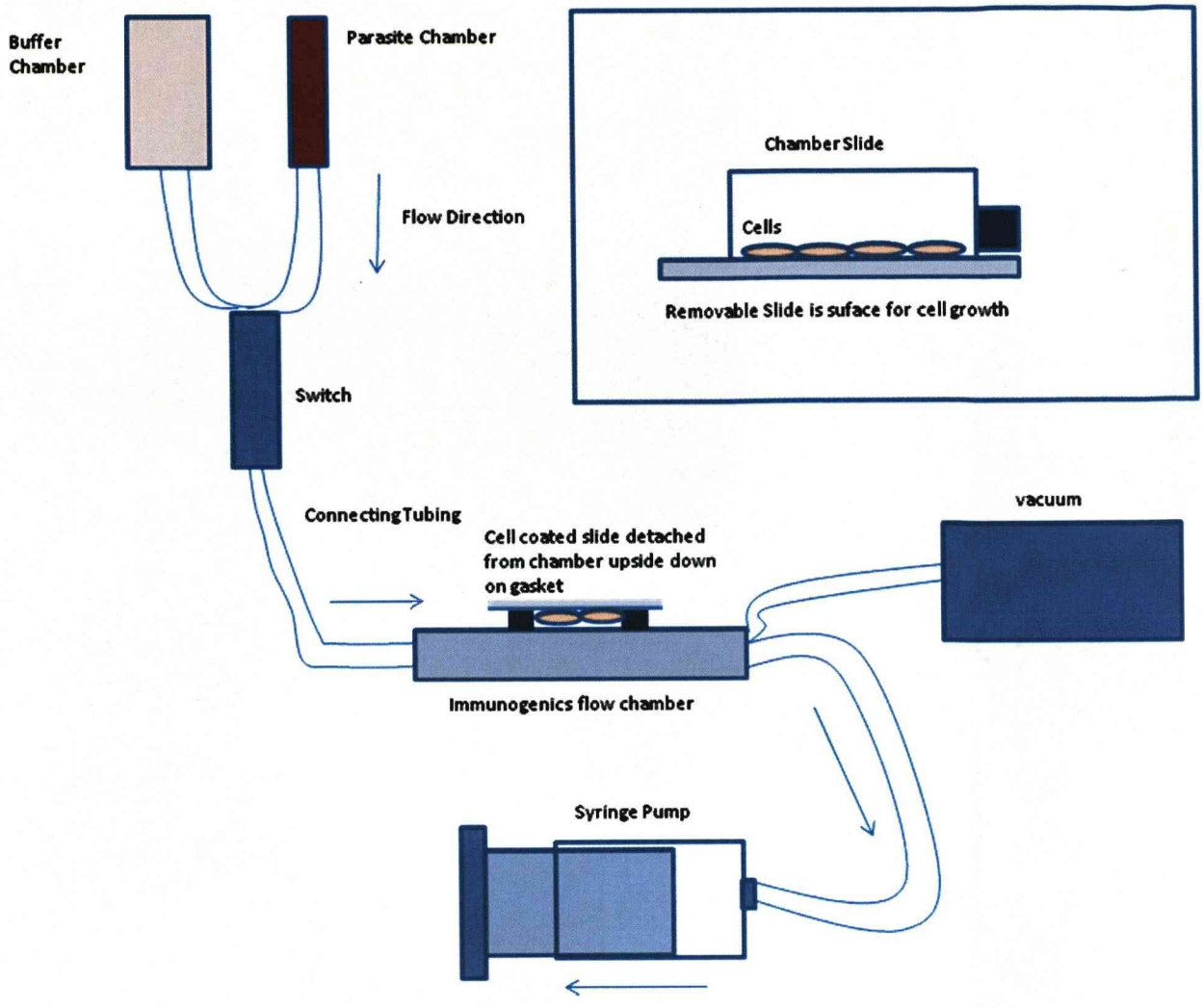

Figure 2.4. Schematic of growth and adhesion assays using chamber slides. Chamber slides act as normal tissue culture flasks for cell growth. Once cells have reached confluency and have been stimulated for assay the chamber part can be removed by levering away from the slide. This leaves the cells on a flat slide which can then be placed cell side down on the Immunetics chamber. A vacuum is applied which seals the slide to the gaskets on the chamber then flow can be applied using the syringe pump set to an appropriate speed to give desired shear stress levels. During the assay the flow can be switched from the parasite or the medium reservoirs.

Comparison of Flow Binding assays using microslides or flow chamber system

Microslides	Flow Chamber
Preparation of slides using acid and APES treatment followed by autoclaving required	No pre-treatment of slides required
Slides Cheap to buy	Slides relatively expensive to buy
One T25 flask of cells sufficient for 6 slides to be confluent the following day	One T25 flask of cells sufficient for 2-3 slides to be confluent the following day
Cells will not grow in microslides	Cells will grow on flow chamber slides
Need adapted incubator with media exchange pump to grow	Can be grown in standard CO2 incubator
Flow system attached to microscope required	Flow system attached to microscope required as well as special flow chamber (immunetics) and vacuum pump
Increased risk of infection during culturing due to media exchange system	No increased risk of infection during culturing over standard culturing
Large volume of medium (>50 ml for 6 slides) required	Smaller volume of medium (2.5 ml per slide) required

Table 2.2 Comparison of flow assay types.

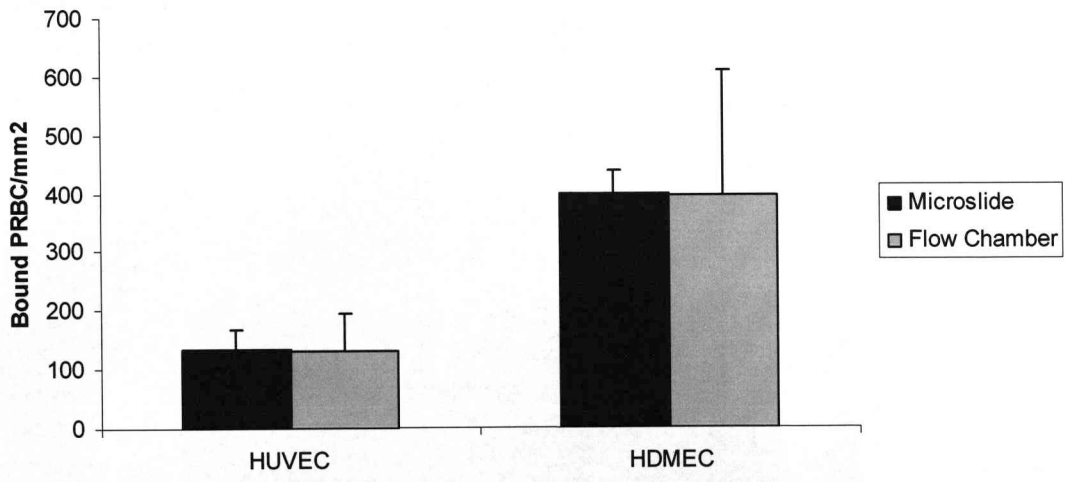

Figure 2.5. Adhesion of ItG PRBC under flow conditions to stimulated HUVEC and HDMEC. Results show mean + SD bound PRBC per mm^2, N=12 for microslides and N=3 for flow chamber for HUVEC. HDMEC N=8 microslides and N=2 flow chamber).

CHAPTER 3 - CYTOADHERENCE OF *P. FALCIPARUM* AFTER ANTIMALARIAL TREATMENT

3-1 INTRODUCTION

An important aspect of the pathogenesis of severe malaria results from the ability of infected red blood cells to sequester in the microvasculature (as described in detail in chapter 1). Post-mortem studies of severe malaria show high levels of infected red blood cells (PRBC) bound to microvasculature (Taylor *et al.*, 2004, Turner, 1997). The involvement of sequestration in pathogenesis could be directly a result of blocking of the blood vessels, and/or downstream effects caused by the interaction between PRBC and the endothelium, including local inflammatory responses (Chakravorty et al., 2008).

Cytoadherence is mediated by a parasite protein PfEMP-1 which is a large protein comprising several external Duffy-binding-like (DBL) domains, encoded for by *var* genes. *P. falciparum* has around 60 *var* genes per genome, of which only one is expressed at a time. This process of antigenic variation is a way in which the parasite evades recognition by host adaptive antibody immune responses and the large number of variants of PfEMP-1 also results in the potential to bind to many different host receptors (Kyes *et al.*, 2007b).

ICAM-1 is a host receptor of interest as it is linked to cerebral malaria (Chakravorty & Craig, 2005). Patients suffering with cerebral malaria have up-regulated levels of ICAM-1 in the brain and parasite isolates from patients suffering from cerebral malaria show higher binding to ICAM-1 protein (Turner et al., 1994, Newbold et al., 1997).

It is known that cytoadherence of PRBC induces signalling events in endothelial cells (Tripathi et al., 2006, Jenkins et al., 2007a). Some of these signalling responses may help protect the host endothelium against damage, as suggested by the down-regulation of apoptotic genes in endothelial cells (Chakravorty et al., 2007). However, other effects may be damaging. For example, the induction of ICAM-1 expression on endothelial cells occurs in response to PRBC (Chakravorty et al., 2007), which could lead to further sequestration of PRBC, as well as local leukocyte recruitment, amplifying pathology caused by adhesion or local inflammatory responses. There is also evidence of induction of apoptosis and leakage in endothelial cells following adhesion of PRBC (Medana & Turner, 2007).

Antimalarial treatments are effective at killing parasites where resistance has not developed; however, there is still a high mortality rate associated with severe malaria with most deaths occurring in the first 24 h after hospital admission (Marsh *et al.*, 1995). It is clear that even after initiation of antimalarial treatment, patients continue to show worrying clinical signs (Marsh et al., 1995). It has been suggested that PRBC after antimalarial treatment may still continue to cytoadhere – as observed in cerebral ultrastructural studies (Pongponratn *et al.*, 2003). Furthermore a potential mechanism for the difference in effectiveness of artesunate versus quinine was suggested to be potentially due to activity in preventing sequestration (Dondorp *et al.*, 2005).

It has not previously been shown using in-vitro assays to known receptors what ability antimalarial-treated PRBC have to cytoadhere. In this study we investigate the hypothesis that non-viable parasites killed by standard antimalarial treatment could contribute to disease pathology by their continued ability to cytoadhere. We have performed *in vitro* assays for cytoadherence with drug-treated *P. falciparum* PRBC to ICAM-1 and human endothelium under both static and flow conditions. Using a range of antimalarials we show that non-viable *P. falciparum* PRBC retain the ability to cytoadhere at least 24 h after drug administration as a result of the slow rate of degradation of the surface protein PfEMP-1.

3-2 MATERIALS AND METHODS

Parasites

The isogenic parasite isolates ItG and A4 were used as described in methods chapter 2. Parasites were synchronised at ring stage using sorbitol lysis as described in methods chapter 2, and to allow for stage-matched controls for 24 hour drug treatment time points parallel cultures were maintained 24 hours apart.

Endothelial Cells

Endothelial cell lines HUVEC and HDMEC were used as described in methods chapter 2. All assays were performed on confluent monolayers of cells.

Adhesion Assays

Adhesion assays to ICAM-1 protein and to endothelial cells under static conditions were performed as described in methods chapter 2. Flow adhesion assays were all performed using the microslide system as described in methods chapter 2.

Measurement of PfEMP-1 levels of the surface of *P. falciparum* A4 PRBC

PfEMP-1 on the surface of live A4 PRBC was visualised by immunofluorescence using BC6 monoclonal primary antibody (1:50 dilution) which specifically recognises an exposed epitope of the A4var41 PfEMP-1 (Horrocks et al., 2002). This was followed by a secondary rabbit anti-mouse antibody (Serotec) (1:100) followed by Alexa488 conjugated goat anti-rabbit antibody (Invitrogen) (1:5000). All washes and antibody dilutions were in Dulbecco's PBS with 1% BSA and each incubation was at 37°C for 30 min. Infected cells were stained with ethidium bromide (1 µg/ml), mounted on a microscope slide and analysed by confocal microscopy using Zeiss LSMPascal microscope and Zeiss Pascal and Photoshop software (Adobe). For flow cytometry analysis staining was carried out as above then infected cells were diluted in PBS and 500,000 events (red blood cells) acquired on Beckman Coulter FACS XL, gated using forward scatter and side scatter to acquire red blood cell populations excluding debris and then FL-1 and FL-2 fluorescence intensity measured. Analysis was performed using WinMDi software. Region R1 was created for A4var41 positive cells based on negative antibody controls. The mean fluorescence intensity (MFI) of region R1 was used to quantitate the level of PfEMP-1 on A4var41 positive infected red blood cells. The percentage of A4 PRBC that were classed as A4var41 positive remained at ~75-85% throughout experiments and was unchanged within an experiment before/after 24 h artesunate treatment.

Drug Treatment

The effect of parasite viability on cytoadherence was tested using artesunate, quinine, lumefantrine and piperaquine. Final drug concentrations were chosen based on published peak plasma levels. These were: 500 nM for artesunate, (Newton *et al.*, 2006, Simpson *et al.*, 2006), 25 µM for quinine (Akoachere *et al.*, 2005, Le Jouan *et al.*, 2005), 15 µM for lumefantrine (McGready *et al.*, 2006, Ashley *et al.*, 2007), and 100 nM for piperaquine (Akoachere et al., 2005, Davis et al., 2005). The concentrations of drugs used were well above the IC_{50} determined for each and were confirmed to inhibit parasite development as assessed by Giemsa staining. Parasites were confirmed non-viable after treatment by continued culture for at least 72 h post-treatment with no growth.

IC_{50} Growth Inhibition Assays

Growth inhibition (IC_{50}) assays were performed on ItG parasites using a standard fluorometric assay (Bennett *et al.*, 2004, Smilkstein *et al.*, 2004). A 10 mM stock concentration of drug was prepared and 1:3 serial dilution series made (400 µl + 800 µl) starting at 2000 nM. Drug dilutions were then plated out 50 µl per well in triplicate over a 96 well plate including controls with no drug, and control with high concentration artemether (1 mM). To each well 50 µl of parasite suspension at 2% rings and 2% Hct in normal culture medium was added resulting in a standard final drug dilution series ranging from 1000 nM to 0.45 nM. This range was adjusted according to the drug. Parasites were incubated under standard culture conditions for 48 hours. Sybr green lysis mix consisted of lysis buffer (20 mM Tris.Cl pH 7.5, 5 mM EDTA, 0.008% Saponin and 0.08% Triton X-100), with the addition of 0.2 µl Sybr green per 1 ml lysis buffer. After 48 hours incubation, 100 µl of Lysis buffer/Sybr green solution was added per well and incubated in the dark for 1 hour. Following this incubation the plate was read at 484 nm excitation 530 nm emission. Percentage growth for each drug concentration compared to positive control was calculated, and the IC_{50} determined using Grafit software.

3-3 RESULTS

Artesunate treatment of ItG

We first assessed the effect of artesunate treatment on parasite development. Unless otherwise stated throughout this chapter the *P. falciparum* isolate ItG was used. Addition of 500 nM artesunate to a culture of mid-trophozoite-stage ItG PRBC resulted in a rapid growth inhibition of the parasite. The concentration of 500 nM was chosen based on published peak plasma concentrations, and is well above the published IC_{50}, and the IC_{50} we determined for ItG (See table 3.1 below) As determined by Giemsa staining, parasite growth stopped after 2-4 hours incubation in 500 nM artesunate (Fig. 3.1) and parasites were not viable for long term culture. Similar results were seen when the artesunate was washed out (3 x 10 ml washes) after time periods of 30 min or greater. However, when artesunate (500 nM) was washed out after 10 min or less incubation time, parasite growth was unaffected.

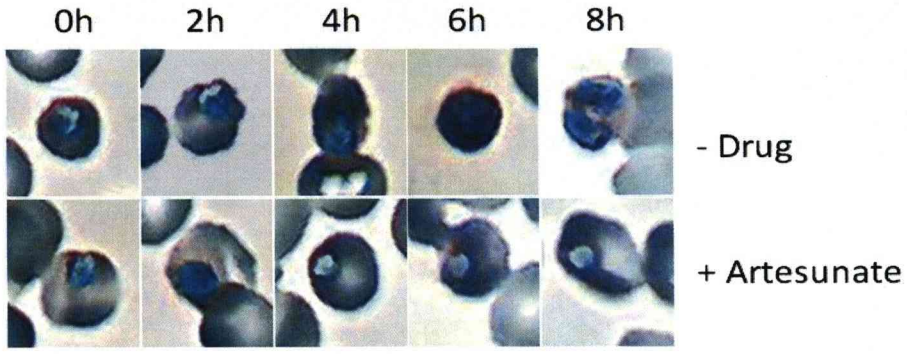

Figure 3.1. Giemsa stained smears of ItG over time course of artesunate incubation. (One experiment, representative of many independent observations)

Addition of artesunate to late-stage trophozoites resulted in some lysis of parasites, noticeable 24h after addition of drug by the presence of some "free" parasites visible in Giemsa stained smears. However, when artesunate was added to younger trophozoites there was little observable lysis, and no apparent lysis on addition of drug to ring-stage parasites (Fig. 3.2).

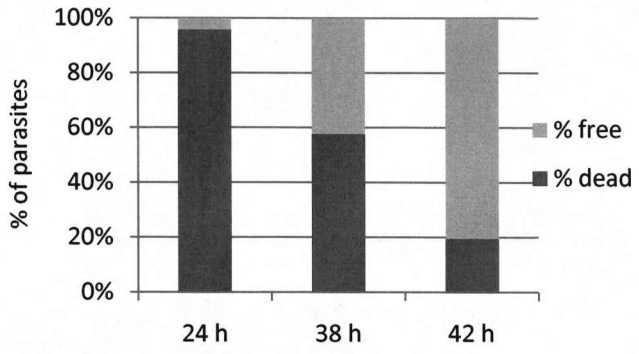

Figure 3.2. Lysis of ItG PRBC after 24h artesunate treatment after addition of drug to parasites at 24, 38 or 42 hours post-invasion representing young and mature trophozoites, and schizont stages. All parasites either free or intraerythrocytic were counted in Giemsa smears and percentage of free or intraerythrocytic (but dead) parasites were plotted. (Compiled from two experiments; representative of several independent observations).

Cytoadherence of artesunate treated *P. falciparum* ItG PRBC to ICAM-1 under flow conditions

The effect of artesunate treatment on the ability of PRBC to cytoadhere was first tested using flow adhesion assays to ICAM-1. As described in the methods section we used ICAM-1 coated microslides and parasite flow at a wall shear stress of 0.05 Pa, as widely used to mimic microvascular shear stress (Gray et al., 2003, Cooke et al., 2002) (See also materials and methods chapter 2). Mid-trophozoite-stage parasites (24 – 28 hours post invasion) were treated with 500 nM artesunate in standard culture conditions for 24 h. Giemsa stained smears were made at time points after drug addiction (Fig. 3.3a) and parasitaemia was adjusted to 3% for ICAM-1 adhesion assays under flow conditions. No significant difference in binding was observed for parasites exposed to artesunate for 4 h compared to untreated parasites (Fig. 3.3a). Following 8 h exposure, a slight reduction in binding was seen and following 24 h artesunate treatment adhesion to ICAM-1 was reduced to ~30% of control levels ($P < 0.01$, Fig. 3.3b). Similar binding phenotypes were observed for artesunate concentrations ranging from 20 nM to 12.5 µM (Fig. 3.3b). As described above, a 30 minute exposure to 500 nM artesunate was sufficient to render parasites non-viable. The adhesion phenotype of parasite exposed to artesunate for 30 min to 24 h was assessed. As before, 500 nM artesunate was added to mid-trophozoite-stage parasites. Drug was washed out after 30 min to 24 h exposure time, and adhesion assayed 24 h after initial drug addition. Similar adhesion phenotypes were observed 24 h after initial addition of artesunate when it was washed out at various time points of 30 min or longer (Fig. 3.3c).

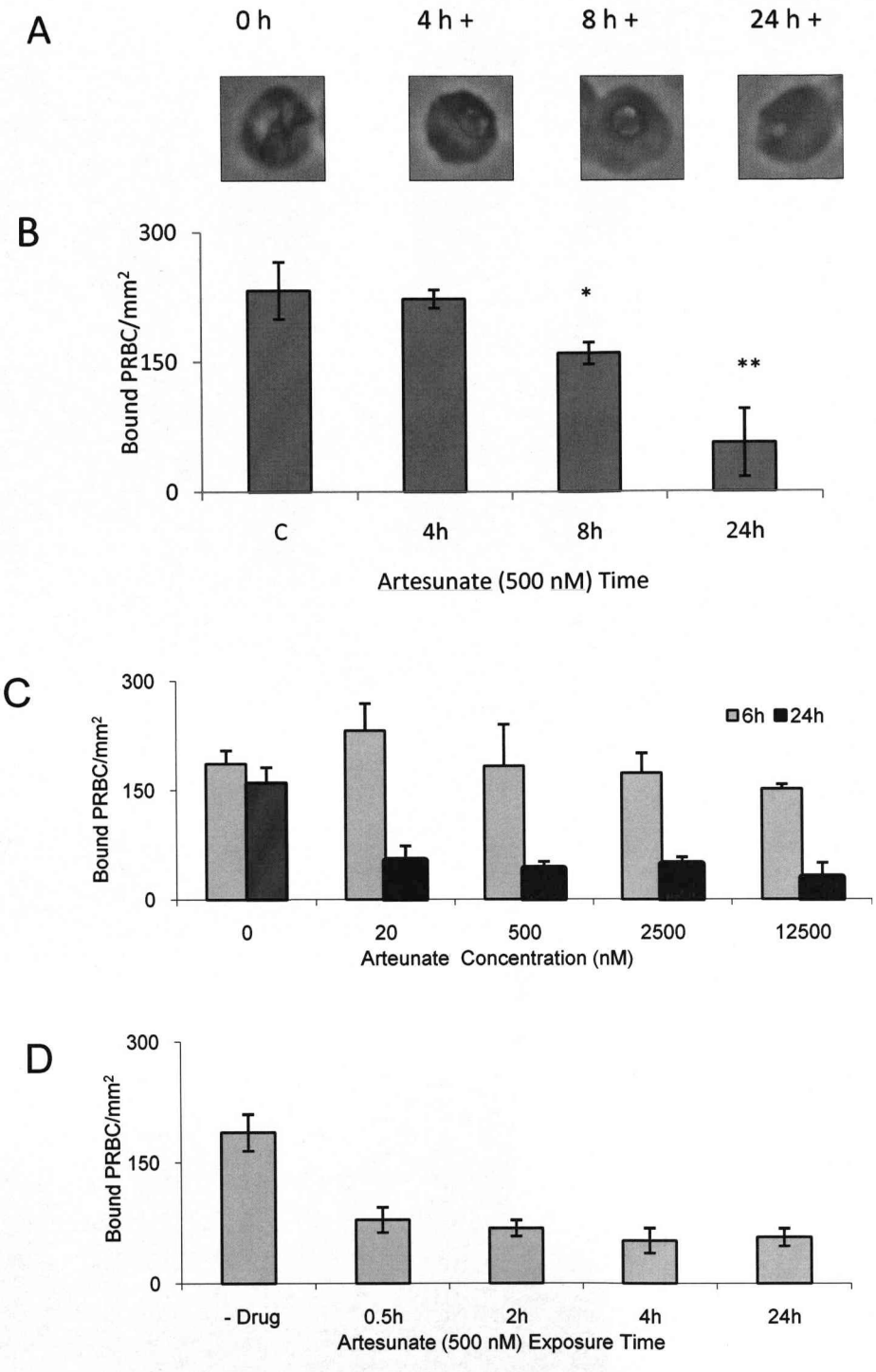

Figure 3.3. Adhesion of artesunate treated PRBC to ICAM-1 under flow conditions. A) Giemsa stained smears of PRBC after 0, 4 8, and 24 h 500 nM Art treatment and B) adhesion level to ICAM-1 protein under flow conditions. C) Adhesion to ICAM-1 under flow after 6h or 24h treatment with a range of artesunate concentrations. D) Adhesion to ICAM-1 under flow 24 h after addition of 500 nM artesunate then subsequent washing out of drug after 30 min to 24 h. Time points < 30 min had reinvaded to ring stage parasites by 24 h following drug addition. * $P<0.05$ and ** $P<0.01$ as determined by T test compared to untreated control.

Cytoadherence of artesunate treated ItG PRBC to human endothelial cells

Having seen the effect of artesunate treatment on adhesion of PRBC to ICAM-1 protein, we wanted to confirm whether the same phenotype was observed measuring the adhesion to endothelial cells. Adhesion of PRBC to human endothelial cells (HUVEC and HDMEC) was assessed under both static and flow conditions following 4, 8 and 24 h artesunate (500 nM) treatment of trophozoite (24 h post invasion) stage parasites.

As described in the Methods section, binding assays were performed with confluent monolayers of TNF (1 ng/ml, 18 h) activated endothelial cells. Under these conditions HUVEC express the receptor ICAM-1, whereas HDMEC express both CD36 and ICAM-1.

Under static conditions, there was no significant difference in the level of binding to either HUVEC or HDMEC of PRBC incubated for 4 h with artesunate (500 nM) compared to the untreated controls to (Fig. 3.4a,b). Following 8 h exposure, a slight reduction in binding was seen and following 24 h artesunate treatment adhesion to both HUVEC ($P<0.01$) and HDMEC ($P<0.05$) was reduced to ~30% of control levels (Fig. 3.4a, b).

Essentially the same binding phenotypes were observed for adhesion measured under flow, with up to 8 h exposure to artesunate (500 nM) not significantly affecting adhesion to both HUVEC or HDMEC, whilst 24 h exposure to artesunate (500 nM) did reduce the levels of binding to both cell types to 25-30% of control levels (Fig. 3.4c,d).

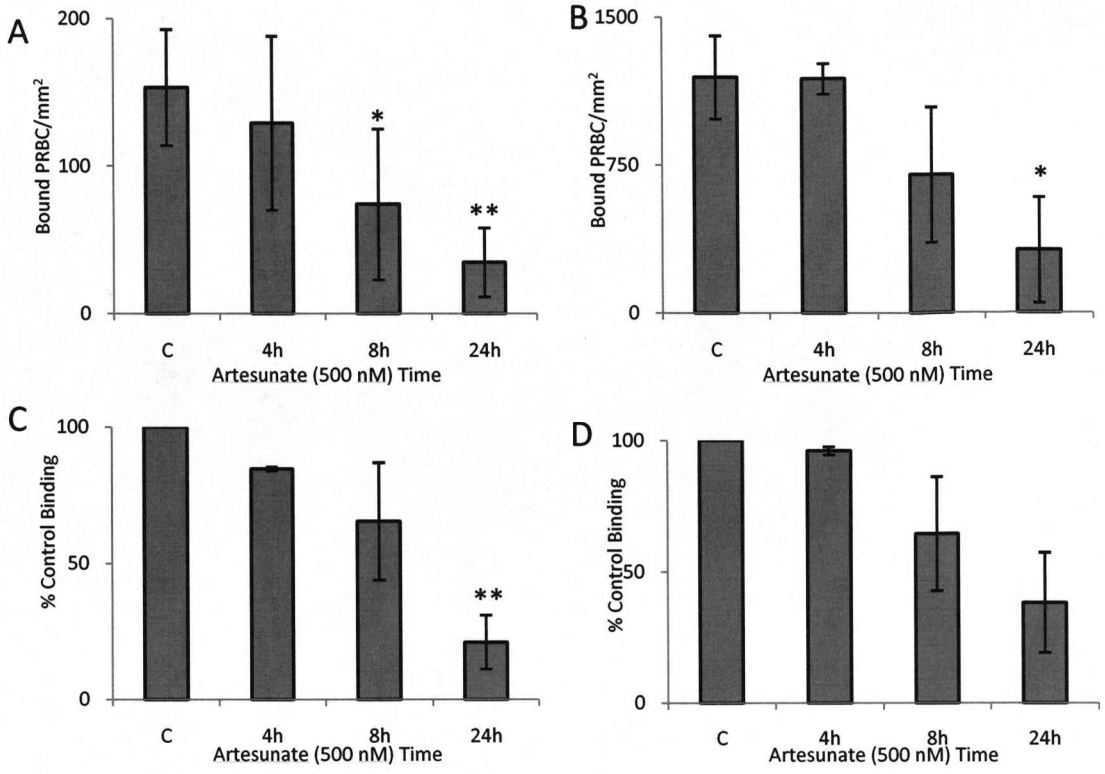

Figure 3.4. Adhesion of ItG to endothelial cells in static and flow adhesion assays. A) HUVEC static B) HDMEC static C) HUVEC Flow D) HDMEC flow. All results are the mean ± SD of three independent triplicate experiments. Statistical significance compared to control levels of adhesion (C, untreated trophozoites) are indicated * $P<0.05$, ** $P<0.01$ as measured by two-tailed independent T test.

Cytoadherence of A4 and CS2 isolates

Similar results to those seen for ItG adhesion after artesunate treatment were also seen with two other parasite isolates. A4, like ItG, binds to both ICAM-1 and CD36 but generally at lower levels than ItG (Gray et al., 2003). The adhesion of A4 to ICAM-1 protein under flow and to HDMEC under static conditions was assessed. No significant reduction in adhesion was seen after 8 h treatment of trophozoite-stage parasites with artesunate (500 nM); however, after 24 hours treatment adhesion was reduced to 25-30% of controls (Fig. 3.5a,b). Additionally the CSA binding strain CS2 (Cooke et al., 1996) was assayed for cytoadherence to CSA protein under flow conditions. No reduction in adhesion was seen after 8 h treatment and significant adhesion at around 25% positive control levels was observed after 24 h treatment (Fig. 3.5c).

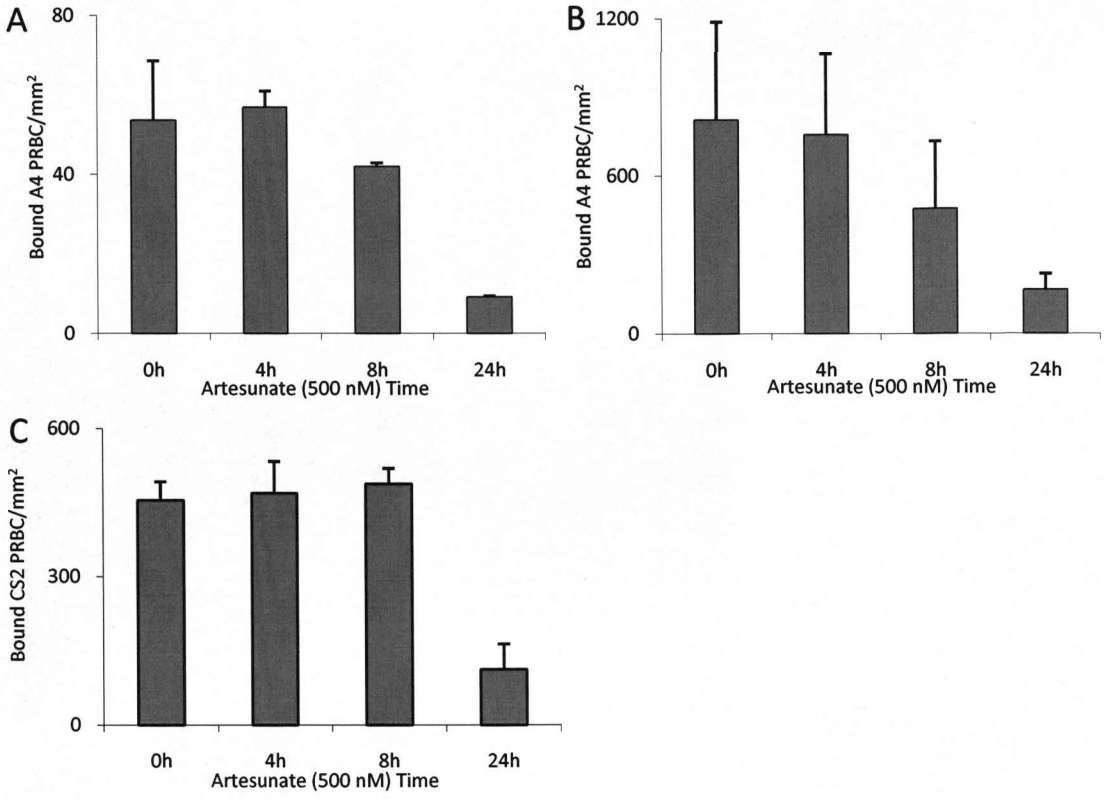

Figure 3.5. Adhesion of A4 and CS2 PRBC. A) Adhesion of A4 PRBC to ICAM-1 under flow conditions and B) adhesion of A4 to HDMEC under static conditions. C) Adhesion of CS2 PRBC to chondroitin sulphate A (CSA) under flow conditions.

PfEMP-1 distribution on the surface of drug treated *P. falciparum* PRBC visualised using confocal microscopy

To determine whether the continued ability of non-viable parasites to adhere is due to the persistence of the PfEMP-1 complex on the infected erythrocyte membrane the distribution of PfEMP-1 on the surface of the A4 PRBC was measured. We used the monoclonal antibody mAb BC6 which is specific for the a surface epitope of the PfEMP-1 A4var41 variant (Roberts et al., 1992), and used unfixed (i.e. non-permeabilised) cells and laser scanning confocal microscopy to observe the A4 PRBC surface. The characteristic punctate distribution of PfEMP-1 on the outer erythrocytic membrane was observed (Fig. 3.6). Membrane permeant ethidium bromide was used to label infected red blood cells, and no BC6 labelling of uninfected cells was observed. Similarly, the specificity of the BC6 antibody for the A4var41 PfEMP-1 was such that other strains, i.e. ItG, showed no positive labelling (result not shown – see also flow cytometry data below). Qualitatively, the distribution of PfEMP-1 was not observably different in A4 PRBC treated for up to 24 h with 500 nM artesunate (Fig. 3.6).

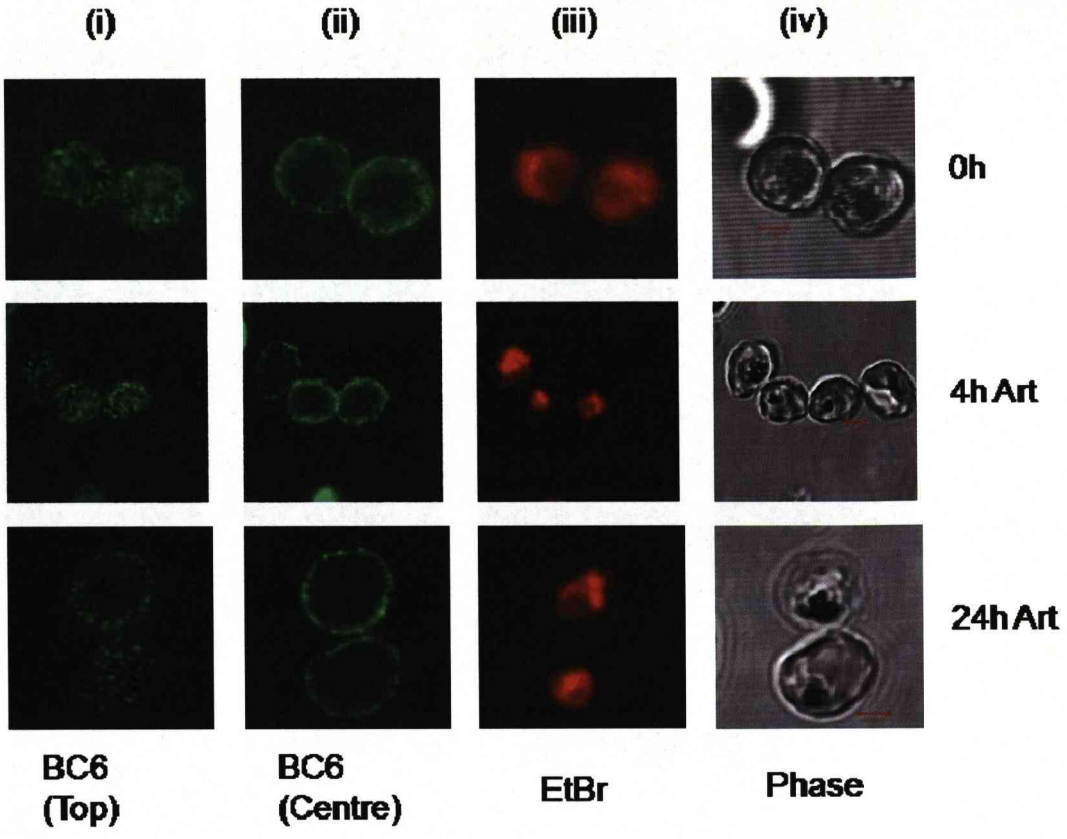

Figure 3.6. Confocal fluorescence microscopy of PfEMP-1 distribution on the surface of A4 PRBC after 4 and 24 h artesunate treatment. Panels i and ii show PfEMP-1 labelled with BC6 antibody and alexa488 conjugated secondary antibody, top (i) and centre (ii) plane of z-stack sections. Panel iii shows ethidium bromide labelling of parasites, and iv) shows bright field (phase) images. Scale bar (2 μM) shown on respective phase images.

Quantitation of PfEMP-1 on the PRBC Surface by Flow Cytometry

PRBC were labelled using immunofluorescence for PfEMP-1 using the BC6 monoclonal antibody as above and an alexa488 coupled secondary antibody detectable using flow cytometry in the FL1 channel. The PRBC could be identified from uninfected RBC using ethidium bromide in the FL2 channel. We confirmed that 75-85% of A4 PRBC used in these experiments expressed detectable levels of A4var41 PfEMP-1 (Fig. 3.7). The specificity of the BC6 antibody for the A4var41 PfEMP-1 was confirmed as there was no staining visible on uninfected RBC, or the antigenically distinct ItG isolate (Fig 3.7).

Following treatment with artesunate (500 nM, 24 h), the mean fluorescence of PfEMP-1 surface positive PRBC was reduced to approximately 65% the level of untreated cells ($P < 0.01$, n=3, Fig. 3.8). This is based on the geometic mean of those cells falling the upper right quadrant as illustrated in figure 3.7. During an experiment there was no

change in the percentage of PRBC that expressed PfEMP-1 (i.e. as illustrated in figure 3.7, the number of cells falling in the upper right quadrant (Ethidium bromide positive and PfEMP-1 positive) compared with upper left (Ethidium bromide positive but PfEMP-1 negative)). Notably, PfEMP-1 could still be detected on PRBC surface after 4 days treatment (data not shown).

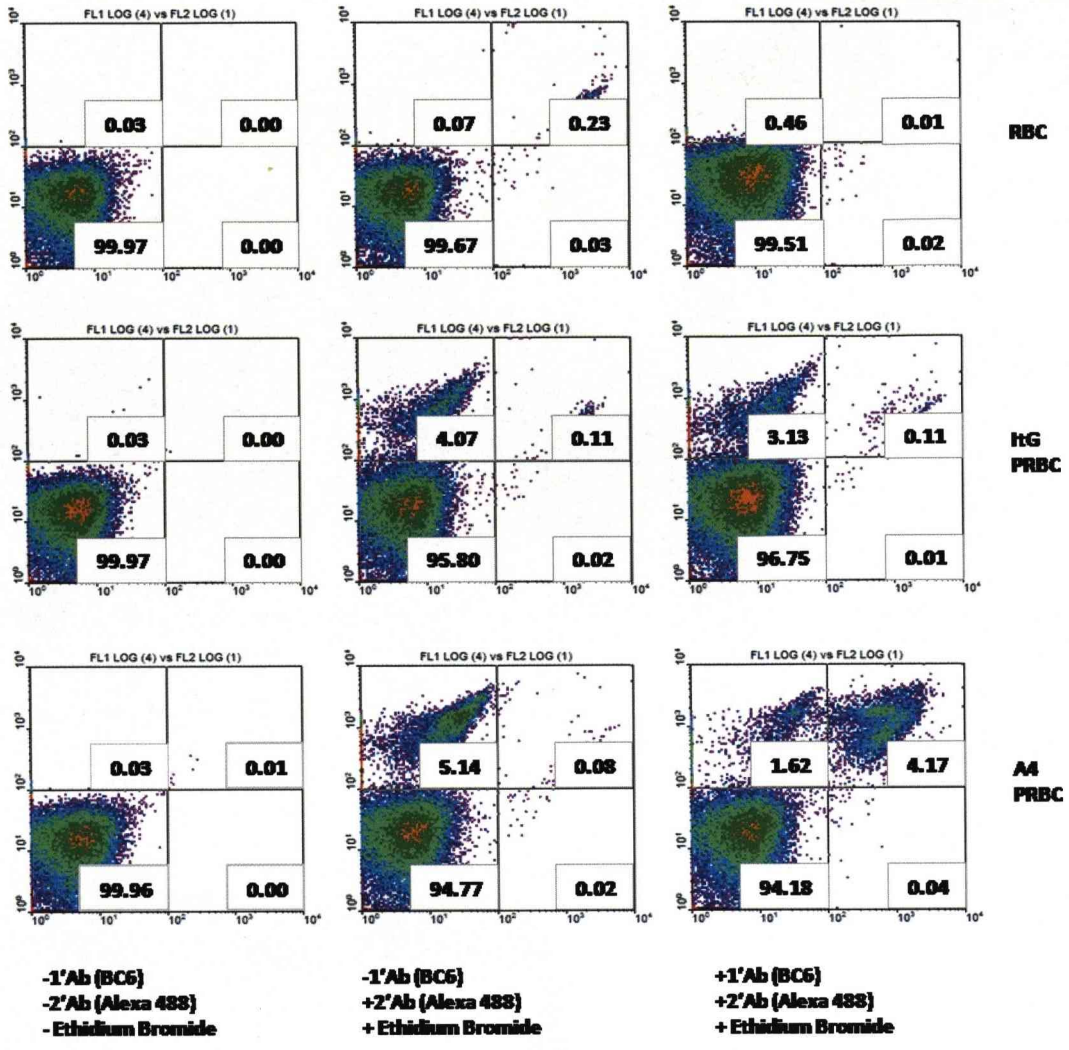

Figure 3.7. Density plots of flow cytometry experiments for surface PfEMP-1 measurement. Cells were immunolabeled for A4var41 specific PfEMP-1 using BC6 primary antibody and an alexa488 coupled secondary antibody. PRBC were labelled using ethidium bromide. Fluorescence in the FL1 channel (Alexa 488, PfEMP-1) is indicated on the x axis, and FL2 (ethidium bromide, indicating parasitized cells) on the Y axis. RBC populations were gated to exclude debris and cell clumps on a forward scatter/side scatter plot before analysis of FL1/FL2 levels. Result representative of several independent experiments. Each plot is the analysis of at least 100,000 RBC. Quadrant lines are identical for each plot, and the values indicate the percentage of the population falling within each quadrant.

Cells in each quadrant can be described as follows:

Lower Left – Uninfected RBC, A4var41 PfEMP-1 Negative

Lower Right – Uninfected RBC, A4var41 PfEMP-1 Positive

Upper Left – PRBC, A4var41 PfEMP-1 Negative

Upper Right – PRBC, A4var41 PfEMP-1 Positive

The top row shows uninfected RBC only, the middle row ItG infected PRBC culture, and bottom row A4 infected PRBC culture. Left column shows no staining, middle shown ethidium bromide, and alexa conjugated antibody staining and right column shows staining including primary BC6 antibody.

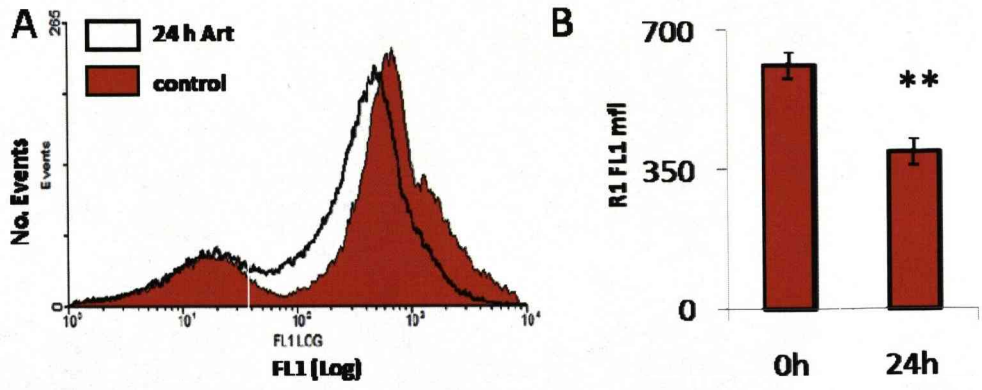

Figure 3.8. PfEMP-1 levels by flow cytometry after artesunate treatment. A) Representative histogram of FL1 mean fluorescence intensity of control (solid) and 24h artesunate treated cells (open black). Gated on ethidium bromide positive population (quadrant upper left and upper right as in figure 3.7). B) mean fluorescence intensity of PfEMP-1 positive populations (quadrant upper right as in figure 3.7) after 24h artesunate treatment, mean ± SD three independent experiments. **P<0.01 as determined by T test compared to untreated control.

Use of other antimalarials – Determination of IC_{50} values

Other antimalarials were chosen to assess cytoadherence of non-viable *P. falciparum.* The IC_{50} for each chosen antimalarial was assessed on ItG using a standard fluorometric (Sybr Green) assay (Bennett et al., 2004, Smilkstein et al., 2004). The IC_{50} values determined for ItG were within the range previously reported for each drug, and the concentration chosen for use was based on previously published peak plasma concentrations (see methods section for references) and were mostly well above the IC_{50} value (Table 3.1). Figure 3.9 show representative IC_{50} curves.

Drug	IC(50) on ItG Mean of three assays +/- SD	Concentration Used
Artesunate	1.6 nM +/- 1.5	500 nM
Quinine	382.48 nM +/- 140	25 µM
Lumefantrine	233.29 nM	15 µM
Piperaquine	52.4 nM +/- 8.16	100 nM

Table 3.1. IC50 values calculated on ItG. Similar results were seen for A4 (not shown). Mean IC_{50} for each is the mean of three independent triplicate experiments. (*lumefantrine two experiments)

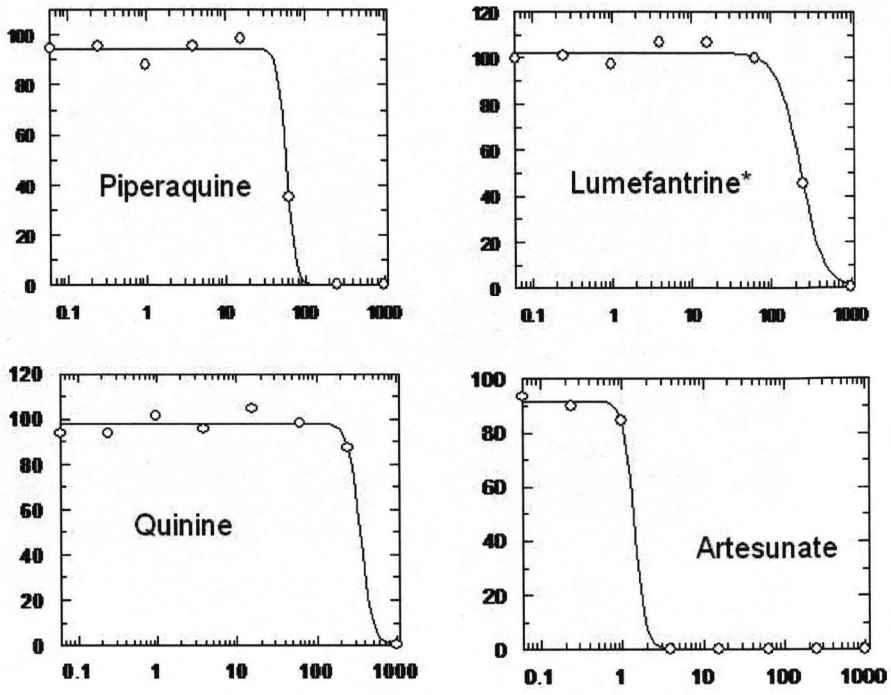

Figure 3.9. Representative IC50 curves on ItG. Y axis shows percentage fluorescence (representing growth) compared to untreated control, and x axis indicates concentration of drug (nM). Each point represents the mean of triplicate values.

Cytoadherence to ICAM-1 after treatment of TROPHOZOITE-stage PRBC with a range of antimalarials

Adhesion of PRBC to ICAM-1 protein under flow was assayed following 4, 8 and 24 h drug treatment of trophozoite (24 h post invasion) stage parasites. The antimalarial drugs tested were artesunate (500 nM), quinine (25 μM), lumefantrine (15 μM) and piperaquine (100 nM).

The binding phenotypes for all treatments were observed to be very similar, with no significant difference in binding observable after 4 h drug exposure (Fig. 3.10a). As observed previously, a small reduction in binding was observed for parasites exposed to 8 h artesunate (Fig. 3.10b) but no significant difference relative to control cells was observed for all other drugs (Fig. 3.10b). A significant reduction in PRBC binding was observed following 24 h exposure to all of the drugs, with binding ~30% of control levels (Fig. 3.10c).

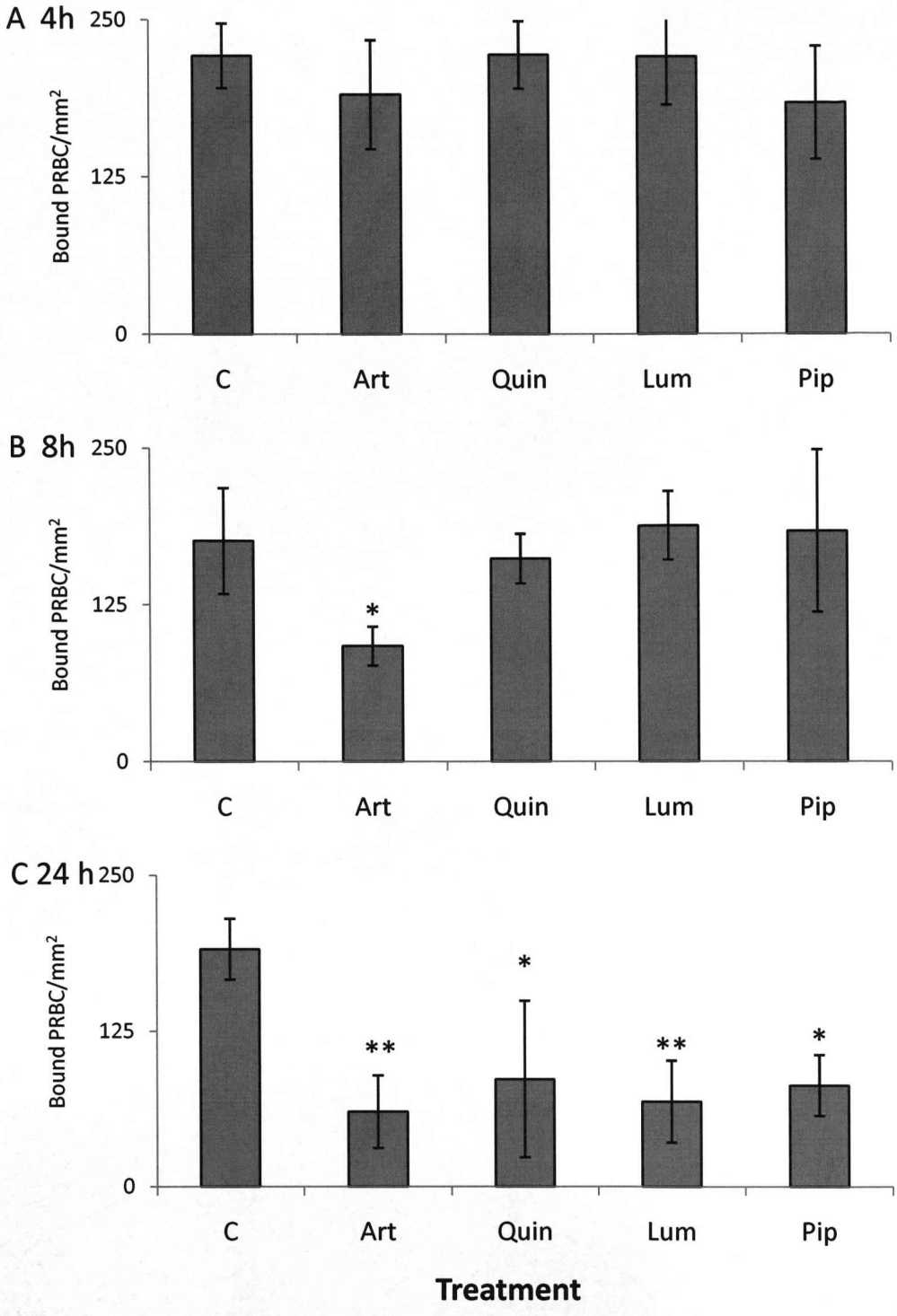

Figure 3.10. Adhesion of drug-treated trophozoite-stage ItG PRBC to ICAM-1 under flow conditions. Adhesion shown as bound PRBC/mm^2 to ICAM-1 under flow conditions after 4 h (A), 8 h (B), and 24 h (C) treatment of trophozoites stage parasites with artesunate (art) 500 nM, quinine (Quin) 25 μM, lumefantrine (Lum) 15 μM, and piperaquine (Pip) 100 nM or untreated trophozoite stage PRBC (C). * $P<0.05$ and **$P<0.01$ as determined by T test compared to untreated control.

Cytoadherence to ICAM-1 after treatment of RING-stage PRBC with a range of antimalarials

As the antimalarial drugs used in this study have different pharmacodynamic properties, especially in regards to cell cycle specificity, binding experiments to ICAM-1 under flow conditions were repeated as described above but drug exposure was performed on ring-stage (12 h post invasion) parasite cultures. These younger ring stage parasites represent the pre-cytoadherent circulating population.

Adhesion to ICAM-1 protein under flow, was determined after 24 h exposure of ring-stage PRBC to artesunate (500 nM), quinine (25 μM), lumefantrine (15 μM) and piperaquine (100 nM) relative to untreated control cells. Significant differences were observed between the various treatments. Artesunate treated parasites were unable to mature to trophozoites and non-viable ring parasites were observed after 24 h exposure (Fig. 3.11a), whilst quinine and lumefantrine treated parasites matured to late trophozoites before dying and appearing pyknotic (Fig. 3.11a). Piperaquine treated parasites appeared to show an intermediate amount of development to late ring/early trophozoite before becoming non-viable. Binding experiments revealed that control parasites allowed to develop for 24 h from ring stage parasites to trophozoites displayed characteristic levels of adhesion whilst control ring-stage parasites, as expected, displayed a very low level of cytoadherence (Fig. 3.11b). Artesunate treated parasites, which had failed to mature showed little cytoadherence, whilst quinine and lumefantrine treated parasites displayed high levels of adhesion comparable to control trophozoite-stage PRBC (Fig. 3.11b). Treatment of parasites with piperaquine resulted in intermediate levels of binding, ~50% of control levels (Fig. 3.11b).

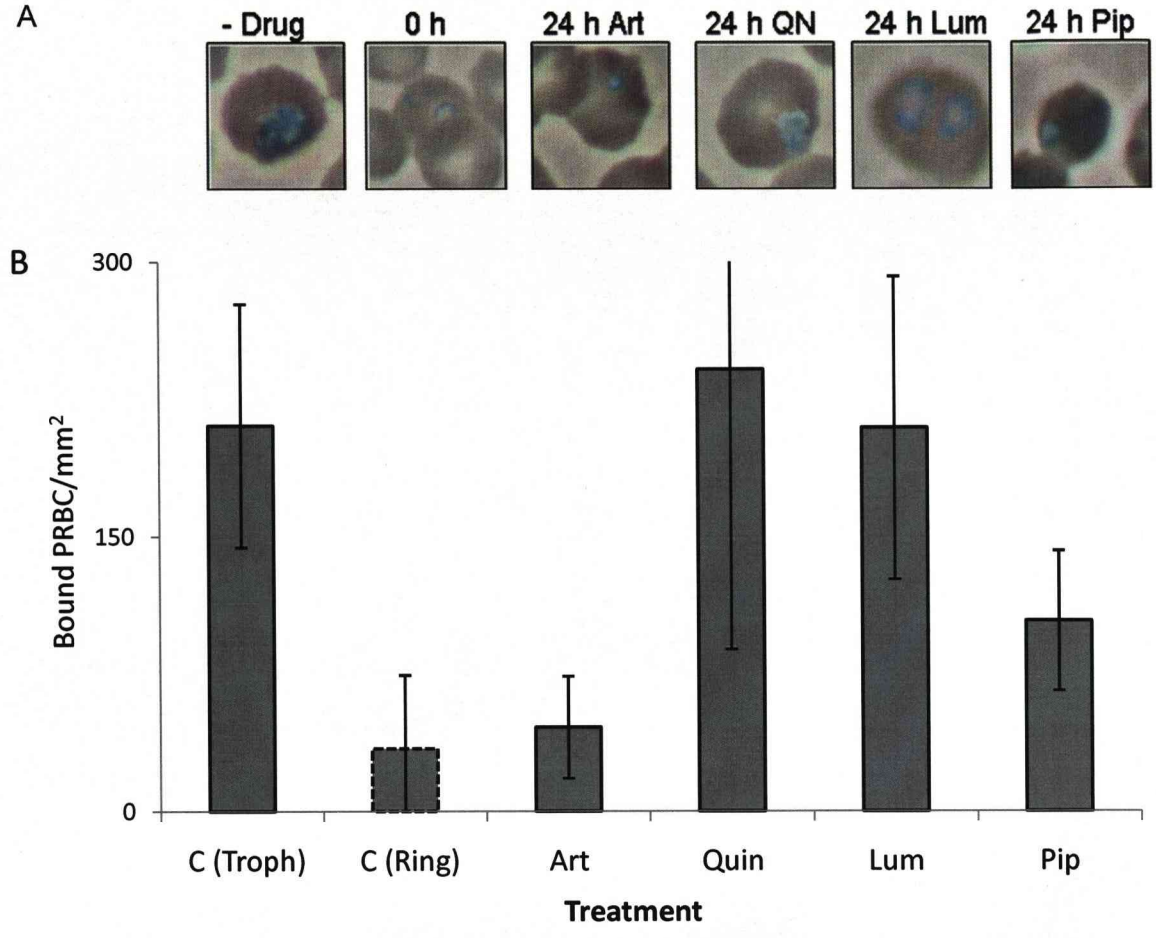

Figure 3.11. Adhesion to ICAM-1 after addition of drugs to ring stages A) Giemsa stained smear of parasites at time of assay, 24h after administration of drug to RING-stage parasites. B) Adhesion to ICAM-1 under flow conditions 24h after administration of drugs to RING stage parasites (Ring stage control is alternate day culture (highlighted by dashed outline), Troph control is 24 h – drug). Mean ± SD three independent triplicate experiments.

3-4 DISCUSSION

We have assessed the ability of non-viable parasites killed by antimalarial treatments to cytoadhere, and our data demonstrate that *P. falciparum* PRBC are capable of cytoadherence for at least 24 h after lethal dosages of a range of antimalarial drugs. The antimalarial drugs tested in this study were artesunate, quinine, lumefantrine and piperaquine at clinically relevant concentrations, chosen to mimic peak plasma drug levels. The cytoadherence phenotype of PRBC was measured using both static and flow assays and using a range of parasite strains (ItG, A4 and CS2) against purified receptor proteins and endothelial cells (HUVEC and HDMEC).

These observations are consistent with observations from a previous ultrastructural analysis of brains from patients with cerebral malaria (Pongponratn et al., 2003) which suggested that they observe morphologically damaged parasites adhered to cerebral endothelium, consistent with parasite death in-situ and maintained ability to adhere.

Consistent with the continued ability to cytoadhere, we observed the characteristic punctate distribution of PfEMP-1 on the surface of *P. falciparum* PRBC following 24 h antimalarial treatment, as shown in figure 3.6. For the measurement of PfEMP-1 levels the A4 isolate was used (rather than the ItG isolate as used for the majority of the adhesion assays) due to the availability of the specific antibody for the A4var41 PfEMP-1. Importantly this antibody, BC6, recognises an external epitope of the PfEMP-1 protein. The ItG isolate was originally used in adhesion assays due to the generally higher level of binding seen to ICAM-1 compared to A4 (Gray et al., 2003). In adhesion assays after drug treatment of A4 the effect of drug treatment on adhesion levels was comparable to the result that we had seen with ItG (Fig 3.5a).

These data illustrate the stability of the changes made to the red blood cell by the parasite such that the remodelling of the infected red blood cells is maintained after the parasite is rendered non-viable. Nevertheless, quantification of the PfEMP-1 levels on PRBC surface showed some reduction after drug treatment, consistent with a degree of degradation/loss of the protein. This reduction in PfEMP-1, combined with potential degradation of other cytoadherence-related parasite proteins, i.e. KAHRP, could explain the reduced levels of cytoadherence seen after 24 h treatment. This could be comparable to that seen when mutations are present in haemoglobin, i.e. haemoglobin C (HbC), and sickle haemoglobin (HbS). In these cases infected erythrocytes show a

slightly reduced and abnormal display of PfEMP-1 and concurrently reduced cytoadherence (Cholera *et al.*, 2008).

Testing a selection of antimalarial drugs showed that the effect on mature trophozoite cytoadherence was not drug specific; the same level of adhesion was seen after 24 h treatment with all of the antimalarials tested.

Previously published data has implied that antimalarial drugs including quinine, halofantrine, artesunate and artemether reduce cytoadherence and/or rosetting in *P. falciparum* (Udomsangpetch *et al.*, 1996). In the Udomsangpetch et al. study, parasites (presumably ring stage circulating parasites) were exposed to antimalarial drugs for 2 to 24 h, washed and grown in culture until control parasites (no drug exposure) were at late trophozoite/early schizont stage. Depending on the drug treatment these authors reported a range of binding phenotypes, most notably parasites exposed to artesunate and artemether were reported to result in ≥50% inhibition of both cytoadherence (static assay) and rosetting. It was concluded by these authors that the observed differences between the various drugs on parasite adhesion probably reflected differences in the susceptibility of asexual stage parasites to antimalarials.

We show a similar effect when drug treatment is added to ring stage (young) parasites. As shown in figure 3.11, the various antimalarials used inhibited parasite growth at different stages of the asexual cycle. This is consistent with previous pharmacodynamic data on the mode of action of these drugs, with artesunate known to be active against young ring stage parasites (Skinner et al., 1996, O'Neill & Posner, 2004). The activity of lumefantrine, quinine and piperaquine, however, is based on the disruption of haem detoxification (Biagini *et al.*, 2003, Biagini *et al.*, 2005) occurring later in development during haemoglobin digestion by trophozoite stage parasites (Skinner et al., 1996, Hempelmann *et al.*, 2003, O'Neill *et al.*, 2006). The pharmacodynamic differences of these drugs when administered to ring stage parasites results in mismatched comparisons of binding phenotypes. Essentially the assays measured the adhesion of dead ring stage parasites for the artesunate treated group, against the adhesion of dead trophozoite stage parasites for the quinine, lumefantrine and piperaquine treated groups. The significant reduction in adhesion seen by artesunate treated parasites in figure 3.11 and in the Udomsangpetch et al., study (Udomsangpetch et al., 1996) reflect that these groups consist of ring stage parasites that have insufficient levels of binding proteins, i.e. PfEMP-1, exported to the erythrocyte membrane surface at that stage.

The significance of this difference between ring-stage acting artemisinin based treatments and treatments that only act on mature parasites (i.e. quinine), has also been discussed in the context of the SEAQUAMAT trial. This trial compared artemisinin and quinine for the treatment of severe malaria in adults and showed an advantage for artesunate over quinine, particularly in groups with high parasitaemia (Dondorp et al., 2005). The authors suggest that this advantage may stem from the mechanism of action of artesunate on immature parasites thereby preventing the next round of sequestration. Our *in vitro* results support this hypothesis.

The significant observation of our study is that dead parasites retain the ability to cytoadhere irrespective of the antimalarial treatment administered. However, we can hypothesise that administration of fast, ring stage acting antimalarials such as artesunate will result in a reduction of de novo cytoadherence when administered *in vivo* due to the ability to prevent maturation of parasites to mature cytoadherent stages. The persistence of cytoadherence for many hours after treatment, despite rapid effects on parasite viability fits with, and may in part explain, the clinical observation of a high mortality rate in first 24 hours after hospital admission after initiation of antimalarial treatment (Marsh et al., 1995). Even though treatment is killing the parasites rapidly, we show that they would still be able to cytoadhere 24 h following treatment, potentially still contributing to disease pathology.

3-5 LIMITATIONS AND FURTHER WORK

We have shown that the PfEMP-1 exported to the surface of the RBC by the parasite is still present for many hours following antimalarial treatment, illustrating the permanent nature of the changes made to the red blood cell by the parasite. In chapter 4 we further investigate the issue of RBC remodelling by the parasite and the effect of antimalarial treatment by looking at the reduced deformability of the PRBC.

A major limitation of this work is that we have been unable to look at the effect of antimalarial treatment on the adhesion of already bound PRBC. We have treated trophozoite stage parasites and then assessed for adhesion up to 24 hours following treatment. In vivo these trophozoite-stage PRBC would already be expected to be sequestered in microvasculature. We have been able to show that PRBC are still capable of adhesion after up to 24 hours treatment, but we have not been able to show whether already bound PRBC would stay adhered. A long term co-culture model would need to be developed to enable us to perform these experiments. We would expect, however, that having shown PRBC are still capable of binding, the interaction between already bound PRBC and endothelium would be maintained to at least the same degree of binding ability that we have seen.

It is conceivable that the predicted continued sequestration of non-viable *P. falciparum* PRBC in patient microvasculature may be targeted by adjuvant therapies designed to prevent or ideally reverse cytoadherence. Indeed, studies have recently been performed with Levamisole, which was shown to reduce sequestration of *P. falciparum* in patients by inhibition of CD36 dephosphorylation (Dondorp et al., 2007). The potential for adjunct therapies to reverse cytoadherence (specifically ICAM-1 mediated cytoadherence) is investigated in chapter 6.

An important consequence of adhesion to host endothelium is signalling events within endothelial cells that may contribute to pathogenesis (Chakravorty et al., 2008). It has been shown that adhesion of PRBC to endothelial cells induces signalling pathways, one example of which results in induction of ICAM-1 on the surface of the endothelial cell (Chakravorty et al., 2007, Tripathi et al., 2006). Preliminary experiments to address whether non-viable PRBC were able to stimulate adhesion molecule expression in a similar way suggested dead PRBC elicited the same response as viable PRBC, however, in our experiments the basal level of simulation by live PRBC was very low

resulting in little confidence when trying to detect differences between live and dead PRBC (results not shown).

Similarly the stimulation of MAP kinase signalling pathways has been shown by endothelial cells in response to cytoadherence (Jenkins *et al.*, 2007b), however, in our experiments the difference between uninfected RBC and PRBC signalling was very small resulting in little confidence in detecting differences (or stating none) between signalling events induced by live PRBC or dead PRBC (results not shown).

Another widely discussed consequence of adhesion to endothelial cells is the induction of apoptosis in the endothelial cells. There are three ways in which endothelial cell apoptosis may be stimulated in malaria. It has been shown that soluble parasite derived factors can induce apoptosis in endothelial cells (Wilson et al., 2008). Host derived inflammatory factors may influence apoptosis (Combes et al., 2006, Wassmer et al., 2006a, Wassmer et al., 2006b, Hemmer et al., 2005), and there is also evidence suggesting that cytoadherence of PRBC can directly induce apoptosis. However, all published data showing *in vitro* evidence for cytoadherence-induced apoptosis is based on assays using human lung endothelial cells (Toure et al., 2008, Pino et al., 2003, Siau et al., 2007). Our adhesion experiments performed on endothelial cells of different origins, HUVEC and HDMEC (and HBEC, not shown), do not result in superficial evidence for endothelial cell disruption in conditions used for our experiments. Indeed, it has been suggested that there is upregulation of pathways protective against apoptosis following cytoadherence in HUVEC (Chakravorty et al., 2007). We have not attempted to assay for apoptosis after adhesion, but suggest that established models for induction of apoptosis, i.e. lung endothelial cells would have to be used to compare the ability of live and antimalarial-treated PRBC to induce any potential cytoadherence-related apoptosis.

We would hypothesise that there would be no difference in the cytoadherence-related signalling between live or dead PRBC adhesion. This would strengthen an argument for an adjunct therapy to prevent or reverse sequestration since it may also prevent endothelial cell damage resulting from cytoadherence related signalling events.

3-6 CONCLUSIONS

In summary, this study has assessed the cytoadherence capability of drug-killed *P. falciparum* PRBC. We demonstrate that non-viable parasites, irrespective of treatment retain the ability to cytoadhere for up to 24 h. This phenomenon is due to the stability of the changes made to the host red blood cell by the parasite, as illustrated by the continued presence of PfEMP-1 on the surface of PRBC after loss of parasite viability. The continued capacity for cytoadherence, and presence of surface PfEMP-1 indicates that the remodelling of the red blood cell is stable.

The continued capacity for cytoadherence could contribute to disease pathology following treatment. It is hypothesised that fast and ring stage acting antimalarials such as the endoperoxides may be therapeutically more favourable by their ability to prevent de novo adhesion, but adjunctive therapy strategies that can also reverse cytoadherence may also be advantageous in addressing the high mortality seen in severe malaria early after hospital admission.

CHAPTER 4 - LORCA ANALYSIS OF THE DEFORMABILITY OF PRBC AFTER ANTIMALARIAL TREATMENT

4-1 INTRODUCTION

The many modifications that a parasite makes to the host RBC are described in detail in chapter 1. As well becoming able to cytoadhere and sequester in microvasculature a PRBC is much more rigid, i.e. less deformable than an uninfected RBC (Cooke et al., 2001, Cranston et al., 1984). The reduction in deformability of PRBC could lead to reduced flow through small vessels contributing to the severe pathologies of malaria. In support of this, a correlation between a lack of deformability and clinical severity has been shown (Dondorp et al., 1997, Dondorp, 2008). Decreased rigidity of PRBC is a particular problem in microvasculature already partially blocked by cytoadherent PRBC. Whereas deformable RBC can squeeze through partially blocked vessels more rigid PRBC are less able to do so and more likely to lead to obstructions (Shelby *et al.*, 2003, Dondorp et al., 2008).

A major determinant of the reduced deformability of a PRBC is the increased membrane cytoskeleton rigidity, which results both from modification of host proteins, and insertion of parasite proteins into the membrane. The role of knobs in the increased rigidity of PRBC has been shown using knobless clones (Paulitschke & Nash, 1993), and using micropipette techniques the involvement of two knob-associated proteins KAHRP and PfEMP-3 has been demonstrated (Glenister et al., 2002). Other possible contributors to the decreased deformability of a PRBC include the physical presence of the parasite as well as a potential increased cytoplasmic viscosity, partly due to increased solute uptake via NPP (Cooke et al., 2001, Cranston et al., 1984). Cytoplasmic viscosity has been suggested to contribute to the determination of deformability of uninfected RBC along with membrane stiffness (Mohandas *et al.*, 1980, Kon *et al.*, 1987).

It has been suggested that there is a decreased deformability of uninfected RBC from malaria patients (Dondorp et al., 1997, Griffiths *et al.*, 2001), or RBC that have been in contact with parasite derived factors (Naumann *et al.*, 1991). However, other studies did not see this (Paulitschke & Nash, 1993, Glenister et al., 2002). These differences may reflect both the different techniques used to measure the deformability of PRBC, and differences between *in vivo*, and *in vitro* studies.

It is widely thought that it is the increased rigidity of *P. falciparum* PRBC that is responsible for the ability of the spleen to recognise and clear PRBC, either through destruction of the PRBC, or through removal of the parasite by the mechanical process of pitting (Engwerda et al., 2005, Chotivanich et al., 2002, Angus et al., 1997, Safeukui et al., 2008). Sequestration in the microvasculature is a mechanism by which the rigid PRBC can escape from circulation and avoid passage through, and destruction by, the spleen. *P. vivax* PRBC are not known to cytoadhere, so remain in peripheral circulation during intraerythrocytic development. However, *P. vivax* infection does not lead to increased rigidity of the PRBC. It has been suggested that the *P. vivax* PRBC are more deformable than uninfected RBC (Suwanarusk et al., 2004). An alternative mechanism for avoidance of splenic clearance of *P. vivax* PRBC has been proposed based on adhesion of *P. vivax* PRBC to barrier cells in the spleen preventing entry into the spleen and subsequent clearance (del Portillo et al., 2004), but there is little (or no) evidence to support this.

In chapter 3 we were interested in the effect of antimalarial treatment on the ability of PRBC to cytoadhere. Since deformability of PRBC has also been correlated with severity of disease (Dondorp et al., 1997, Dondorp, 2008), we were interested in looking at the effect that antimalarial treatment of trophozoite stage PRBC may have on deformability. The effect of antimalarial treatment on the deformability of PRBC has been looked at in one previous study (Chotivanich *et al.*, 2000), where it was suggested that treatment of ring-stage parasites with artesunate restricted further decreases in deformability, while quinine had a more limited effect. However, this study assessed deformability of PRBC after addition of drugs to ring stage parasites. We sought to extend this study by analysing the effect of antimalarial treatment on the already remodelled trophozoite-stage PRBC, to see whether, as with cytoadherence, the phenotype is maintained after the parasite is rendered non-viable by antimalarial treatment.

Methods to Study Deformability

Three main techniques have been used to study deformability of RBC/PRBC. Micropipette studies can be used to measure the elasticity of the cell membrane, which is determined by the membrane cytoskeleton (Nash *et al.*, 1989). This is calculated by measuring the shear elastic modulus, the length of membrane that can be aspirated into a micropipette (1 – 1.5 μm diameter) with a given pressure (Fig 4.1 a) (Glenister et al., 2002).

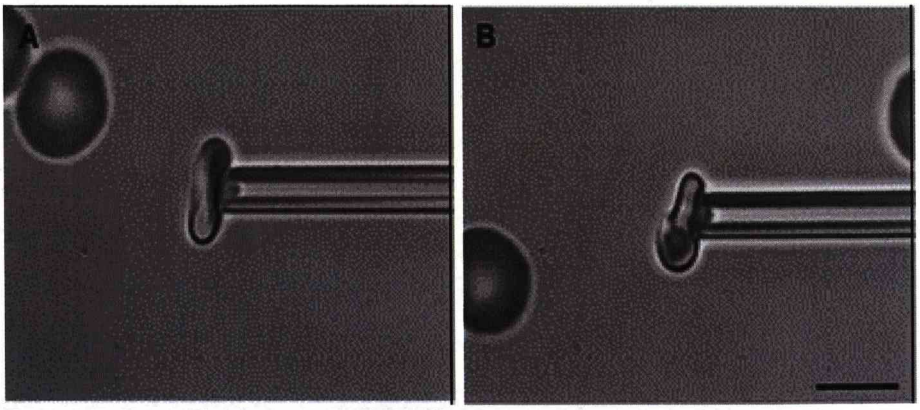

Figure 4.1 a. Determination of membrane shear elastic modulus by micropipette aspiration.
(Figure taken from Glenister 2002 (Glenister et al., 2002)) Bright-field digitally captured images of a typical micropipette (1.3 μm internal diameter) used for determination of the shear elastic modulus of (A) an uninfected RBC and (B) an RBC infected with a mature *P. falciparum* parasite. A portion of the RBC membrane aspirated into the pipette can be visualized clearly, shown here at a pressure of 2.0mm H2O (A) and 4.0 mm H2O (B). Scale bar, 5 μm.

Microfluidics methods measure ability of cells to pass through narrow constrictions in channels (Fig. 4.1 b) (Shelby et al., 2003). Video capturing of cells passing through microfluidic channels of 2 to 8 μm allow visualisation of channel blockage by PRBC at different stages.

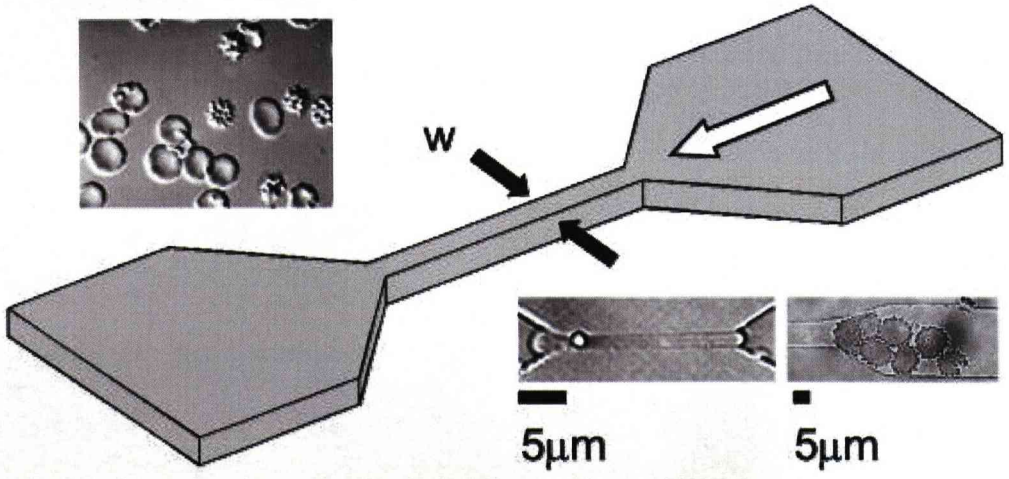

Figure 4.1 b. Schematic of a microchannel. (Figure taken from Shelby 2003 (Shelby et al., 2003))
Schematic illustrating the geometry of the microchannel. The constricted segment of the channel (width denoted by w) was sized at 8, 6, 4, and 2 μm. The white arrow represents the direction of fluid flow. (*Upper Inset*)A differential interference contrast image of normal (smooth) and infected RBCs. (*Lower Left Inset*) A normal RBC passing through a 2-μm constriction. (*Lower Right Inset*) Infected RBCs blocking a 6-μm constriction.

The method that we have used to measure deformability is an ektacytometry based method (Mohandas et al., 1980, Dondorp et al., 1997) using a Laser-assisted Optical Rotational Cell Analyzer (Lorca) (http://www.mechatronics.nl/products/lorrca/index.htm). In this technique, erythrocytes are placed in a narrow gap between two concentric cylinders and the outer cylinder rotates to create a defined shear force on the red blood cells. A camera connected to a computer allows images to be taken, each image being a composite of 500 cells. The elongation index of the red blood cells, the ratio of length to width, is calculated on a composite image of the 500 cells and used as the measure of deformability at a given shear stress (Fig. 4.1c). Deformability is generally measured over a range of shear stress from 0.5 Pa to 30 Pa, and at each shear stress the mean of 50 calculations is used.

Whereas micropipette studies generally measure the deformability of the cell membrane/membrane cytoskeleton of individual cells, Lorca enables measurement of the deformability of the whole cell. Microfluidics based studies also measure the deformability of the cell as a whole. However, microfluidics studies show the effect of the deformability changes of individual cells since relatively few rigid cells in a population will be sufficient to block the microfluidic channels. Lorca enables the study of the deformability of the whole population of RBC and allows us to quantitate the deformability changes based on a large number of RBC.

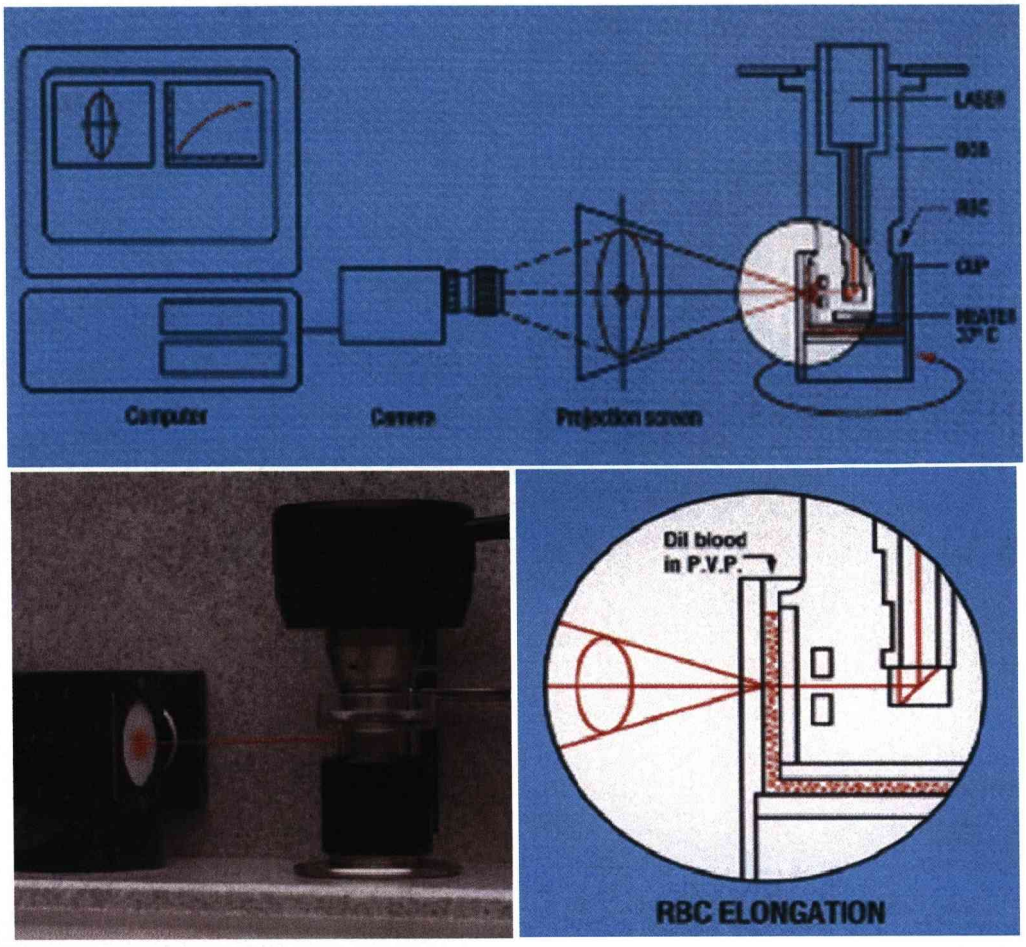

Figure 4.1 c. Laser-assisted Optical Rotational Cell Analyzer (Lorca).

A thin layer of red blood cell suspension is sheared between two concentric cylinders. The rotation of the outer cylinder (cup) causes deformation (elongation) of the red blood cells. The laser-beam diffraction pattern is detected with a video camera and analyzed by a computer. (http://www.mechatronics.nl/products/lorrca/index.htm).

In this study our main aim was to investigate the rigidity of PRBC after treatment with antimalarials. This is a continuation of work presented in chapter 3 which looked at cytoadherence after antimalarial treatment. The chapter is split into three main parts; first, controls to establish our use of Lorca to measure PRBC rigidity; second, the effect of antimalarial treatment on deformability; and finally, we have attempted to dissect the relative contributions of the various changes in the erythrocyte brought on by parasite infection, i.e. changes to cytoplasmic viscosity and membrane changes.

4-2 MATERIALS AND METHODS

Strains and Culture conditions

P. falciparum was maintained under standard conditions as described in chapter 2. Most experiments were performed using the A4 isolate, and some repeated using ItG as described in chapter 2. The KAHRP deletion strain 1C10 was also used. This isolate originates from A4 but has a truncation on chromosome 2 resulting in a deletion of the KAHRP gene and a knobless phenotype (Horrocks et al., 2005). This phenotype was confirmed by assessing the (lack of) ability to float on Plasmagel. Parasite cultures were regularly synchronised at ring stage using sorbitol lysis, however this was shown to affect the deformability of cells for up to 2 days post treatment so synchronisation using this technique was carried at least 3 days before experiments.

Enrichment for Trophozoite stage parasites

Since Lorca measures the deformability of a population of RBC, PRBC were generally enriched to 50% parasitaemia. In order to enrich a culture either Plasmagel flotation or magnetic separation method was used as described in methods chapter 2. After enrichment using either method PRBC were washed three times in incomplete medium, parasitaemia was checked and PRBC diluted to usually 50% using matched cultured uninfected red blood cells. Final parasitaemia achieved was checked before experiments.

LORCA (Laser assisted optical rotational cell analyser)

A 12.5 µl pellet of packed RBC at 50% parasitaemia was diluted with 12.5 µl of serum free medium and mixed gently into 5 ml of polyvinylpyrrolidone (PVP) at 37°C. Before taking readings the Lorca was washed twice with 1 ml sample. 1 ml sample was then added to the Lorca and measurements taken over 9 shear stress levels from 0.5 Pa to 30 Pa. The cup was washed once more with 1 ml sample before a second reading was taken. All measurements were taken at 37°C. Control uninfected red blood cells were measured along with each experiment. Plasmagel treatment was shown to have no effect on the deformability of red blood cells (data not shown), however, in all experiments control RBC were exposed to Plasmagel as for PRBC before deformability assays.

Uninfected cell experiments

To assess the deformability of uninfected cells in a culture, a culture at 12% parasitaemia at mid-trophozoite stage was cleared of infected cells by magnetic

purification using the VarioMacs magnet and column as described in methods chapter 2. Unbound cells were collected from the magnet and the process repeated 2 – 4 times. This resulted in cultures containing <2% infected cells, and remaining infected cells were usually infected with early stage parasites (as determined by Giemsa stained smear).

Drug Treatment

Artesunate was made up to a 10 mM stock solution in dimethylsufoxide (DMSO) immediately prior to the experiment. Drug was added to mid-trophozoite stage cultures into normal culture medium to 500 nM. Furosemide and quinine stocks were made to 100 mM stock solution and used at 100 µM concentrations. For long drug incubations drugs were added to normal culture parasitaemia (8 -12%) and cultures Plasmagel enriched at appropriate time points before Lorca analysis. For short time course furosemide experiments parasites were enriched prior to drug addition, and drug was added to the enriched culture. The untreated control was from the same enrichment.

Sorbitol Lysis

As a control for the activity of furosemide the ability of sorbitol to lyse trophozoite-stage PRBC was quantitated by measuring absorbance at 546 nm. A 20 µl sample of cells at 50% haematocrit and 50% parasitaemia was mixed with 180 µl 5% sorbitol, or 180 µl 5% sorbitol plus 100 µM furosemide, or incomplete medium. Uninfected red blood cells were used as controls in the same way. At 5 minute time points a 30 µl sample was taken, centrifuged at 5000 rpm for 1 min in an Eppendorf centrifuge and 25 µl of the supernatant diluted with 475 µl of appropriate buffer and transferred to a cuvette. Absorbance at 546 nm was measured compared to relevant blank.

4-3 RESULTS

Part I - Deformability of PRBC

Deformability of PRBC is reduced compared to uninfected red blood cells

We first confirmed that we could use Lorca to detect deformability changes in PRBC. Unless otherwise stated we have used the A4 *P. falciparum* isolate. We could detect the reduced deformability of un-enriched PRBC cultures at a parasitaemia of 12%, as well as on Plasmagel enriched cultures at 50% parasitaemia (Fig. 4.2a).

To determine whether parasites alter the deformability of uninfected cells within a culture, a culture at 12% parasitaemia mid-trophozoite stage was cleared of infected cells using magnetic separation, and deformability of these parasite-exposed but uninfected RBC were measured against a control RBC "culture" that had been maintained in parallel. PRBC from this culture measured at 50% parasitaemia after magnetic enrichment showed a significant reduction in deformability compared to control RBC. Uninfected RBC from within the culture were no less deformable than the control RBC (Fig. 4.2b). Results are shown for A4 PRBC, showing the mean and standard error of three experiments in separate batches of blood. The same result was obtained using the KAHRP deletion isolate 1C10 in two experiments (data not shown).

In figure 4.2a we established that we could detect reduced deformability at a parasitaemia as low as 12%, although the difference was clearer at higher parasitaemia. To detect deformability of a culture from ring through to schizont stages we used a culture at a relatively high parasitaemia but that still enabled healthy growth, in this case we used a culture at 17% parasitaemia. Deformability of a culture of PRBC measured (un-enriched) at 17% parasitaemia over the 48 hour parasite growth cycle showed increasing rigidity of red cells as the parasite matures (Fig. 4.2c). When comparing freshly washed RBC with RBC that had been stored washed at 4°C for > 1 week it was apparent that stored washed RBC become more rigid with time. (see also Fig. 4.5c). However, over the time course of the experiments (< 48h), there was no appreciable difference in the deformability of RBC maintained under culture conditions (Fig. 4.2d).

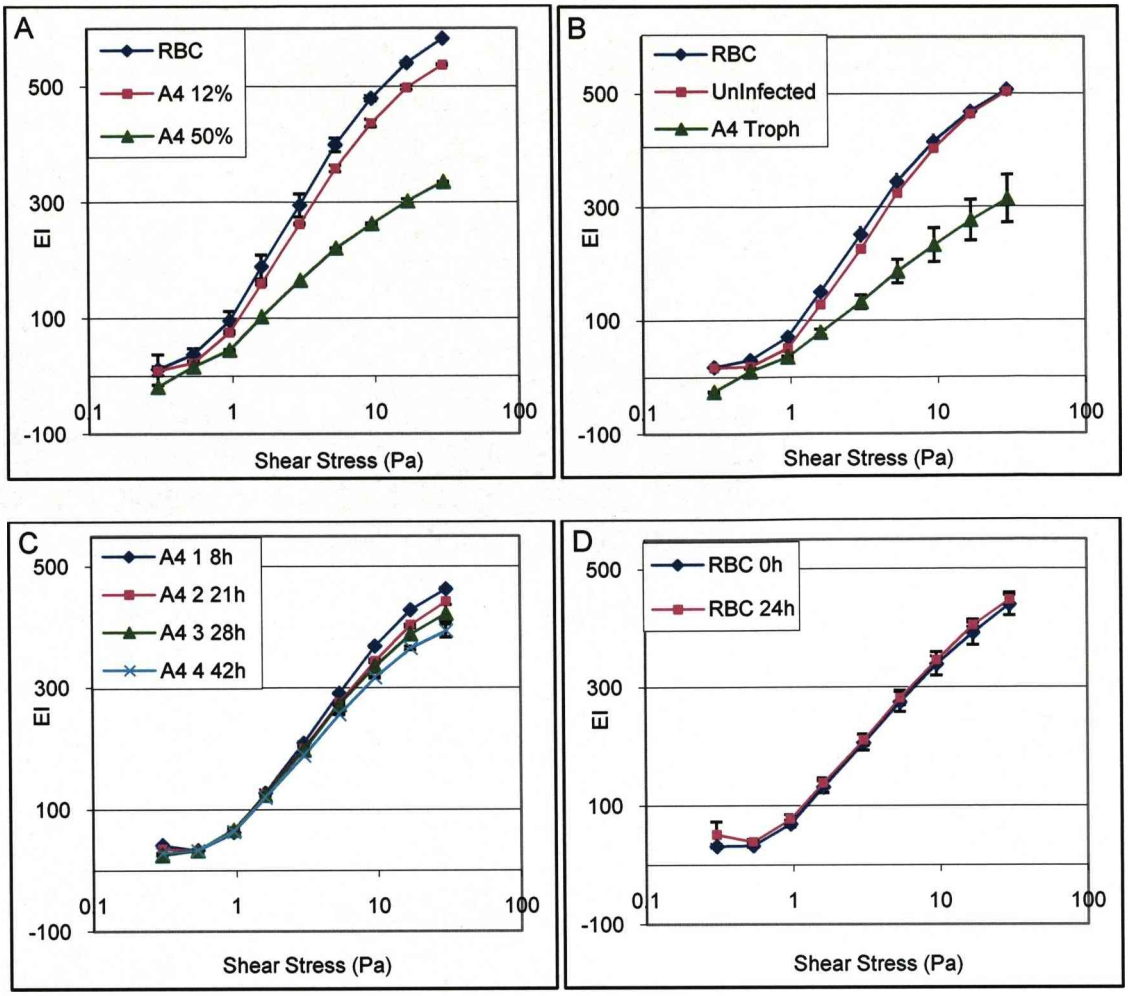

Figure 4.2. Deformability of PRBC A) A4 PRBC measured at 12% parasitaemia and 50% parasitaemia are less deformable than uninfected red cells. Y axis indicates deformability measured as an Elongation index (EI). B) Uninfected RBC that have been exposed to PRBC (Uninfected) are not detectably different to red cells from control culture (RBC). Mean ±SE of three independent experiments. C) Deformability of parasite culture reduces as parasites mature. Time indicates hours post-invasion from 8h (rings) to 42h (mature schizonts). Measured on an un-enriched culture at 17% parasitaemia. Representative of two independent experiments D) Deformability of control RBC "cultured" in parallel is unchanged over the experimental time course.

These results indicate that we can use Lorca to detect the expected increase in PRBC rigidity during parasite maturation, and suggest that the changes we are measuring in a population are due to parasite induced changes to the infected red blood cells only.

Deformability of PRBC after 24 hours antimalarial treatment is slightly reduced compared to the culture before treatment

The deformability of mature trophozoite stage PRBC (28-30h post invasion) was measured before addition of artesunate (500 nM) to the culture. After 24 hours the original culture with no artesunate had matured and reinvaded to ring stage parasites, however, as expected, the artesunate treated parasites were dead and pyknotic (as determined by Giemsa stained smears, not shown). PRBC could still be enriched using Plasmagel after 24h artesunate treatment indicating maintenance of knob structures. The deformability of uninfected red blood cells was not affected by 24 hours artesunate treatment, and the deformability of artesunate treated PRBC was slightly reduced at most shear stress compared to the 0 h time point (Fig. 4.3a). Figure 4.3 a shows the mean and standard error of three independent experiments. Deformability of stage-matched (mature trophozoite) untreated PRBC at the 24 hour time point was not significantly different to the 0 h time point (not shown).

The apparent increase in the deformability of PRBC at very low shear stress is most likely an artefact due to the presence of free parasites in the culture resulting from low levels (< 10%) lysis of PRBC after artesunate treatment.

Artesunate and quinine were next added to young trophozoites (~18 h post invasion) and deformability assessed after 24 hours with or without treatment. The artesunate treated parasites had become slightly more rigid than the starting culture but had not progressed to become as rigid as the untreated PRBC now matured to schizonts. Quinine treated PRBC showed a similar result, although had become slightly more rigid (Fig. 4.3b). The same result was seen in two independent experiments, figure 4.3b shows one representative experiment.

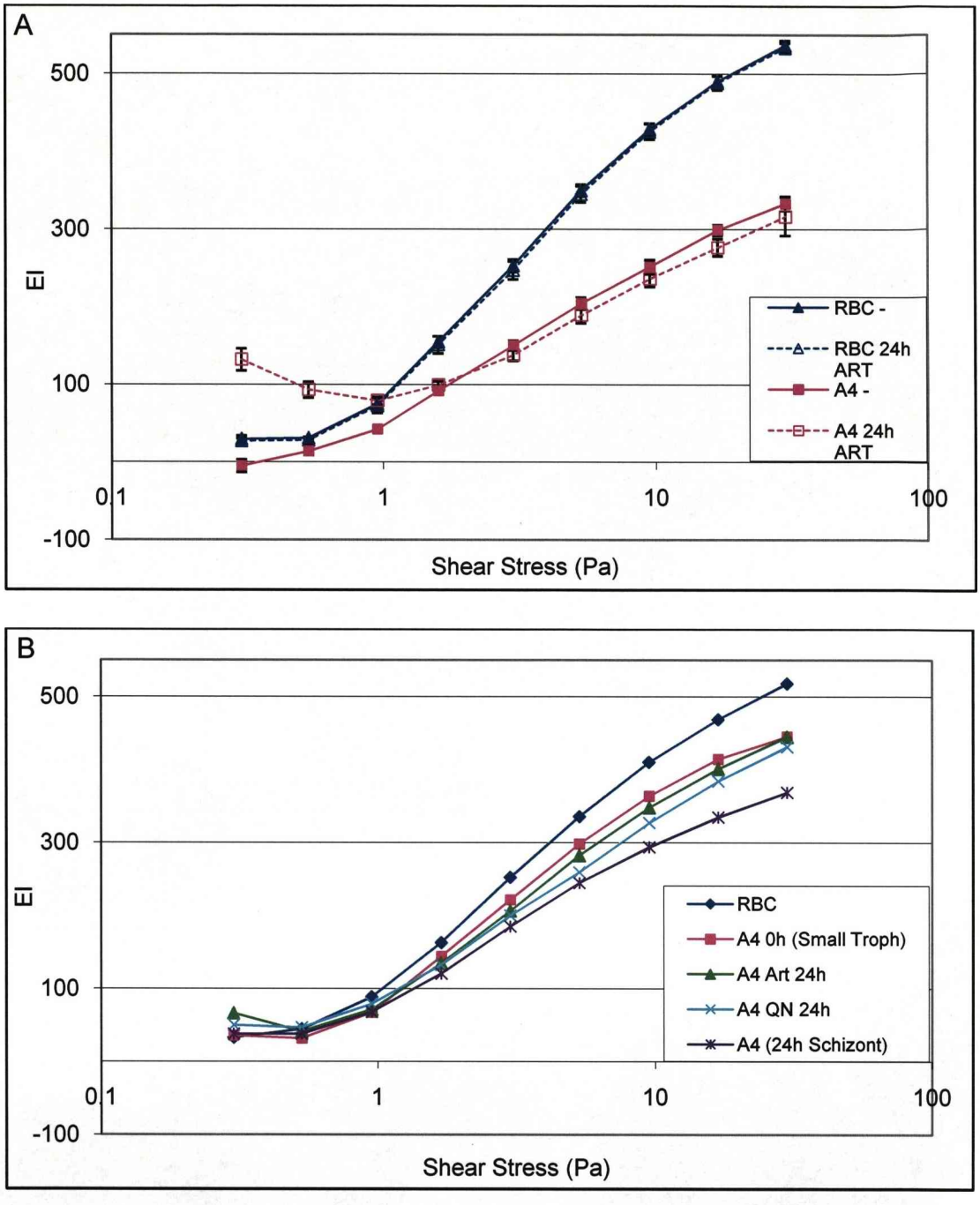

Figure 4.3. Effect of antimalarials on PRBC deformability A) A4 PRBC after 24 hour incubation with artesunate (500 nM) (treated at mid-trophozoite stage) show a slight reduction in deformability when compared to untreated PRBC, mean ± SE of three independent duplicate experiments. A4 - represents mean of both the 0h culture and 24h stage matched untreated alternate culture which were not significantly different. B) Deformability of artesunate (Art 24h) or quinine treated (QN 24 h) PRBC 24 hours after addition of drug to young trophozoites (0 h Small troph) compared with untreated PRBC which had matured to schizonts (24h Schizont).

KAHRP deletion strain appears to be more deformable than A4

To confirm the role of parasite induced membrane cytoskeletal changes in the increased rigidity of PRBC we used a knobless strain. The KAHRP deletion strain 1C10 (Horrocks et al., 2005) was used as an isolate with a compromised membrane cytoskeletal structure. This isolate is a derivative of A4 with a truncation of chromosome 2 that knocks out KAHRP and therefore knobs, resulting in reduced membrane rigidity compared to wild type PRBC (Horrocks et al., 2005, Glenister et al., 2002, Paulitschke & Nash, 1993). The 1C10 KAHRP deletion PRBC ($PRBC^{\Delta KAHRP}$) showed virtually no ability to float on Plasmagel when compared directly over 30 minutes with wild type A4 PRBC ($PRBC^{A4}$), an observation that is consistent with the lack of knobs. The $PRBC^{\Delta KAHRP}$ were less rigid than $PRBC^{A4}$. Over several independent Lorca experiments the difference between $PRBC^{A4}$ and $PRBC^{\Delta KAHRP}$ deformability at mid-trophozoite stage was confirmed (Fig. 4.4). Figure 4.4 a illustrates the deformability of $PRBC^{A4}$ and $PRBC^{\Delta KAHRP}$ at mature trophozoite stage (~ 28 h post invasion) compared to uninfected RBC, shown is the mean and standard error of three independent experiments. Figure 4.4 b illustrates Giemsa stains pictures of PRBC used from one experiment. As seen with $PRBC^{A4}$, the $PRBC^{\Delta KAHRP}$ did not affect the deformability of uninfected cells within a culture (two experiments, data not shown).

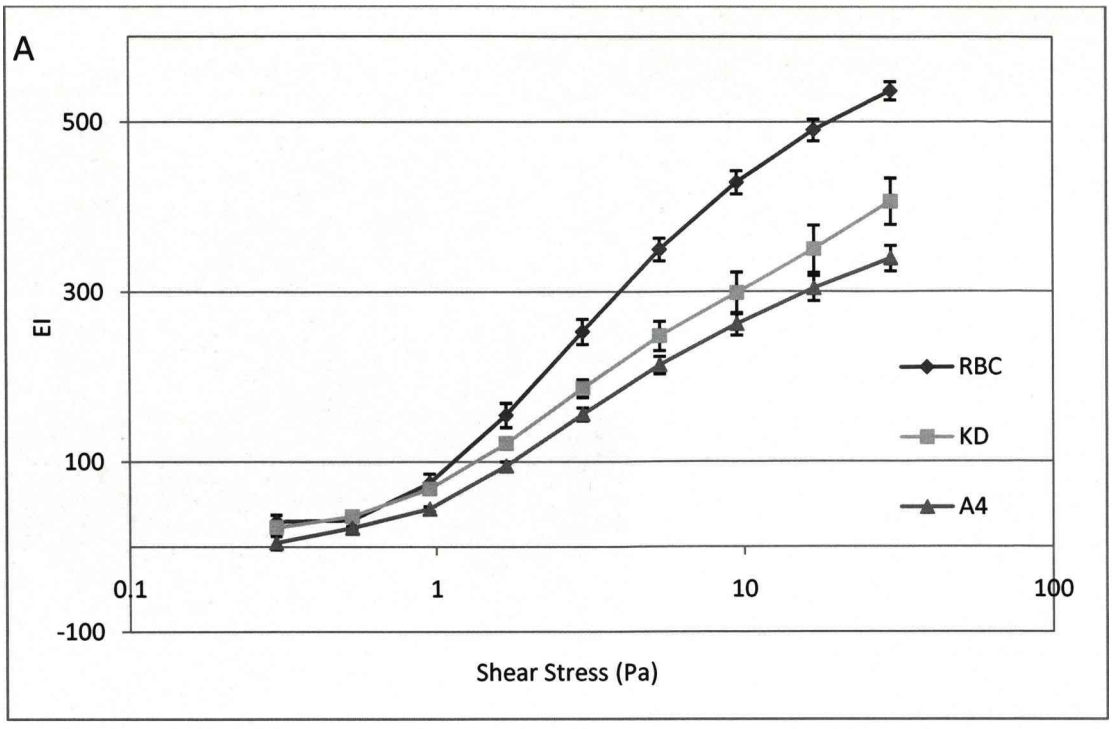

B

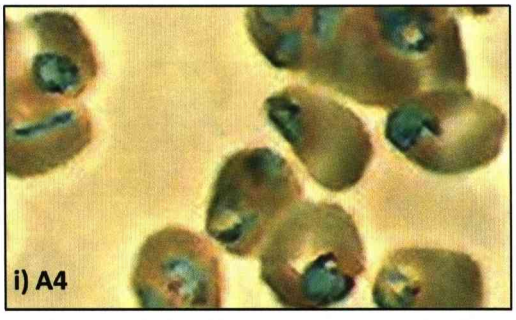

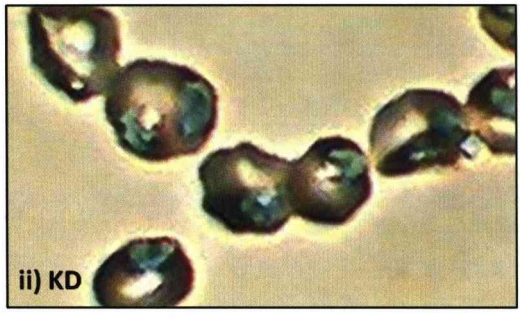

Figure 4.4. Effect of KAHRP deletion on deformability of PRBC A) Comparison of A4 and KD at mid-trophozoite stage. Mean of results from three independent experiments (six readings) Error bars show standard error. B) Giemsa stained smears illustrating stage matched mid-trophozoite PRBC after Plasmagel enrichment. i)A4 and ii) KAHRP deletion PRBC 1C10 (KD)

Furosemide blocks NPP and Inhibits Solute Uptake in PRBC

The increased uptake of solutes through parasite induced new permeability pathways (NPP) in PRBC could be responsible for an altered cytoplasmic viscosity (Kirk et al., 1994), which could contribute to the increased rigidity of PRBC (Cooke et al., 2001). Furosemide is a diuretic that has been suggested to lead to a slight reduction in RBC mean cell volume (MCV) (Biagini unpublished) (although this has not been seen in other studies (Hasler & Reinhart, 1998)), but is also known to block NPP in PRBC

(Kirk et al., 1994). To test the effect of NPP on overall PRBC deformability we used furosemide to inhibit NPP then assayed deformability of PRBC using Lorca.

The activity of furosemide on PRBC was confirmed by the blocking of sorbitol lysis of $PRBC^{A4}$. Sorbitol lysis of mature PRBC selectively is dependent on the NPP which allow uptake of sorbitol normally excluded from RBC, and result in the lysis of PRBC. This lysis can be quantitated by measuring haemoglobin release through its absorption at 545 nm. On addition of 5% sorbitol to mid-trophozoite stage $PRBC^{A4}$ a rapid lysis of the PRBC could be measured (Fig. 4.5a). However on addition of furosemide this lysis was almost completely inhibited showing that furosemide can inhibit NPP as measured by the ability to inhibit osmotic lysis due to sorbitol uptake.

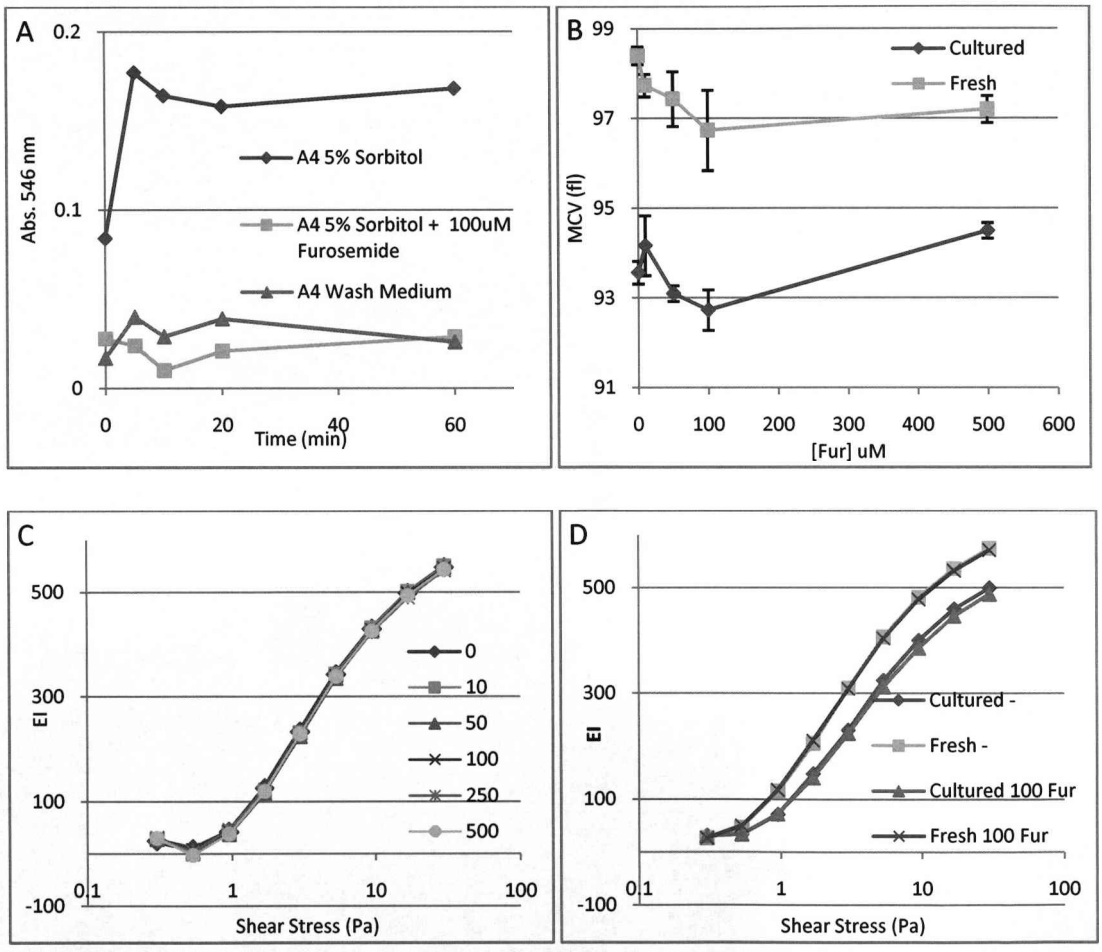

Figure 4.5. Effect of furosemide on RBC and PRBC A) Inhibition of sorbitol lysis of PRBC by 100 µM furosemide. Lysis measured by absorbance of released haemoglobin at 456 nm (y axis). B) Reduction in mean cell volume (MCV) measured in fl (y axis) of RBC incubated in furosemide for 15 min. Comparison of fresh and mock-cultured RBC. Mean +- SD of three readings. C) Deformability of RBC after incubation in varying concentrations, 0 to 500 µM, of furosemide for 15 min. D) Deformability of fresh and mock-cultured RBC after incubation with or without 100 µM furosemide for 15 min.

Furosemide does not affect RBC deformability

To determine whether furosemide affected RBC, furosemide was added in concentrations from 10 to 500 µM for 15 minutes. We first measure the mean cell volume (MCV) and found a very slight reduction in MCV after 15 min exposure to between 10 µM and 100 µM furosemide (figure 4.5b). The same effect on MCV was seen after 2 h incubation (not shown). However, no effect on deformability of RBC was observed (Fig. 4.5c). The same result was seen with the 100 µM furosemide at time points of 2h, 4h and 24 hours (not shown). We found that cultured RBC were smaller and less deformable than fresh RBC (Fig 4.5c and d). However, the effect of furosemide treatment on RBC in terms of MCV and deformability was the same for both fresh and "cultured" cells.

Furosemide does not affect the deformability of A4 PRBC

The deformability of $PRBC^{A4}$ was not affected by treatment with furosemide for 15 minutes (Fig. 4.6 a). This was consistent in four independent experiments, and also at longer time points (up to 4 hours). After 24 hours incubation in furosemide parasites had developed to schizonts but not burst and showed low deformability consistent with the mature schizont stage (not shown).

Furosemide reduces the rigidity of KAHRP deletion PRBC

Interestingly 15 min incubation with 100 µM furosemide did lead to a reduction in the rigidity of $PRBC^{\Delta KAHRP}$. This was consistent in three independent experiments, shown in figure 4.6a is one representative experiment and figure 4.6b shows the mean and SD of the relative change in EI for for furosemide treated compared to untreated control for three independent experiments. A third parasite isolate, ItG which, like A4, has knobs, showed similar results to that seen with A4.

This showed that as well as being initially more deformable than the wild type PRBC, the PRBC with a compromised membrane structure were more sensitive to furosemide treatment, resulting in an even further reduced rigidity compared to wild type PRBC.

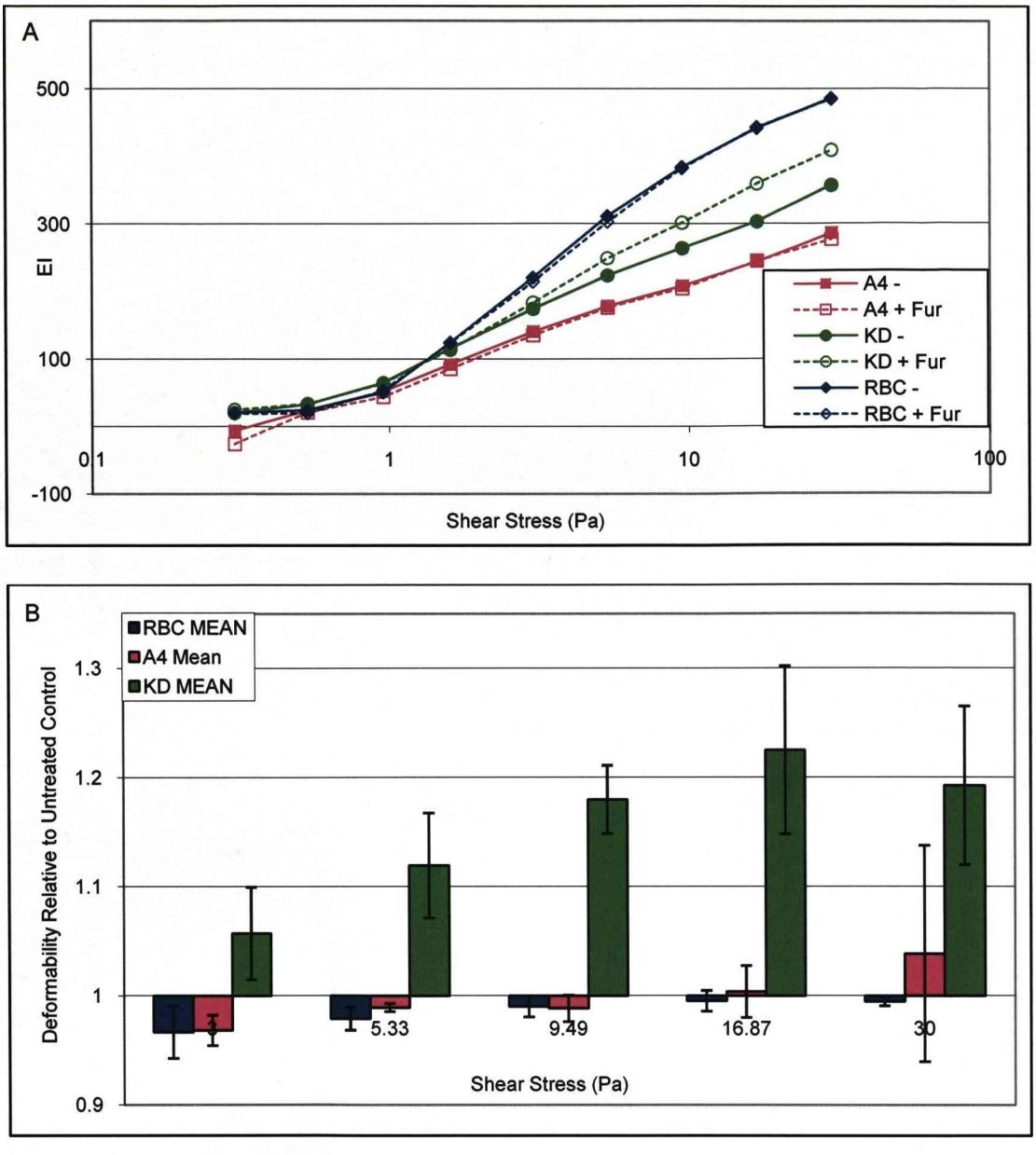

Figure 4.6. Effect of furosemide on A4 and KD PRBC A) Representative experiment comparing A4 (A4) and the KAHRP Deletion strain 1C10 (KD) PRBC after furosemide treatment. B) Relative deformability compared to untreated control for a range of shear stress for A4 and KAHRP deletion PRBC mean ± SD for three independent experiments.

4-4 DISCUSSION

As the increased rigidity of PRBC compared to uninfected RBC is thought to be a contributory factor to severe disease we looked at these changes, and the effect that antimalarial treatment may have on the deformability of PRBC. Our significant result is that the deformability of PRBC remains reduced compared to uninfected RBC for long after the administration of antimalarial treatment.

There are three main parts to this chapter that will be discussed: firstly, the series of controls that established Lorca as a tool to measure the deformability of PRBC. Secondly, the main aim of the study which was to determine the effect of antimalarial treatment on PRBC; and finally some insights into the contributory factors to the increased rigidity of PRBC.

Part I – Use of Lorca to measure PRBC Deformability

Deformability of A4 PRBC compared to uninfected RBC

The first results presented in this chapter were controls to establish that we could use Lorca to detect the expected deformability changes in PRBC. As Lorca measures the mean rigidity of the whole population of RBC it was important that we established at what parasitaemia we could detect the changes in the PRBC resulting from parasite infection. We could easily detect these changes at 50% parasitaemia after enrichment for trophozoites, but this could also be detected even with fewer parasites present, in cultures at only 12% parasitaemia (Fig. 4.2a). This enabled us to look at the changes in rigidity through parasite development from young ring stages which cannot be easily enriched for, through to schizonts. We were able to show that PRBC became increasingly rigid as the parasites matured (Fig. 4.2c). We had also observed that washed RBC stored at 4°C became increasingly rigid with storage (Fig. 4.6d) so a control "culture" of uninfected red blood cells was always maintained in parallel with the PRBC culture to ensure matched RBC controls. These "cultured" RBC were diluted with fresh RBC in parallel with the PRBC culture and maintained in the same culture conditions. Over the time course of experiments (<48 hours) there was no measurable change in the deformability of uninfected RBC (Fig. 4.2d). For many of the experiments we were enriching for trophozoite-stage PRBC using Plasmagel so we also confirmed that this treatment had no effect on the deformability of uninfected RBC.

Deformability of uninfected RBC from parasite culture

Some previous studies on the deformability of PRBC have also shown that uninfected RBC that have been in contact with PRBC, or exposed to parasite derived factors also show increased rigidity compared to normal uninfected RBC (Dondorp et al., 1997, Naumann et al., 1991). However, other studies have not seen this (Paulitschke & Nash, 1993, Glenister et al., 2002). To test this in our cultures we used the magnetic separation technique to clear a culture of PRBC. After two clearings on the magnet RBC were ~98% uninfected, and the remaining infected cells contained younger parasites.

This cleared culture was compared to uninfected RBC that had been "cultured" in parallel (as described above). Using Lorca we could not detect a significant difference in the deformability of uninfected RBC from the culture, compared to the control uninfected RBC. This was shown over the whole shear stress range from 0.5 Pa to 30 Pa, in several independent experiments and with two parasite isolates (Fig. 4.2 b).

The reduction in deformability of uninfected RBC previously reported could have several explanations. Deformability of uninfected PRBC from patients has been shown (Dondorp et al., 1997, Griffiths et al., 2001) . However, our study is in-vitro so no host-factors are involved. Host responses to infection, including fever (Marinkovic *et al.*, 2008), could cause an increase in rigidity of all RBC, including uninfected.

Changes in deformability of uninfected cells due to 4-hydroxynonenal (HNE) adducts from haemozoin were shown to be detectable (Skorokhod *et al.*, 2007). However, the compound is insoluble so not expected to diffuse to affect a large number of RBC. Only uninfected RBC in close contact with PRBC would likely to be affected by this. If relatively few individual RBC are affected by compounds such as HNE we would not detect this on our system which measures an average deformability of the whole cell population. For the purposes of our experiments, this result, i.e. that we cannot detect changes to uninfected RBC, allows us to say that all the changes that we are measuring using Lorca in our experiments are due to parasite-induced changes to infected PRBC only.

Part II – The effect of antimalarial treatment on the deformability of PRBC

Increased rigidity of PRBC over RBC is maintained after antimalarial treatment

As the increased rigidity of PRBC is possibly linked to the pathophysiology of severe disease we wanted to determine whether the rigidity of PRBC was reversed or maintained after antimalarial treatment. In chapter 3 we established that cytoadherence of PRBC can continue for several hours after antimalarial treatment, and showed that the remodelling of PRBC, including factors responsible for cytoadherence including knobs and PfEMP-1, were maintained after loss of parasite viability. This suggested that the remodelling of the parasite was stable even after loss of parasite viability, and to test this hypothesis further we wanted to determine the effect of antimalarial treatment on the rigidity of the PRBC.

We observed a maintained reduction in deformability of PRBC for 24 hours after artesunate treatment (Fig. 4.3). This result is consistent with a permanent remodelling of the RBC by the parasite, and corresponds well to the results presented in chapter 3 showing the prolonged cytoadherent ability of drug treated parasites.

Artesunate is known to have a very rapid effect on the parasites, and very short exposure times are sufficient to kill parasites (chapter 3). However, the parasites are not immediately affected by the drug (ter Kuile et al., 1993), and as determined by Giemsa staining appear to mature slightly before dying and becoming increasingly pyknotic (as shown in chapter 3, figure 3.1a). By comparing a time course of growing parasite cultures with an artesunate killed culture we suggest that the decrease in deformability seen in drug killed cultures is consistent with a small amount of development of the parasites after treatment. There was little further change in deformability of PRBC if the same culture was compared after 4h and 24h treatment (result not shown), suggesting that no further changes in the parasite deformability occurred after parasite death.

Similar results were seen after treatment with quinine suggesting that the deformability of the PRBC after artesunate treatment remains consistent with the developmental stage of the parasite when the parasite was killed. After drug treatment PRBC remain more rigid than uninfected RBC for at least 24 hours after parasite death. This is consistent with cytoadherence results seen after antimalarial treatment (chapter 3), and confirms that the changes made to the RBC by the parasite are stable for long after the parasite has been killed.

Any pathophysiological effects resulting from the increased rigidity could be occurring for many hours after administration of antimalarials, however, it is also the increased rigidity of PRBC that makes them a target for clearance by the spleen. It has been suggested that mature, circulating PRBC are retained by the spleen for either parasite removal, a mechanical process known as pitting, or for destruction. Furthermore it has recently been shown that a subset of ring-stage PRBC can also be retained by the spleen (Angus et al., 1997, Safeukui et al., 2008). There is also evidence for circulating dead PRBC after artesunate treatment in splenectomised patients (Chotivanich et al., 2002). The increase in the number of observed dead PRBC in patients with no spleen suggests a role for the spleen in destroying PRBC or removing parasites that may be dead and circulating after antimalarial treatments. The maintained increase in PRBC rigidity explains how non-viable PRBC after antimalarial treatment are a target for clearance by the spleen. Although we have shown that cytoadherence can also continue after antimalarial treatment, if desequestration could be achieved releasing PRBC into circulation, (see chapter 6) these remodelled PRBC could still potentially be cleared by the spleen.

Part III – Determinants of increased rigidity of PRBC

As discussed in the introduction there are three main types of technique used to measure deformability of RBC, each giving slightly different information, and having different limitations. One of the advantages of Lorca is that it provides information about the RBC deformability as a whole, whereas micropipette studies are generally restricted to the deformability (or elasticity) of the cell membrane alone. We sought to take advantage of this property of the technique to investigate how different factors contribute to the increased rigidity of the PRBC. While it is known that the increased rigidity of PRBC membrane is an important factor in the increased rigidity of the cell (Paulitschke & Nash, 1993, Glenister et al., 2002), the contribution of other factors, such as the presence of the parasite and the change in composition of the RBC cytoplasm (Cooke et al., 2001, Cranston et al., 1984), has not been previously investigated. The aim of the last series of results presented in this chapter was to determine whether factors other than the increased membrane rigidity are contributing to the observed increase in rigidity of PRBC.

Effect of inhibition of NPP on deformability of infected Red Blood cells.

The lack of organelles in an uninfected RBC, along with a simple cytoplasm comprising mainly of haemoglobin results in a low cytoplasmic viscosity. The viscosity of the cytoplasm of an uninfected RBC is determined by the concentration of haemoglobin (Gennaro *et al.*, 1996), and it has been shown that the internal viscosity of the RBC cytoplasm does contribute to the overall deformability of the RBC (Mohandas et al., 1980, Kon et al., 1987). PRBC take up more solutes than uninfected RBC (Kirk et al., 1994), much of this increased uptake is through the as-yet poorly characterised NPP. The NPP are also responsible for the removal of waste products, including amino acids from the haemoglobin breakdown by the parasite. It is possible that a result of the haemoglobin breakdown by the parasite is a decrease in cytoplasmic viscosity. However, it has been hypothesised that the increased solute concentration in the PRBC cytoplasm leads to an increased cytoplasmic viscosity when compared to uninfected RBC (Cooke et al., 2001).

In order to try to determine the contribution of cytoplasmic viscosity to the increased rigidity of PRBC we used furosemide. Furosemide inhibits NPP in infected red blood cells. It is a diuretic drug that is known to act on channels in other cell types, and there is some evidence that it also acts on uninfected red blood cells. As the cytoplasmic viscosity of PRBC is thought to be increased because of uptake of solutes through NPP, by inhibiting this solute uptake into the PRBC cytoplasm cytoplasmic viscosity might be reverted to a native state, as seen in uninfected RBC.

We found that furosemide had a very slight effect on reducing the mean cell volume (MCV) of uninfected red blood cells (Biagini, unpublished and figure 4.5b) suggesting it has some effect on uninfected RBC. However, the deformability of uninfected red blood cells appeared to be not significantly affected by the drug.

Before testing the effect of furosemide on deformability of PRBC we used its effect on sorbitol lysis as a control that furosemide was indeed inhibiting NPP in PRBC. Sorbitol lyses PRBC due to it being taken up though NPP, which are only present in mature infected RBC. Uninfected RBC and PRBC containing young rings do not have NPP activity and do not take up sorbitol – hence are not osmotically lysed by sorbitol. As furosemide can block NPP the addition of furosemide to trophozoite-stage PRBC blocks lysis by sorbitol. This effect was observed indicating that in our experiments the furosemide was inhibiting NPP.

However, the deformability of A4 PRBC was not changed after furosemide treatment, suggesting that inhibition of NPP did not affect the overall deformability of A4 PRBC as we could measure by Lorca.

Effect of Cytoplasmic Viscosity and Cytoskeletal Changes – using a KAHRP deletion mutant

To further test the possible contributions of increased cytoplasmic viscosity in PRBC we used the KAHRP deletion (therefore knobless) parasite isolate 1C10 (Horrocks et al., 2005). As expected, we were unable to enrich this isolate using Plasmagel flotation – indicative of a lack of knobs. For these experiments a magnetic separation method was used to enrich for trophozoite-stage parasites. Consistent with previously published results this strain also showed reduced rigidity compared to wild type parasites, although deformability was not restored to the level of uninfected RBC (Fig. 4.4). These results confirm that the cytoskeletal changes to the RBC by parasites, including knob formation involving KAHRP contribute to the overall reduced deformability seen in PRBC (Glenister et al., 2002).

Using furosemide as for A4 above, we found that the KAHRP deletion strain showed a significant increase in deformability when NPP were inhibited. One possible explanation could be the contribution of an increased cytoplasmic viscosity in PRBC resulting from increased solute uptake through NPP. When NPP are inhibited in the KAHRP deletion strain the cytoplasmic viscosity is again reduced resulting in a more deformable cell. In our model, the increased cytoplasmic viscosity in PRBC compared to RBC does contribute to the increased rigidity of PRBC. However, in WT PRBC such as A4 the overriding contribution to the reduced deformability is that of the rigidification of the cytoskeleton. When the cytoskeletal rigidity is compromised as seen in the KAHRP deletion isolate the contribution of the cytoplasmic viscosity can be seen. This potential model is illustrated in figure 4.7.

These results have implications for any adjunct therapy potentially aimed at reducing the rigidity of PRBC with the aim of improving circulation. Therapies aimed at reducing rigidity by affecting cytoplasmic viscosity would be unlikely to have a significant effect in the presence of a wild-type *P. falciparum* membrane cytoskeletal modifications. To result in an observable reduction in PRBC rigidity the membrane cytoskeletal modifications would have to be targeted.

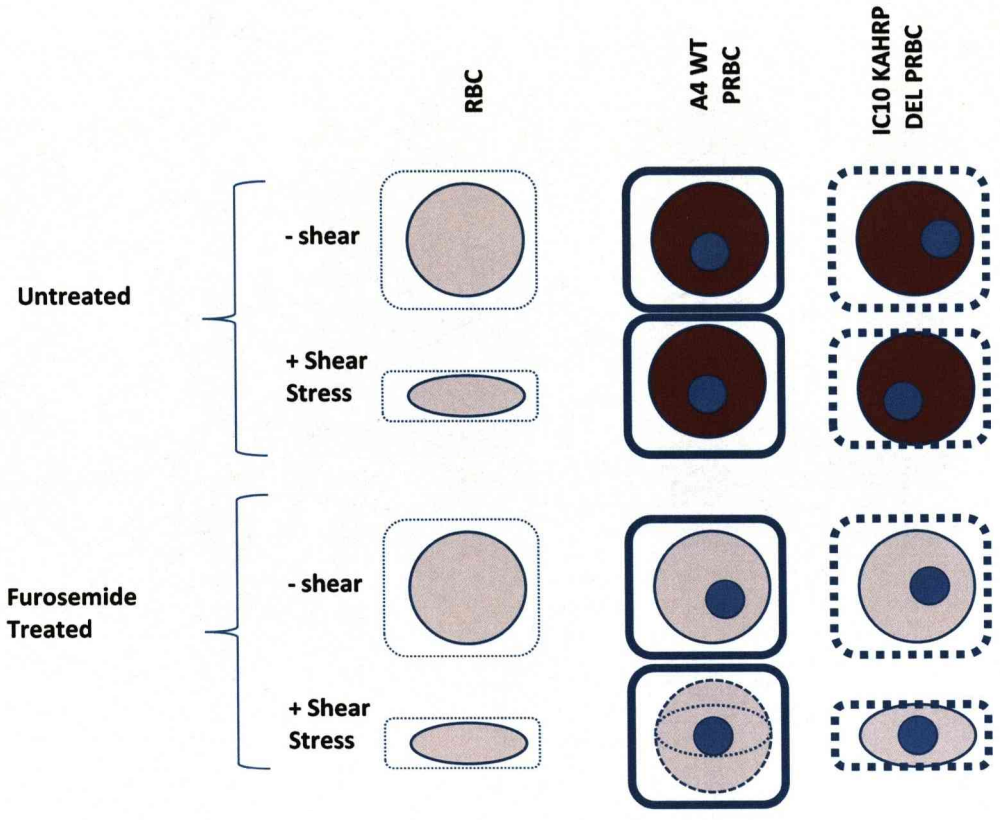

Figure 4.7. Possible model for cytoplasmic and cytoskeletal determinants of rigidity in PRBC

- Uninfected red blood cells have an elastic membrane cytoskeleton (thin blue box) and low viscosity cytoplasm (pale pink). This results in them being highly deformable and able to elongate under shear stress.
- PRBC contain a parasite within its parasitophorous vacuole (solid blue), contain more solutes in the RBC cytoplasm increasing the viscosity (dark pink) and have a modified cytoskeleton (Thick blue box). This results in the parasite being able to withstand shear stress without elongating.
- The KAHRP deletion PRBC as with WT infected red blood cells contain a parasite, and have an increased solute content of RBC cytoplasm leading to increased viscosity. While modified to some extent, the membrane cytoskeleton is less rigid than that of WT PRBC. These cells deform more than WT (A4) PRBC under shear stress but remain more rigid than uninfected RBC.
- When treated with furosemide there is no effect on uninfected RBC which remain deformable.
- The WT (A4) PRBC lose cytoplasmic viscosity to a nearer uninfected state, but there is no change in deformability observed due to the rigid cytoskeleton
- The KAHRP deletion strain (1C10), when treated with furosemide loses cytoplasmic viscosity and the effect of this on whole cell rigidity can be observed as there is no reinforcing rigid cytoskeleton.

4-5 LIMITATIONS AND FURTHER WORK

There are many limitations to this work regarding the contribution of an altered cytoplasmic viscosity to the rigidity of PRBC. Firstly, the conclusions are drawn based on the comparison of one knobless and one knobby strain, although in one experiment ItG (knobby) gave the same result as the A4 strain (not shown). Also the knobless strain used is lacking in KAHRP due to a chromosomal truncation resulting in potentially other deletions that may be relevant. Confirmation of the result using other deletion strains, and specific (KAHRP) mutations would be essential to confirm the results.

A major limitation is that this interpretation is based on an assumption that the cytoplasmic viscosity of PRBC is increased compared to RBC, and importantly, that the inhibition of NPP using furosemide results in a reduction of the cytoplasmic viscosity. Furosemide is a broad ranging inhibitor of transport channels, and may act on host RBC channels (as indicated by the possible loss of MCV in RBC) as well as plasmodial NPP and plasmodial folate transporters (Wang *et al.*, 2007). Also, the NPP are not yet completely characterised. As a result we are unable to predict the effect that furosemide would have on PRBC cytoplasmic viscosity. Our model assumes that inhibition of NPP inhibits uptake of solutes to result in a loss of PRBC cytoplasmic viscosity. Should this not be the case then the differences between the two isolates may be due to more subtle differences in the interaction of furosemide with the PRBC. It is possible that, for example, the KAHRP knock out strain has changes in the NPP channels that are affected by furosemide resulting in the differences seen.

Our model could be tested in several ways. The involvement of NPP specifically could be tested by using chymotrypsin to effectively turn off the NPP (Baumeister et al., 2006), or use other inhibitors more specific for NPP i.e. 5-nitro-2-(3-phenylpropylamino) benzoic acid (NPPB) (Kirk et al., 1994). The increased viscosity of the PRBC cytoplasm over uninfected RBC cytoplasm could be measurable as an increased osmotic fragility. This is seen by lysis of mature trophozoite PRBC earlier in a series of lysis buffers of increasing relative tonicity (Lew *et al.*, 2003). An effect of furosemide on this change in osmotic fragility could easily be tested for. A return to a reduced osmotic fragility as seen in uninfected RBC after furosemide treatment would support the model that furosemide is leading to a reduction in PRBC cytoplasmic osmolarity. However, a complication is that the cytoplasmic viscosity may not be directly related to the osmolarity as many solutes may contribute to cytoplasmic viscosity without affecting osmolarity.

4-6 CONCLUSIONS

In summary, we have shown that the observed rigidity of PRBC is due to changes in the RBC membrane cytoskeleton structure made by the parasite. Our hypothesis from this work is that the increased cytoplasmic viscosity of a PRBC also has a role in the increased rigidity, however, this effect can only be seen when membrane cytoskeleton integrity is compromised.

Increased rigidity of PRBC is maintained after the parasite has been killed – indicative of the permanent remodelling of the RBC by the parasite. This is significant as it implies that any pathophysiological features resulting from the increased rigidity of the PRBC can potentially still be continuing long after antimalarial treatment has been administered. However, it also indicates that if PRBC were to be released from sequestration the increased rigidity of the cells would still make them a potential target for splenic clearance.

CHAPTER 5 - REDUCED CYTOADHERENCE TO ENDOTHELIAL CELLS EXPOSED TO FEVER

5-1 INTRODUCTION

An important symptom of *P.* falciparum malaria is fever, which may occur as classically predicted fever peaks recurring every 48 hours, or a more general raised temperature as commonly observed in acute malaria (Peters, 1995) [www.who.int].

Febrile temperatures may have an effect on the growth, and cytoadherence capacity of *P. falciparum* parasites. There is some evidence that trophozoite stage parasites are sensitive to higher temperatures *(*Oakley *et al.,* 2007, Kwiatkowski, 1989*)*, resulting in inhibition of growth and loss of viability of parasites, while the young ring stage parasites may mature quicker at febrile temperatures (Long et al., 2001, Kwiatkowski, 1989, Pavithra et al., 2004). This has been suggested to result in an increased synchronicity of cultures.

It has been shown by Udomsangpetch et al. (Udomsangpetch et al., 2002), that the ability of PRBC to cytoadhere may be increased after growth at febrile temperatures, possibly due to increased PfEMP-1 trafficking at higher temperatures. However, other studies have shown no evidence for increased levels of PfEMP-1 on the surface of PRBC matured under febrile conditions (Oakley et al., 2007). However, the Udomsangpetch et al. study only looked at the effect of fever on PRBC, and not the effect that fever may have on the host endothelial cells to which the PRBC adhere.

Host endothelial cells respond to febrile temperatures, and as described in chapter 1, there are differences between the responses to febrile temperatures and heat shock (Hasday & Singh, 2000, Park et al., 2005). We define febrile, or fever-range temperatures as physiologically relevant temperatures generally between 39°C and 41°C, whereas heat shock temperatures are non-physiological temperatures over 42.5°C (up to 55°C was used in one study (Zhou *et al.*, 2007)). Some studies have reported that exposure to febrile temperatures increase the response to cytokines such as TNF (Chen et al., 2006), whereas other studies have seen the opposite, i.e. fever exposure reduces the response to cytokines (Hasday et al., 2001). Some of these differences are due to differences between different endothelial cell types. One relevant phenotype of increased ICAM-1 expression in response to febrile temperatures appears limited to the specialized High Endothelial Venule (HEV) endothelial cells (Chen et al., 2006).

There have been more studies looking at the effect of non-physiological heat shock conditions on endothelial cells but again varying results have been seen with some studies showing a stimulatory effect of heat shock (Lefor et al., 1994), whereas others show a reduced response to cytokines in cells exposed to heat shock (Nakabe et al., 2007, Kohn et al., 2002).

One expected response to heat shock is the induction of the heat shock response pathway. This is a stress pathway that is well known to be induced in many cell types in response to a range of environmental stresses, including heat shock. The response is characterised by the activation of a transcription factor, HSF-1, which induces transcription of several genes, mainly those encoding heat shock proteins, including HSP70. Heat shock proteins include several families of proteins with mainly chaperone functions that may exist to protect against deleterious effects of fever on protein folding (Lindquist & Craig, 1988, Hartl, 1996).

Antipyretic (fever-reducing) treatment is standard adjunct therapy for malaria (Winstanley & Ward, 2006), however, studies assessing the effects of antipyretic treatment on disease have not shown evidence (in terms of parasite clearance time or disease outcome) for an advantage of giving antipyretic treatment (Meremikwu et al., 2000). In one study paracetamol led to a significantly increased time to parasite clearance when compared to mechanical antipyresis alone (Brandts et al., 1997). Similar results were seen with other antipyretics metamizol and naproxen, where a slight difference in parasite clearance time was observed but this could not be linked to any significant difference in fever reduction compared to controls (Lell et al., 2001).

As fever is a universal symptom in malaria, knowing whether fever affects cytoadherence could have implications for symptom management, as well as being interesting in terms of host-pathogen interactions. From available literature it is not clear how endothelial cells respond to febrile temperatures with respect to phenotypes relevant for cytoadherence, i.e. adhesion receptor expression. Since there have been some studies looking at the effect of febrile temperatures on parasites, we focus on the possible cytoadherence-related effects of fever on endothelial cells. In order to simply look at effects on endothelial cells in this study we expose only the endothelial cells to physiologically relevant febrile temperatures and assess effects on subsequent PRBC cytoadherence. We have found that exposure of endothelial cells to febrile temperatures results in a reduction in cytoadherence, illustrating the protective nature of host responses.

5-2 MATERIALS AND METHODS

Parasites

Parasite isolates used were C24, ItG, A4, JDP8 as described in Methods chapter 2 and the patient isolate 8146 described in chapter 6. All were maintained at 37°C throughout and used at mid-trophozoite stage for assays.

Endothelial Cells

HUVEC and HDMEC were obtained from Promocell and maintained as described in Methods chapter 2. In addition, individual isolates of HUVEC were used which were obtained by Neil Jenkins in Kilifi (N. Jenkins PhD Thesis 2007, LSTM. Ethics were approved locally for HUVEC isolation (Kilifi), and cells were cultured before shipment to LSTM). These were maintained as described in methods chapter 2 for Promocell HUVEC. The human pulmonary microvascular (Lung) endothelial cell line (HLEC) were obtained from Sciencell and maintained as for HDMEC as described in chapter 2. The transformed brain microvascular endothelial cell line HB13 (Tripathi et al., 2006) was a gift from M. Stins. HB13 were maintained in DMEM (high glucose with sodium bicarbonate, without L-Glutamine and sodium pyruvate) (Gibco) with 10% (vol/vol) foetal bovine serum (Sigma) and supplemented with 2 mM L-glutamine, 10 ng/ml epidermal growth factor (EGF), 1 µg/ml hydrocortisone. Cells were incubated at 37°C in 5% CO_2 in a humidified incubator and trypsinisation for passage was carried out on sub-confluent cells as described for HUVEC/HDMEC. HUVEC, HDMEC and HLEC were used at passage number 3 – 6 and HB13 were used at passage number 12 – 15.

Immunofluorescence and Flow Cytometry

ICAM-1 expression on endothelial cells was measured by flow cytometry after immunofluorescence staining using and anti-ICAM-1 monoclonal antibody mAb 15.2 conjugated to FITC, as described in methods chapter 2. For fluorescent confocal microscopy cells were grown to confluence on 13 mm permanox cover slips (Nunc) and exposed to TNF/fever conditions as appropriate. Cells were washed in PBS with 1% BSA (PBSBSA) and incubated with primary anti-ICAM-1 antibody (mAb 15.2) 1:50 dilution in PBSBSA for 45 min at 37°C. After washing with PBSBSA secondary FITC-conjugated anti-mouse secondary antibody at 1:50 dilution was incubated in the cells in the dark for 45 min at 37°C. Cells were then fixed in 4% paraformaldehyde for 30 min. The cells were then permeabilised with PBSBSA with this addition of 0.1% triton X-100 for 30 min, then washed before incubation with Rhodamine Phalloidin at 1:50 dilution along with 1:1000 dilution DAPI in PBSBSA with 0.005% triton for 45 min. Cells were

washed with PBSBSA, then washed with PBS and mounted in vector shield and sealed. Analysis was using a Zeiss LSM Pascal confocal microscope and Zeiss pascal software. Minor image processing carried out using Adobe Photoshop was performed in the same way for all experimental conditions.

Adhesion Assays

Static adhesion assays to endothelial cells were performed at 37°C as described in chapter 2. Flow adhesion assays to endothelial cells were performed at 37°C using the chamber slide system as described in chapter 2.

Fever Treatment

Confluent cells were incubated at febrile temperatures of 39.5°C or 41°C in an identical 5% CO_2 humidified incubator as the control cells (37°C) (Heraeus incubator). Actual temperature was monitored using a thermometer on the same shelf as the cells in each incubator and was found to be ± 0.5°C expected temperature. For most experiments fever exposure was for 16 hours, however other exposure times were used in some cases as described in the text. Controls maintained at 37°C were included in every experiment.

Heat Shock Treatment

Heat shock (as opposed to "fever") was performed by incubating endothelial cells in a sealed (parafilm) 24 well plate in a water bath carefully measured to be at 42.5°C for 1 hour. Control cells were incubated in the same way in a water bath at 37°C. After 1 h incubation the plates were unsealed and returned to the 37°C CO_2 incubator for 4 h recovery time before experiment.

Protein Samples

Whole cell lysates were obtained from confluent cells in one well of a 24 well plate. Cells were washed twice with dPBS then incubated in 40 µl 2 X SDS sample buffer for 30 seconds before harvesting by scraping with a yellow pipette tip. Samples were boiled for 4 min before use and 5-10 µl loaded on sodium dodecyl sulfate (SDS) gels for Coomassie staining or western analysis. Comparable protein concentration in each sample was confirmed by analysing a coomassie stained gel.

SDS-PAGE and Western Blotting

For Western blotting, 5 - 10 µl samples of whole cell lysate (0.5 – 1 x 10^4 cell equivalents) were separated on a 10% SDS gel according to standard procedures

(Sambrook et. al) before transfer onto Hybond-P membrane (Amersham) using Bio-rad mini-protean transfer kit (using a Tris-Glycine transfer buffer as standard procedures Amersham/Bio-rad). Low or High molecular weight protein markers (Amersham) were loaded alongside. After transfer the membrane was blocked in 5% Marvel Low fat milk in TBST (Tris-buffered saline solution with 0.1% Tween20) overnight at 4°C. Primary anti-HSP70 antibody (A gift of Yang Wu) was used at 1:50,000 dilution in TBST for 1 h at room temperature. After washing for 1 h at room temperature with 4 x changes of TBST a horseradish peroxidase (HRP)-coupled secondary antibody was incubated at 1:5000 for 1 h at room temperature. The membrane was washed 1 h at room temperature with at least 4 changes of buffer and visualised using ECL system (Amersham) and exposure to X-ray film (Pierce). After exposure blots were stripped with 2 x 5 min washes in 0.2N NaOH followed by 2 x washes in dH_2O before re-blocking with 5% marvel as above. For loading control the blot was then probed with β-Actin antibody (Abcam) used at 1:5000 dilution and proceeded as above.

Viability Assay

The Cell-Titer Blue metabolic assay (Promega) was used to determine endothelial cell viability. The assay is based on the ability of living cells to convert a redox dye (resazurin) into a fluorescent end product (resorufin). Nonviable cells will have lost metabolic capacity and therefore will not generate the fluorescent signal. From trypsinisation of 1 x confluent T25 flask cells were counted and two-fold serial dilutions of endothelial cells were seeded from 1 x 10^4 cells/well to 625 cells/well, in triplicate 2X in a 96 well plate. After settling for two hours medium was replaced with 150 µl/ well of growth medium and cells grown overnight. Controls included wells containing no endothelial cells and dead endothelial cells treated with sodium azide before addition of reagent. After overnight growth at 37°C or fever temperature, in triplicate with/without 1 ng/ml TNF cells were incubated in 100 µl of a 1:20 dilution of cell-titer blue reagent in HUVEC medium for 4 h at 37°C. Fluorescence at 560/590 nm was measured and plotted after subtraction of background (medium alone negative control).

5-3 RESULTS

Part I – Effect of Febrile Temperatures on Cytoadherence

Adhesion of ItG to fever treated and stimulated HUVEC is reduced

To examine the effect that exposure of endothelial cells to fever had on cytoadherence, we first used Human endothelial umbilical vein endothelial cells (HUVEC). We chose a modest febrile temperature of 39.5°C which is within physiologically relevant fever range. We initially exposed cells to fever for 16h which would be relevant for observations of generally raised temperatures during acute infection, or corresponds to the maximum length of fever peaks in a classical model of *P. falciparum* malaria febrile episodes.

A confluent monolayer of HUVEC was incubated at a fever temperature of 39.5°C or standard temperature of 37°C for 16 h. Resting HUVEC do not express ICAM-1, so TNF (1ng/ml) was used in most experiments to induce expression of ICAM-1 on these cells. Since it has been shown that fever peaks and TNF levels coincide in malaria infection, TNF (when used) was added concurrently with fever exposure for the stimulation of ICAM-1 adhesion receptor expression. Adhesion of parasite isolates to these cells was then assayed. Parasites had been maintained at 37°C and assays were carried out at 37°C in order to only assess the affect of fever on the endothelial cells.

The *P. falciparum* isolate C24 which is not expected to adhere to HUVEC showed very low levels of binding in static assays, and this was the same regardless of overnight incubation temperature or TNF exposure (Fig. 5.1a). ItG showed low levels of adhesion to non-stimulated HUVEC and significantly increased levels of adhesion to TNF stimulated cells. However, adhesion to fever treated TNF stimulated HUVEC was lower than that seen to control HUVEC maintained at 37°C (Fig. 5.1b). A similar reduction in adhesion to fever treated HUVEC was seen in assays under flow conditions where <50% adherent PRBC were present on fever treated cells compared to those maintained at 37°C (Fig. 5.1c).

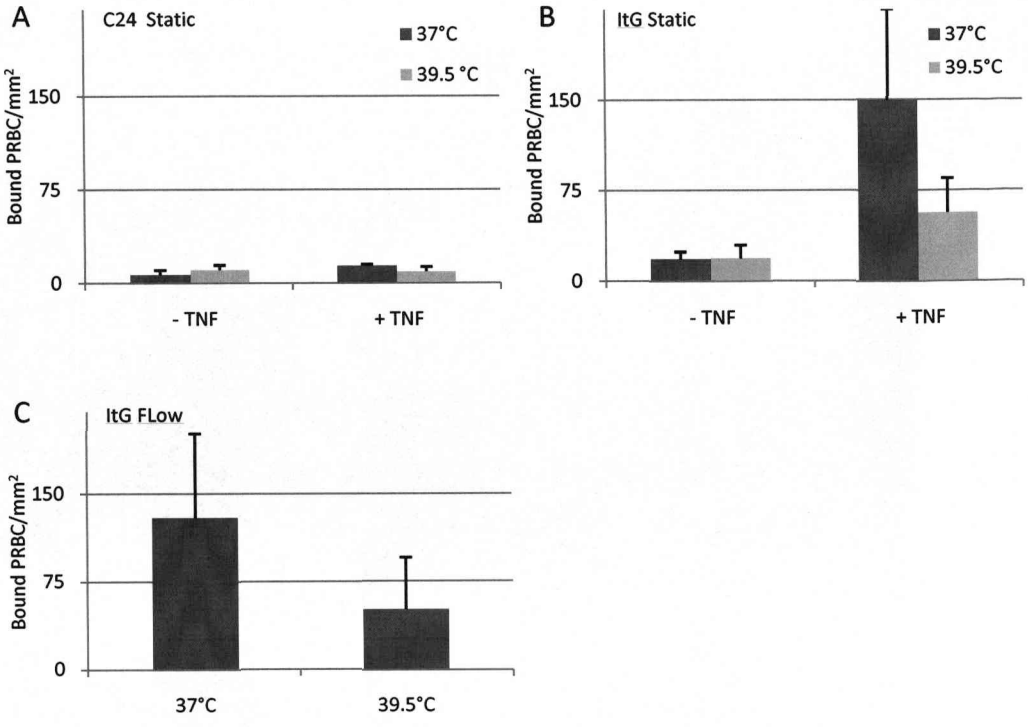

Figure 5.1. Adhesion to HUVEC exposed to 16 h 39.5°C fever. A,B) Static adhesion assays. Adhesion of C24 PRBC (a) and ItG PRBC (b) to HUVEC with or without 16h 1 ng/ml TNF and concurrent 16h 37°C or 39.5°C fever exposure in static adhesion assays. Results shown are bound PRBC/mm^2 ± SD from 3 (C24) or 6 (ItG) Independent experiments. C) Flow adhesion assay ItG to HUVEC stimulated with 1 ng/ml TNF concurrent with/without 16 h 39.5°C fever. Result shown as bound PRBC/mm^2 ± SD from 3 independent experiments

ICAM-1 Expression levels are the same after fever treatment

The first explanation we considered for the reduction in adhesion seen to HUVEC after fever exposure was the possibility of reduced levels of ICAM-1 stimulation. We first showed that, as predicted, there was no induction of ICAM-1 expression on unstimulated cells after fever treatment, as measured by flow cytometry after immunofluorescence for ICAM-1 (Fig. 5.2a solid lines). Following TNF exposure ICAM-1 was strongly stimulated, and this level of stimulation did not appear to be affected by exposure to febrile temperatures (Fig. 5.2 a dashed lines).

HUVEC Viability is unaffected by fever treatment

To exclude that the reduced cytoadherence observed was due to reduced cell viability we used a resorufin-based assay Cell-titer blue (Promega) to determine viability of HUVEC after exposure to fever temperatures. Cells were seeded at a range of densities in a 96 well plate in order to distinguish between any potential cell death or reduced growth phenotype in case of differences in viability observed. There was no

significant difference in viability after incubation at 39.5°C compared to control 37°C with viability at all seeding densities being >90% of control (Fig. 5.2b).

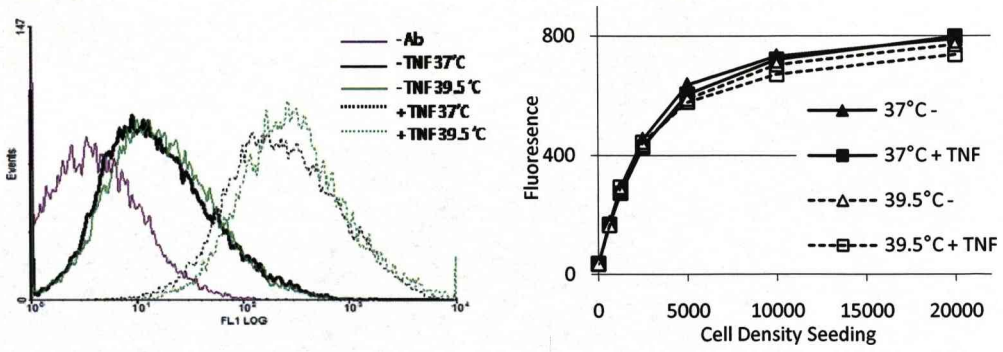

Figure 5.2. ICAM-1 expression and viability of HUVEC after 16h fever. A) ICAM-1 expression on the surface of HUVEC measured by flow cytometry. Result is representative of three independent experiments. B) Viability of HUVEC measured by resorufin assay at different cell seeding densities. Mean of three independent experiments.

Addition of TNF to HUVEC after fever exposure results in protection against cytoadherence

It could be possible that the reduced adhesion seen is due to reduced efficacy of TNF when it is added at higher temperature, conceivably simply due to reduced stability of TNF at the higher temperatures. To control for this we added TNF independently of fever treatment. HUVEC were exposed to 39.5°C fever for 16 h in the absence of TNF, then cells were returned to 37°C and TNF was added at 10 ng/ml for 5 h after fever exposure before static adhesion assays. As discussed later, this is probably less physiologically relevant than addition of TNF and fever concurrently, but may also reveal clues to the mechanism of protection.

These preliminary experiments showed a reduction in adhesion to fever exposed cells compared to that seen to cells maintained at 37°C when TNF was added after fever exposure (Fig. 5.3a), similar to the protection shown in figure 5.1b when TNF and fever were added together. However, when cells were exposed to fever after TNF stimulation no effect on adhesion was seen (Fig. 5.3a). The reduced adhesion to overnight fever exposed cells was similar after a 30 min, or 6 h recovery time (Fig. 5.3b). Exposure of HUVEC to fever for < 6h did not appear to affect adhesion levels (not shown).

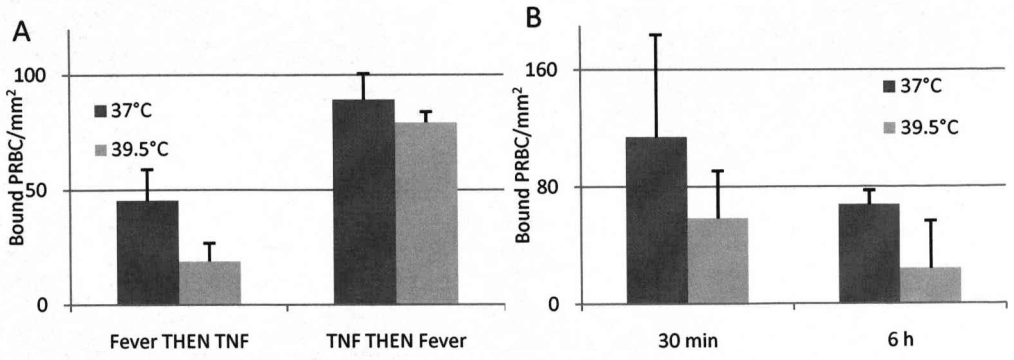

Figure 5.3. Adhesion if ItG to HUVEC after different fever/TNF exposure conditions. Static adhesion assays. A) Adhesion levels after exposure of HUVEC to 16 h fever either before addition of 10 ng/ml TNF for 6 h (first column), or exposure to 10 ng/ml TNF for 6 h before exposure to 16 h fever (second column). B) Recovery time at 37°C after exposure to fever and TNF (1 ng/ml) for 16 h.

Febrile temperatures of 41°C result in protection against cytoadherence

Adhesion of ItG to HUVEC after exposure to a fever temperature of 41°C also showed a reduction in adhesion compared to that seen on HUVEC maintained at 37°C. (Fig. 5.4a). The level of reduction in adhesion was similar to that seen after exposure to a 39.5°C fever, and similarly ICAM-1 expression levels were unaffected (Fig 5.4b). Although cell morphology appeared generally unaffected (Fig. 5.4c) viability was slightly reduced to ~85-90% of control cells maintained at 37°C (Fig. 5.4d).

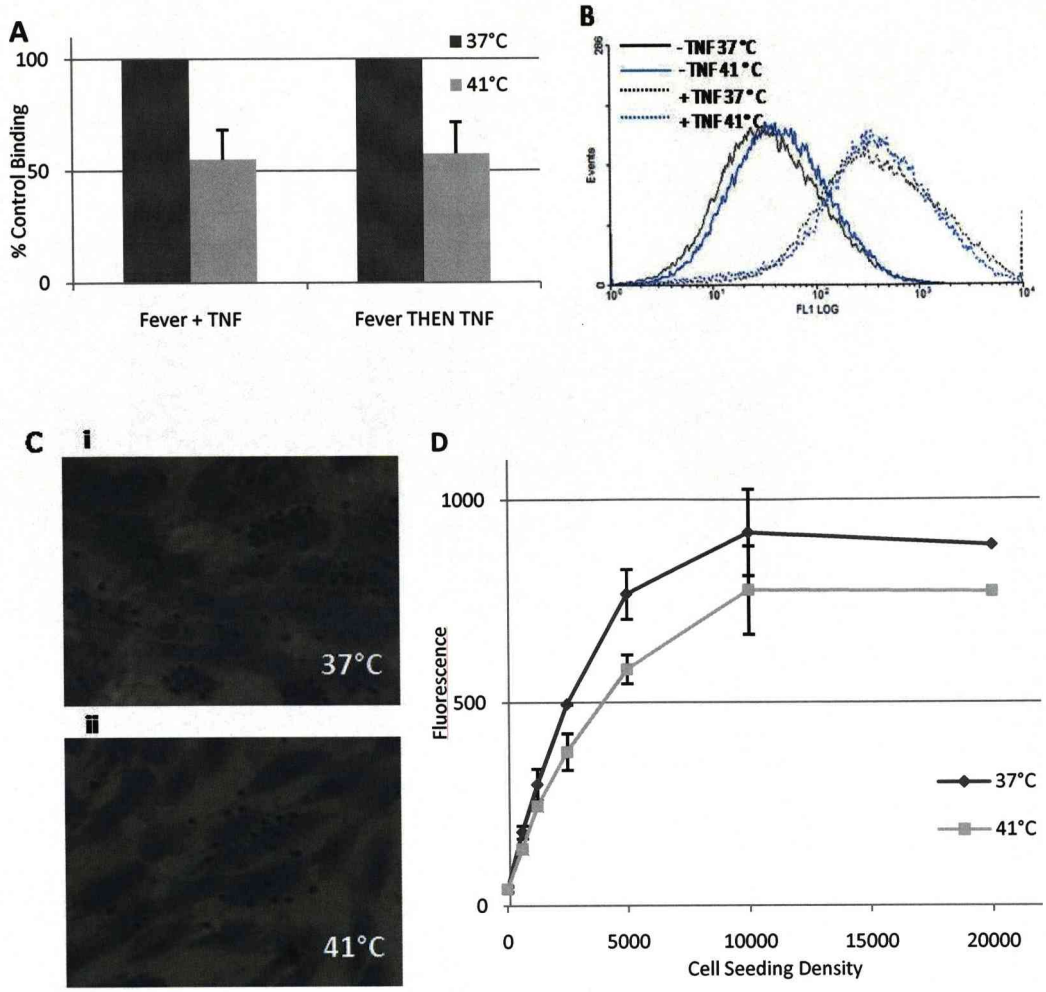

Figure 5.4. Effect of 41°C fever on HUVEC. A) adhesion of ItG to HUVEC after either overnight fever with 1 ng/ml TNF (column 1) or after 16 h fever followed by 10 ng/ml TNF (column2) Mean + SD of 3 or 2 independent triplicate experiments. B) Expression of ICAM-1 after exposure to fever at 41°C 16 h with 1 ng/ml TNF. C) Giemsa staining morphology of HUVEC after adhesion assay. D) Viability of HUVEC after exposure to 41°C fever. Mean ± SD of two independent experiments.

ICAM-1 Distribution on HUVEC

Although levels of ICAM-1 appeared the same in flow cytometry analysis we used fluorescence microscopy to analyse the distribution of ICAM-1 on the surface of HUVEC. ICAM-1 expression in HUVEC was visualised by immunofluorescence staining on live (unfixed) cells (to ensure surface staining only), using mAb 15.2 and a FITC conjugated secondary antibody and counter stained with rhodamine conjugated phalloidin to stain filamentous actin (f-actin) cytoskeleton, and DAPI stain for nuclear DNA. With no primary anti-ICAM-1 antibody there was no visible background in the FITC channel (not shown). In the absence of TNF there was minimal visible staining of HUVEC for ICAM-1 (Fig. 5.5a, c). The ICAM-1 distribution on TNF stimulated HUVEC

was an uneven patchy distribution over the surface of the cell which was unchanged after ItG adhesion assays (Fig. 5.5b,d).

Immunofluorescence Analysis of HUVEC after fever Treatment

Immunofluorescence staining for ICAM-1 and f-Actin was carried out as above on HUVEC that had been exposed to 16 h 39.5°C. The pattern of ICAM-1 expression and the phalloidin staining appeared no different between cells maintained at 37°C and those exposed to 39.5°C fever for 16h (Fig. 5.6). Similar results were seen when staining was carried out after ItG adhesion assay and no ICAM-1 expression was visible in unstimulated cells (not shown).

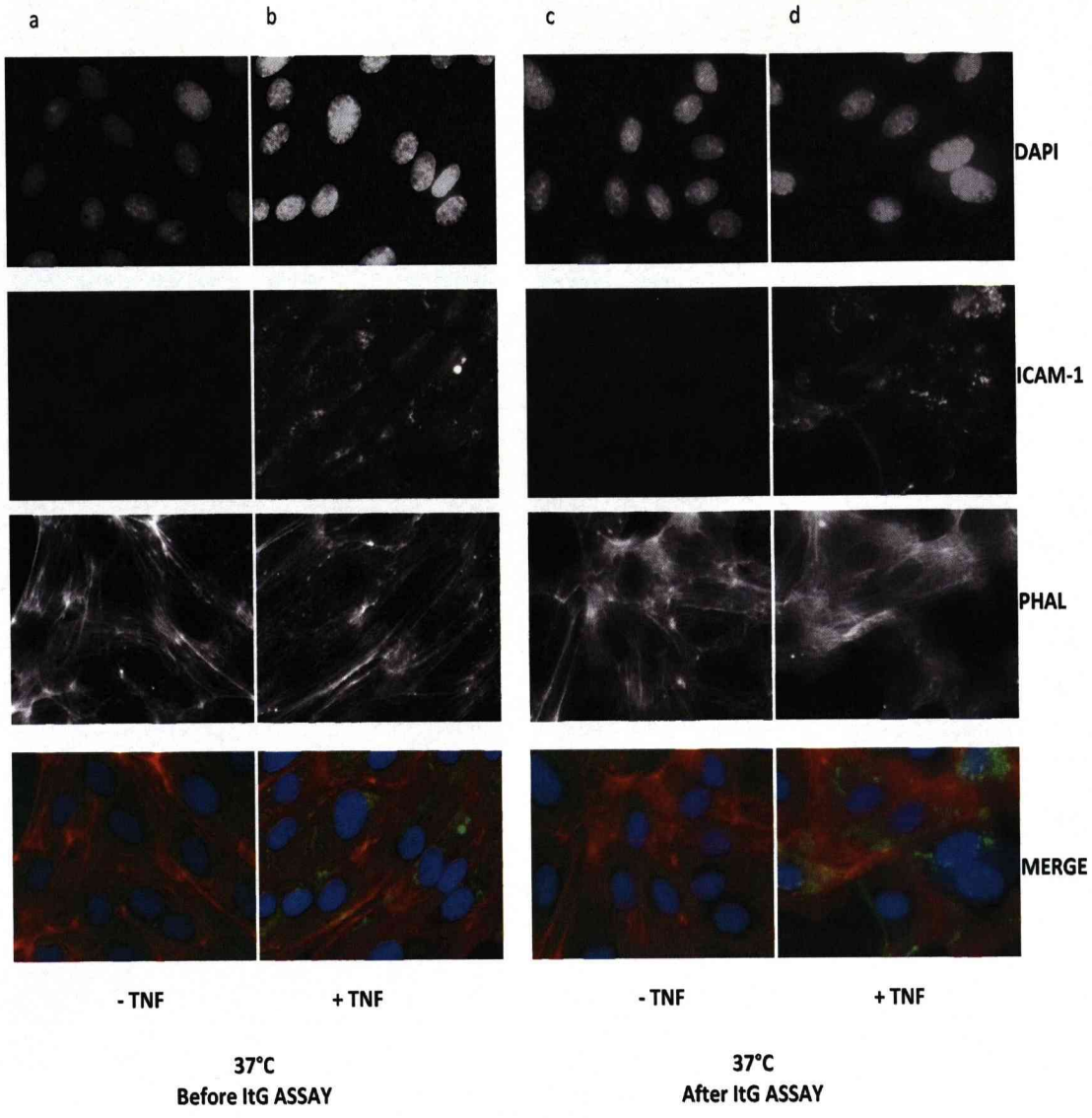

Figure 5.5. Immunofluorescence labelling of ICAM-1 on HUVEC. DAPI stain for nuclear DNA (row 1), Surface labelling of ICAM-1 on HUVEC using mAb 15.2 followed by FITC conjugated secondary antibody prior to fixation (row 2). F-Actin staining using rhodamine phalloidin after paraformaldehyde fixation and permeabilisation (row 3), and merged images (row 4). Cells were stimulated with TNF (1ng/ml 16h) (b,d) or without stimulation (a,c). Immunofluorescence procedure were carried out before (a,b) or after (c,d) ItG adhesion assay.

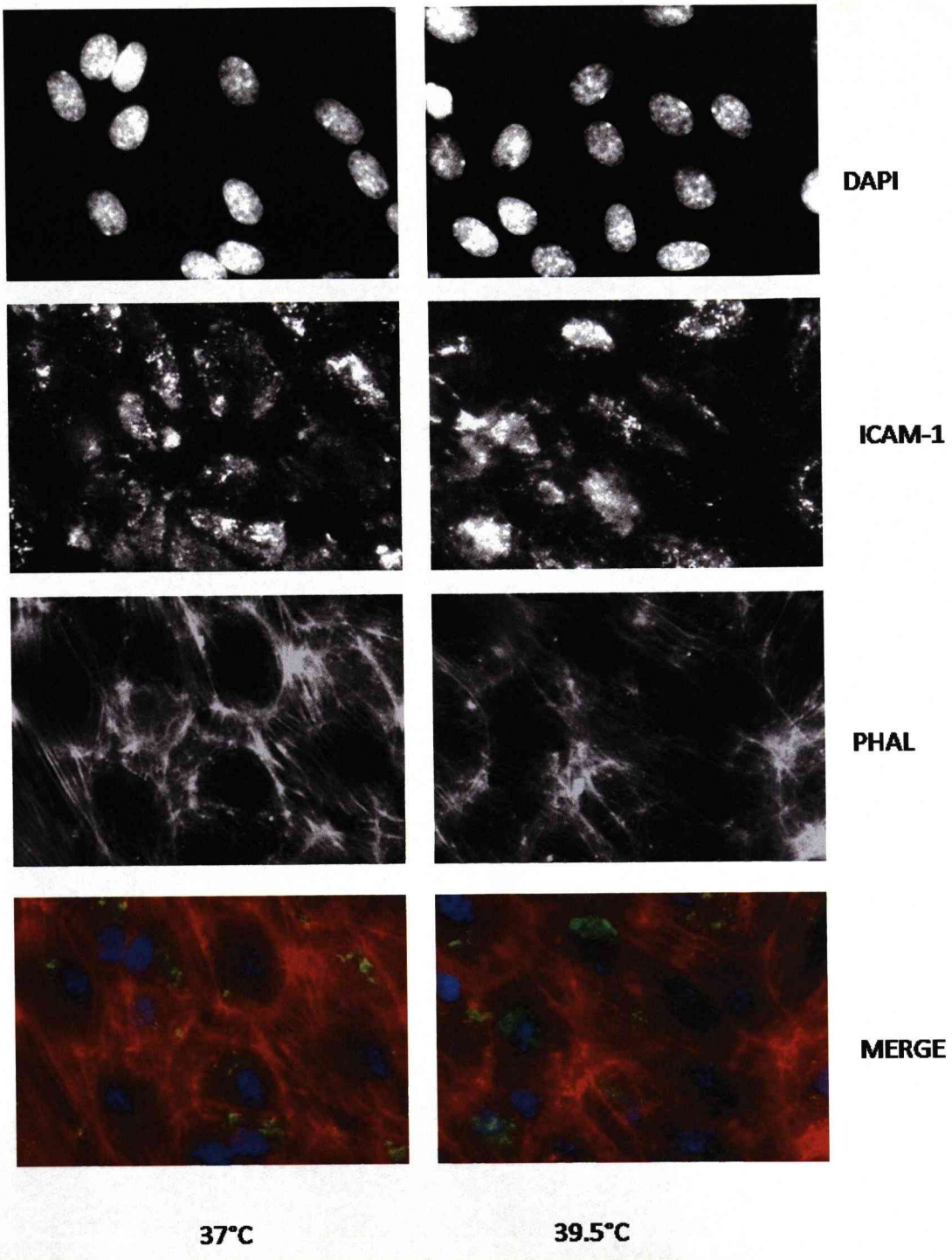

Figure 5.6. ICAM-1 Immunofluorescence on HUVEC after 16h 39.5°C fever. DAPI stain for nuclear DNA (row 1), Surface labelling of ICAM-1 on HUVEC using mAb 15.2 followed by FITC conjugated secondary antibody prior to fixation (row 2). F-Actin staining using rhodamine phalloidin after paraformaldehyde fixation and permeabilisation (row 3), and merged images (row 4). Cells were stimulated with TNF (1 ng/ml 16 h) along with treatment (16 h) at 37°C (left column) or 39.5°C (right column).

Part II - Heat Shock Response Pathway Activation

The next series of experiments attempt to determine something of the mechanism of the observed protection against cytoadherence. We have not seen any evidence of changes to the endothelial cells in response to fever, so we next assessed the stimulation of the heat shock response pathway. We have used HSP70 which is expressed in response to heat shock temperatures and other environmental stresses to analyse whether heat shock pathways are activated in response to our fever conditions. As a control we used standard heat shock conditions of a 42.5°C heat shock for 1 hour followed by 4 h recovery at 37°C to allow for protein expression. These conditions, as expected, showed strong HSP70 stimulation in HUVEC (Fig. 5.7 lanes 5-8).

Heat Shock Response Pathway is activated in response to 16 h 39.5°C fever

HSP70 was seen to be strongly stimulated in response to standard heat shock conditions (42.5°C for 1 h followed by a 4 h recovery at 37°C to allow for protein expression) (Fig. 5.7 lanes 5-8). HSP70 was also strongly induced by exposure of HUVEC to our fever conditions of 39.5°C for 16 h (Fig. 5.7 lanes 1-4). The presence of 1 ng/ml TNF had no effect on HSP70 level stimulation.

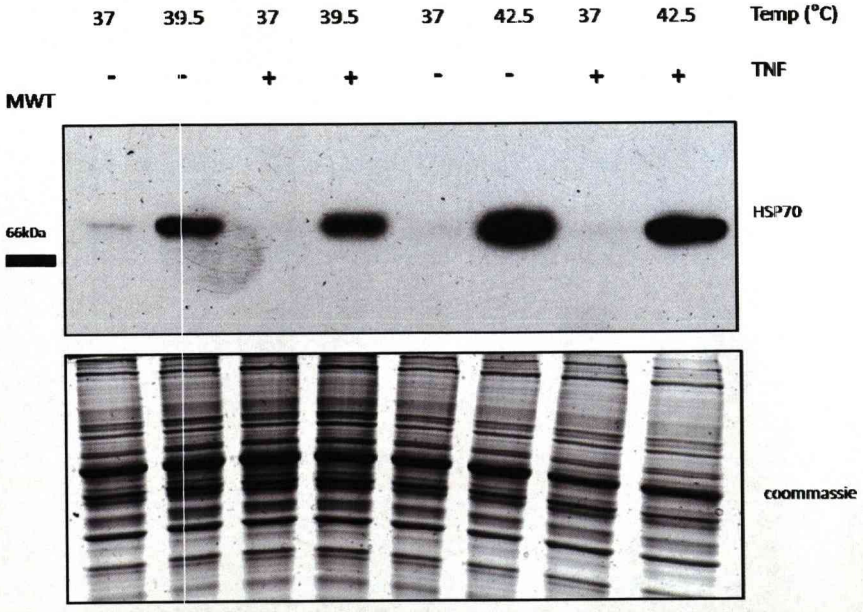

Figure 5.7. Induction of HSP70 in HUVEC. Western blot probed for HSP70 of HUVEC samples after exposure to heat shock conditions (right) or febrile temperatures (left). Coomassie stained membrane (bottom panel) used as indication of loading. Amersham high range molecular weight markers were run alongside, approximate position of 66 kDa marker is indicated.

Individual HUVEC isolates have similar HSP70 activation and adhesion assay phenotypes

All experiments we have presented so far have been performed on pooled HUVEC from one commercial supplier (Promocell). To ensure that our observations were not unusual to these cells we used HUVEC isolates obtained from individuals (Neil Jenkins, Liverpool/Kilifi) as opposed to pooled batches from Promocell. We assayed individual isolates both for adhesion phenotype after fever exposure, and HSP70 expression. Four isolates tested and compared in parallel with Promocell HUVEC showed similar results.

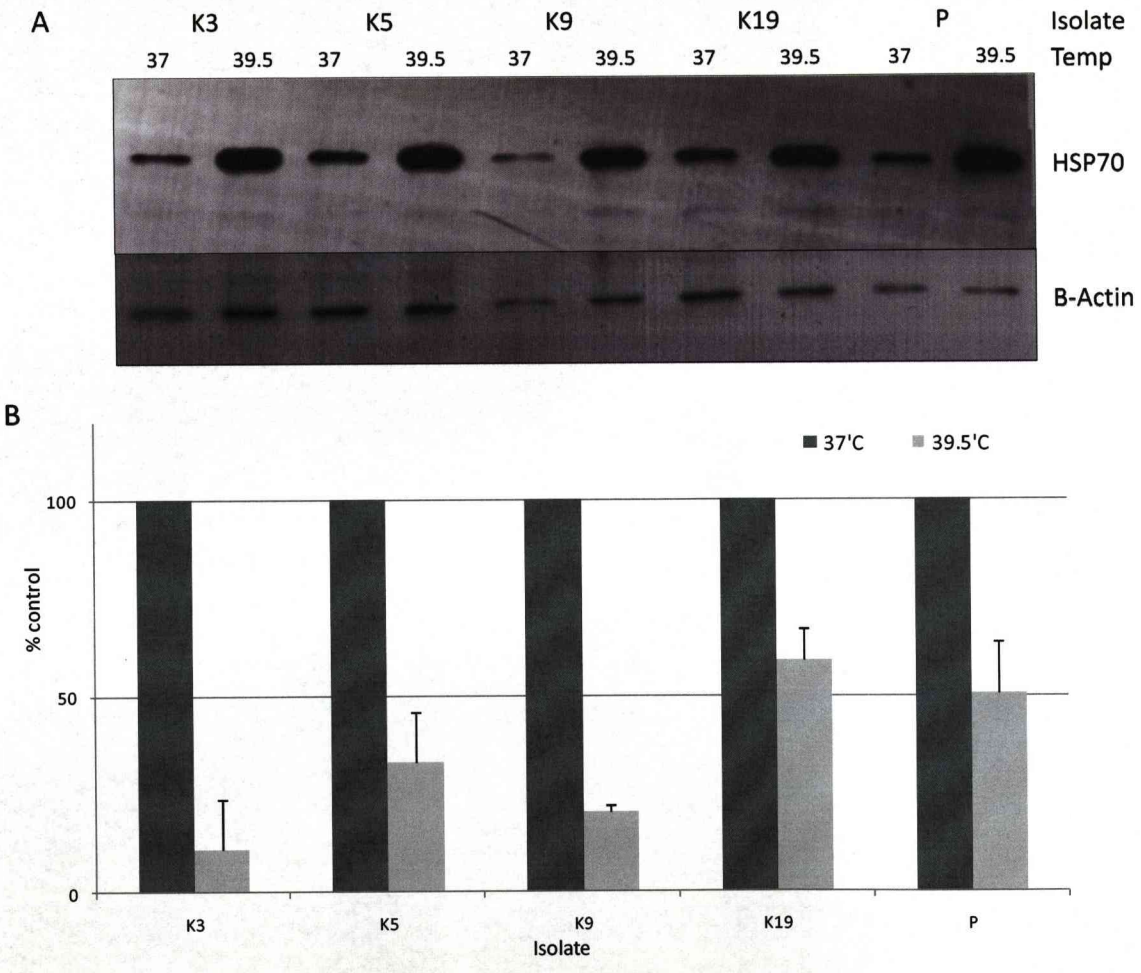

Figure 5.8. Effect of fever on individual HUVEC isolates. A) Induction of HSP70 in individual HUVEC isolates after exposure to 39.5C for 16h. The same blot was probed for b-actin as a loading control. B) Adhesion of ltG to different HUVEC isolates after exposure to 39.5'C 16h (grey bars) compared to maintained at 37'C (black bars). Adhesion expressed as a percentage of 37'C control and mean + SD of two slides. All assays and protein extraction were carried out at the same time.

All isolates showed HSP70 induction after exposure to 16h 39.5°C (Fig. 5.8a). Although actual numbers of adherent PRBC varied between isolates, all isolates showed reduced levels of adhesion to cells exposed to 16h 39.5°C compared with controls maintained at 37°C (Fig. 5.8b).

Adhesion to HDMEC is not affected by exposure to fever

HDMEC express CD36 constitutively as well as ICAM-1 after TNF stimulation, and adhesion of ItG PRBC to stimulated HDMEC is known to use both receptors. In contrast to the reduced adhesion seen to stimulated fever-exposed HUVEC, adhesion of both C24 and ItG PRBC to both unstimulated and stimulated HDMEC was relatively unaffected by 16 h exposure to 39.5°C temperatures (Fig. 5.9a). Similarly, under flow conditions there was no difference in adhesion of ItG to stimulated HDMEC (Fig. 5.9b).

To separate out CD36 mediated adhesion and ICAM-1 mediated adhesion a monoclonal antibody which blocks adhesion to CD36 was used. As shown in figure 5.9c, after inhibiting CD36 mediated adhesion there was a reduced level of adhesion which was slightly, but not significantly, reduced after exposure to 16 h 39.5°C fever (Fig. 5.9c +block). Without blocking treatment adhesion was ~85% of 37°C control, however after CD36 blocking, adhesion was ~70% of control.

After blocking of ICAM-1 adhesion using the anti-ICAM-1 monoclonal antibody mAb15.2 we could see that febrile temperature exposure had no effect on the CD36 mediated adhesion (result not shown) even after TNF stimulation, suggesting that only ICAM-1 mediated adhesion is affected by febrile temperatures (Fig. 5.9d).

To further investigate this, a different parasite isolate, JDP8, which favours ICAM-1 adhesion and shows comparatively little adhesion to CD36 was used (Chattopadhyay et al., 2004). JDP8 PRBC showed the expected higher adhesion than ItG to stimulated HDMEC with mean adhesion of 995 PRBC/mm^2, whereas CD36 mediated adhesion to unstimulated HDMEC was lower than ItG at 215 PRBC/mm^2. JDP8 showed a subtle reduction in adhesion to stimulated HDMEC (Fig. 5.9e), a mean adhesion of 71% compared to 37°C controls was observed (Fig. 5.9e) but again this was not statistically significant.

As seen with HUVEC there was no difference in the level of ICAM-1 after exposure to 16 h 39.5°C fever (Fig. 5.9f). These experiments indicate that there is much less response of HDMEC to febrile temperatures than we previously observed with HUVEC, with no reduction in adhesion being statistically significant although some reduced binding was observed in most experiments. The results also hint that any possible reduction in adhesion seen is due to ICAM-1 mediated adhesion only.

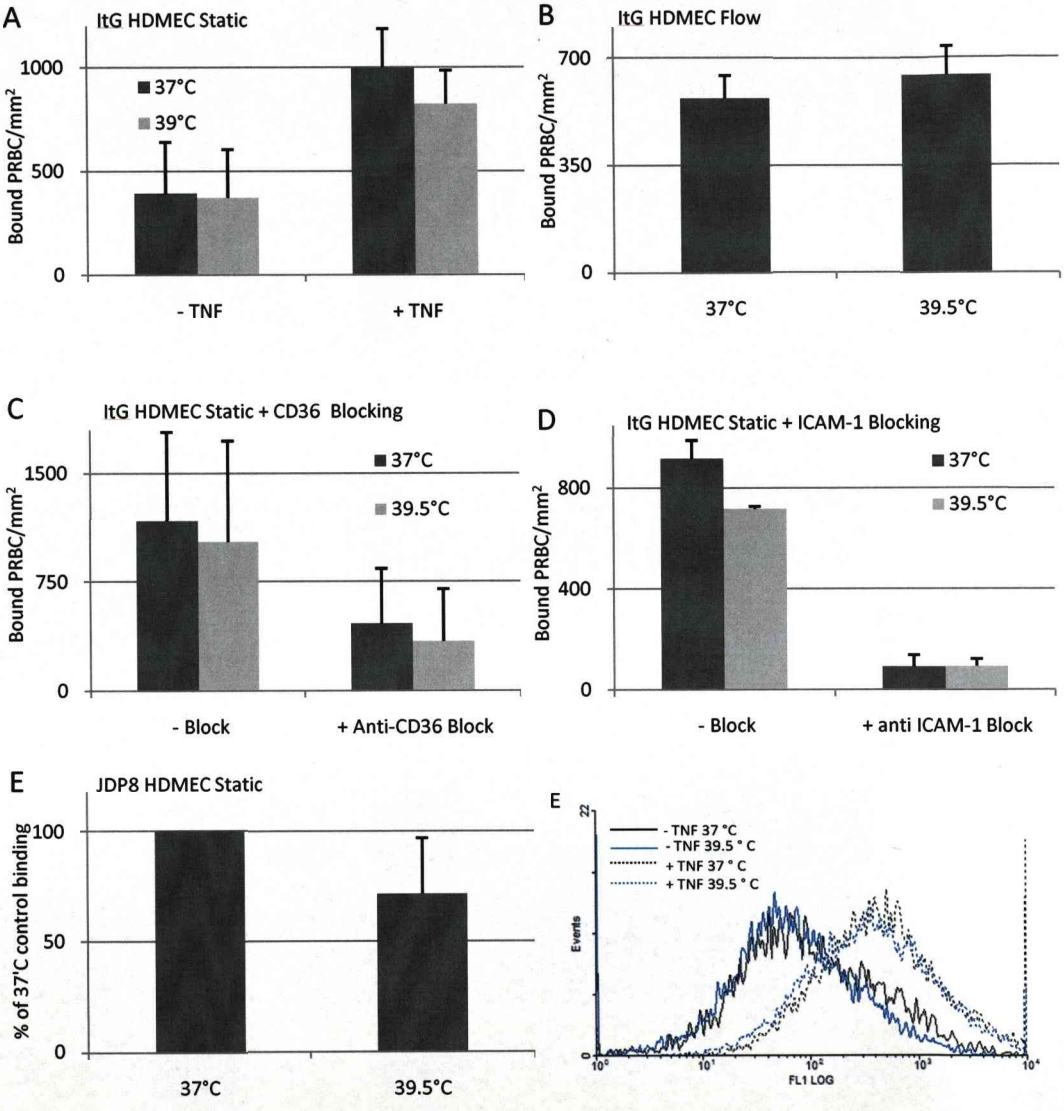

Figure 5.9. Adhesion to HDMEC after fever exposure. A) Adhesion of ItG to HDMEC in static assays. Bound PRBC/mm^2, mean + SD three independent experiments. B) Adhesion of ItG to TNF stimulated HDMEC in flow adhesion assays. Expressed as bound PRBC/mm^2, mean ± SD of two independent duplicate experiments. C) Adhesion of ItG to TNF stimulated HDMEC in static assays. Bound PRBC/mm^2 mean + SD of two independent duplicate experiments. D) Adhesion of ItG to TNF stimulated HDMEC in static assays with blocking of ICAM-1 adhesion using mAb 15.2. E) Adhesion of JDP8 to HDMEC in static assays. Percent of 37°C control binding, mean + SD four independent duplicate experiments. F) Expression of ICAM-1 on HDMEC

Adhesion to HBEC but not HLEC is reduced by fever

Human pulmonary vein (lung) endothelial cells (HLEC) express CD36 and ICAM-1 after TNF stimulation (Muanza *et al.*, 1996). These cells showed very similar adhesion behaviour to HDMEC. There was no difference in the adhesion to unstimulated HLEC after fever exposure, representing mainly CD36 mediated adhesion. (Fig. 5.10a), and there was a slight effect on adhesion to TNF stimulated HLEC after exposure to 16h 39.5°C fever (Fig. 5.10a). The brain endothelial cell line HB13 is a transformed cell line derived from human brain microvascular endothelial cells. These cells have been shown to express ICAM-1 after TNF stimulation, however have very low levels of CD36 expression (Tripathi et al., 2006). Preliminary experiments with these cells have indicated that the response to fever is more similar to that seen with HUVEC, i.e. a reduction in cytoadherence of ~ 50% is seen.

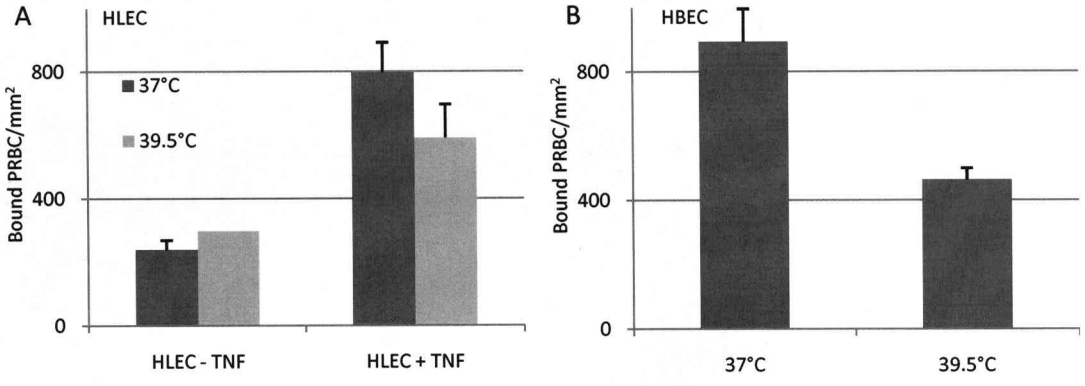

Figure 5.10. Adhesion of ItG to HLEC and HBEC. Showing bound PRBC/mm^2 to a) HLEC, mean + SD two independent duplicate experiments, and b) HBEC mean + SD of triplicate experiment.

Adhesion of A4 to fever-exposed HUVEC is reduced

Preliminary experiments suggest that the adhesion of A4 to fever-exposed HUVEC shows a similar pattern to that seen with ItG, i.e. a reduction in adhesion to cells exposed to 16 h 39.5°C compared to those maintained at 37°C.

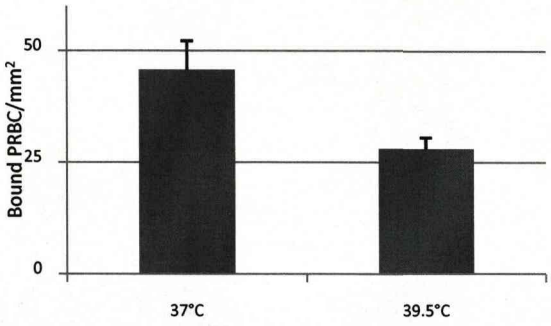

Figure 5.11. Adhesion of A4 to HUVEC. Mean of triplicate experiment. + SD.

HDMEC show a reduced HSP response to fever compared to HUVEC

The ability of febrile temperatures to induce heat shock response pathways in HUVEC and HDMEC was compared. The level of HSP70 induction was measured over a time course of incubation at 39.5°C. Samples were taken from both cell lines at the same time, and were run on the same gel to ensure equivalent blotting and antibody exposure conditions. The results suggest that HDMEC show a lower level of HSP70 expression in response to febrile temperature, suggesting lower levels of heat shock response pathway activation (Fig. 5.12). The same result was seen in two independent experiments.

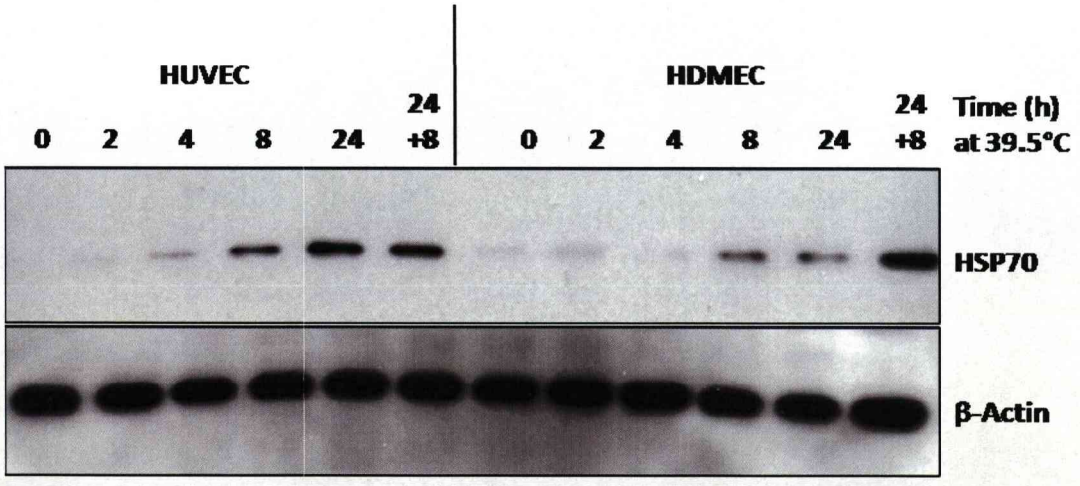

Figure 5.12. Western blot for HSP70 as a marker of heat shock pathway activation after exposure to febrile temperatures. Representative of two independent experiments. Upper panel, membrane probed for HSP70, and membrane was stripped and re-probed for beta-actin as a loading control (lower panel). HUVEC and HDMEC samples were taken at the same time, processed in the same way and run on the same gel.

The role of the heat shock response pathway in response to fever

In order to determine whether the heat shock response pathway was important in the observed protection against fever we sought to inhibit the activation of this pathway. Two chemical inhibitors of the heat shock pathway induction were used, quercetin and KNK437 (Powers & Workman, 2007, Dokladny *et al.*, 2008, Nagai *et al.*, 1995, Hosokawa *et al.*, 1992). Quercetin was shown to reduce the level of heat shock pathway following fever treatment by western blotting for HSP70 protein levels (Fig. 5.13a). At the higher concentrations of quercetin 10 μM, 50 μM and 100 μM cellular morphology was disrupted, and extensive cell death appeared to have occurred at 50 μM and 100 μM concentrations. No effect was seen at equivalent maximum concentration of DMSO solvent. Quercetin has previously been reported to also affect the TNF stimulation of ICAM-1 expression (Kobuchi *et al.*, 1999), so we measured ICAM-1 levels on quercetin treated HUVEC. There was a slight reduction in ICAM-1 level of quercetin treated HUVEC compared to untreated (Fig. 5.13b,c). After overnight quercetin treatment of HUVEC adhesion was significantly reduced (Fig. 5.13c) although again at higher concentrations of quercetin (50 μM and 100 μM) cells were visibly affected by the treatment. The effect of 2 μM quercetin on fever- exposed HUVEC was assessed (Fig. 5.13d) but the effect of quercetin on basal adhesion levels masks any effect related to heat shock response pathway. At the concentration of KNK437 recommended for use (10 μM) there was a slight reduction in ICAM-1 level (80% of control, not shown) but cells were visibly affected by the treatment so any effect on binding phenotype (not shown) could not be directly attributed to effect on heat shock pathway over general cell death effects.

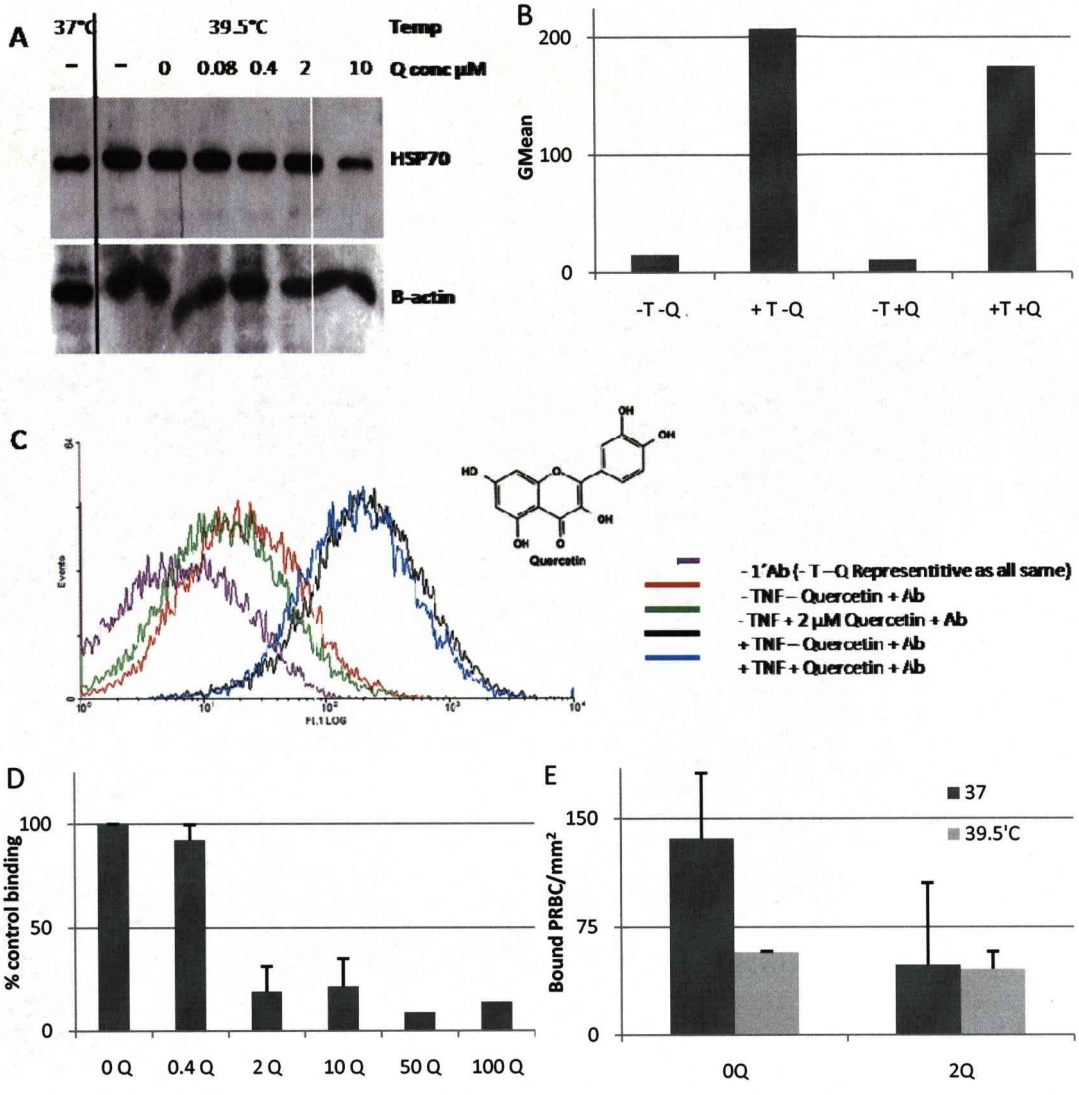

Figure 5.13. Effect of quercetin treatment of HUVEC on HSP induction, ICAM-1 expression and cytoadherence. A) Western blot for HSP70 Induction by 16h 39.5°C fever with addition of Quercetin at 0–10 µM concentration. 0 µM quercetin represents DMSO solvent only compared to – indicates no treatment. Blot was stripped and reprobed for β-actin as a loading control (lower panel). B) Geometric mean quantitation of ICAM-1 expression after 16 h TNF (1ng/ml) stimulation with 2 µM quercetin. And C) FACS trace of ICAM-1 levels after 16h TNF (1 ng/ml). D) Effect of quercetin at concentrations of 0.4 to 100 µM on ItG adhesion. Mean +SD 1–3 independent experiments expressed as a percentage of control (untreated) adhesion. E) Adhesion of ItG to HUVEC treated with quercetin 2 µM and 16 h 39.5°C fever. Bound PRBC/mm^2, mean + SD two independent triplicate experiments.

5-4 DISCUSSION

We have assessed the response of endothelial cells to fever in terms of PRBC cytoadherence. The striking result that we have shown is that host endothelial cells respond to fever in a way that is protective against ICAM-1 cytoadherence. All assays were performed at 37°C using parasites that had been maintained at 37°C in order to only analyse the effect that febrile temperatures had on the host endothelial cell.

The first observation was that fever had no stimulatory effect on adhesion. C24 which is known not to bind to HUVEC showed very low levels of adhesion to HUVEC that had been exposed to fever either with or without TNF stimulation. This suggested that fever was not making the endothelial cells "stickier" in any non-specific way. Similarly, HUVEC not exposed to TNF stimulation are known to support only very low levels of ItG cytoadherence, and this was not increased on fever exposure.

After TNF stimulation under febrile conditions, adhesion of ItG PRBC to HUVEC was reduced compared to adhesion to TNF stimulated cells maintained at 37°C. In individual experiments the degree of adhesion varied between 30% and 80% of controls. This variability could be explained by variations in the temperature of the incubators, both of which were found to vary by ± 0.5°C. Alternatively previous exposure of cells to fever or heat shock is known to confer protection against subsequent exposures, thermotolerance, it is possible that batches of cells may have been exposed to slightly raised temperatures at some point during growth or expansion which affected their response.

Although cell morphology appeared unaffected by fever, (as determined by observations of cell monolayers during adhesion assays), we used a resazurin based metabolic assay to quantitate cell viability. This showed that HUVEC exposed to 39.5°C fever for 16 h were still >90% viable compared to controls maintained at 37°C. Furthermore, analysis of cells using fluorescence microscopy to look at cell cytoskeleton showed no gross morphological changes and an intact monolayer of cells remained despite fever treatment.

A second explanation for the reduced adhesion that we considered was the possibility of a reduction in the level of ICAM-1 induced by the TNF stimulation. Flow cytometry

analysis of surface ICAM-1 levels suggested equivalent ICAM-1 stimulation in fever treated cells compared to those maintained at 37°C.

A reduction in the response to TNF could conceivably be due to increased degradation of TNF at the higher temperature resulting in an effectively lower concentration. Although this appeared not to be the case as ICAM-1 levels were equivalent, a second control for this involved adding TNF separately from the fever exposure. We found that cells exposed to fever then stimulated with TNF at 37°C showed a similar phenotype to those exposed to fever and TNF simultaneously, i.e. there was a reduction in adhesion to the fever exposed cells compared with those maintained at 37°C. Interestingly, preliminary experiments suggested that the converse was not true. Cells stimulated with TNF before fever exposure did not show a reduced binding phenotype. This hints at the possibility that the reduction in adhesion seen could be due to effects on newly synthesised proteins resulting from TNF stimulation under fever conditions or after fever exposure.

We also looked at ICAM-1 distribution across the surface of HUVEC. Initial experiments looked at ICAM-1 distribution before and after ItG adhesion assay, as well as without / with TNF stimulation. Before TNF stimulation there was very little ICAM-1 staining visible, and controls with no primary antibody showed no background fluorescence from secondary antibody alone (result not shown). After the ItG assay few PRBC were remaining after wash steps so any potential redistribution of ICAM-1 to PRBC adhesion sites would be difficult to analyse. This is probably due to the use of mAb 15.2 which is known to inhibit PRBC cytoadherence, and as we describe in chapter 6 can also reverse binding of already adherent parasites. Phalloidin staining of the actin cytoskeleton revealed possible hints of cytoskeletal changes to HUVEC (and HDMEC, not shown) after parasite adhesion (Fig. 5.5 phaloidin panel), however, this is under investigation elsewhere (Srabasti Chakravorty).

The distribution of ICAM-1 across the surface of HUVEC appeared broadly unaffected by fever exposure, similarly there was no evidence for effects on the F-actin network after exposure to fever. We also looked at HUVEC (and HDMEC) after adhesion assays on both control cells and those exposed to fever (not shown) and, similarly, there was no difference between cells exposed to fever and those maintained at 37°C.

We then chose to investigate the heat shock response pathway. This is a stress response pathway present in all mammalian cells which activates protective responses in response to environmental stresses including heat shock and heavy metal exposure (Wagner *et al.*, 1999). Standard heat shock conditions involve a short (1h) exposure to heat shock temperature generally between 42°C and 43°C followed by a recovery period at 37°C for around 4h to allow for protein synthesis. Under these conditions in HUVEC we could see significant upregulation of the heat shock response protein HSP70. This was the same whether TNF was absent or present. After exposure to our fever conditions of 39.5°C for 16 h we found that HSP70 was also induced, and again expression was unaffected by the presence of TNF. Upregulation of HSP70 in HUVEC could first be detected by western blotting after 4 h exposure to 39.5°C. This showed that exposure even to physiological range temperatures induces this stress response in endothelial cells.

HUVEC from different sources were shown to behave similarly in terms of cytoadherence phenotype and heat shock response after fever exposure (Fig. 5.8), however, significant differences could be seen between different types of endothelial cells. Whereas there was a clear reduction in adhesion to fever-exposed HUVEC, there was much less effect of fever on adhesion to HDMEC. This could be in part explained by the adhesion to constitutively expressed CD36 on the HDMEC. C24 adhesion to CD36 on HDMEC, and ItG binding to CD36 (after blocking of ICAM-1 adhesion) on HDMEC appeared unaffected by fever treatment (Fig. 5.9). When the CD36 mediated adhesion was blocked using the monoclonal antibody some further reduction in adhesion was seen after fever treatment – but the adhesion seen was still ~70% of controls compared with the <50% of control adhesion seen with HUVEC.

We also observed a reduced heat shock pathway response in HDMEC compared to HUVEC. This lesser response may explain this discrepancy in adhesion after fever, and hints at a role for the heat shock response pathway (or subsequent downstream effects) as having a role in the protection observed in HUVEC. Differences between different endothelial cell types are not unexpected as have been seen in previous studies looking at responses of endothelial cell to fever and heat shock (Ketis *et al.*, 1988). A specific example of this is the upregulation of ICAM-1 expression in specialised HEV cells (Chen et al., 2006), whereas, as we show, other endothelial cell types show little response (Hasday et al., 2001).

We assessed heat shock response pathway activation by looking at the stress response protein HSP70 which is known to be upregulated in response to heat stress

through the Heat Shock Transcription Factor (HSF-1). HSF-1 is a protein that in a resting state is complexed with HSP90. On exposure to heat stress HSF-1 becomes dissociated from HSP90 and trimerises, autophosphorylates and becomes an active transcription factor able to stimulate transcription of other heat shock pathway proteins, including HSP70 (Morimoto, 1998).

To determine the role of this pathway in protection against cytoadherence in HUVEC chemical inhibitors of the heat shock response pathway were used. Quercetin is a flavonoid which is found in onions, apples, tea and red wine, and can reach peak plasma concentrations of up to 2 μM from dietary intake (Moon *et al.*, 2008). It can inhibit heat shock response by inhibiting trimerisation and activation of HSF-1 (Nagai et al., 1995). However, quercetin has wide ranging inhibitory properties and has been shown to inhibit JNK pathways (Nagai et al., 1995), as well as TNF stimulation of NF-kB and conversely NF-kB pathway induced upregulation of TNF (Nair *et al.*, 2006). We found that the chemical appeared slightly toxic to HUVEC at concentrations previously published to be effective against HSF-1 activation, even in the absence of heat stress.

Quercetin alone in the absence of heat stress appeared able to significantly reduce levels of adhesion. The ability of this readily available dietary chemical alone to exert significant protective effects against cytoadherence may in itself be interesting. However, as a result of this effect on cytoadherence we were unable to use quercetin to help determine the importance of the heat shock response pathway in response to fever.

The downstream effector of the protection against cytoadherence was not elucidated. There are several possibilities which are described below and illustrated in figure 5.14b.

We have hints that the protective effect is seen only on adhesion to ICAM-1 newly synthesised in the presence of heat shock response proteins. This was evidenced by the lack of reduction in adhesion following fever when TNF stimulation, and therefore ICAM-1 production, preceded fever exposure (Fig. 5.3a). While when ICAM-1 was stimulated concurrently with fever, or following fever exposure, adhesion levels were reduced. Many of these proteins are chaperones which are involved in the folding of newly synthesised proteins. It is conceivable that the presence of one of more of these chaperones (i.e. HSP70) could result in subtly different folding of newly synthesised ICAM-1 resulting in a different display of the PfEMP-1 adhesion site on ICAM-1 (Fig. 5.14b).

Alternatively there may be effects of heat shock response pathway proteins inhibiting adhesion. HSP70 can be localised on the surface of cells after heat shock (although this has mainly been demonstrated in tumour cells (Multhoff *et al.*, 1995)) – this (or other proteins) could be providing direct inhibition of adhesion to ICAM-1 (Fig. 5.14d).

ICAM-1 dimerisation and clustering may be important for adhesion of the endogenous ligand LFA-1 (Miller *et al.*, 1995, Yang et al., 2004, Jun et al., 2001a), and could also be important for optimal adhesion of PRBC. The presence of heat shock pathway-activated proteins in the cell membrane i.e. small HSPs (sHSPs) such as HSP17 (Tsvetkova *et al.*, 2002) could be reducing the fluidity of the cell membrane (Fig. 5.14c).

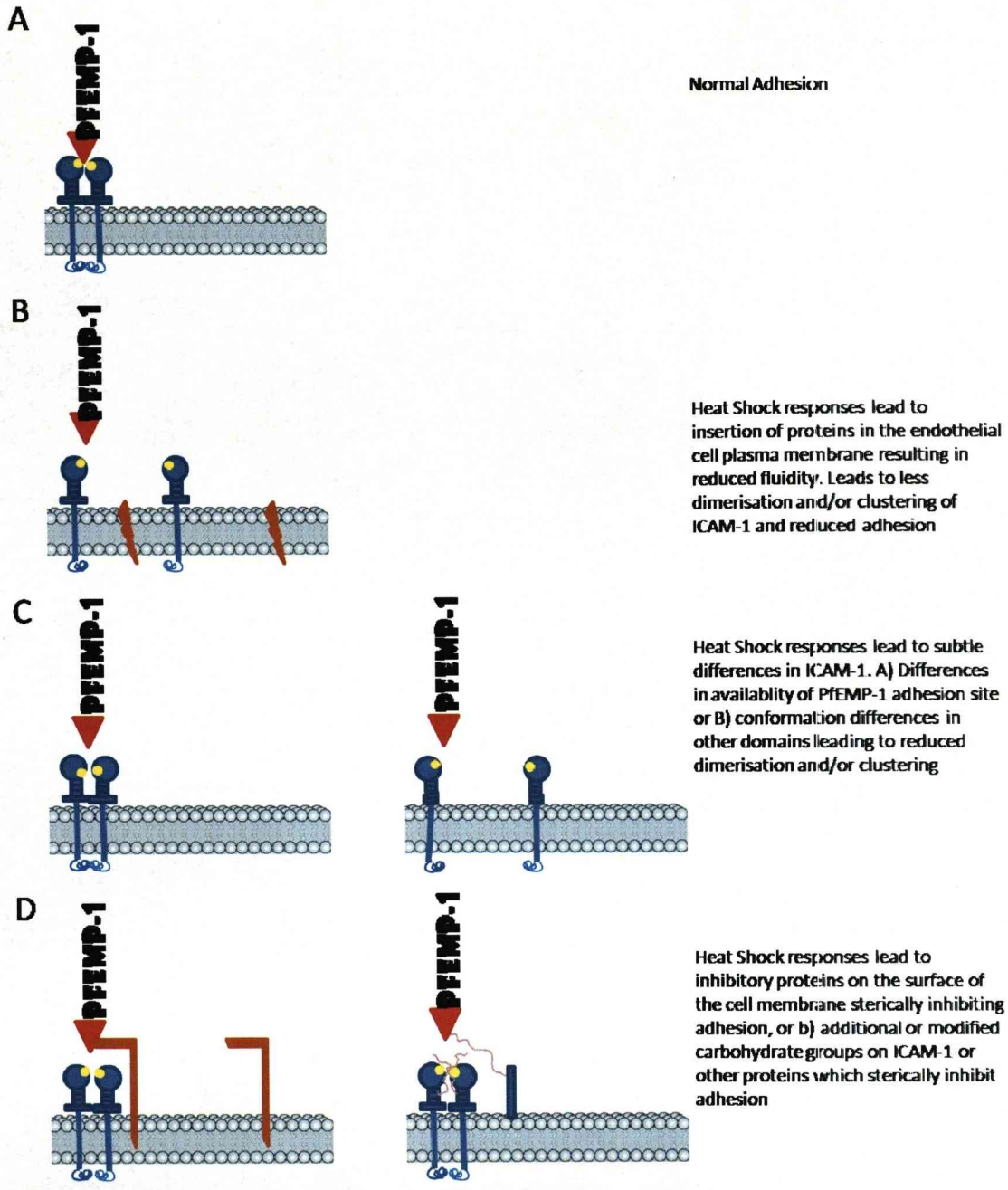

Figure 5.14. Model of possible mechanisms for the reduction in ICAM-1 cytoadherence after fever. Illustration of suggested mechanisms, as described in the text, for the protection against cytoadherence observed after exposure of endothelial cells to febrile temperatures.

5-5 LIMITATIONS AND FURTHER WORK

One limitation of this work is that most assays were carried out using just one *P. falciparum* isolate, ItG. To further confirm the observations in this chapter, this work needs to be extended by using further parasite isolates as it is known that different isolates have slightly different mechanisms of adhesion to ICAM-1 (Tse et al., 2004). Preliminary results suggested that the JDP8 and A4 *P. falciparum* isolates, both of which are known to adhere to ICAM-1, showed the same behaviour as the ItG. However, further repeats should confirm this, and the use of fresh patient isolates would be important to show that the phenomenon is not unusual to established laboratory isolates. The availability of new ICAM-1 binding patient isolates from a separate project (Lucy Ochola and Tadge Szestak), as used in chapter 6, will be advantageous.

Our results using HDMEC have suggested that the reduced adhesion following fever exposure in our experiments was limited to ICAM-1 binding, as there was no apparent effect on CD36 mediated adhesion. Whether this is due to CD36 being constitutively expressed, or that the febrile temperatures are specifically affecting ICAM-1 is not clear. Further work could be carried out to determine this, and the effect on adhesion to other receptors could also be determined.

Further experiments to elucidate how fever exposure is protecting against PRBC cytoadherence need to be carried out to distinguish between the possibilities illustrated in figure 5.14. These could include using a range of conformation sensitive ICAM-1 antibodies to detect potential subtle differences in ICAM-1. Adhesion of other ICAM-1 ligands, i.e. LFA-1 could show how general the effect is or whether it is limited to PRBC adhesion. Detection of changes in cellular membrane fluidity using FRAP of a GFP-labelled ICAM-1 protein (Yang *et al.*, 2006) could show whether ICAM-1 is less mobile within the membrane after fever exposure. A general screen for differences in protein, or carbohydrate content of the membranes of fever treated compared to untreated endothelial cells might reveal differences that prove to be the effector in the protection against cytoadherence. A 2-d DIGE approach combined with mass-spec identification of spots could be employed.

We suggest that the heat shock response pathway may play a role in the protection, although we were unable to provide any evidence for this. The use of chemical inhibitors of the heat shock response pathway was not successful. An RNAi knockdown

of the effecter transcription factor, HSF-1 (Zhao & Shen, 2007), could be attempted. RNAi has been increasingly used in HUVEC, and RNAi of HSF-1 has been successfully achieved in other endothelial cell types.

The opposite approach to determining whether heat shock response pathway was having a role in protection was also considered. Stimulation of heat shock response pathways in two alternative ways to the 16h 39.5°C fever was attempted. This first involved exposure to heavy metals (Wagner et al., 1999), however at concentrations around those previously reported to stimulated heat shock response pathways negative effects on cellular integrity were observed. Similarly, using heat shock (42.5°C, 1 h) to stimulate heat shock response pathways there was a fine line between just stimulating heat shock response pathways and reducing cellular integrity. Careful optimisation of these types of experiments would be required for any conclusions to be made.

5-6 CONCLUSIONS

We have provided evidence for the protective nature of natural host responses against cytoadherence. Specifically, we have shown that exposure of endothelial cells to physiologically relevant febrile range temperatures can protect against subsequent ICAM-1 mediated PRBC adhesion. Future work will determine what the mediator of this protective response is, and whether the heat shock response pathway plays any role in the protection.

CHAPTER 6 - BLOCKING AND REVERSAL OF ICAM-1 CYTOADHERENCE

6-1 INTRODUCTION

Cytoadherence of PRBC to endothelium is thought to have an important role in the pathogenesis of malaria, and as shown in chapter three this cytoadherence could be continuing for long after the initiation of antimalarial treatment. If this continued sequestration of PRBC is contributing to the continuation of disease symptoms, i.e. coma in the case of cerebral malaria, then it could be advantageous to reverse the cytoadherence interaction.

Although many experiments have addressed inhibition of adhesion, meaning the prevention of de-novo adhesion, there have been fewer studies looking at the potential to reverse the cytoadherence of already adherent PRBC. Reversal of adhesion, or "desequestration" of CSA-binding PRBC to placental sections has, however, been achieved by flushing through with CSA (Gysin *et al.*, 1999). Reversal of specific adhesion to CD36 has also been previously described. CD36 adhesion was reversed in standard static (Baruch *et al.*, 1997) and flow (Cooke *et al.*, 1998) conditions by addition of a recombinant protein derived from the CD36 binding region of the CIDR domain from PfEMP-1. Under flow conditions reversal of up to 50% was achieved after two hours of flow with 2 μM recombinant protein (Cooke et al., 1998). This recombinant protein was also shown to be able to reverse around 80% adhesion of PRBC to human endothelial cells expressing CD36 in a small number of skin-graft mouse models (Yipp *et al.*, 2003a).

Adhesion to ICAM-1 can be inhibited using monoclonal antibodies against ICAM-1 (Tse et al., 2004). The monoclonal antibody mAb 15.2 against the L42 loop of domain 1 of ICAM-1 is commonly used as a control antibody to inhibit ICAM-1 mediated cytoadherence. However, the reversal of adhesion to ICAM-1 has not been previously reported. Furthermore, while adhesion to ICAM-1 has been inhibited using antibodies, the use of proteins to inhibit adhesion has not been reported. Attempts to inhibit cytoadherence using a soluble ICAM-1 protein have been unsuccessful (Craig et al., 1997) – although this approach has been used for the inhibition of adhesion of rhinovirus to ICAM-1 (Casasnovas & Springer, 1994). A recombinant protein based on an ICAM-1 binding domain has not previously been available. However, we were able to access a recombinant protein based on the DBL-β domain which was produced as part of a project aiming to solve a crystal structure for the ICAM-1 binding DBL-beta

domain from PfEMP-1 (M. Higgins). This DBL-β domain derives from IT4var13 (Kraemer et al., 2007) which is a DBL-β domain containing *var* from *var* group B1 (Ups type B1), i.e. in the same *var* group as known ICAM-1 binders A4var and IT-ICAM (as expressed in A4 and ItG).

In this chapter we look at the ability of the recombinant DBL-β domain as well as mAb 15.2 to not only inhibit but to reverse adhesion of PRBC to ICAM-1.

6-2 MATERIALS AND METHODS

Parasites

P. falciparum isolates A4 and ItG were maintained as described in methods chapter 2. The patient isolate 8146 was obtained as part of larger project (Lucy Ochola, Kilifi, Kenya. Samples were obtained in Kilifi, Kenya with local ethical approval and parasites cultured at for at least 24 h before shipping to LSTM). Parasites were isolated from a patient in Kilifi, and after overnight growth to trophozoite-stage were assessed for their ability to adhere to ICAM-1 (Lucy Ochola, methods used as described in methods chapter 2). Since this isolate had some affinity for ICAM-1 it was maintained in culture and subjected to three rounds of selection on ICAM-1 (by Tadge Szestak, selection as described in methods chapter 2). All assays were carried out on parasites at mid-trophozoite stage (26 – 34 h post-invasion). Parasites were used at 3% parasitaemia and 1% haematocrit and were washed once then resuspended in binding buffer for assays (see methods chapter 2).

DBL Domain Proteins

DBL-β and DBL-3x domains were prepared by Matt Higgins (Dept. Biochemistry, Cambridge). Both were expressed as His tagged recombinant proteins in *E. coli* and purified using Ni-NTA affinity to a concentration of 10 mg/ml as described in (Higgins, 2008a). The DBL-β domain used is a 45 kDa fragment from the *var* gene IT4_var13 (EF158072) (Kraemer et al., 2007). The DBL-3X domain is a 37 kDa CSA-binding fragment from the *var* gene *var2csa* (Higgins, 2008a).

ICAM-1 Proteins

ICAM-1 proteins were prepared by Tadge Szestak (LSTM), as full length FC proteins and purified to concentrations of 200 – 700 µg/ml. The wild type, or reference ICAM-1 (ICAM-1 ref), and two ICAM-1 variants, ICAM-1 Kilifi and ICAM-1 S22A were used. Proteins were diluted to 25 µg/ml in Dulbecco's PBS (dPBS) for use. CD36 protein was obtained from R&D systems.

Static Adhesion Assays

Static adhesion assays to protein were carried out as described in methods chapter 2. In each dish ICAM-1 ref, (and the mutants ICAM-1 Kilifi and ICAM-1 S22A when used) were spotted at a concentration of 25 µg/ml, a CD36 spot was always included at 25 µg/ml to control for non-specific loss of PRBC binding, and a PBS spot included to control for background binding. Triplicate protein spots per dish were used. Counts

from the PBS spot for each dish were subtracted from each protein count, (however, these PBS counts were always very low, in the range of 0 – 6 PRBC/mm^2).

Static Adhesion Blocking Assays

Dishes were pre-incubated with 1.5 ml of binding buffer with or without blocking antibody or protein, at 37°C for 30 minutes, before proceeding with adhesion assay as above. The monoclonal antibody mAb 15.2 was used at 5 µg/ml in binding buffer. DBL-β domain protein was diluted to 25 µg/ml in binding buffer and serial five-fold dilutions were made for concentration dependence assays. Control DBL-3X protein was used at 25 µg/ml in binding buffer.

Reversal Assays – Static Protein

For reversal assays controls were always carried out in the same experiment such that in a given experiment there were at least 4 conditions (see also schematic figure 6.3a): Dishes 1 and 2 were treated as a standard binding / blocking assay (no blocking, mAb blocking (and DBL-β blocking when used)). Dishes 3 and 4 were treated as a standard binding assay along with dishes 1–2 up to the end of 8 x 2 ml binding buffer washes. At this point dishes 1–2 were fixed in 1% glutaraldheyde in PBS while dishes 3–4 were incubated for a further 1 hour with either binding buffer alone, or mAb 15.2 (5 µg/ml in binding buffer), or DBL-β protein when used, with gentle mixing every 10 min. After the further incubation dishes were washed 4 X 2 ml binding buffer and fixed in 1% glutaraldehyde in PBS. All experiments were carried out with duplicate dishes each containing triplicate spots. After overnight fixing at room temperature, dishes were stained for 30 min in 5% Giemsa, washed with water and air dried before counting (see below).

Reversal Assays – Static Endothelial Cell

HUVEC were maintained and static cell assays carried out as described in methods chapter 2. For reversal assays PRBC were allowed to bind as for normal assay then following two dip washes coverslips were placed in a gravity wash for 30 min. After 30 min coverslips were placed cell-side up into a well containing binding buffer with (and control without) mAb 15.2 at 5 µg/ml. After 30 min coverslips were transferred to a second gravity wash for 10 min then fixed in 1% glutaraldehyde. As with static protein assays, controls were carried out which were fixed before the second incubation. All cell assays were carried out in triplicate.

Reversal Assays – Under Flow Conditions

Flow reversal assays were carried out on microslides coated in ICAM-1 ref at 50 µg/ml. Slides were prepared and assays carried out as described in Methods Chapter 2. PRBC at 3% parasitaemia and 1% haematocrit were flowed through the microslide for 5 min to allow for PRBC adhesion. Flow was continuous throughout the experiment at 0.05 Pa shear stress. After 5 min PRBC flow, flow was switched to binding medium alone to remove unbound PRBC and clear flow lines of PRBC. Timing was started at the start of this wash which continued for 2 min before the binding medium was swapped for medium containing mAb or DBL-β protein. The number of bound cells in six fields alone the slide was counted at 2 min, 5 min, 10 min 15 min and 20 min time points (see figure 6.7a for schematic). Reversal of adhesion to HUVEC under flow conditions was carried out in a similar way on TNF (1 ng/ml 16h) stimulated HUVEC grown overnight on microslides.

Counting Static Assays

Static adhesion assays were counted using a macro developed on Image-pro plus by Doug Paton as a Masters student project. Images were captured using the X10 objective on a Nikon microscope using a camera and image pro-plus software. 8 images for each protein spot were captured and saved as 8 bit grayscale files. Once all images from each dish had been captured, files were all opened and the macro initiated to count spots from each image. Doug's work optimised the analysis so that the program correctly recognised and counted only PRBC, this was statistically verified by comparison with manual counts (Doug Paton, Masters Project 2007).

6-3 RESULTS

Part I - USE OF PROTEIN TO INHIBIT ADHESION TO ICAM-1

DBL-β protein blocks adhesion of ItG and A4 PRBC to ICAM-1

The ability of the recombinant DBL-β domain protein to bind to ICAM-1 has been shown (Tadge Szestak, LSTM, unpublished), suggesting a functional domain. We wanted to test the ability of this protein to inhibit adhesion of PRBC to ICAM-1, and first tested this using static protein adhesion assays. Adhesion of both ItG and A4 PRBC to immobilised ICAM-1 could be blocked with 25 μg/ml of DBL-β protein (Fig. 6.1). Blocking compared to control of 84% ± 12% for ItG and 93.4% ± 3% for A4 was achieved ($P<0.001$ (T-test) for both). The monoclonal antibody, mAb 15.2, has been previously used to inhibit adhesion, and in these experiments was shown to inhibit adhesion by >95% for both isolates (Fig. 6.1).

As a control for the specificity of the blocking by the DBL-β domain we used a DBL-3X domain which is a domain known to adhere to CSA but not ICAM-1. The DBL-3X protein is a similar size and produced in the same way to the DBL-β protein used (Higgins, 2008a). The DBL-3X domain protein did not significantly affect adhesion of A4 or ItG PRBC to ICAM-1 (Fig. 6.1). Adhesion to CD36 was not affected by either DBL-β or DBL-3X protein (data not shown). Adhesion is expressed as a % of control (no blocking) adhesion for each independent experiment, and results show the mean and SD of three independent experiments. The mean ± SD of bound A4 PRBC in the control dishes was 534 ± 195 PRBC/mm^2, whereas ItG PRBC showed higher levels of adhesion at 1634 ± 598 PRBC/mm^2.

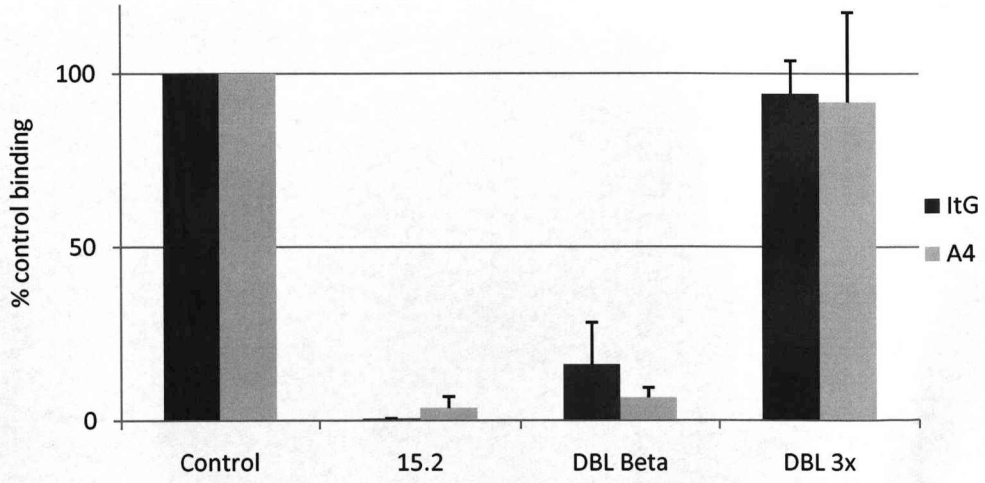

Figure 6.1. Adhesion of ItG and A4 to ICAM-1 protein in static assays. Blocking using mAb 15.2 at 5 μg/ml, DBL-β at 25 μg/ml or DBL-3X at 25 μg/ml. Expressed as a percent of the control binding in each experiment. Mean + SD of three independent duplicate experiments

Concentration Dependence of DBL-β blocking of adhesion to ICAM-1 variants

The concentration dependence of this inhibition of adhesion was assessed over a range of concentrations from 0.2 μg/ml to 25 μg/ml for both A4 and ItG PRBC. Since these two *P. falciparum* isolates are isogenic, well established laboratory isolate, we also used a recent patient isolate, 8146. This strain was isolated from a patient in Kilifi, Kenya as part of a larger study (Lucy Ochola). This isolate was tested for adhesion to ICAM-1 and since showed some levels of adhesion was then subjected to three rounds of selection on ICAM-1 protein (Tadge Szestak, LSTM). We found that the isolate 8146 was able to adhere to ICAM-1 ref in static assays at similar levels to A4 (not shown).

As illustrated in figure 6.2a, there was clear concentration dependent inhibition of adhesion for all three isolates. Curves illustrated the relative inhibition of adhesion, and the bar charts for each experiment show adhesion levels of the controls as bound PRBC/mm^2 (Fig. 6.2). Control adhesion assays with blocking using the DBL-3X domain show no inhibition of adhesion, and control inhibition using the mAb 15.2 in each experiment showed ~95% inhibition of adhesion (Fig. 6.2a, bar chart). Adhesion to CD36 protein was tested in each experiment and was not inhibited by either of the DBL domains at any concentration, or by the mAb 15.2 (not shown).

Having shown the ability of DBL-β to inhibit adhesion to ICAM-1 ref, we also looked at ability of the DBL-β protein to block adhesion to ICAM-1 variants. The variant ICAM-1 Kilifi has a K29M substitution (see introduction chapter 1 figure 1.8). It is known that ItG PRBC show similar levels of adhesion to ICAM-1 Kilifi as to the wild type, or reference ICAM-1 (referred to as ICAM-1 ref), whereas A4 PRBC do not adhere to ICAM-1 Kilifi. A second ICAM-1 variant with a substitution S22A was also used. The adhesion phenotypes to ICAM-1 S22A is reversed, with A4 PRBC able to adhere to ICAM-1 S22A whereas ItG PRBC show no binding to ICAM-1 S22A (Tse et al., 2004). We found that the isolate 8146 was able to adhere to ICAM-1 ref at similar levels to A4. It was also able to adhere to ICAM-1 Kilifi, and at slightly lower levels to ICAM-1 S22A.

The adhesion of ItG PRBC to the ICAM-1 mutant ICAM-1 Kilifi was inhibited by DBL-β in a similar concentration dependent manner to the inhibition of adhesion to ICAM-1 ref (Fig. 6.2b). As expected A4 PRBC showed no adhesion to ICAM-1 Kilifi (Fig. 6.2b, bar chart). Preliminary experiments showed that the patient isolate 8146 also showed adhesion to ICAM-1 Kilifi and this could be inhibited in a similar manner using DBL-β (Fig. 6.2b).

As expected no adhesion of ItG PRBC to ICAM-1 S22A was seen (Fig. 6.2c bar chart). However adhesion of both A4 PRBC and 8146 PRBC could be inhibited using DBL-β protein (Fig. 6.2c).

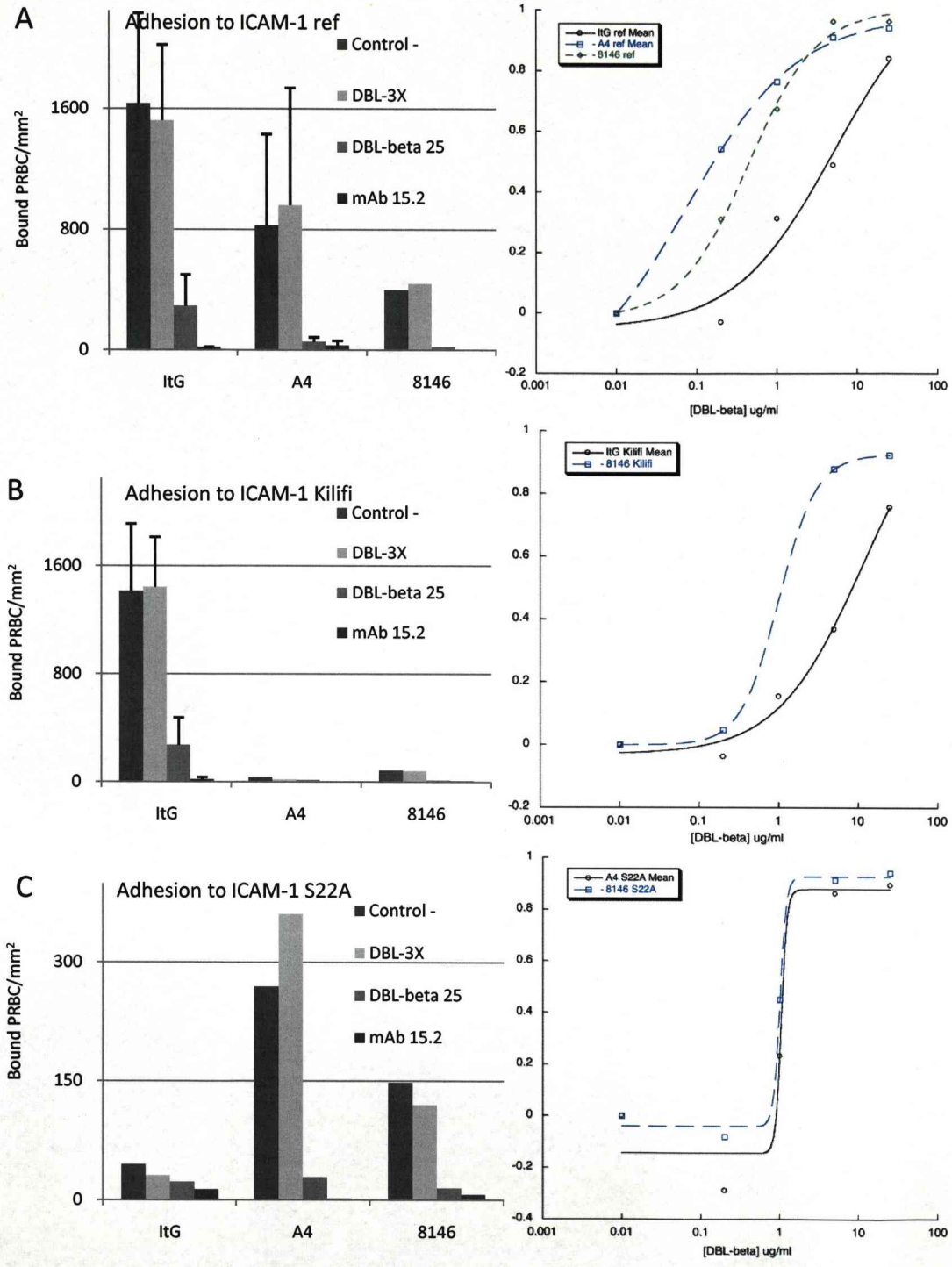

Figure 6.2. Adhesion to ICAM-1 protein variants and concentration dependent inhibition by DBL-beta. i) Bar charts show number of PRBC bound per mm^2 for controls for assays including untreated positive control (i.e. 0 µg/ml DBL-β), DBL-3X at 25 µg/ml, mAb 15.2 at 5 µg/ml and DBL-beta domain at 25 µg/ml. ii) Curves show plots of relative inhibition of adhesion by DBL-beta protein concentrations 0.2 to 25 µg/ml. Plotted as relative inhibition of control (untreated) binding where 1 represents complete inhibition of adhesion and 0 represents control levels of adhesion. ItG and A4 results represent the mean of three independent experiments + SD. Adhesion to: A) ICAM-1 ref, B) ICAM-1 Kilifi and C) ICAM-1 S22A.

The DBL-3X protein at 25 µg/ml showed no inhibitory effect on adhesion to any of the ICAM-1 variants (Fig. 6.2a-c bar charts). As expected, the monoclonal antibody mAb 15.2 strongly inhibited adhesion of all isolates to all ICAM-1 variants, as shown in figure 6.2 bar charts a-c.

The IC_{50} concentration for DBL-β blocking represents the concentration at which DBL-β can block 50% of PRBC adhesion. These values varied slightly between isolates, which IC_{50} values highest for the strong ItG PRBC adhesion compared to the moderate levels of adhesion of A4 and 8146 PRBC (Table 6.1).

	ItG	**A4**	**8146**
ICAM-1 ref	5.14	0.07	0.435
ICAM-1 Kilifi	11.23	n/a	0.993
ICAM-1 S22A	n/a	1.04	0.998

Table 6.1. IC50 concentrations of DBL-β protein for ICAM-1 variants. IC_{50} value (DBL-β concentration µg/ml) calculated using for each isolate ItG, A4 and 8146 on each ICAM-1 variant, ICAM-1 ref, ICAM-1 Kilifi and ICAM-1 S22A. Values based on three independent experiments (except for 8146 and A4 S22A).

Part II - REVERSAL OF ADHESION TO ICAM-1

The ability of mAb 15.2 to block adhesion has been shown, and we have established that the DBL-β domain can also block adhesion. However, the reversal of PRBC already bound to ICAM-1 has not been shown. We next test the ability of both the monoclonal antibody mAb 15.2 and the DBL-β domain to reverse already adhered PRBC.

Reversal of adhesion using Monoclonal Antibody – Static assays

In conjunction with James Callery as a Masters project (J. Callery 2008) we first assessed the ability of the mAb 15.2 to remove PRBC bound to ICAM-1 (Fig. 6.6). PRBC were allowed to adhere as for a standard static assay, and unbound cells washed off before incubation of the dish with the mAb 15.2 to reverse adhesion (See materials and methods and figure 6.3a). In these experiments the mAb 15.2 at 5 μg/ml was able to achieve >95% inhibition of adhesion and >80% reversal of ItG adhesion to 50 μg/ml ICAM-1 (Fig. 6.3). In figure 6.3 the positive control refers to adhesion levels with no blocking antibody after the first round of washing, and positive control (2) refers to the adhesion levels of control dishes after the second incubation and second round of washing, i.e. the reversal step (see also schematic figure 6.3a). It is clear that there is some reduction in adhesion in these experiments due to the extra incubations and wash steps, however this reversal was greatly increased by addition of the mAb 15.2. The value of 80% reversal refers to comparison of adhesion levels after the reversal wash steps either with or without mAb 15.2.

A

B

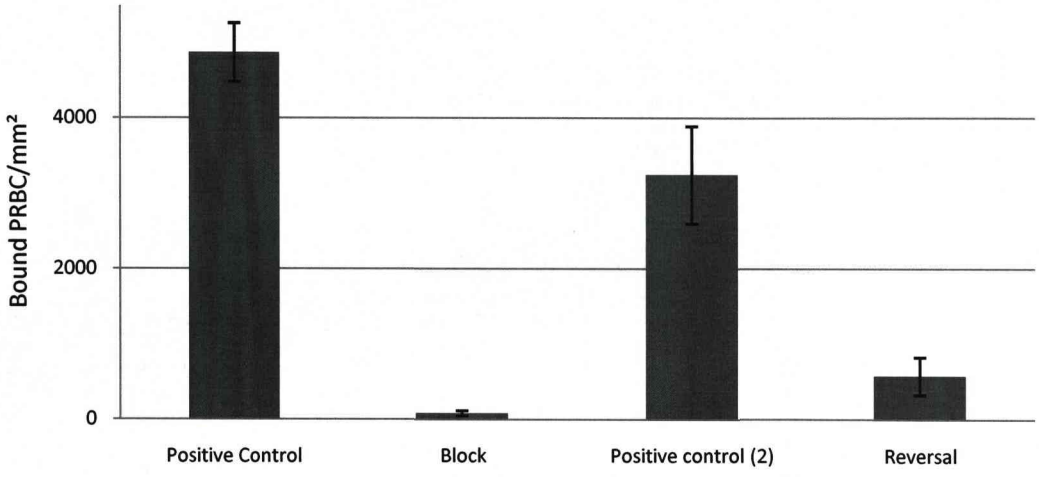

Figure 6.3 (KH & JC). Reversal of adhesion of ItG PRBC to ICAM-1. A) Schematic of assay for reversal as described in materials and methods. Each circle represents an assay dish over incubation and wash steps (left to right). B) Reversal of adhesion to ICAM-1 in static protein assays using 5 µg/ml mAb 15.2. Expressed as bound PRBC/mm^2 mean of three independent experiments, error bars indicate 95% confidence intervals.

Reversal of Adhesion using mAb 15.2 – Flow assays

The monoclonal antibody mAb 15.2 was also shown to reverse adhesion to ICAM-1 under physiologically relevant flow conditions. PRBC were allowed to adhere to ICAM-1 under standard flow conditions then washed at the same flow rate with binding buffer containing mAb 15.2. Counts of bound parasites showed a reduction in the number of adhered PRBC over 20 min flow with mAb 15.2 at either 1 µg/ml or 5 µg/ml concentration (Fig. 6.4). A 67% reduction in adhesion was seen when comparing the number of adherent PRBC before and after 20 min flow with 5 µg/ml mAb 15.2. Control

slides washed with binding buffer alone showed that 90% of adhered PRBC remained bound after 20 min. The same concentration of antibody was able to block 98% of adhesion (not shown).

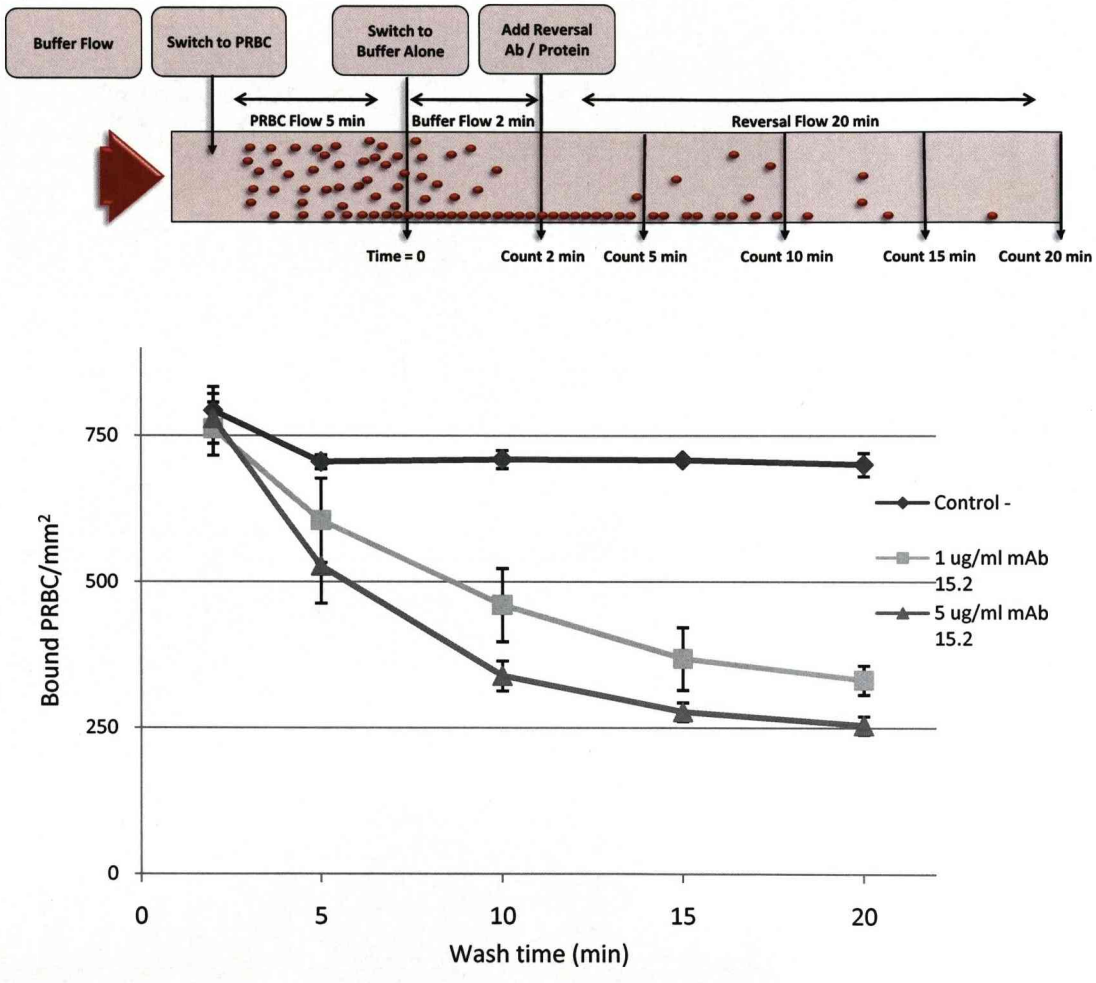

Figure 6.4 (KH & JC). Reversal of adhesion of ItG PRBC to ICAM-1 protein in flow assays. A) Schematic of assay as described in methods. B) Reversal of flow adhesion to ICAM-1 protein using 1 µg/ml or 5 µg/ml mAb 15.2. Results expressed as bound PRBC/mm^2, showing the mean of three independent experiments. Error bars indicate 95% confidence intervals.

Reversal of Adhesion using mAb 15.2 – HUVEC Static assays

The reversal of ICAM-1 mediated adhesion on endothelial cells was assessed using TNF stimulated human umbilical vein endothelial cell (HUVEC). Reversal was achieved using mAb 15.2 (Fig. 6.5). A 93% reduction in adhesion was seen after a wash with 5 µg/ml mAb 15.2 compared to washing in binding buffer alone.

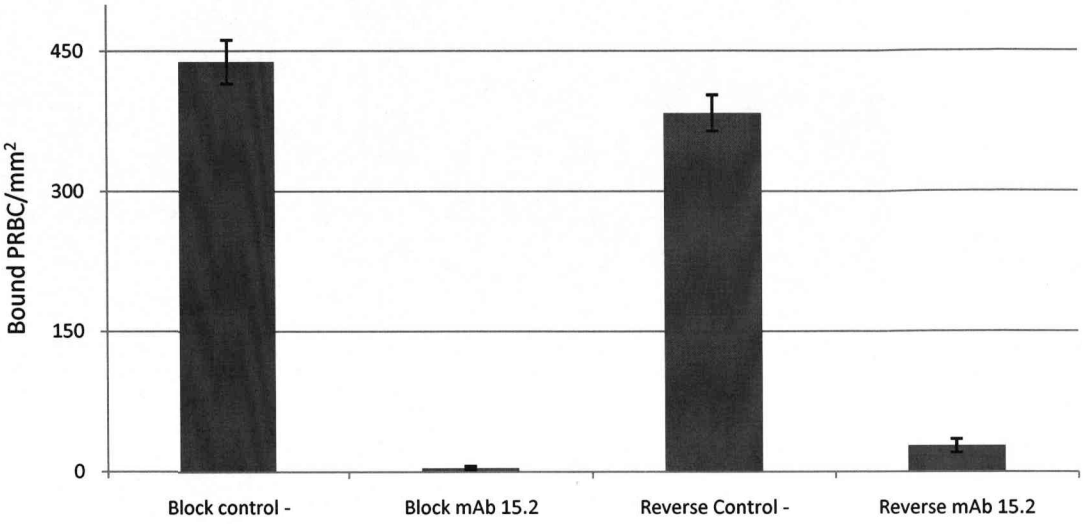

Figure 6.5 (KH & JC). Reversal of adhesion of ItG to TNF stimulated HUVEC. Monoclonal antibody mAb 15.2 at 5 µg/ml was used to block or reverse adhesion to HUVEC. Results expressed as bound ItG PRBC/mm^2, showing the mean of three independent experiments. Error bars indicate 95% confidence intervals

Reversal of Adhesion using DBL-β – Static Assays

The ability of the DBL-β domain protein to reverse adhesion in static protein assays was tested in the same way as the monoclonal antibody (as illustrated in schematic figure 6.3a). As described in materials and methods the mAb was used in the same experiment as a control. We were able to achieve significant reversal of 60% with DBL-β at 25 µg/ml compared to binding buffer alone, whereas in these experiments treatment with mAb 15.2 resulted in >90% reversal (Fig. 6.9). Adhesion to CD36 was not significantly reversed by either the anti-ICAM-1 antibody or DBL-β protein (not shown).

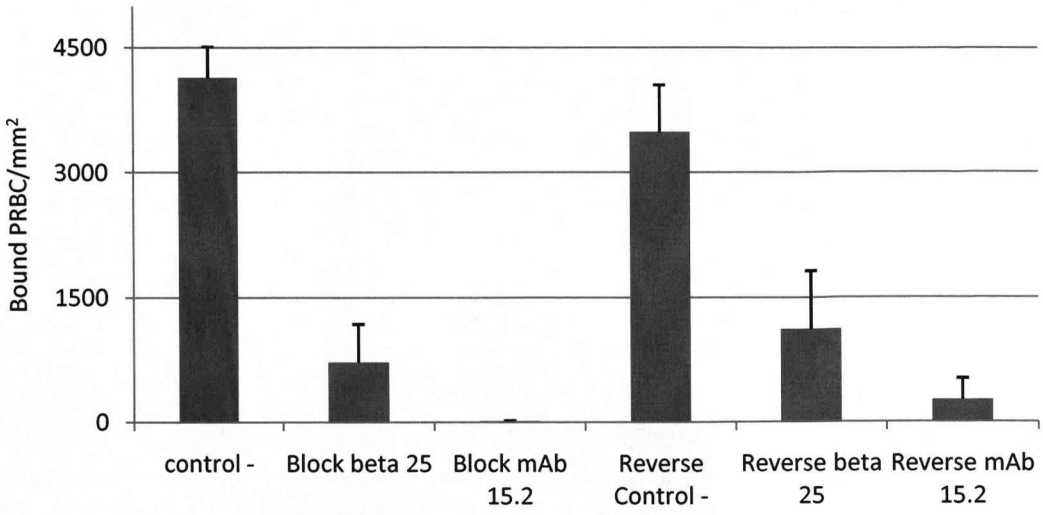

Figure 6.6. Reversal of adhesion of ItG to ICAM-1 protein in static assays using DBL-β. DBL-β protein at 25 µg/ml or mAb 15.2 at 5 µg/ml was used to block or reverse adhesion to ICAM-1 protein in static assays. Results are expressed as bound PRBC per mm^2 showing the mean ± SD of three independent duplicate experiments

Reversal of Adhesion using DBL-β – Flow Assays

In order to confirm the ability of the DBL-β protein to reverse sequestered PRBC under flow conditions we used the same experimental conditions as used for the monoclonal antibody (see schematic figure 6.4a). Similarly to mAb 15.2 the DBL-β protein was able to inhibit around 95% of adhesion to ICAM-1 under flow conditions (Fig. 6.7 block). Reversal of 70% of adherent PRBC to ICAM-1 under flow conditions was achieved after 20 min flow with 25 µg/ml DBL-β. (Fig. 6.7).

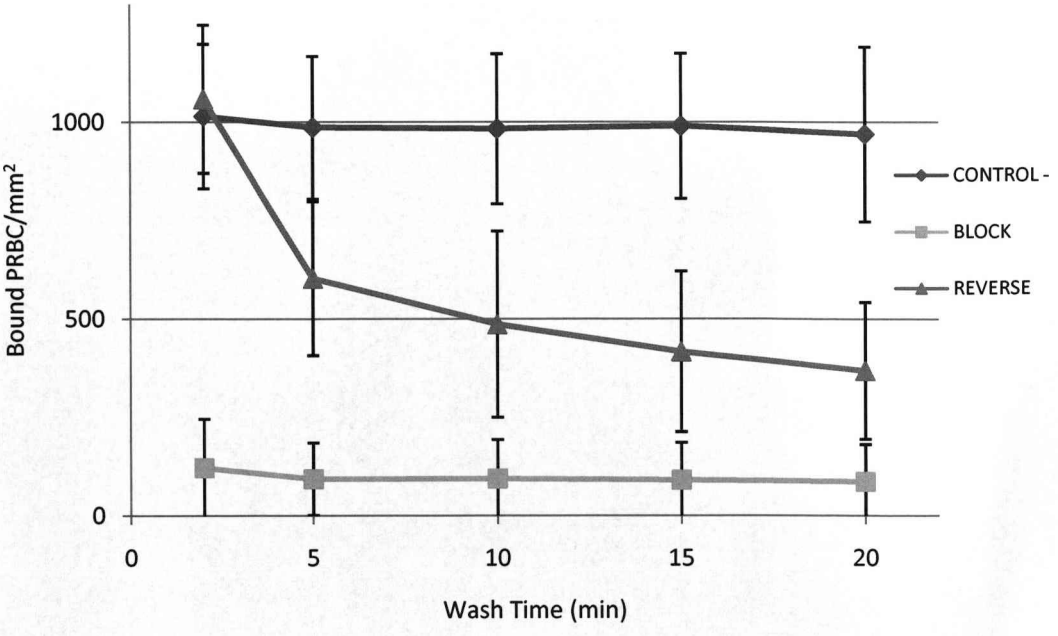

Figure 6.7. Reversal of adhesion to ICAM-1 protein under flow conditions using DBL-β protein. Protein used at 25 µg/ml, assay as illustrated in figure 6.3a. Mean of four slides ±95% confidence intervals

6-4 DISCUSSION

It has been widely discussed that an adjunct therapy which can reverse cytoadherence, leading to desequestration of PRBC could be advantageous to improve prognosis in severe malaria cases. Our results in chapter 3, which illustrate that PRBC maintain the ability to cytoadhere for many hours after administration of antimalarial treatments, support the idea that such a therapy, to be administered alongside conventional antimalarial treatment, could be beneficial. However, there is little *in vitro* work showing that this is feasible, and no studies have specifically addressed reversal of ICAM-1 mediated adhesion. We set out to test whether we could reverse specific adhesion to ICAM-1 *in vitro*. We also assessed the ability of a recombinant protein to inhibit and reverse adhesion, since most work published has used only monoclonal antibody to inhibit ICAM-1 mediated cytoadherence. We have found that both an anti-ICAM-1 monoclonal antibody, and a DBL-β recombinant protein can reverse adhesion of PRBC to ICAM-1.

Use of protein to inhibit ICAM-1 adhesion

Monoclonal antibodies have been widely used to inhibit ICAM-1 adhesion. Here, we have provided the first evidence of a recombinant protein that can inhibit PRBC adhesion to ICAM-1.

Two well characterised, established laboratory *P. falciparum* isolates were used. ItG which is known to have a high binding affinity for ICAM-1 and a moderate ICAM-1 binder A4. These are isogenic isolates which express antigenically (and phenotypically) distinct PfEMP-1 proteins. The expected *var* or PfEMP-1 expression for each strain was confirmed before experiments were carried out (see materials and methods chapter 2). In order to confirm that the results seen were not unusual to long-established laboratory isolates, a more recent patient isolate was used. The isolate was obtained from Kilifi, Kenya as part of a large project to analyse the ICAM-1 binding phenotype of patient isolates. The isolate used here, 8146, was shown to adhere to ICAM-1, and had undergone three rounds of selection *in vitro* for adhesion to ICAM-1 in order to homogenise the population before sequencing of the expressed *var* gene could be carried out (Tadge Szestak).

The three isolates used differ subtly in their binding to ICAM-1. ItG showed the highest adhesion to ICAM-1, followed by A4 and 8146 showing similar moderate levels of adhesion. However, as well as the difference in affinity for ICAM-1 the three isolates show different binding ability to two ICAM-1 variants, ICAM-1 Kilifi which has a K29M

substitution and the mutant ICAM-1 S22A. As previously shown (Tse et al., 2004), ItG showed no binding to the S22A mutant, but high binding to ICAM-1 Kilifi, whereas A4 showed no binding to ICAM-1 Kilifi but significant adhesion to ICAM-1 S22A. In contrast, the new patient isolate, 8146, was able to bind to all three ICAM-1 variants, although adhesion to the two mutant ICAM-1 proteins appeared to be at slightly lower levels than that seen to ICAM-1ref (Fig. 6.3).

The recombinant DBL-β protein used to inhibit adhesion was based on a domain from a different PfEMP-1 to those expressed by any of the three parasite isolates used. However, it was clearly able to inhibit adhesion of all parasite isolates to each of the ICAM-1 variants used, including the high levels of adhesion seen of ItG to ICAM-1ref.

It is known that PRBC expressing different ICAM-1 adhesive DBL-β domains may bind slightly differently to ICAM-1, as illustrated by different sensitivity to ICAM-1 mutations (Tse et al., 2004). Our use of three parasite isolates, and three ICAM-1 variants illustrate that our observed inhibition of ICAM-1 mediated adhesion was not limited to one specific PRBC type but could inhibit adhesion of PRBC expressing divergent ICAM-1 binding DBL-β domains. We did show, however, that the observed inhibition by the protein was specific, and not due to any generic stickiness of the recombinant protein. The DBL-β protein, at the highest concentration used, did not inhibit adhesion (of any of the tested isolates) to CD36 (data not shown). Furthermore, a DBL-3x domain protein produced in a similar way to the DBL-β domain protein did not lead to any inhibition of adhesion to either ICAM-1 or CD36.

The concentration dependence of the inhibition of adhesion was slightly different between ItG and A4 (Fig. 6.2), reflecting the different strengths of adhesion between the two parasite isolates.

Reversal of PRBC adhesion to ICAM-1

We have also shown for the first time the ability to reverse ICAM-1 mediated cytoadherence. This was possible using both the monoclonal antibody mAb 15.2 and the recombinant DBL-β protein. The antibody used is known to map to the L42 loop in the predicted DBL-β binding region of domain 1 of ICAM-1 (see introduction chapter 1, figure 1.7), and has previously been used to block ICAM-1 mediated adhesion of PRBC (Tse et al., 2004, Chakravorty et al., 2007). Reversal of the strong adhesion of ItG to ICAM-1 was possible in static conditions when bound PRBC were incubated in buffer containing antibody, and also under flow conditions when the same concentration of

antibody was flowed at a physiologically relevant shear stress of 0.05 Pa over adhered PRBC.

We have also shown that the reversal effect can be achieved under physiologically relevant flow conditions, to both ICAM-1 protein and ICAM-1 expressing HUVEC endothelial cells. In flow assays the effect of the DBL-β protein was rapid with PRBC release from the microslide observed as soon as the DBL-β containing buffer reached the slide (at 4 min).

The ability of both the mAb and the recombinant protein to not only inhibit but to reverse adhesion has important therapeutic implications. Results presented in chapter 3 showed that the cytoadherence of PRBC to endothelium can continue for long after administration of antimalarial treatment. As we discussed, and has been discussed before (Checkley & Whitty, 2007, Dondorp et al., 2005), reversal of these cytoadherent parasites has the potential to be highly advantageous. The continued sequestered parasite population has the potential to still be contributing to disease severity by impeding blood flow and contributing to endothelial damage as well as enhancing local inflammatory responses (Chakravorty et al., 2007). Furthermore, we showed in chapter 4 that these antimalarial treated PRBC remain rigid after loss of parasite viability, meaning that released PRBC would still potentially be able to be recognised and cleared by the spleen.

It has been shown previously that adhesion to CD36 can be reversed to some extent using a recombinant protein designed against the CD36-binding CIDR domain of PfEMP-1 (Baruch et al., 1997, Cooke et al., 1998, Yipp et al., 2003a). Here we show that a recombinant protein derived from the ICAM-1 binding DBL-β domain of PfEMP-1 can reverse ICAM-1 adhesion. Although CD36 adhesion is common to many parasite isolates, CD36 is highly expressed in a wide range of endothelial and other cells types and is important in many inflammatory processes. The high levels of expression of CD36 on a wide range of cell types and the lack of correlation of CD36 adhesion and clinical severity may make targeting of CD36 adhesion an inefficient way to remove sequestered PRBC populations. Given the proposed link between ICAM-1 adhesion and cerebral malaria (Chakravorty & Craig, 2005, Turner et al., 1994) it may be that targeting ICAM-1 adhesion may be an efficient way to improve prognosis in this severe subset of malaria cases.

6-5 LIMITATIONS AND FURTHER WORK

Most of the work presented here looks at reversal of adhesion specifically to ICAM-1 protein. Preliminary experiments suggest that the reversal of adhesion to ICAM-1 on endothelial cells would be possible in a similar way. The most physiologically relevant *in vitro* experiment that we could perform would be to assay for reversal of PRBC bound to endothelial cells under flow conditions. A potential complication of this would be maintaining the health/viability of the endothelial cells during the prolonged flow assay process. However, preliminary experiments over a 20 minute reversal suggested that a monolayer of generally morphologically healthy looking HUVEC could be maintained. This assay revealed that a reversal of over 50% could be achieved from HUVEC both with the DBL-β domain, and the mAb 15.2 (result not shown). However, the much lower levels of adherent PRBC initially may mask larger real differences. Significant optimisation of these experiments would be necessary to ensure we were working with healthy cells and statistically relevant adhesion levels.

The results presented here show that a 45 kDa recombinant protein derived from a previously uncharacterised ICAM-1 binding DBL-β domain is an efficient way to inhibit and reverse adhesion of even the strong ICAM-1 binding isolate ItG. Further knowledge of the mechanism of ICAM-1 adhesion by different variant DBL-β domains could allow a targeted development of a protein or peptide with a higher affinity for ICAM-1 allowing more efficient reversal of adhesion. A crystal structure of the adhesion of DBL-β domains bound to ICAM-1 will be invaluable for establishing the detail of the binding interaction. This work is currently in progress and was the reason for the availability of the recombinant DBL-β protein (M. Higgins, Cambridge). The structure of the CSA binding DBL-3X domain has already been solved both alone and in a co-crystal with CSA (Higgins, 2008b, Singh et al., 2008).

A major limitation is that we are looking at adhesion only to ICAM-1, whereas it is known that *in vivo* adhesion may be mediated by co-operation between more than one receptor. We could model a more complicated adhesion process using an alternative endothelial cell type, HDMEC which, in addition to ICAM-1 also express CD36. As described above optimisation experiments would be necessary, as would inclusion of similar experiments using an anti-CD36 antibody or protein. However, since adhesion in the brain in cerebral malaria is thought to be mediated at least mainly by ICAM-1 adhesion, reversal of simple ICAM-1 adhesion could well still be relevant in these severe cases.

The results we have presented are a complete, although simplified analysis of the ability of both monoclonal antibody, and DBL-β protein to inhibit and reverse ICAM-1 adhesion.

6-6 CONCLUSIONS

We have shown that a monoclonal antibody and a recombinant DBL-β domain protein can both inhibit and reverse adhesion of different PRBC isolates to ICAM-1 in both static and flow conditions. This has significant implications for the viability of an adjunct therapy that may be able to reverse sequestration, potentially during the first 24 hours of antimalarial therapy while PRBC are still potentially capable of cytoadherence (chapter 3). Further development of this work and the development of an optimised binding protein based on the DBL-β:ICAM-1 binding interaction could conceivably lead to a viable adjunct therapy that could be administered along with antimalarial treatment particularly in cases of cerebral malaria.

CHAPTER 7 – SUMMARY

This thesis has focussed on cytoadherence of *P. falciparum* infected red blood cells to endothelial cells, and the potential effects that natural host responses, i.e. fever, as well as interventions, i.e. antimalarial drugs, have on this interaction. Within each chapter we have discussed our major findings, and their significance and limitations. Here we briefly summarise our results.

The first part of the thesis, presented in chapters 3 and 4 addressed the question of what happens in terms of cytoadherence after antimalarial treatment. Our main findings were that the cytoadherence of PRBC could continue for long periods after administration of antimalarial treatment. Consistent with this, the remodelling of PRBC could be seen to be maintained after treatment, in terms of both the expression of PfEMP-1 on the surface of the PRBC and the increased rigidity of the PRBC. The maintained capacity for cytoadherence of PRBC after antimalarial treatment had been suggested previously. However we have provided the first evidence using a range of cytoadherence assays of the maintained ability of non-viable parasites to cytoadhere.

This work also illustrates that there may be an advantage for antimalarials that act on younger, i.e. circulating, ring stage parasites as these prevent the maturation of this round of parasites to cytoadherent trophozoite stages. While this result had been predicted elsewhere it had not previously been shown. When this stage was treated with a range of antimalarials we could show that PRBC treated with drugs that prevented maturation to cytoadherent trophozoite stages showed no adhesion 24 h following treatment. Ring-stage PRBC treated with drugs that allowed maturation to cytoadherence trophozoite stages showed high levels of cytoadherence 24 h following treatment, which would be expected to slowly decline over the next 24 + hours.

The maintained capacity for cytoadherence after antimalarial treatment suggests that there may be a therapeutic advantage for the administration of anti-adhesive adjunct therapies that can not only inhibit, but can reverse cytoadherence. This issue was addressed in chapter 6. We have shown that both a monoclonal anti-ICAM-1 antibody, and a recombinant protein derived from a PfEMP-1 DBL-β domain, can not only inhibit but also reverse cytoadherence. This is the first work showing that a recombinant protein can not only inhibit but reverse cytoadherence to ICAM-1. The study suggests that the development of adjunct therapies to reverse cytoadherence based on the PfEMP-1:ICAM-1 interaction could be feasible.

The second main focus of this thesis was the effect of febrile temperatures on cytoadherence. This work arose from the realisation that fever is a major consequence of *P. falciparum* infection, however, most studies on cytoadherence, including our own, are carried out under non-febrile conditions at a temperature of 37°C. Since the effect of febrile temperatures on parasites has previously been reported, we looked specifically at host responses in the endothelial cells, and the effect on cytoadherence. The striking result here was that the host response to fever appears to be protective against cytoadherence. This could be related to heat shock response pathway activation, although we were unable to elucidate an exact mechanism. Revealing the mechanisms behind this protection will be a significant undertaking, although we have already ruled out simple effects on ICAM-1 levels and cell viability.

Overall our results may contribute to the understanding of why there is still a high mortality rate from malaria, especially during the first 24 hours after hospital admission. We suggest that continued cytoadherence may contribute to this and indicate the feasibility of approaches to reverse this cytoadherence interaction.

ACKNOWLEDGEMENTS

I'd like to thank my supervisors Alister and Giancarlo for all their help and support over the last three years. Thank you to all members of Alister's group – Tadge, Srabasti and Yang for all their help and support in the lab. Also specific thanks to Tadge for the making all the ICAM-1 protein, Matt Higgins for the DBL proteins, members of Steve Ward's group for help with the antimalarial drugs and members of Mike Lehane's group for use of the incubator for fever experiments. Thanks also to project students Doug and James for their work and I'd like to wish Khairul good luck continuing the projects.

PUBLICATIONS AND PRESENTATIONS

Work in this thesis has been presented for publication, or is in preparation for publication, and has been presented at meetings in the following forms:

Publications:

Exported proteins required for virulence and rigidity of Plasmodium falciparum infected human erythrocytes. *Maier AG, Rug M, O'Neill MT, Brown M, Chakravorty S, Szestak T, Chesson J, Wu Y,* ***Hughes K****, Coppel RL, Newbold C, Beeson JG, Craig A, Crabb BS, Cowman AF.* **Cell. 2008 Jul 11;134(1):48-61.**

Host response to cytoadherence in Plasmodium falciparum.
Chakravorty SJ, ***Hughes KR****, Craig AG.* **Biochem Soc Trans. 2008 Apr;36(Pt 2):221-8. Review**

Publications in Preparation:

Continued cytoadherence of Plasmodium falciparum infected red blood cells after antimalarial treatment. ***Hughes KR****, Biagini G, Craig AG.* **Molecular and biochemical parasitology 2009** (manuscript accepted subject to minor revisions December 2008)

Reversal of adhesion of Plasmodium falciparum infected red blood cells to ICAM-1 using antibody and recombinant protein ***Hughes KR****, Callery J, Higgins M, Craig AG*

Presentations:

Continued cytoadherence of Plasmodium falciparum infected red blood cells after antimalarial treatment. ***Hughes KR****, Biagini G, Craig AG*

Has been presented at the following meetings:

Poster presentation Molecular Parasitology Meeting, Woods Hole, September 2007

Oral Presentation BSP Malaria Meeting, Newcastle, April 2008

Oral Presentation BioMalPar Meeting, Heidleberg, May 2008

REFERENCES

Aitcheson, N., S. Talbot, J. Shapiro, K. Hughes, C. Adkin, T. Butt, K. Sheader & G. Rudenko, (2005) VSG switching in Trypanosoma brucei: antigenic variation analysed using RNAi in the absence of immune selection. *Mol Microbiol* **57**: 1608-1622.

Akoachere, M., K. Buchholz, E. Fischer, J. Burhenne, W. E. Haefeli, R. H. Schirmer & K. Becker, (2005) In vitro assessment of methylene blue on chloroquine-sensitive and -resistant Plasmodium falciparum strains reveals synergistic action with artemisinins. *Antimicrob Agents Chemother* **49**: 4592-4597.

Alano, P., (2007) Plasmodium falciparum gametocytes: still many secrets of a hidden life. *Mol Microbiol* **66**: 291-302.

Angus, B. J., K. Chotivanich, R. Udomsangpetch & N. J. White, (1997) In vivo removal of malaria parasites from red blood cells without their destruction in acute falciparum malaria. *Blood* **90**: 2037-2040.

Antia, M., T. Herricks & P. K. Rathod, (2007) Microfluidic Modeling of Cell-Cell Interactions in Malaria Pathogenesis. *PLoS Pathog* **3**: e99.

Ashley, E. A., K. Stepniewska, N. Lindegardh, R. McGready, A. Annerberg, R. Hutagalung, T. Singtoroj, G. Hla, A. Brockman, S. Proux, J. Wilahphaingern, P. Singhasivanon, N. J. White & F. Nosten, (2007) Pharmacokinetic study of artemether-lumefantrine given once daily for the treatment of uncomplicated multidrug-resistant falciparum malaria. *Trop Med Int Health* **12**: 201-208.

Barnwell, J. W., A. S. Asch, R. L. Nachman, M. Yamaya, M. Aikawa & P. Ingravallo, (1989) A human 88-kD membrane glycoprotein (CD36) functions in vitro as a receptor for a cytoadherence ligand on Plasmodium falciparum-infected erythrocytes. *J Clin Invest* **84**: 765-772.

Barnwell, J. W., C. F. Ockenhouse & D. M. d. Knowles, (1985) Monoclonal antibody OKM5 inhibits the in vitro binding of Plasmodium falciparum-infected erythrocytes to monocytes, endothelial, and C32 melanoma cells. *J Immunol* **135**: 3494-3497.

Baruch, D. I., X. C. Ma, H. B. Singh, X. Bi, B. L. Pasloske & R. J. Howard, (1997) Identification of a region of PfEMP1 that mediates adherence of Plasmodium falciparum infected erythrocytes to CD36: conserved function with variant sequence. *Blood* **90**: 3766-3775.

Baruch, D. I., B. L. Pasloske, H. B. Singh, X. Bi, X. C. Ma, M. Feldman, T. F. Taraschi & R. J. Howard, (1995) Cloning the P. falciparum gene encoding PfEMP1, a malarial variant antigen and adherence receptor on the surface of parasitized human erythrocytes [see comments]. *Cell* **82**: 77-87.

Basco, L. K., J. Bickii & P. Ringwald, (1998) In vitro activity of lumefantrine (benflumetol) against clinical isolates of Plasmodium falciparum in Yaounde, Cameroon. *Antimicrob Agents Chemother* **42**: 2347-2351.

Baum, J., A. G. Maier, R. T. Good, K. M. Simpson & A. F. Cowman, (2005) Invasion by P. falciparum Merozoites Suggests a Hierarchy of Molecular Interactions. *PLoS Pathog* **1**: e37.

Baumeister, S., M. Winterberg, C. Duranton, S. M. Huber, F. Lang, K. Kirk & K. Lingelbach, (2006) Evidence for the involvement of Plasmodium falciparum proteins in the formation of new permeability pathways in the erythrocyte membrane. *Mol Microbiol* **60**: 493-504.

Bennett, B. J., N. Mohandas & R. L. Coppel, (1997) Defining the minimal domain of the Plasmodium falciparum protein MESA involved in the interaction with the red cell membrane skeletal protein 4.1. *J Biol Chem* **272**: 15299-15306.

Bennett, T. N., M. Paguio, B. Gligorijevic, C. Seudieu, A. D. Kosar, E. Davidson & P. D. Roepe, (2004) Novel, rapid, and inexpensive cell-based quantification of antimalarial drug efficacy. *Antimicrob Agents Chemother* **48**: 1807-1810.

Berendt, A. R., A. McDowall, A. G. Craig, P. A. Bates, M. J. Sternberg, K. Marsh, C. I. Newbold & N. Hogg, (1992) The binding site on ICAM-1 for Plasmodium falciparum-infected erythrocytes overlaps, but is distinct from, the LFA-1-binding site. *Cell* **68**: 71-81.

Bertonati, C. & A. Tramontano, (2007) A model of the complex between the PfEMP1 malaria protein and the human ICAM-1 receptor. *Proteins* **69**: 215-222.

Biagini, G. A., P. M. O'Neill, P. G. Bray & S. A. Ward, (2005) Current drug development portfolio for antimalarial therapies. *Curr Opin Pharmacol* **5**: 473-478.

Biagini, G. A., P. M. O'Neill, A. Nzila, S. A. Ward & P. G. Bray, (2003) Antimalarial chemotherapy: young guns or back to the future? *Trends Parasitol* **19**: 479-487.

Biswas, A. K., A. Hafiz, B. Banerjee, K. S. Kim, K. Datta & C. E. Chitnis, (2007) Plasmodium falciparum uses gC1qR/HABP1/p32 as a receptor to bind to vascular endothelium and for platelet-mediated clumping. *PLoS Pathog* **3**: 1271-1280.

Blythe, J. E., T. Surentheran & P. R. Preiser, (2004) STEVOR--a multifunctional protein? *Mol Biochem Parasitol* **134**: 11-15.

Borst, P., W. Bitter, R. McCulloch, F. Van Leeuwen & G. Rudenko, (1995) Antigenic variation in malaria. *Cell* **82**: 1-4.

Brandts, C. H., M. Ndjave, W. Graninger & P. G. Kremsner, (1997) Effect of paracetamol on parasite clearance time in Plasmodium falciparum malaria [see comments]. *Lancet* **350**: 704-709.

Bray, P. G., R. E. Martin, L. Tilley, S. A. Ward, K. Kirk & D. A. Fidock, (2005) Defining the role of PfCRT in Plasmodium falciparum chloroquine resistance. *Mol Microbiol* **56**: 323-333.

Bull, P. C., M. Berriman, S. Kyes, M. A. Quail, N. Hall, M. M. Kortok, K. Marsh & C. I. Newbold, (2005) Plasmodium falciparum Variant Surface Antigen Expression Patterns during Malaria. *PLoS Pathog* **1**: e26.

Bull, P. C., B. S. Lowe, M. Kortok, C. S. Molyneux, C. I. Newbold & K. Marsh, (1998) Parasite antigens on the infected red cell surface are targets for naturally acquired immunity to malaria. *Nat Med* **4**: 358-360.

Casasnovas, J. M. & T. A. Springer, (1994) Pathway of rhinovirus disruption by soluble intercellular adhesion molecule 1 (ICAM-1): an intermediate in which ICAM-1 is bound and RNA is released. *J. Virol.* **68**: 5882-5889.

Casasnovas, J. M., T. Stehle, J. H. Liu, J. H. Wang & T. A. Springer, (1998) A dimeric crystal structure for the N-terminal two domains of intercellular adhesion molecule-1. *Proc Natl Acad Sci U S A* **95**: 4134-4139.

Chakravorty, S. J. & A. Craig, (2005) The role of ICAM-1 in Plasmodium falciparum cytoadherence. *Eur J Cell Biol* **84**: 15-27.

Chakravorty, S. J., C. Carret, G. B. Nash, A. Ivens, T. Szestak & A. Craig, (2007) Altered phenotype and gene transcription in endothelial cells induced by Plasmodium falciparum - infected red blood cells: pathogenic or protective? *Int. J. Parasitol.* **37**: 975-987.

Chakravorty, S. J., K. R. Hughes & A. G. Craig, (2008) Host response to cytoadherence in Plasmodium falciparum. *Biochem Soc Trans* **36**: 221-228.

Chattopadhyay, R., T. Taneja, K. Chakrabarti, C. R. Pillai & C. E. Chitnis, (2004) Molecular analysis of the cytoadherence phenotype of a Plasmodium falciparum field isolate that binds intercellular adhesion molecule-1. *Mol Biochem Parasitol* **133**: 255-265.

Checkley, A. M. & C. J. Whitty, (2007) Artesunate, artemether or quinine in severe Plasmodium falciparum malaria? *Expert Rev Anti Infect Ther* **5**: 199-204.

Chen, Q., D. T. Fisher, K. A. Clancy, J. M. Gauguet, W. C. Wang, E. Unger, S. Rose-John, U. H. von Andrian, H. Baumann & S. S. Evans, (2006) Fever-range thermal stress promotes lymphocyte trafficking across high endothelial venules via an interleukin 6 trans-signaling mechanism. *Nat Immunol* **7**: 1299-1308.

Cholera, R., N. J. Brittain, M. R. Gillrie, T. M. Lopera-Mesa, S. A. Diakite, T. Arie, M. A. Krause, A. Guindo, A. Tubman, H. Fujioka, D. A. Diallo, O. K. Doumbo, M. Ho, T. E. Wellems & R.

M. Fairhurst, (2008) Impaired cytoadherence of Plasmodium falciparum-infected erythrocytes containing sickle hemoglobin. *Proc Natl Acad Sci U S A* **105**: 991-996.

Chotivanich, K., R. Udomsangpetch, A. Dondorp, T. Williams, B. Angus, J. A. Simpson, S. Pukrittayakamee, S. Looareesuwan, C. I. Newbold & N. J. White, (2000) The mechanisms of parasite clearance after antimalarial treatment of Plasmodium falciparum malaria. *J Infect Dis* **182**: 629-633.

Chotivanich, K., R. Udomsangpetch, R. McGready, S. Proux, P. Newton, S. Pukrittayakamee, S. Looareesuwan & N. J. White, (2002) Central role of the spleen in malaria parasite clearance. *J Infect Dis* **185**: 1538-1541.

Cockburn, I. A., M. J. Mackinnon, A. O'Donnell, S. J. Allen, J. M. Moulds, M. Baisor, M. Bockarie, J. C. Reeder & J. A. Rowe, (2004) A human complement receptor 1 polymorphism that reduces Plasmodium falciparum rosetting confers protection against severe malaria. *Proc Natl Acad Sci U S A* **101**: 272-277.

Combes, V., N. Coltel, D. Faille, S. C. Wassmer & G. E. Grau, (2006) Cerebral malaria: role of microparticles and platelets in alterations of the blood-brain barrier. *Int J Parasitol* **36**: 541-546.

Comeaux, C. A. & M. T. Duraisingh, (2007) Unravelling a histone code for malaria virulence. *Mol Microbiol* **66**: 1291-1295.

Cooke, B. M., A. R. Berendt, A. G. Craig, J. MacGregor, C. I. Newbold & G. B. Nash, (1994) Rolling and stationary cytoadhesion of red blood cells parasitized by Plasmodium falciparum: separate roles for ICAM-1, CD36 and thrombospondin. *Br J Haematol* **87**: 162-170.

Cooke, B. M. & G. B. Nash, (1995) Plasmodium falciparum: characterization of adhesion of flowing parasitized red blood cells to platelets. *Exp Parasitol* **80**: 116-123.

Cooke, B. M., S. J. Rogerson, G. V. Brown & R. L. Coppel, (1996) Adhesion of malaria-infected red blood cells to chondroitin sulfate A under flow conditions. *Blood* **88**: 4040-4044.

Cooke, B. M., C. L. Nicoll, D. I. Baruch & R. L. Coppel, (1998) A recombinant peptide based on PfEMP-1 blocks and reverses adhesion of malaria-infected red blood cells to CD36 under flow. *Mol Microbiol* **30**: 83-90.

Cooke, B. M., N. Mohandas & R. L. Coppel, (2001) The malaria-infected red blood cell: structural and functional changes. *Adv Parasitol* **50**: 1-86.

Cooke, B. M., R. L. Coppel & G. B. Nash, (2002) Analysis of the adhesive properties of Plasmodium falciparum-infected red blood cells under conditions of flow. *Methods Mol Med* **72**: 561-569.

Cox-Singh, J., T. M. Davis, K. S. Lee, S. S. Shamsul, A. Matusop, S. Ratnam, H. A. Rahman, D. J. Conway & B. Singh, (2008) Plasmodium knowlesi malaria in humans is widely distributed and potentially life threatening. *Clin Infect Dis* **46**: 165-171.

Crabb, B. S., B. M. Cooke, J. C. Reeder, R. F. Waller, S. R. Caruana, K. M. Davern, M. E. Wickham, G. V. Brown, R. L. Coppel & A. F. Cowman, (1997) Targeted gene disruption shows that knobs enable malaria-infected red cells to cytoadhere under physiological shear stress. *Cell* **89**: 287-296.

Craig, A. G., R. Pinches, S. Khan, D. J. Roberts, G. D. Turner, C. I. Newbold & A. R. Berendt, (1997) Failure to block adhesion of Plasmodium falciparum-infected erythrocytes to ICAM-1 with soluble ICAM-1. *Infect Immun* **65**: 4580-4585.

Craig, A. & A. Scherf, (2001) Molecules on the surface of the Plasmodium falciparum infected erythrocyte and their role in malaria pathogenesis and immune evasion. *Mol Biochem Parasitol* **115**: 129-143.

Crandall, I., K. M. Land & I. W. Sherman, (1994) Plasmodium falciparum: pfalhesin and CD36 form an adhesin/receptor pair that is responsible for the pH-dependent portion of cytoadherence/sequestration. *Exp Parasitol* **78**: 203-209.

Cranston, H. A., C. W. Boylan, G. L. Carroll, S. P. Sutera, J. R. Williamson, I. Y. Gluzman & D. J. Krogstad, (1984) Plasmodium falciparum maturation abolishes physiologic red cell deformability. *Science* **223**: 400-403.

Davis, T. M., T. Y. Hung, I. K. Sim, H. A. Karunajeewa & K. F. Ilett, (2005) Piperaquine: a resurgent antimalarial drug. *Drugs* **65**: 75-87.

del Portillo, H. A., M. Lanzer, S. Rodriguez-Malaga, F. Zavala & C. Fernandez-Becerra, (2004) Variant genes and the spleen in Plasmodium vivax malaria. *Int J Parasitol* **34**: 1547-1554.

Diamond, M. S., D. E. Staunton, S. D. Marlin & T. A. Springer, (1991) Binding of the integrin Mac-1 (CD11b/CD18) to the third immunoglobulin-like domain of ICAM-1 (CD54) and its regulation by glycosylation. *Cell* **65**: 961-971.

Dokladny, K., D. Ye, J. C. Kennedy, P. L. Moseley & T. Y. Ma, (2008) Cellular and molecular mechanisms of heat stress-induced up-regulation of occludin protein expression: regulatory role of heat shock factor-1. *Am J Pathol* **172**: 659-670.

Dondorp, A. M., B. J. Angus, M. R. Hardeman, K. T. Chotivanich, K. Silamut, R. Ruangveerayuth, P. A. Kager, N. J. White & J. Vreeken, (1997) Prognostic significance of reduced red blood cell deformability in severe falciparum malaria. *Am J Trop Med Hyg* **57**: 507-511.

Dondorp, A. M., P. A. Kager, J. Vreeken & N. J. White, (2000) Abnormal blood flow and red blood cell deformability in severe malaria. *Parasitol Today* **16**: 228-232.

Dondorp, A., F. Nosten, K. Stepniewska, N. Day & N. White, (2005) Artesunate versus quinine for treatment of severe falciparum malaria: a randomised trial. *Lancet* **366**: 717-725.

Dondorp, A. M., K. Silamut, P. Charunwatthana, S. Chuasuwanchai, R. Ruangveerayut, S. Krintratun, N. J. White, M. Ho & N. P. Day, (2007) Levamisole inhibits sequestration of infected red blood cells in patients with falciparum malaria. *J Infect Dis* **196**: 460-466.

Dondorp, A. M., (2008) Clinical significance of sequestration in adults with severe malaria. *Transfus Clin Biol* **15**: 56-57.

Dondorp, A. M., C. Ince, P. Charunwatthana, J. Hanson, A. van Kuijen, M. A. Faiz, M. R. Rahman, M. Hasan, E. Bin Yunus, A. Ghose, R. Ruangveerayut, D. Limmathurotsakul, K. Mathura, N. J. White & N. P. Day, (2008) Direct in vivo assessment of microcirculatory dysfunction in severe falciparum malaria. *J Infect Dis* **197**: 79-84.

Duraisingh, M. T., T. S. Voss, A. J. Marty, M. F. Duffy, R. T. Good, J. K. Thompson, L. H. Freitas-Junior, A. Scherf, B. S. Crabb & A. F. Cowman, (2005) Heterochromatin silencing and locus repositioning linked to regulation of virulence genes in Plasmodium falciparum. *Cell* **121**: 13-24.

Dzikowski, R., F. Li, B. Amulic, A. Eisberg, M. Frank, S. Patel, T. E. Wellems & K. W. Deitsch, (2007) Mechanisms underlying mutually exclusive expression of virulence genes by malaria parasites. *EMBO Rep* **8**: 959-965.

Eda, S., J. Lawler & I. W. Sherman, (1999) Plasmodium falciparum-infected erythrocyte adhesion to the type 3 repeat domain of thrombospondin-1 is mediated by a modified band 3 protein. *Mol Biochem Parasitol* **100**: 195-205.

Engwerda, C. R., L. Beattie & F. H. Amante, (2005) The importance of the spleen in malaria. *Trends Parasitol* **21**: 75-80.

Freitas-Junior, L. H., R. Hernandez-Rivas, S. A. Ralph, D. Montiel-Condado, O. K. Ruvalcaba-Salazar, A. P. Rojas-Meza, L. Mancio-Silva, R. J. Leal-Silvestre, A. M. Gontijo, S. Shorte & A. Scherf, (2005) Telomeric heterochromatin propagation and histone acetylation control mutually exclusive expression of antigenic variation genes in malaria parasites. *Cell* **121**: 25-36.

Fried, M., F. Nosten, A. Brockman, B. J. Brabin & P. E. Duffy, (1998) Maternal antibodies block malaria [letter]. *Nature* **395**: 851-852.

Fried, M. & P. E. Duffy, (2002) Two DBLgamma subtypes are commonly expressed by placental isolates of Plasmodium falciparum. *Mol Biochem Parasitol* **122**: 201-210.

Gamain, B., A. R. Trimnell, C. Scheidig, A. Scherf, L. H. Miller & J. D. Smith, (2005) Identification of multiple chondroitin sulfate A (CSA)-binding domains in the var2CSA gene transcribed in CSA-binding parasites. *J Infect Dis* **191**: 1010-1013.

Gaur, D., D. C. Mayer & L. H. Miller, (2004) Parasite ligand-host receptor interactions during invasion of erythrocytes by Plasmodium merozoites. *Int J Parasitol* **34**: 1413-1429.

Gennaro, A. M., A. Luquita & M. Rasia, (1996) Comparison between internal microviscosity of low-density erythrocytes and the microviscosity of hemoglobin solutions: an electron paramagnetic resonance study. *Biophys J* **71**: 389-393.

Glenister, F. K., R. L. Coppel, A. F. Cowman, N. Mohandas & B. M. Cooke, (2002) Contribution of parasite proteins to altered mechanical properties of malaria-infected red blood cells. *Blood* **99**: 1060-1063.

Glushakova, S., D. Yin, T. Li & J. Zimmerberg, (2005) Membrane transformation during malaria parasite release from human red blood cells. *Curr Biol* **15**: 1645-1650.

Gnant, M. F., E. M. Turner & H. R. Alexander, Jr., (2000) Effects of hyperthermia and tumour necrosis factor on inflammatory cytokine secretion and procoagulant activity in endothelial cells. *Cytokine* **12**: 339-347.

Gravenor, M. B. & D. Kwiatkowski, (1998) An analysis of the temperature effects of fever on the intra-host population dynamics of Plasmodium falciparum. *Parasitology* **117**: 97-105.

Gray, C., C. McCormick, G. Turner & A. Craig, (2003) ICAM-1 can play a major role in mediating P. falciparum adhesion to endothelium under flow. *Mol Biochem Parasitol* **128**: 187-193.

Greenwood, J., C. L. Amos, C. E. Walters, P. O. Couraud, R. Lyck, B. Engelhardt & P. Adamson, (2003) Intracellular domain of brain endothelial intercellular adhesion molecule-1 is essential for T lymphocyte-mediated signaling and migration. *J Immunol* **171**: 2099-2108.

Griffiths, M. J., F. Ndungu, K. L. Baird, D. P. Muller, K. Marsh & C. R. Newton, (2001) Oxidative stress and erythrocyte damage in Kenyan children with severe Plasmodium falciparum malaria. *Br J Haematol* **113**: 486-491.

Guerra, C. A., P. W. Gikandi, A. J. Tatem, A. M. Noor, D. L. Smith, S. I. Hay & R. W. Snow, (2008) The limits and intensity of Plasmodium falciparum transmission: implications for malaria control and elimination worldwide. *PLoS Med* **5**: e38.

Gysin, J., B. Pouvelle, N. Fievet, A. Scherf & C. Lepolard, (1999) Ex vivo desequestration of plasmodium falciparum-infected erythrocytes from human placenta by chondroitin sulfate A [In Process Citation]. *Infect Immun* **67**: 6596-6602.

Hanssen, E., R. Sougrat, S. Frankland, S. Deed, N. Klonis, J. Lippincott-Schwartz & L. Tilley, (2008) Electron tomography of the Maurer's cleft organelles of Plasmodium falciparum-infected erythrocytes reveals novel structural features. *Mol Microbiol* **67**: 703-718.

Hartl, F. U., (1996) Molecular chaperones in cellular protein folding. *Nature* **381**: 571-579.

Hasday, J. D., D. Bannerman, S. Sakarya, A. S. Cross, I. S. Singh, D. Howard, B. E. Drysdale & S. E. Goldblum, (2001) Exposure to febrile temperature modifies endothelial cell response to tumor necrosis factor-alpha. *J Appl Physiol* **90**: 90-98.

Hasday, J. D. & I. S. Singh, (2000) Fever and the heat shock response: distinct, partially overlapping processes. *Cell Stress Chaperones* **5**: 471-480.

Hasler, C. R. & W. H. Reinhart, (1998) No influence of furosemide on human erythrocyte shape and volume and blood viscosity in vitro. *Clin Hemorheol Microcirc* **18**: 43-46.

Helmby, H., L. Cavelier, U. Pettersson & M. Wahlgren, (1993) Rosetting Plasmodium falciparum-infected erythrocytes express unique strain-specific antigens on their surface. *Infect Immun* **61**: 284-288.

Hemmer, C. J., H. A. Lehr, K. Westphal, M. Unverricht, M. Kratzius & E. C. Reisinger, (2005) Plasmodium falciparum Malaria: reduction of endothelial cell apoptosis in vitro. *Infect Immun* **73**: 1764-1770.

Hempelmann, E., C. Motta, R. Hughes, S. A. Ward & P. G. Bray, (2003) Plasmodium falciparum: sacrificing membrane to grow crystals? *Trends Parasitol* **19**: 23-26.

Higgins, M. K., (2008a) Overproduction, purification and crystallization of a chondroitin sulfate A-binding DBL domain from a Plasmodium falciparum var2csa-encoded PfEMP1 protein. *Acta Crystallogr Sect F Struct Biol Cryst Commun* **64**: 221-223.

Higgins, M. K., (2008b) The Structure of a Chondroitin Sulfate-binding Domain Important in Placental Malaria. *J. Biol. Chem.* **283**: 21842-21846.

Ho, M., T. Schollaardt, X. Niu, S. Looareesuwan, K. D. Patel & P. Kubes, (1998) Characterization of Plasmodium falciparum-infected erythrocyte and P- selectin interaction under flow conditions. *Blood* **91**: 4803-4809.

Ho, M. & N. J. White, (1999) Molecular mechanisms of cytoadherence in malaria. *Am J Physiol* **276**: C1231-1242.

Ho, M., H. L. Hoang, K. M. Lee, N. Liu, T. MacRae, L. Montes, C. L. Flatt, B. G. Yipp, B. J. Berger, S. Looareesuwan & S. M. Robbins, (2005) Ectophosphorylation of CD36 regulates cytoadherence of Plasmodium falciparum to microvascular endothelium under flow conditions. *Infect Immun* **73**: 8179-8187.

Horrocks, P., R. Pinches, S. Kyes, N. Kriek, S. Lee, Z. Christodoulou & C. I. Newbold, (2002) Effect of var gene disruption on switching in Plasmodium falciparum. *Mol Microbiol* **45**: 1131-1141.

Horrocks, P., R. Pinches, Z. Christodoulou, S. A. Kyes & C. I. Newbold, (2004) Variable var transition rates underlie antigenic variation in malaria. *Proc Natl Acad Sci U S A* **101**: 11129-11134.

Horrocks, P., R. A. Pinches, S. J. Chakravorty, J. Papakrivos, Z. Christodoulou, S. A. Kyes, B. C. Urban, D. J. Ferguson & C. I. Newbold, (2005) PfEMP1 expression is reduced on the surface of knobless Plasmodium falciparum infected erythrocytes. *J Cell Sci* **118**: 2507-2518.

Hosokawa, N., K. Hirayoshi, H. Kudo, H. Takechi, A. Aoike, K. Kawai & K. Nagata, (1992) Inhibition of the activation of heat shock factor in vivo and in vitro by flavonoids. *Mol Cell Biol* **12**: 3490-3498.

Hughes, K., M. Wand, L. Foulston, R. Young, K. Harley, S. Terry, K. Ersfeld & G. Rudenko, (2007) A novel ISWI is involved in VSG expression site downregulation in African trypanosomes. *EMBO J* **26**: 2400-2410.

Jenkins, N., Y. Wu, S. Chakravorty, O. Kai, K. Marsh & A. Craig, (2007a) Plasmodium falciparum intercellular adhesion molecule-1-based cytoadherence-related signaling in human endothelial cells. *J Infect Dis* **196**: 321-327.

Jenkins, N., Y. Wu, S. J. Chakravorty, O. Kai, K. Marsh & A. Craig, (2007b) Plasmodium falciparum ICAM-1-based cytoadherence-related signalling in human endothelial cells. *J. Infect. Dis.* **196**: 321-327.

Jensen, J. B., (1978) Concentration from Continuous Culture of Erythrocytes Infected with Trophozoites and Schizonts of Plasmodium Falciparum. *Am J Trop Med Hyg* **27**: 1274-1276.

Jolly, C., Y. Usson & R. I. Morimoto, (1999) Rapid and reversible relocalization of heat shock factor 1 within seconds to nuclear stress granules. *Proc Natl Acad Sci U S A* **96**: 6769-6774.

Jun, C. D., C. V. Carman, S. D. Redick, M. Shimaoka, H. P. Erickson & T. A. Springer, (2001a) Ultrastructure and function of dimeric, soluble intercellular adhesion molecule-1 (ICAM-1). *J Biol Chem* **276**: 29019-29027.

Jun, C. D., M. Shimaoka, C. V. Carman, J. Takagi & T. A. Springer, (2001b) Dimerization and the effectiveness of ICAM-1 in mediating LFA-1-dependent adhesion. *Proc Natl Acad Sci U S A* **98**: 6830-6835.

Ketis, N. V., R. L. Hoover & M. J. Karnovsky, (1988) Effects of hyperthermia on cell survival and patterns of protein synthesis in endothelial cells from different origins. *Cancer Res* **48**: 2101-2106.

Kirk, K., H. A. Horner, B. C. Elford, J. C. Ellory & C. I. Newbold, (1994) Transport of diverse substrates into malaria-infected erythrocytes via a pathway showing functional characteristics of a chloride channel. *J Biol Chem* **269**: 3339-3347.

Kirk, K., (2001) Membrane transport in the malaria-infected erythrocyte. *Physiol Rev* **81**: 495-537.

Kobuchi, H., S. Roy, C. K. Sen, H. G. Nguyen & L. Packer, (1999) Quercetin inhibits inducible ICAM-1 expression in human endothelial cells through the JNK pathway. *Am J Physiol* **277**: C403-411.

Kohn, G., H. R. Wong, K. Bshesh, B. Zhao, N. Vasi, A. Denenberg, C. Morris, J. Stark & T. P. Shanley, (2002) Heat shock inhibits tnf-induced ICAM-1 expression in human endothelial cells via I kappa kinase inhibition. *Shock* **17**: 91-97.

Kon, K., N. Maeda & T. Shiga, (1987) Erythrocyte deformation in shear flow: influences of internal viscosity, membrane stiffness, and hematocrit. *Blood* **69**: 727-734.

Kraemer, S. M., L. Gupta & J. D. Smith, (2003) New tools to identify var sequence tags and clone full-length genes using type-specific primers to Duffy binding-like domains. *Mol Biochem Parasitol* **129**: 91-102.

Kraemer, S. M., S. A. Kyes, G. Aggarwal, A. L. Springer, S. O. Nelson, Z. Christodoulou, L. M. Smith, W. Wang, E. Levin, C. I. Newbold, P. J. Myler & J. D. Smith, (2007) Patterns of gene recombination shape var gene repertoires in Plasmodium falciparum: comparisons of geographically diverse isolates. *BMC Genomics* **8**: 45.

Kwiatkowski, D., (1989) Febrile temperatures can synchronize the growth of Plasmodium falciparum in vitro. *J Exp Med* **169**: 357-361.

Kwiatkowski, D., M. E. Molyneux, S. Stephens, N. Curtis, N. Klein, P. Pointaire, M. Smit, R. Allan, D. R. Brewster, G. E. Grau & et al., (1993) Anti-TNF therapy inhibits fever in cerebral malaria [see comments]. *Q J Med* **86**: 91-98.

Kwiatkowski, D., C. A. Bate, I. G. Scragg, P. Beattie, I. Udalova & J. C. Knight, (1997) The malarial fever response--pathogenesis, polymorphism and prospects for intervention. *Ann Trop Med Parasitol* **91**: 533-542.

Kyes, S. A., J. A. Rowe, N. Kriek & C. I. Newbold, (1999) Rifins: a second family of clonally variant proteins expressed on the surface of red cells infected with Plasmodium falciparum. *Proc Natl Acad Sci U S A* **96**: 9333-9338.

Kyes, S., R. Pinches & C. Newbold, (2000) A simple RNA analysis method shows var and rif multigene family expression patterns in Plasmodium falciparum. *Mol Biochem Parasitol* **105**: 311-315.

Kyes, S., Z. Christodoulou, R. Pinches, N. Kriek, P. Horrocks & C. Newbold, (2007a) Plasmodium falciparum var gene expression is developmentally controlled at the level of RNA polymerase II-mediated transcription initiation. *Mol Microbiol* **63**: 1237-1247.

Kyes, S. A., S. M. Kraemer & J. D. Smith, (2007b) Antigenic variation in Plasmodium falciparum: gene organization and regulation of the var multigene family. *Eukaryot Cell* **6**: 1511-1520.

Lawler, J. & R. O. Hynes, (1986) The structure of human thrombospondin, an adhesive glycoprotein with multiple calcium-binding sites and homologies with several different proteins. *J Cell Biol* **103**: 1635-1648.

Le Jouan, M., V. Jullien, E. Tetanye, A. Tran, E. Rey, J. M. Treluyer, M. Tod & G. Pons, (2005) Quinine pharmacokinetics and pharmacodynamics in children with malaria caused by Plasmodium falciparum. *Antimicrob Agents Chemother* **49**: 3658-3662.

Lefor, A. T., C. E. Foster, 3rd, W. Sartor, B. Engbrecht, D. F. Fabian & D. Silverman, (1994) Hyperthermia increases intercellular adhesion molecule-1 expression and lymphocyte adhesion to endothelial cells. *Surgery* **116**: 214-220; discussion 220-211.

Lell, B., M. Sovric, D. Schmid, D. Luckner, K. Herbich, H. Y. Long, W. Graninger & P. G. Kremsner, (2001) Effect of antipyretic drugs in children with malaria. *Clin Infect Dis* **32**: 838-841.

Lew, V. L., T. Tiffert & H. Ginsburg, (2003) Excess hemoglobin digestion and the osmotic stability of Plasmodium falciparum-infected red blood cells. *Blood* **101**: 4189-4194.

Lindquist, S. & E. A. Craig, (1988) The heat-shock proteins. *Annu Rev Genet* **22**: 631-677.

Long, H. Y., B. Lell, K. Dietz & P. G. Kremsner, (2001) Plasmodium falciparum: in vitro growth inhibition by febrile temperatures. *Parasitol Res* **87**: 553-555.

Lopez-Rubio, J. J., A. M. Gontijo, M. C. Nunes, N. Issar, R. Hernandez Rivas & A. Scherf, (2007a) 5' flanking region of var genes nucleate histone modification patterns linked to

phenotypic inheritance of virulence traits in malaria parasites. *Mol Microbiol* **66**: 1296-1305.

Lopez-Rubio, J. J., L. Riviere & A. Scherf, (2007b) Shared epigenetic mechanisms control virulence factors in protozoan parasites. *Curr Opin Microbiol* **10**: 560-568.

Lucas, J. Z. & I. W. Sherman, (1998) Plasmodium falciparum: thrombospondin mediates parasitized erythrocyte band 3-related adhesin binding. *Exp Parasitol* **89**: 78-85.

Luchavez, J., F. Espino, P. Curameng, R. Espina, D. Bell, P. Chiodini, D. Nolder, C. Sutherland, K. S. Lee & B. Singh, (2008) Human Infections with Plasmodium knowlesi, the Philippines. *Emerg Infect Dis* **14**: 811-813.

Lustigman, S., R. F. Anders, G. V. Brown & R. L. Coppel, (1990) The mature-parasite-infected erythrocyte surface antigen (MESA) of Plasmodium falciparum associates with the erythrocyte membrane skeletal protein, band 4.1. *Mol Biochem Parasitol* **38**: 261-270.

Magowan, C., R. L. Coppel, A. O. Lau, M. M. Moronne, G. Tchernia & N. Mohandas, (1995) Role of the Plasmodium falciparum mature-parasite-infected erythrocyte surface antigen (MESA/PfEMP-2) in malarial infection of erythrocytes. *Blood* **86**: 3196-3204.

Maier, A. G., M. Rug, M. T. O'Neill, M. Brown, S. Chakravorty, T. Szestak, J. Chesson, Y. Wu, K. Hughes, R. L. Coppel, C. Newbold, J. G. Beeson, A. Craig, B. S. Crabb & A. F. Cowman, (2008) Exported proteins required for virulence and rigidity of Plasmodium falciparum-infected human erythrocytes. *Cell* **134**: 48-61.

Marinkovic, M., M. Diez-Silva, I. Pantic, J. J. Fredberg, S. Suresh & J. P. Butler, (2008) Febrile temperature leads to significant stiffening of Plasmodium falciparum parasitized erythrocytes. *Am J Physiol Cell Physiol*.

Marsh, K., D. Forster, C. Waruiru, I. Mwangi, M. Winstanley, V. Marsh, C. Newton, P. Winstanley, P. Warn, N. Peshu & et al., (1995) Indicators of life-threatening malaria in African children [see comments]. *N Engl J Med* **332**: 1399-1404.

Marti, M., R. T. Good, M. Rug, E. Knuepfer & A. F. Cowman, (2004) Targeting malaria virulence and remodeling proteins to the host erythrocyte. *Science* **306**: 1930-1933.

McCormick, C. J., A. Craig, D. Roberts, C. I. Newbold & A. R. Berendt, (1997) Intercellular adhesion molecule-1 and CD36 synergize to mediate adherence of Plasmodium falciparum-infected erythrocytes to cultured human microvascular endothelial cells. *J Clin Invest* **100**: 2521-2529.

McGready, R., K. Stepniewska, S. A. Ward, T. Cho, G. Gilveray, S. Looareesuwan, N. J. White & F. Nosten, (2006) Pharmacokinetics of dihydroartemisinin following oral artesunate treatment of pregnant women with acute uncomplicated falciparum malaria. *Eur J Clin Pharmacol* **62**: 367-371.

Medana, I. M. & G. D. Turner, (2006) Human cerebral malaria and the blood-brain barrier. *Int J Parasitol* **36**: 555-568.

Medana, I. M. & G. D. Turner, (2007) Plasmodium falciparum and the blood-brain barrier--contacts and consequences. *J Infect Dis* **195**: 921-923.

Mercier, P. A., N. A. Winegarden & J. T. Westwood, (1999) Human heat shock factor 1 is predominantly a nuclear protein before and after heat stress. *J Cell Sci* **112 (Pt 16)**: 2765-2774.

Meremikwu, M., K. Logan & P. Garner, (2000) Antipyretic measures for treating fever in malaria. *Cochrane Database Syst Rev*: CD002151.

Miller, J., R. Knorr, M. Ferrone, R. Houdei, C. P. Carron & M. L. Dustin, (1995) Intercellular adhesion molecule-1 dimerization and its consequences for adhesion mediated by lymphocyte function associated-1. *J Exp Med* **182**: 1231-1241.

Miltenyi, S., W. Muller, W. Weichel & A. Radbruch, (1990) High gradient magnetic cell separation with MACS. *Cytometry* **11**: 231-238.

Mohandas, N., M. R. Clark, M. S. Jacobs & S. B. Shohet, (1980) Analysis of factors regulating erythrocyte deformability. *J Clin Invest* **66**: 563-573.

Montgomery, J., F. A. Mphande, M. Berriman, A. Pain, S. J. Rogerson, T. E. Taylor, M. E. Molyneux & A. Craig, (2007) Differential var gene expression in the organs of patients dying of falciparum malaria. *Mol Microbiol* **65**: 959-967.

Moon, Y. J., L. Wang, R. DiCenzo & M. E. Morris, (2008) Quercetin pharmacokinetics in humans. *Biopharm Drug Dispos* **29**: 205-217.

Morimoto, R. I., (1998) Regulation of the heat shock transcriptional response: cross talk between a family of heat shock factors, molecular chaperones, and negative regulators. *Genes Dev* **12**: 3788-3796.

Muanza, K., F. Gay, C. Behr & A. Scherf, (1996) Primary culture of human lung microvessel endothelial cells: a useful in vitro model for studying Plasmodium falciparum-infected erythrocyte cytoadherence. *Res Immunol* **147**: 149-163.

Mueller, I., P. A. Zimmerman & J. C. Reeder, (2007) Plasmodium malariae and Plasmodium ovale--the "bashful" malaria parasites. *Trends Parasitol* **23**: 278-283.

Multhoff, G., C. Botzler, M. Wiesnet, E. Muller, T. Meier, W. Wilmanns & R. D. Issels, (1995) A stress-inducible 72-kDa heat-shock protein (HSP72) is expressed on the surface of human tumor cells, but not on normal cells. *Int J Cancer* **61**: 272-279.

Nagai, N., A. Nakai & K. Nagata, (1995) Quercetin suppresses heat shock response by down regulation of HSF1. *Biochem Biophys Res Commun* **208**: 1099-1105.

Nair, M. P., S. Mahajan, J. L. Reynolds, R. Aalinkeel, H. Nair, S. A. Schwartz & C. Kandaswami, (2006) The flavonoid quercetin inhibits proinflammatory cytokine (tumor necrosis factor alpha) gene expression in normal peripheral blood mononuclear cells via modulation of the NF-kappa beta system. *Clin Vaccine Immunol* **13**: 319-328.

Nakabe, N., S. Kokura, M. Shimozawa, K. Katada, N. Sakamoto, T. Ishikawa, O. Handa, T. Takagi, Y. Naito, N. Yoshida & T. Yoshikawa, (2007) Hyperthermia attenuates TNF-alpha-induced up regulation of endothelial cell adhesion molecules in human arterial endothelial cells. *Int J Hyperthermia* **23**: 217-224.

Nash, G. B., E. O'Brien, E. C. Gordon-Smith & J. A. Dormandy, (1989) Abnormalities in the mechanical properties of red blood cells caused by Plasmodium falciparum. *Blood* **74**: 855-861.

Naumann, K. M., G. L. Jones, A. Saul & R. Smith, (1991) A Plasmodium falciparum exo-antigen alters erythrocyte membrane deformability. *FEBS Lett* **292**: 95-97.

Navarro, M. & K. Gull, (2001) A pol I transcriptional body associated with VSG mono-allelic expression in Trypanosoma brucei. *Nature* **414**: 759-763.

Newbold, C., P. Warn, G. Black, A. Berendt, A. Craig, B. Snow, M. Msobo, N. Peshu & K. Marsh, (1997) Receptor-specific adhesion and clinical disease in Plasmodium falciparum [see comments]. *Am J Trop Med Hyg* **57**: 389-398.

Newman, P. J., M. C. Berndt, J. Gorski, G. C. White, 2nd, S. Lyman, C. Paddock & W. A. Muller, (1990) PECAM-1 (CD31) cloning and relation to adhesion molecules of the immunoglobulin gene superfamily. *Science* **247**: 1219-1222.

Newton, P. N., K. I. Barnes, P. J. Smith, A. C. Evans, W. Chierakul, R. Ruangveerayuth & N. J. White, (2006) The pharmacokinetics of intravenous artesunate in adults with severe falciparum malaria. *Eur J Clin Pharmacol* **62**: 1003-1009.

Ng, O. T., E. E. Ooi, C. C. Lee, P. J. Lee, L. C. Ng, S. W. Pei, T. M. Tu, J. P. Loh & Y. S. Leo, (2008) Naturally acquired human Plasmodium knowlesi infection, Singapore. *Emerg Infect Dis* **14**: 814-816.

Nonaka, T., T. Akimoto, N. Mitsuhashi, Y. Tamaki & T. Nakano, (2003) Changes in the number of HSF1 positive granules in the nucleus reflects heat shock semiquantitatively. *Cancer Lett* **202**: 89-100.

Nunes, M. C. & A. Scherf, (2007) Plasmodium falciparum during pregnancy: a puzzling parasite tissue adhesion tropism. *Parasitology* **134**: 1863-1869.

O'Neill, P. M. & G. H. Posner, (2004) A medicinal chemistry perspective on artemisinin and related endoperoxides. *J Med Chem* **47**: 2945-2964.

O'Neill, P. M., S. A. Ward, N. G. Berry, J. P. Jeyadevan, G. A. Biagini, E. Asadollaly, B. K. Park & P. G. Bray, (2006) A medicinal chemistry perspective on 4-aminoquinoline antimalarial drugs. *Curr Top Med Chem* **6**: 479-507.

Oakley, M. S., S. Kumar, V. Anantharaman, H. Zheng, B. Mahajan, J. D. Haynes, J. K. Moch, R. Fairhurst, T. F. McCutchan & L. Aravind, (2007) Molecular factors and biochemical pathways induced by febrile temperature in intraerythrocytic Plasmodium falciparum parasites. *Infect Immun* **75**: 2012-2025.

Ockenhouse, C. F., R. Betageri, T. A. Springer & D. E. Staunton, (1992a) Plasmodium falciparum-infected erythrocytes bind ICAM-1 at a site distinct from LFA-1, Mac-1, and human rhinovirus [published erratum appears in Cell 1992 Mar 6;68(5):following 994]. *Cell* **68**: 63-69.

Ockenhouse, C. F., N. N. Tandon, C. Magowan, G. A. Jamieson & J. D. Chulay, (1989) Identification of a platelet membrane glycoprotein as a falciparum malaria sequestration receptor [see comments]. *Science* **243**: 1469-1471.

Ockenhouse, C. F., T. Tegoshi, Y. Maeno, C. Benjamin, M. Ho, K. E. Kan, Y. Thway, K. Win, M. Aikawa & R. R. Lobb, (1992b) Human vascular endothelial cell adhesion receptors for Plasmodium falciparum-infected erythrocytes: roles for endothelial leukocyte adhesion molecule 1 and vascular cell adhesion molecule 1. *J Exp Med* **176**: 1183-1189.

Oh, S. S., S. Voigt, D. Fisher, S. J. Yi, P. J. LeRoy, L. H. Derick, S. Liu & A. H. Chishti, (2000) Plasmodium falciparum erythrocyte membrane protein 1 is anchored to the actin-spectrin junction and knob-associated histidine-rich protein in the erythrocyte skeleton. *Mol Biochem Parasitol* **108**: 237-247.

Park, H. G., S. I. Han, S. Y. Oh & H. S. Kang, (2005) Cellular responses to mild heat stress. *Cell Mol Life Sci* **62**: 10-23.

Parker, P. D., L. Tilley & N. Klonis, (2004) Plasmodium falciparum induces reorganization of host membrane proteins during intraerythrocytic growth. *Blood* **103**: 2404-2406.

Patel, K. D., M. U. Nollert & R. P. McEver, (1995) P-selectin must extend a sufficient length from the plasma membrane to mediate rolling of neutrophils. *J Cell Biol* **131**: 1893-1902.

Paul, F., S. Roath, D. Melville, D. C. Warhurst & J. O. Osisanya, (1981) Separation of malaria-infected erythrocytes from whole blood: use of a selective high-gradient magnetic separation technique. *Lancet* **2**: 70-71.

Paulitschke, M. & G. B. Nash, (1993) Membrane rigidity of red blood cells parasitized by different strains of Plasmodium falciparum. *J Lab Clin Med* **122**: 581-589.

Pavithra, S. R., G. Banumathy, O. Joy, V. Singh & U. Tatu, (2004) Recurrent fever promotes Plasmodium falciparum development in human erythrocytes. *J Biol Chem* **279**: 46692-46699.

Pei, X., X. An, X. Guo, M. Tarnawski, R. Coppel & N. Mohandas, (2005) Structural and functional studies of interaction between Plasmodium falciparum knob-associated histidine-rich protein (KAHRP) and erythrocyte spectrin. *J Biol Chem* **280**: 31166-31171.

Pei, X., X. Guo, R. Coppel, N. Mohandas & X. An, (2007) Plasmodium falciparum erythrocyte membrane protein 3 (PfEMP3) destabilizes erythrocyte membrane skeleton. *J Biol Chem* **282**: 26754-26758.

Peters, W. G., H, (1995) *Tropical Medicine and Parasitology*. Mosby-Wolfe.

Pino, P., I. Vouldoukis, J. P. Kolb, N. Mahmoudi, I. Desportes-Livage, F. Bricaire, M. Danis, B. Dugas & D. Mazier, (2003) Plasmodium falciparum--infected erythrocyte adhesion induces caspase activation and apoptosis in human endothelial cells. *J Infect Dis* **187**: 1283-1290.

Pongponratn, E., G. D. Turner, N. P. Day, N. H. Phu, J. A. Simpson, K. Stepniewska, N. T. Mai, P. Viriyavejakul, S. Looareesuwan, T. T. Hien, D. J. Ferguson & N. J. White, (2003) An ultrastructural study of the brain in fatal Plasmodium falciparum malaria. *Am J Trop Med Hyg* **69**: 345-359.

Pouvelle, B., V. Matarazzo, C. Jurzynski, J. Nemeth, M. Ramharter, G. Rougon & J. Gysin, (2007) Neural cell adhesion molecule, a new cytoadhesion receptor for Plasmodium falciparum-infected erythrocytes capable of aggregation. *Infect Immun* **75**: 3516-3522.

Powers, M. V. & P. Workman, (2007) Inhibitors of the heat shock response: biology and pharmacology. *FEBS Lett* **581**: 3758-3769.

Price, R., M. van Vugt, F. Nosten, C. Luxemburger, A. Brockman, L. Phaipun, T. Chongsuphajaisiddhi & N. White, (1998) Artesunate versus artemether for the treatment of recrudescent multidrug-resistant falciparum malaria. *Am J Trop Med Hyg* **59**: 883-888.

Price, R. N., E. Tjitra, C. A. Guerra, S. Yeung, N. J. White & N. M. Anstey, (2007) Vivax malaria: neglected and not benign. *Am J Trop Med Hyg* **77**: 79-87.

Prudencio, M., A. Rodriguez & M. M. Mota, (2006) The silent path to thousands of merozoites: the Plasmodium liver stage. *Nat Rev Microbiol* **4**: 849-856.

Ralph, S. A., C. Scheidig-Benatar & A. Scherf, (2005) Antigenic variation in Plasmodium falciparum is associated with movement of var loci between subnuclear locations. *Proc Natl Acad Sci U S A* **102**: 5414-5419.

Rayner, J. C., (2006) Erythrocyte exit: Out, damned merozoite! Out I say! *Trends Parasitol* **22**: 189-192.

Reeder, J. C., A. F. Cowman, K. M. Davern, J. G. Beeson, J. K. Thompson, S. J. Rogerson & G. V. Brown, (1999) The adhesion of Plasmodium falciparum-infected erythrocytes to chondroitin sulfate A is mediated by P. falciparum erythrocyte membrane protein 1. *Proc Natl Acad Sci U S A* **96**: 5198-5202.

Roberts, D. D., J. A. Sherwood, S. L. Spitalnik, L. J. Panton, R. J. Howard, V. M. Dixit, W. A. Frazier, L. H. Miller & V. Ginsburg, (1985) Thrombospondin binds falciparum malaria parasitized erythrocytes and may mediate cytoadherence. *Nature* **318**: 64-66.

Roberts, D. J., A. G. Craig, A. R. Berendt, R. Pinches, G. Nash, K. Marsh & C. I. Newbold, (1992) Rapid switching to multiple antigenic and adhesive phenotypes in malaria [see comments]. *Nature* **357**: 689-692.

Rock, E. P., E. F. Roth, Jr., R. R. Rojas-Corona, J. A. Sherwood, R. L. Nagel, R. J. Howard & D. K. Kaul, (1988) Thrombospondin mediates the cytoadherence of Plasmodium falciparum-infected red cells to vascular endothelium in shear flow conditions. *Blood* **71**: 71-75.

Rogerson, S. J., S. C. Chaiyaroj, K. Ng, J. C. Reeder & G. V. Brown, (1995) Chondroitin sulfate A is a cell surface receptor for Plasmodium falciparum-infected erythrocytes. *J Exp Med* **182**: 15-20.

Rowe, A., J. Obeiro, C. I. Newbold & K. Marsh, (1995) Plasmodium falciparum rosetting is associated with malaria severity in Kenya. *Infect Immun* **63**: 2323-2326.

Rowe, J. A., J. M. Moulds, C. I. Newbold & L. H. Miller, (1997) P. falciparum rosetting mediated by a parasite-variant erythrocyte membrane protein and complement-receptor 1. *Nature* **388**: 292-295.

Rug, M., S. W. Prescott, K. M. Fernandez, B. M. Cooke & A. F. Cowman, (2006) The role of KAHRP domains in knob formation and cytoadherence of P falciparum-infected human erythrocytes. *Blood* **108**: 370-378.

Safeukui, I., J. M. Correas, V. Brousse, D. Hirt, G. Deplaine, S. Mule, M. Lesurtel, N. Goasguen, A. Sauvanet, A. Couvelard, S. Kerneis, H. Khun, I. Vigan-Womas, C. Ottone, T. J. Molina, J. M. Treluyer, O. Mercereau-Puijalon, G. Milon, P. H. David & P. A. Buffet, (2008) Retention of Plasmodium falciparum ring-infected erythrocytes in the slow, open microcirculation of the human spleen. *Blood* **112**: 2520-2528.

Scherf, A., R. Hernandez-Rivas, P. Buffet, E. Bottius, C. Benatar, B. Pouvelle, J. Gysin & M. Lanzer, (1998) Antigenic variation in malaria: in situ switching, relaxed and mutually exclusive transcription of var genes during intra-erythrocytic development in Plasmodium falciparum. *Embo J* **17**: 5418-5426.

Scherf, A., J. J. Lopez-Rubio & L. Riviere, (2008) Antigenic variation in Plasmodium falciparum. *Annu Rev Microbiol* **62**: 445-470.

Scherf, A., B. Pouvelle, P. A. Buffet & J. Gysin, (2001) Molecular mechanisms of Plasmodium falciparum placental adhesion. *Cell Microbiol* **3**: 125-131.

Schieck, E., J. M. Pfahler, C. P. Sanchez & M. Lanzer, (2007) Nuclear run-on analysis of var gene expression in Plasmodium falciparum. *Mol Biochem Parasitol* **153**: 207-212.

Schofield, L. & F. Hackett, (1993) Signal transduction in host cells by a glycosylphosphatidylinositol toxin of malaria parasites. *J Exp Med* **177**: 145-153.

Schofield, L., S. Novakovic, P. Gerold, R. T. Schwarz, M. J. McConville & S. D. Tachado, (1996) Glycosylphosphatidylinositol toxin of Plasmodium up-regulates intercellular adhesion molecule-1, vascular cell adhesion molecule-1, and E-selectin expression in vascular endothelial cells and increases leukocyte and parasite cytoadherence via tyrosine kinase-dependent signal transduction. *J Immunol* **156**: 1886-1896.

Shah, A., E. Unger, M. D. Bain, R. Bruce, J. Bodkin, J. Ginnetti, W. C. Wang, B. Seon, C. C. Stewart & S. S. Evans, (2002) Cytokine and adhesion molecule expression in primary human endothelial cells stimulated with fever-range hyperthermia. *Int J Hyperthermia* **18**: 534-551.

Shelby, J. P., J. White, K. Ganesan, P. K. Rathod & D. T. Chiu, (2003) A microfluidic model for single-cell capillary obstruction by Plasmodium falciparum-infected erythrocytes. *Proc Natl Acad Sci U S A* **100**: 14618-14622.

Siau, A., F. S. Toure, O. Ouwe-Missi-Oukem-Boyer, L. Ciceron, N. Mahmoudi, C. Vaquero, P. Froissard, U. Bisvigou, S. Bisser, J. Y. Coppee, E. Bischoff, P. H. David & D. Mazier, (2007) Whole-transcriptome analysis of Plasmodium falciparum field isolates: identification of new pathogenicity factors. *J Infect Dis* **196**: 1603-1612.

Simpson, J. A., T. Agbenyega, K. I. Barnes, G. Di Perri, P. Folb, M. Gomes, S. Krishna, S. Krudsood, S. Looareesuwan, S. Mansor, H. McIlleron, R. Miller, M. Molyneux, J. Mwenechanya, V. Navaratnam, F. Nosten, P. Olliaro, L. Pang, I. Ribeiro, M. Tembo, M. van Vugt, S. Ward, K. Weerasuriya, K. Win & N. J. White, (2006) Population pharmacokinetics of artesunate and dihydroartemisinin following intra-rectal dosing of artesunate in malaria patients. *PLoS Med* **3**: e444.

Singh, B., L. Kim Sung, A. Matusop, A. Radhakrishnan, S. S. Shamsul, J. Cox-Singh, A. Thomas & D. J. Conway, (2004) A large focus of naturally acquired Plasmodium knowlesi infections in human beings. *Lancet* **363**: 1017-1024.

Singh, K., A. G. Gittis, P. Nguyen, D. C. Gowda, L. H. Miller & D. N. Garboczi, (2008) Structure of the DBL3x domain of pregnancy-associated malaria protein VAR2CSA complexed with chondroitin sulfate A. *Nat Struct Mol Biol* **15**: 932-938.

Skinner, T. S., L. S. Manning, W. A. Johnston & T. M. Davis, (1996) In vitro stage-specific sensitivity of Plasmodium falciparum to quinine and artemisinin drugs. *Int J Parasitol* **26**: 519-525.

Skorokhod, A., E. Schwarzer, G. Gremo & P. Arese, (2007) HNE produced by the malaria parasite Plasmodium falciparum generates HNE-protein adducts and decreases erythrocyte deformability. *Redox Rep* **12**: 73-75.

Smilkstein, M., N. Sriwilaijaroen, J. X. Kelly, P. Wilairat & M. Riscoe, (2004) Simple and inexpensive fluorescence-based technique for high-throughput antimalarial drug screening. *Antimicrob Agents Chemother* **48**: 1803-1806.

Smith, J. D., C. E. Chitnis, A. G. Craig, D. J. Roberts, D. E. Hudson-Taylor, D. S. Peterson, R. Pinches, C. I. Newbold & L. H. Miller, (1995) Switches in expression of Plasmodium falciparum var genes correlate with changes in antigenic and cytoadherent phenotypes of infected erythrocytes [see comments]. *Cell* **82**: 101-110.

Smith, J. D., A. G. Craig, N. Kriek, D. Hudson-Taylor, S. Kyes, T. Fagen, R. Pinches, D. I. Baruch, C. I. Newbold & L. H. Miller, (2000) Identification of a Plasmodium falciparum intercellular adhesion molecule-1 binding domain: a parasite adhesion trait implicated in cerebral malaria. *Proc Natl Acad Sci U S A* **97**: 1766-1771.

Smith, J. D., B. Gamain, D. I. Baruch & S. Kyes, (2001) Decoding the language of var genes and Plasmodium falciparum sequestration. *Trends Parasitol* **17**: 538-545.

Smith, J. D., S. Kyes, A. G. Craig, T. Fagan, D. Hudson-Taylor, L. H. Miller, D. I. Baruch & C. I. Newbold, (1998) Analysis of adhesive domains from the A4VAR Plasmodium falciparum erythrocyte membrane protein-1 identifies a CD36 binding domain. *Mol Biochem Parasitol* **97**: 133-148.

Springer, A. L., L. M. Smith, D. Q. Mackay, S. O. Nelson & J. D. Smith, (2004) Functional interdependence of the DBLbeta domain and c2 region for binding of the Plasmodium falciparum variant antigen to ICAM-1. *Mol Biochem Parasitol* **137**: 55-64.

Staalsoe, T., H. A. Giha, D. Dodoo, T. G. Theander & L. Hviid, (1999) Detection of antibodies to variant antigens on Plasmodium falciparum- infected erythrocytes by flow cytometry. *Cytometry* **35**: 329-336.

Staunton, D. E., M. L. Dustin, H. P. Erickson & T. A. Springer, (1990) The arrangement of the immunoglobulin-like domains of ICAM-1 and the binding sites for LFA-1 and rhinovirus. *Cell* **61**: 243-254.

Su, X. Z., V. M. Heatwole, S. P. Wertheimer, F. Guinet, J. A. Herrfeldt, D. S. Peterson, J. A. Ravetch & T. E. Wellems, (1995) The large diverse gene family var encodes proteins involved in cytoadherence and antigenic variation of Plasmodium falciparum-infected erythrocytes [see comments]. *Cell* **82**: 89-100.

Suwanarusk, R., B. M. Cooke, A. M. Dondorp, K. Silamut, J. Sattabongkot, N. J. White & R. Udomsangpetch, (2004) The deformability of red blood cells parasitized by Plasmodium falciparum and P. vivax. *J Infect Dis* **189**: 190-194.

Taylor, T. E., W. J. Fu, R. A. Carr, R. O. Whitten, J. S. Mueller, N. G. Fosiko, S. Lewallen, N. G. Liomba & M. E. Molyneux, (2004) Differentiating the pathologies of cerebral malaria by postmortem parasite counts. *Nat Med* **10**: 143-145.

ter Kuile, F., N. J. White, P. Holloway, G. Pasvol & S. Krishna, (1993) Plasmodium falciparum: in vitro studies of the pharmacodynamic properties of drugs used for the treatment of severe malaria. *Exp Parasitol* **76**: 85-95.

Tilley, L., R. Sougrat, T. Lithgow & E. Hanssen, (2008) The twists and turns of Maurer's cleft trafficking in P. falciparum-infected erythrocytes. *Traffic* **9**: 187-197.

Toure, F. S., O. Ouwe-Missi-Oukem-Boyer, U. Bisvigou, O. Moussa, C. Rogier, P. Pino, D. Mazier & S. Bisser, (2008) Apoptosis: a potential triggering mechanism of neurological manifestation in Plasmodium falciparum malaria. *Parasite Immunol* **30**: 47-51.

Trager, W. & J. B. Jensen, (1976) Human malaria parasites in continuous culture. *Science* **193**: 673-675.

Treutiger, C. J., A. Heddini, V. Fernandez, W. A. Muller & M. Wahlgren, (1997) PECAM-1/CD31, an endothelial receptor for binding Plasmodium falciparum- infected erythrocytes [see comments]. *Nat Med* **3**: 1405-1408.

Tripathi, A. K., D. J. Sullivan & M. F. Stins, (2006) Plasmodium falciparum-infected erythrocytes increase intercellular adhesion molecule 1 expression on brain endothelium through NF-kappaB. *Infect Immun* **74**: 3262-3270.

Tripathi, A. K., D. J. Sullivan & M. F. Stins, (2007) Plasmodium falciparum-infected erythrocytes decrease the integrity of human blood-brain barrier endothelial cell monolayers. *J Infect Dis* **195**: 942-950.

Tse, M. T., K. Chakrabarti, C. Gray, C. E. Chitnis & A. Craig, (2004) Divergent binding sites on intercellular adhesion molecule-1 (ICAM-1) for variant Plasmodium falciparum isolates. *Mol Microbiol* **51**: 1039-1049.

Tsvetkova, N. M., I. Horvath, Z. Torok, W. F. Wolkers, Z. Balogi, N. Shigapova, L. M. Crowe, F. Tablin, E. Vierling, J. H. Crowe & L. Vigh, (2002) Small heat-shock proteins regulate membrane lipid polymorphism. *Proc Natl Acad Sci U S A* **99**: 13504-13509.

Turner, G., (1997) Cerebral malaria. *Brain Pathol* **7**: 569-582.

Turner, G. D., H. Morrison, M. Jones, T. M. Davis, S. Looareesuwan, I. D. Buley, K. C. Gatter, C. I. Newbold, S. Pukritayakamee, B. Nagachinta & et al., (1994) An immunohistochemical study of the pathology of fatal malaria. Evidence for widespread endothelial activation

and a potential role for intercellular adhesion molecule-1 in cerebral sequestration. *Am J Pathol* **145**: 1057-1069.

Udomsangpetch, R., B. Pipitaporn, S. Krishna, B. Angus, S. Pukrittayakamee, I. Bates, Y. Suputtamongkol, D. E. Kyle & N. J. White, (1996) Antimalarial drugs reduce cytoadherence and rosetting Plasmodium falciparum. *J Infect Dis* **173**: 691-698.

Udomsangpetch, R., B. Pipitaporn, K. Silamut, R. Pinches, S. Kyes, S. Looareesuwan, C. Newbold & N. J. White, (2002) Febrile temperatures induce cytoadherence of ring-stage Plasmodium falciparum-infected erythrocytes. *Proc Natl Acad Sci U S A* **99**: 11825-11829.

Udomsangpetch, R., P. H. Reinhardt, T. Schollaardt, J. F. Elliott, P. Kubes & M. Ho, (1997) Promiscuity of clinical Plasmodium falciparum isolates for multiple adhesion molecules under flow conditions. *J Immunol* **158**: 4358-4364.

Viebig, N. K., E. Levin, S. Dechavanne, S. J. Rogerson, J. Gysin, J. D. Smith, A. Scherf & B. Gamain, (2007) Disruption of var2csa gene impairs placental malaria associated adhesion phenotype. *PLoS ONE* **2**: e910.

Voss, T. S., J. Healer, A. J. Marty, M. F. Duffy, J. K. Thompson, J. G. Beeson, J. C. Reeder, B. S. Crabb & A. F. Cowman, (2006) A var gene promoter controls allelic exclusion of virulence genes in Plasmodium falciparum malaria. *Nature* **439**: 1004-1008.

Wagner, M., I. Hermanns, F. Bittinger & C. J. Kirkpatrick, (1999) Induction of stress proteins in human endothelial cells by heavy metal ions and heat shock. *Am J Physiol* **277**: L1026-1033.

Waller, K. L., L. M. Stubberfield, V. Dubljevic, W. Nunomura, X. An, A. J. Mason, N. Mohandas, B. M. Cooke & R. L. Coppel, (2007) Interactions of Plasmodium falciparum erythrocyte membrane protein 3 with the red blood cell membrane skeleton. *Biochim Biophys Acta* **1768**: 2145-2156.

Wang, P., Q. Wang, P. F. Sims & J. E. Hyde, (2007) Characterisation of exogenous folate transport in Plasmodium falciparum. *Mol Biochem Parasitol* **154**: 40-51.

Wassmer, S. C., V. Combes, F. J. Candal, I. Juhan-Vague & G. E. Grau, (2006a) Platelets potentiate brain endothelial alterations induced by Plasmodium falciparum. *Infect Immun* **74**: 645-653.

Wassmer, S. C., J. B. de Souza, C. Frere, F. J. Candal, I. Juhan-Vague & G. E. Grau, (2006b) TGF-beta1 released from activated platelets can induce TNF-stimulated human brain endothelium apoptosis: a new mechanism for microvascular lesion during cerebral malaria. *J Immunol* **176**: 1180-1184.

Wassmer, S. C., C. Lepolard, B. Traore, B. Pouvelle, J. Gysin & G. E. Grau, (2004) Platelets reorient Plasmodium falciparum-infected erythrocyte cytoadhesion to activated endothelial cells. *J. Infect. Dis.* **189**: 180-189.

Waterkeyn, J. G., M. E. Wickham, K. M. Davern, B. M. Cooke, R. L. Coppel, J. C. Reeder, J. G. Culvenor, R. F. Waller & A. F. Cowman, (2000) Targeted mutagenesis of Plasmodium falciparum erythrocyte membrane protein 3 (PfEMP3) disrupts cytoadherence of malaria-infected red blood cells. *Embo J* **19**: 2813-2823.

Wickham, M. E., M. Rug, S. A. Ralph, N. Klonis, G. I. McFadden, L. Tilley & A. F. Cowman, (2001) Trafficking and assembly of the cytoadherence complex in Plasmodium falciparum-infected human erythrocytes. *EMBO J* **20**: 5636-5649.

Williams, T. N. & C. I. Newbold, (2003) Reevaluation of flow cytometry for investigating antibody binding to the surface of Plasmodium falciparum trophozoite-infected red blood cells. *Cytometry* **56A**: 96-103.

Wilson, N. O., M. B. Huang, W. Anderson, V. Bond, M. Powell, W. E. Thompson, H. B. Armah, A. A. Adjei, R. Gyasi, Y. Tettey & J. K. Stiles, (2008) Soluble factors from Plasmodium falciparum-infected erythrocytes induce apoptosis in human brain vascular endothelial and neuroglia cells. *Mol Biochem Parasitol* **162**: 172-176.

Winstanley, P. & S. Ward, (2006) Malaria chemotherapy. *Adv Parasitol* **61**: 47-76.

Yang, L., J. R. Kowalski, P. Yacono, M. Bajmoczi, S. K. Shaw, R. M. Froio, D. E. Golan, S. M. Thomas & F. W. Luscinskas, (2006) Endothelial cell cortactin coordinates intercellular adhesion molecule-1 clustering and actin cytoskeleton remodeling during polymorphonuclear leukocyte adhesion and transmigration. *J Immunol* **177**: 6440-6449.

Yang, Y., C. D. Jun, J. H. Liu, R. Zhang, A. Joachimiak, T. A. Springer & J. H. Wang, (2004) Structural basis for dimerization of ICAM-1 on the cell surface. *Mol Cell* **14**: 269-276.

Yipp, B. G., D. I. Baruch, C. Brady, A. G. Murray, S. Looareesuwan, P. Kubes & M. Ho, (2003a) Recombinant PfEMP1 peptide inhibits and reverses cytoadherence of clinical Plasmodium falciparum isolates in vivo. *Blood* **101**: 331-337.

Yipp, B. G., M. J. Hickey, G. Andonegui, A. G. Murray, S. Looareesuwan, P. Kubes & M. Ho, (2007) Differential roles of CD36, ICAM-1, and P-selectin in Plasmodium falciparum cytoadherence in vivo. *Microcirculation* **14**: 593-602.

Yipp, B. G., S. M. Robbins, M. E. Resek, D. I. Baruch, S. Looareesuwan & M. Ho, (2003b) Src-family kinase signaling modulates the adhesion of Plasmodium falciparum on human microvascular endothelium under flow. *Blood* **101**: 2850-2857.

Zhao, R. & G. X. Shen, (2007) Involvement of heat shock factor-1 in glycated LDL-induced upregulation of plasminogen activator inhibitor-1 in vascular endothelial cells. *Diabetes* **56**: 1436-1444.

Zhou, M., A. Zhang, B. Lin, J. Liu & L. X. Xu, (2007) Study of heat shock response of human umbilical vein endothelial cells (HUVECs) using cDNA microarray. *Int J Hyperthermia* **23**: 225-258.